

**STUDIES ON POLYMER NANOCOMPOSITES WITH  
SPECIAL REFERENCE TO POLYESTER-CLOISITE15A  
NANOCOMPOSITE**

*A THESIS*

Submitted by

**BINU P.P.**

*for the award of the degree*

*of*

**DOCTOR OF PHILOSOPHY**



**DIVISION OF MECHANICAL ENGINEERING  
SCHOOL OF ENGINEERING  
COCHIN UNIVERSITY OF SCIENCE AND TECHNOLOGY  
KOCHI – 22, KERALA, INDIA**

**JULY 2017**

## **CERTIFICATE**

This is to certify that the thesis entitled **STUDIES ON POLYMER NANOCOMPOSITES WITH SPECIAL REFERENCE TO POLYESTER-CLOISITE15A NANOCOMPOSITE** submitted by **Binu P.P.** to the Cochin University of Science and Technology, Kochi for the award of the degree of Doctor of Philosophy is a bonafide record of research work carried out by him under our supervision and guidance at the Division of Mechanical Engineering, School of Engineering, Cochin University of Science and Technology. The contents of this thesis, in full or in parts, have not been submitted to any other University or Institute for the award of any degree or diploma. All the relevant corrections and modifications suggested by the audience and recommended by the doctoral committee of the candidate during the pre-synopsis seminar have been incorporated in the thesis.

Kochi-22  
31/07/2017

**Prof. (Dr.) M.N. Vinodkumar**  
(Supervising Guide)

**Prof. (Dr.) K.E. George**  
(Co- Guide)

## **DECLARATION**

I hereby declare that the work presented in the thesis entitled **STUDIES ON POLYMER NANOCOMPOSITES WITH SPECIAL REFERENCE TO POLYESTER-CLOISITE15A NANOCOMPOSITE** is based on the original research work carried out by me under the supervision and guidance of Prof.(Dr.) M.N. Vinodkumar, Dept. of Fire and Safety, Cochin University of Science and Technology, Kochi-22 and Prof.(Dr.) K.E. George, Former Head, Dept. of Polymer Science and Rubber Technology, Cochin University of Science and Technology, Kochi-22, for the award of degree of Doctor of Philosophy with Cochin University of Science and Technology. I further declare that the contents of this thesis in full or in parts have not been submitted to any other University or Institute for the award any degree or diploma.

Kochi - 22  
31/07/2017

**Binu P. P.**

## **ACKNOWLEDGEMENTS**

I bow to God almighty for the blessings showered on me, without which this project could not have been completed.

Also the thesis would not have been completed successfully but for the sincere help of many others and I wish to express my sincere gratitude to them at this juncture. I would like to express my deep sincere gratitude to my supervising guide, Prof.(Dr.) M.N Vinodkumar, Professor Department of Fire & Safety, School of Engineering, CUSAT and Prof. (Dr.) K.E. George, former Professor and Head, Dept. of Polymer Science and Rubber Technology, CUSAT (former Principal, Albertian Institute of Science and Technology) for providing guidance and support to carry out my research. Their inspiration and continuous monitoring helped me in every step of my research activity.

I express my gratitude and respect to Prof. (Dr.) M.R.R. Panikkar, Principal, School of Engineering, CUSAT for his support and permission for carrying out my research work.

I extend my gratitude and respect to Prof. (Dr.) G. Madhu, Professor and former Principal, School of Engineering, CUSAT and also member of my doctoral committee for his support and timely directions to bring my research activity to a fulfillment. I am also grateful to Prof. Dr. P.S. Sreejith, former Principal School of Engineering and Present Dean for the inspiration he has provided.

I extend my gratitude and thanks to Prof. Narayanan Kutty, Head of the Department, PSRT, CUSAT for giving me all support and permission to use the facilities in the department for the conduct of research experiments. I also extend my heartfelt thanks to Prof. (Dr.) Eby Thachil, former HOD, PSRT, CUSAT.

I extend my gratitude to all other members of teaching faculty in the department of PSRT, Division of Fire and Safety and Division of Mechanical Engineering of School of Engineering, for their valuable help and suggestions. I am also thankful to all the non-teaching staff for the support I received from them.

I sincerely acknowledge the services rendered by staff of STIC, CUSAT for testing analysis of my samples.

I acknowledge my sincere thanks and gratitude to all my fellow research scholars of PSRT and SOE for their continuous support and advice.

I am greatly indebted to late Prof. (Dr.) A.V. Zacharias, for his inspiration and support he has rendered at the beginning of this project work.

I am also greatly indebted to Prof. K. Rajendran, Prof. (Dr.) C.E. Krishnan, Prof. (Dr.) P.N. Joshy, former Principals, Sree Narayana Gurukulam College of Engineering, Kadayiruppu, where I am working. I am also indebted to Prof. (Dr.) Saji C.B., Present Principal, Sree Narayana Gurukulam college of Engineering and Prof. K.R. Rajan, HOD, Mechanical, Sree Narayana Gurukulam College of Engineering for the timely help and support they have rendered.

I am greatly indebted to Associate Prof. Rajeshkumar, my colleague for his support.

Last but not the least I express my gratitude to my family members for being a pillar of support and inspiration.

**Binu P P**

## ABSTRACT

**Keywords:** nanocomposite; nanoclay; mechanical property; thermal property.

Extensive use of composites in a wide range of engineering applications has been the inspiration for selecting this study. Composites are the material of choice in many critical engineering applications. Nanofillers are now widely used for reinforcing polymers and the nanomodified polymer composite represents a new class of engineering materials. In the large field of nanotechnology, polymer based nanocomposites have become a prominent area of current research and development.

Uniform dispersion of the reinforcing filler in the polymer is absolutely essential for the property enhancement of the polymer. Uniform distribution as well as optimum quantity of filler or reinforcement is critical for developing useful composites. Nanofillers can improve the properties of the composite even at very low concentration of the filler because of their surface area and hence do not adversely affect the processing or weight of the composite. Nanofillers can also improve the mechanical behavior of conventional polymer composites. Analysis of nanoclay filled polymer as well as nanoclay filled conventional polymer a composite is the topic of this study.

Locally available low cost nanokaoline clays were used as the nanofiller for modifying a widely used thermosetting polymer- unsaturated polyester resin. Both modified and un modified forms of nanoclays were employed for the reinforcement. Mechanical and thermal characterizations of the nanocomposites were done to ascertain the quantum of improvement and application of the composites.

Since unsaturated polyesters are widely used for generating conventional fiber reinforced polymer composites, the study of using nanoclay for modifying the

polymer was extended to reinforced polymer composites also. The study was also done with standard montmorillonite clay, Cloisite15A. Mechanical properties of isophthalic polyester resin improve when modified with nanokaoline clay. The effect is more remarkable in the case of modified nanokaolineclay.

Maximum improvement in mechanical properties was observed with Cloisite15A at a filler content of 1% weight of the resin. Optimum concentration for Cloisite15A is found to be in the range 0.5 to 1.5 %. This concentration is found to be relevant for dynamic loading also. Dynamic mechanical analysis shows storage modulus to be maximum for the nanocomposite with 1% filler. The loss modulus curve peaks around 80 to 100 °C. The nature of thermal degradation obtained from TGA indicates that the thermal stability marginally improves with the addition of nanofiller.

The optimum nanoclay composition in the conventional fiber reinforced polyester is found to be around 0.5 to 1% weight of the polyester resin for getting balanced performance characteristics such as good impact strength, tensile modulus and dynamic mechanical properties. The thermal degradation does not show any remarkable change with the addition of nanofiller and the thermal degradation begins at around 320 °C.

Resistance to creep behavior improves with the addition of nanofiller as shown by tensile creep behavior of both polymer nanocomposite (PNC) and glass fiber reinforced polymer nanocomposite (GFRPNC). Creep compliance is minimum for 1% cloisite15A filled PNC as well as GFRPNC. Also, it remains steady for a long period.

# TABLE OF CONTENTS

|  |           |
|--|-----------|
| ACKNOWLEDGEMENTS                                       | i         |
| ABSTRACT   | iii       |
| TABLE OF CONTENTS                                      | v         |
| LIST OF TABLES   | ix        |
| LIST OF FIGURES  | xii       |
| ABBREVIATIONS  | xviii     |
| <b>CHAPTER 1 INTRODUCTION</b>                          | <b>1</b>  |
| 1.1 POLYMER MATRIX COMPOSITES (PMC)                    | 3         |
| 1.2 PARTICULATE FILLED COMPOSITE                       | 5         |
| 1.3 POLYMER NANOCOMPOSITES                             | 6         |
| 1.4 STRUCTURE OF CLAY PARTICLES                        | 11        |
| 1.5 POLYMER NANOCOMPOSITE STRUCTURES                   | 12        |
| 1.6 SYNTHESIS OF POLYMER-CLAY NANOCOMPOSITES           | 14        |
| 1.7 PROPERTIES OF POLYMER-BASED NANOCOMPOSITES         | 15        |
| 1.8 PROPERTY ENHANCEMENT OF POLYMERS BY<br>NANOFILLERS | 17        |
| 1.9 NANOCLAY MODIFIED FIBER REINFORCED POLYMER         | 19        |
| 1.10 CREEP BEHAVIOR OF NANOCOMPOSITE                   | 23        |
| 1.11 BACKGROUND OF PRESENT WORK                        | 27        |
| 1.12 SCOPE AND OBJECTIVES                              | 28        |
| 1.13 RESEARCH METHODOLOGY                              | 32        |
| <b>CHAPTER 2 EXPERIMENTAL</b>                          | <b>33</b> |
| 2.1 INTRODUCTION                                       | 33        |
| 2.2 MATERIALS  | 33        |
| 2.2.1 Polyester Resin                                  | 33        |
| 2.2.2 Nanoclay   | 34        |
| 2.2.3 Glass fiber mat                                  | 37        |
| 2.3 MATERIAL PREPARATION                               | 37        |
| 2.3.1 Specimen Preparation                             | 37        |
| 2.4 CHARACTERIZATION TECHNIQUES                        | 39        |
| 2.4.1 Tensile Tests (ASTM D 638, ISO 527-1)            | 40        |
| 2.4.2 Impact Tests (ASTM D 4812)                       | 42        |

|   |   |           |
|---|---|-----------|
| 2.4.3   | Flexural Tests (ASTM D790M) -----             | 43        |
| 2.4.4   | Scanning Electron Microscopy (SEM) -----      | 44        |
| 2.4.5   | Dynamic Mechanical Analysis (DMA) -----       | 45        |
| 2.4.6   | X-Ray Diffraction (XRD)-----                  | 47        |
| 2.4.7   | Thermogravimetric Analysis (TGA) -----        | 49        |
| 2.4.8   | Differential Scanning Calorimetry (DSC) ----- | 50        |
| 2.4.9   | Creep Test -----                              | 51        |
| <b>CHAPTER 3 ANALYSIS OF ISOPHTHALIC POLYESTER<br/>/NANO-KAOLIN CLAY NANOCOMPOSITE -----</b>                              |   | <b>53</b> |
| 3.1   | INTRODUCTION -----                            | 53        |
| 3.2   | METHODOLOGY -----                             | 55        |
| 3.2.1   | Raw materials -----                           | 55        |
| 3.2.2   | Material Preparation -----                    | 56        |
| 3.2.3   | Mechanical Characterization -----             | 56        |
| 3.2.4   | Study of Fracture surface -----               | 57        |
| 3.3   | RESULTS AND DISCUSSION -----                  | 57        |
| 3.3.1   | Tensile Properties -----                      | 57        |
| 3.3.2   | Impact Properties-----                        | 67        |
| 3.3.3   | SEM Analysis -----                            | 72        |
| 3.4   | CONCLUSIONS -----                             | 74        |
| <b>CHAPTER 4 MECHANICAL AND THERMAL<br/>CHARACTERIZATION OF ISOPHTHALIC<br/>POLYESTER-CLOISITE15A NANOCOMPOSITE -----</b> |   | <b>75</b> |
| 4.1   | INTRODUCTION -----                            | 75        |
| 4.2   | METHODOLOGY -----                             | 78        |
| 4.2.1   | Raw materials -----                           | 78        |
| 4.2.2   | Specimen Preparation-----                     | 78        |
| 4.2.3   | Mechanical Characterization -----             | 79        |
| 4.2.4   | Dynamic Mechanical Analysis -----             | 80        |
| 4.2.5   | Thermal Analysis -----                        | 80        |
| 4.2.6   | Study of fracture surface -----               | 81        |
| 4.3   | RESULTS AND DISCUSSION -----                  | 82        |
| 4.3.1   | Tensile Test -----                            | 82        |

|                  |  |            |
|------------------|--|------------|
| 4.3.2            | Impact Test -----  | 85         |
| 4.3.3            | Flexural Test -----  | 86         |
| 4.3.4            | Dynamic Mechanical Analysis (DMA) -----  | 88         |
| 4.3.5            | Model Analysis -----   | 102        |
| 4.3.6            | X-ray diffraction -----  | 106        |
| 4.3.7            | Thermogravimetric Analysis -----   | 108        |
| 4.3.8            | Differential Scanning Calorimetry -----  | 110        |
| 4.3.9            | SEM Analysis -----   | 111        |
| 4.3.10           | Statistical Analysis -----   | 114        |
| 4.4              | CONCLUSIONS -----  | 119        |
| <br>             |  |            |
| <b>CHAPTER 5</b> | <b>MECHANICAL AND THERMAL<br/>CHARACTERIZATION OF GLASS FIBER<br/>REINFORCED POLYESTER NANOCOMPOSITE -----</b> | <b>121</b> |
| 5.1              | INTRODUCTION -----   | 121        |
| 5.2              | METHODOLOGY -----  | 123        |
| 5.2.1            | Raw materials -----  | 123        |
| 5.2.2            | Specimen Preparation -----   | 124        |
| 5.2.3            | Mechanical Characterization -----  | 124        |
| 5.2.4            | Dynamic Mechanical Analysis -----  | 125        |
| 5.2.5            | Thermal Analysis -----   | 126        |
| 5.2.6            | Study of fracture surface -----  | 126        |
| 5.3              | RESULTS AND DISCUSSION -----   | 128        |
| 5.3.1            | Tensile Test -----   | 128        |
| 5.3.2            | Impact Test -----  | 132        |
| 5.3.3            | Dynamic Mechanical Analysis -----  | 133        |
| 5.3.4            | Model Analysis -----   | 142        |
| 5.3.5            | X-ray diffraction -----  | 149        |
| 5.3.6            | Thermogravimetric Analysis -----   | 150        |
| 5.3.7            | Differential Scanning Calorimetry -----  | 152        |
| 5.3.8            | SEM Analysis -----   | 153        |
| 5.3.9            | Statistical Analysis -----   | 157        |
| 5.4              | CONCLUSIONS -----  | 162        |

|                             |  |            |
|-----------------------------|--|------------|
| <b>CHAPTER 6</b>            | <b>TENSILE CREEP BEHAVIOR OF NANOCOMPOSITE ---</b>   | <b>163</b> |
| 6.1                         | INTRODUCTION -----                                   | 163        |
| 6.2                         | METHODOLOGY -----                                    | 166        |
| 6.2.1                       | Raw materials -----                                  | 166        |
| 6.2.2                       | Specimen Preparation-----                            | 167        |
| 6.2.3                       | Creep Study -----                                    | 167        |
| 6.3                         | RESULTS AND DISCUSSION -----                         | 168        |
| 6.3.1                       | Dynamic Mechanical Analysis in frequency sweep ----- | 168        |
| 6.3.2                       | Creep data Analysis-----                             | 195        |
| 6.3.3                       | Statistical Analysis -----                           | 197        |
| 6.4                         | CONCLUSIONS -----                                    | 200        |
| <b>CHAPTER 7</b>            | <b>CONCLUSIONS AND SCOPE FOR FURTHER STUDY ----</b>  | <b>201</b> |
| <b>REFERENCES</b>           |  |            |
| <b>LIST OF PUBLICATIONS</b> |  |            |
| <b>CURRICULUM VITAE</b>     |  |            |

## LIST OF TABLES

| <i>Table</i> | <i>Title</i>   | <i>Page No.</i> |
|--------------|--|-----------------|
| Table 2-1    | Properties of isophthalic polyester -----  | 34              |
| Table 2-2    | Properties of nanokaoline clay-----  | 35              |
| Table 2-3    | Properties of Cloisite15A-----   | 35              |
| Table 3-1    | Tensile properties of polyester nanocomposite with<br>different type of nanokaoline clay as filler-----  | 57              |
| Table 3-2    | Tensile properties of polyester nanocomposite with<br>unmodified nanokaoline clay (N100) as filler -----   | 62              |
| Table 3-3    | Tensile properties of polyester nanocomposite with amino<br>modified nanokaoline clay (N 100A) as filler -----                                       | 62              |
| Table 3-4    | Tensile properties of polyester nanocomposite with dialkyl<br>modified nanokaoline clay (N 100Z) as filler -----                                     | 62              |
| Table 3-5    | Tensile properties polyester nanocomposite with mercapton<br>modified nanokaoline clay (N 100M) as filler-----                                       | 63              |
| Table 3-6    | Variation Impact strength of polyester nanocomposite with<br>different type of nanokaoline clay as filler-----                                       | 68              |
| Table 3-7    | Variation of impact strength of polyester nanocomposite<br>with nanoclay ( N 100) content -----  | 68              |
| Table 3-8    | Variation of impact strength of polyester nanocomposite<br>with nanoclay (N 100A) content -----  | 68              |
| Table 3-9    | Variation of impact strength of polyester nanocomposite<br>with nanoclay (N 100Z) content-----   | 68              |
| Table 3-10   | Variation of impact strength of polyester nanocomposite<br>with nanoclay (N 100M) content -----  | 69              |
| Table 4-1    | Tensile properties of polyester nanocomposite with filler<br>content (% weight of Cloisite15A) at different testing speed -----                      | 82              |
| Table 4-2    | Variation of impact strength of polyester nanocomposite<br>with filler content (% weight of Cloisite15A) -----                                       | 82              |
| Table 4-3    | Variation of flexural properties of polyester nanocomposite<br>with filler content (Cloisite15A) at different testing speeds -----                   | 84              |
| Table 4-4    | Values of parameters A,B ,C and regression coefficient of<br>the mathematical model obtained from polynomial fit for<br>mechanical properties. ----- | 98              |

|            |  |     |
|------------|--|-----|
| Table 4-5  | Values of parameters and regression coefficient of the mathematical model obtained from Boltzmann fit for storage modulus at different testing frequencies -----         | 99  |
| Table 4-6  | Values of parameters and regression coefficient of the mathematical model obtained from Loretz fit for loss modulus at different testing frequencies-----                | 100 |
| Table 4-7  | Values of parameters and regression coefficient of the mathematical model obtained from Gaussian fit for tandelta ( $\tan\delta$ ) at different testing frequencies----- | 101 |
| Table 4-8  | Statistical analysis, Tensile modulus-----   | 114 |
| Table 4-9  | Statistical analysis, Impact strength-----   | 115 |
| Table 4-10 | Statistical analysis, Flexural modulus -----   | 116 |
| Table 4-11 | Statistical analysis, Storage modulus -----  | 117 |
| Table 4-12 | Statistical analysis, Thermal degradation -----  | 118 |
| Table 5-1  | Variation of Tensile properties of glass fiber reinforced polyester nanocomposite (GFRPNC) with filler content at different testing speed-----                           | 127 |
| Table 5-2  | Variation of Impact strength of glass fiber reinforced polyester nanocomposite (GFRPNC) with filler content -----  | 128 |
| Table 5-3  | Values of parameters A,B,C and regression coefficient of mathematical model obtained from polynomial fit for mechanical properties-----                                  | 142 |
| Table 5-4  | Value of parameters in Boltzmann model for storage modulus of GFRPNCs -----  | 146 |
| Table 5-5  | Values of parameters in Lorentzian model for loss modulus of GFRPNCs -----   | 147 |
| Table 5-6  | Values of parameters in Gaussian model for $\tan\delta$ of GFRPNCs -----   | 148 |
| Table 5-7  | Statistical analysis, Tensile Modulus -----  | 158 |
| Table 5-8  | Statistical analysis, Impact Strength -----  | 159 |
| Table 5-9  | Statistical analysis, Storage Modulus -----  | 160 |
| Table 5-10 | Statistical analysis, Thermal degradation -----  | 161 |
| Table 6-1  | Dynamic mechanical properties at various frequencies for neat resin (Polyester)-----   | 170 |
| Table 6-2  | Dynamic mechanical properties at various frequencies for 1% Cloisite15A filled PNC -----   | 171 |
| Table 6-3  | Dynamic mechanical properties at various frequencies for 2% Cloisite15A filled PNC -----   | 172 |
| Table 6-4  | Dynamic mechanical properties at various frequencies for 0% Cloisite15A filled GFRPNC -----  | 173 |

|            |  |     |
|------------|--|-----|
| Table 6-5  | Dynamic mechanical properties at frequency sweep for<br>1% Cloisite15A filled GFRPNC ----- | 174 |
| Table 6-6  | Dynamic mechanical properties at frequency sweep for<br>2% Cloisite15A filled GFRPNC ----- | 175 |
| Table 6-7  | Creep compliance of PNCs at stress 1MPa -----  | 176 |
| Table 6-8  | Creep strain of PNCs at stress 1MPa -----  | 177 |
| Table 6-9  | Creep compliance of GFRPNCs at stress 1MPa -----   | 178 |
| Table 6-10 | Creep strain of GFRPNCs at stress 1MPa-----  | 179 |
| Table 6-11 | Creep compliance of GFRPNCs at stress 2 MPa-----   | 180 |
| Table 6-12 | Creep strain of GFRPNCs at stress 2 MPa-----   | 181 |
| Table 6-13 | Statistical analysis, creep compliance of PNCs at stress<br>1MPa -----                     | 198 |
| Table 6-14 | Statistical analysis, creep compliance of GFRPNCs at<br>stress 1MPa-----                   | 199 |
| Table 6-15 | Statistical analysis, creep compliance of GFRPNC at stress<br>2 MPa -----                  | 199 |

## LIST OF FIGURES

| <i>Figure</i> | <i>Title</i>  | <i>Page</i> |
|---------------|---|-------------|
| Figure 1-1    | Different types of nanofillers -----  | 8           |
| Figure 1-2    | Structure of 2:1 layered silicate -----   | 12          |
| Figure 1-3    | Scheme of different types of composite arising from the interaction of layered silicates and polymers -----             | 13          |
| Figure 1-4    | Schematic representation of PLS nanocomposite obtained by insitu polymerization -----                                   | 15          |
| Figure 1-5    | Schematic representation of PLS nanocomposite obtained by intercalation of polymer from solution -----                  | 15          |
| Figure 1-6    | Schematic representation of PLS nanocomposite obtained by direct melt intercalation -----                               | 15          |
| Figure 1-7    | Schematic representation of Methodology adopted for the study -----   | 31          |
| Figure 2-1    | SEM image of modified nanoclay, Cloisite 15A -----  | 36          |
| Figure 2-2    | Image of glass fiber mat -----  | 36          |
| Figure 2-3    | Ultrasonicator -----  | 38          |
| Figure 2-4    | Universal Testing Machine -----   | 41          |
| Figure 2-5    | Resil impact tester -----   | 43          |
| Figure 2-6    | Scanning Electron Microscope -----  | 45          |
| Figure 2-7    | Clamping in duel cantilever mode -----  | 46          |
| Figure 2-8    | Dynamic Mechanical Analyzer -----   | 47          |
| Figure 2-9    | X-Ray Diffractometer -----  | 48          |
| Figure 2-10   | Thermogravimetric analyzer -----  | 50          |
| Figure 2-11   | Differential Scanning Calorimeter -----   | 51          |
| Figure 3-1    | Maximum strain under tensile load for polyester nanocomposite with different type of nanokaoline clay as filler -----   | 59          |
| Figure 3-2    | Tensile modulus of polyester nanocomposite with different nanokaoline clay as filler -----                              | 59          |
| Figure 3-3    | Tensile strength of polyester nanocomposite with different type of nanokaoline clay s filler -----                      | 61          |
| Figure 3-4    | Variation of tensile modulus of polyester nanocomposite with nanoclay (N 100) content at different testing speed -----  | 63          |
| Figure 3-5    | Variation of Tensile strength of polyester nanocomposite with nanoclay(N 100) content at different testing speed -----  | 64          |
| Figure 3-6    | Variation of tensile modulus of polyester nanocomposite with nanoclay (N 100A) content at different testing speed ----- | 64          |

|             |  |    |
|-------------|--|----|
| Figure 3-7  | Variation of tensile strength of polyester nanocomposite with nanoclay (N 100A) content at different testing speed -----   | 65 |
| Figure 3-8  | Variation of tensile modulus of polyester nanocomposite with nanoclay content (N N 100Z) at different testing speed-----   | 65 |
| Figure 3-9  | Variation of tensile strength of polyester nanocomposite with nanoclay content (N 100Z) at different testing speed -----   | 66 |
| Figure 3-10 | Variation of tensile modulus of polyester nanocomposite with nanoclay (N 100M) content at different testing speed -----  | 66 |
| Figure 3-11 | Variation of tensile strength of polyester nanocomposite with nanoclay (N 100M) content at different testing speed -----   | 67 |
| Figure 3-12 | Variation Impact strength of polyester nanocomposite with different type of nanokaoline clay as filler at 1% weight-----   | 70 |
| Figure 3-13 | Variation of impact strength of polyester nanocomposite with nanoclay (N 100) content -----  | 70 |
| Figure 3-14 | Variation of impact strength of polyester nanocomposite with nanoclay (N 100A) content -----   | 71 |
| Figure 3-15 | Variation of impact strength of polyester nanocomposite with nanoclay (N 100Z) content-----  | 71 |
| Figure 3-16 | Variation of impact strength of polyester nanocomposite with nanoclay (N 100M) content-----  | 72 |
| Figure 3-17 | SEM micrographs of fracture surface (a) 1% unmodified nanokaoline filled polyester (b) 1% mercapton modified nanokaoline filled polyester (c) 2% unmodified nanokaoline filled polyester (d) 2% mercapton modified nanokaoline filled polyester and (e) pure polyester ----- | 73 |
| Figure 4-1  | Specimen prepared for tensile test -----   | 79 |
| Figure 4-2  | Specimen prepared for impact test -----  | 80 |
| Figure 4-3  | Specimen prepared for flexural test-----   | 80 |
| Figure 4-4  | Variation of tensile modulus of polyester nanocomposite with filler content (% weight of Cloisite15A) at different testing speeds-----   | 84 |
| Figure 4-5  | Variation of impact strength of polyester nanocomposite with filler content (% weight of Cloisite15A)-----   | 86 |
| Figure 4-6  | Variation of flexural modulus of polyester nanocomposite with filler content (% weight of Cloisite15A) at different testing speeds-----  | 87 |
| Figure 4-7  | Variation of storage modulus of polyester nanocomposite with temperature for different filler (Cloisite15A) content at frequency 1 Hz-----   | 90 |

|             |  |     |
|-------------|--|-----|
| Figure 4-8  | Variation of storage modulus of polyester nanocomposite with temperature for different filler (Cloisite15A) content at frequency 10 Hz -----               | 91  |
| Figure 4-9  | Variation of storage modulus of polyester nanocomposite with temperature for different filler (Cloisite15A) content at frequency 100 Hz-----               | 91  |
| Figure 4-10 | Variation of loss modulus of polyester nanocomposite with temperature for different filler (Cloisite15A) content at frequency 1 Hz-----                    | 93  |
| Figure 4-11 | Variation of loss modulus of polyester nanocomposite with temperature for different filler (Cloisite15A) content at frequency 10 Hz -----                  | 94  |
| Figure 4-12 | Variation of loss modulus of polyester nanocomposite with temperature for different filler (Cloisite15A) content at frequency 100 Hz-----                  | 94  |
| Figure 4-13 | Variation of $\tan\delta$ of polyester nanocomposite with temperature for different filler (Cloisite15A) content at frequency 1 Hz-----                    | 96  |
| Figure 4-14 | Variation of $\tan\delta$ of polyester nanocomposite with temperature for different filler (Cloisite15A) content at frequency 10 Hz -----                  | 97  |
| Figure 4-15 | Variation of $\tan\delta$ of polyester nanocomposite with temperature for different filler (Cloisite15A) content at frequency 100 Hz-----                  | 97  |
| Figure 4-16 | XRD pattern of pure nanoclay (Cloisite15A) -----   | 107 |
| Figure 4-17 | XRD pattern of PNC (1% Cloisite15A)-----   | 107 |
| Figure 4-18 | TGA thermogram of PNC, Variation of % weight loss with temperature at different filler (Cloisite15A) contents -----  | 109 |
| Figure 4-19 | TGA thermogram of PNC, variation of % derived weight with temperature at different filler (Cloisite15A) contents -----                                     | 110 |
| Figure 4-20 | DSC curves of PNC at different filler (Cloisite15A) contents-----  | 111 |
| Figure 4-21 | SEM images of (a) pure polyester, (b) 1% nanoclay filled polyester, (c) 2% nanoclay filled polyester (d) 2% nanoclay filled polyester magnified view ----- | 113 |
| Figure 4-22 | SEM images of (a) pure polyester, (b) 1% nanoclay filled polyester of the fracture surface after impact test-----  | 113 |
| Figure 5-1  | Sample specimen for tensile test -----   | 127 |
| Figure 5-2  | Sample specimen for flexural test-----   | 127 |
| Figure 5-3  | Sample specimen for impact test -----  | 127 |

|             |  |     |
|-------------|--|-----|
| Figure 5-4  | Variation of tensile modulus of glass fiber reinforced polyester nanocomposite with filler content (% weight of Cloisite15A) at different testing speeds -----       | 130 |
| Figure 5-5  | Variation of tensile strength of glass fiber reinforced polyester nanocomposite with filler content (% weight of Cloisite15A) at different testing speeds -----      | 131 |
| Figure 5-6  | Variation of impact strength of glass fiber reinforced polyester nanocomposite with filler content (% weight of Cloisite15A) -----                                   | 131 |
| Figure 5-7  | Variation of storage modulus of Glass Fiber Reinforced Polyester Nanocomposite with temperature for different filler (Cloisite15A) content at frequency 1Hz -----    | 135 |
| Figure 5-8  | Variation of storage modulus of Glass Fiber Reinforced Polyester Nanocomposite with temperature for different filler (Cloisite15A) content at frequency 10 Hz-----   | 136 |
| Figure 5-9  | Variation of storage modulus of Glass Fiber Reinforced Polyester Nanocomposite with temperature for different filler (Cloisite15A) content at frequency 100 Hz ----- | 136 |
| Figure 5-10 | Variation of Loss modulus of glass fiber reinforced polyester nanocomposite with temperature for different filler (Cloisite15A) content at frequency 1 Hz -----      | 138 |
| Figure 5-11 | Variation of Loss modulus of glass fiber reinforced polyester nanocomposite with temperature for different filler (Cloisite15A) content at frequency 10 Hz-----      | 139 |
| Figure 5-12 | Variation of Loss modulus of glass fiber reinforced polyester nanocomposite with temperature for different filler (Cloisite15A) content at frequency 100 Hz -----    | 139 |
| Figure 5-13 | Variation of $\tan\delta$ of glass fiber reinforced polyester nanocomposite with temperature for different filler (Cloisite15A) content at frequency 1 Hz-----       | 140 |
| Figure 5-14 | Variation of $\tan\delta$ of glass fiber reinforced polyester nanocomposite with temperature for different filler (Cloisite15A) content at frequency 10 Hz-----      | 141 |
| Figure 5-15 | Variation of $\tan\delta$ of glass fiber reinforced polyester nanocomposite with temperature for different filler (Cloisite15A) content at frequency 100 Hz -----    | 141 |
| Figure 5-16 | XRD pattern of GFRPNC (1% Cloisite15A)-----  | 149 |
| Figure 5-17 | Variation of % weight loss of glass fiber reinforced polyester nanocomposite with temperature for different filler (Cloisite15A) content -----                       | 151 |

|             |  |     |
|-------------|--|-----|
| Figure 5-18 | Variation of % derived weight of glass fiber reinforced polyester nanocomposite with temperature at different filler (Cloisite15A) content ----- | 151 |
| Figure 5-19 | DSC curves of glass fiber reinforced polyester nanocomposite at different filler (Cloisite15A) content -----                                     | 152 |
| Figure 5-20 | SEM images of fracture surfaces, (a) pure polyester, GFRP (b) 1% nanoclay filled GFRPNC (c) 2% nanoclay filled GFRPNC-----                       | 154 |
| Figure 5-21 | Fracture surface of 0% Cloisite15A filled sample under tensile load of CHS 5 mm/min -----  | 155 |
| Figure 5-22 | Fracture surface of 0% Cloisite15A filled sample under tensile load of CHS 50 mm/min -----   | 155 |
| Figure 5-23 | Fracture surface of 1% Cloisite15A filled sample under tensile load of CHS 5 mm/min -----  | 155 |
| Figure 5-24 | Fracture surface of 1% Cloisite15A filled sample under tensile load of CHS 50 mm/min -----   | 156 |
| Figure 5-25 | Fracture surface of 2% Cloisite15A filled sample under tensile load of CHS 5 mm/min -----  | 156 |
| Figure 5-26 | Fracture surface of 2% Cloisite15A filled sample under tensile load of CHS 50 mm/min -----   | 156 |
| Figure 5-27 | Fracture surface impact tested specimen with (a) 0% Cloisite15A, (b) 1% Cloisite15A-----   | 157 |
| Figure 6-1  | Variation of storage modulus with temperature for different frequencies at filler content 0% -----   | 182 |
| Figure 6-2  | Variation of storage modulus with temperature for different frequencies at filler content 1% -----   | 182 |
| Figure 6-3  | Variation of storage modulus with temperature for different frequencies at filler content 2% -----   | 183 |
| Figure 6-4  | Variation of loss modulus with temperature for different frequencies at filler content 0% -----  | 183 |
| Figure 6-5  | Variation of loss modulus with temperature for different frequencies at filler content 1% -----  | 184 |
| Figure 6-6  | Variation of loss modulus with temperature for different frequencies at filler content 2% -----  | 184 |
| Figure 6-7  | Variation of tandelta with temperature for different frequencies at filler content 0% -----  | 185 |
| Figure 6-8  | Variation of tan delta with temperature for different frequencies at filler content 1% -----   | 185 |
| Figure 6-9  | Variation of tandelta with temperature for different frequencies at filler content 2% -----  | 186 |

|             |  |     |
|-------------|--|-----|
| Figure 6-10 | Variation of storage modulus with temperature for different frequencies at filler content 0%                         | 186 |
| Figure 6-11 | Variation of storage modulus with temperature for different frequencies at filler content 1%                         | 187 |
| Figure 6-12 | Variation of storage modulus with temperature for different frequencies at filler content 2%                         | 187 |
| Figure 6-13 | Variation of loss modulus with temperature for different frequencies at filler content 0%                            | 189 |
| Figure 6-14 | Variation of loss modulus with temperature for different frequencies at filler content 1%                            | 190 |
| Figure 6-15 | Variation of loss modulus with temperature for different frequencies at filler content 2%                            | 190 |
| Figure 6-16 | Variation of tandelta with temperature for different frequencies at filler content 0%                                | 191 |
| Figure 6-17 | Variation of tandelta with temperature for different frequencies at filler content 1%                                | 191 |
| Figure 6-18 | Variation of tandelta with temperature for different frequencies at filler content 2%                                | 192 |
| Figure 6-19 | Variation of tensile creep strain with time for different filler (Cloisite15A) content at stress 1MPa for PNC        | 192 |
| Figure 6-20 | Variation of tensile creep compliance with time for different filler (Cloisite15A) content at stress 1MPa for PNC    | 193 |
| Figure 6-21 | Variation of tensile creep strain with time for different filler (Cloisite15A) content at stress 1MPa for GFRPNC     | 193 |
| Figure 6-22 | Variation of tensile creep compliance with time for different filler (Cloisite15A) content at stress 1MPa of GFRPNC  | 194 |
| Figure 6-23 | Variation of tensile creep strain with time for different filler (Cloisite15A) content at stress 2 MPa for GFRPNC    | 194 |
| Figure 6-24 | Variation of tensile creep compliance with time for different filler (Cloisite15A) content at stress 2MPa for GFRPNC | 195 |

## ABBREVIATIONS

|                 |   |  |
|-----------------|---|--|
| $\varepsilon$   | - | Strain   |
| $\sigma$        | - | Stress   |
| $\varepsilon_T$ | - | True Strain                                    |
| $\sigma_T$      | - | True Stress                                    |
| ABS             | - | Acrylo Nitrile Butadiene styrene               |
| ANOVA           | - | Analysis of Variance                           |
| ASTM            | - | American Society for Testing Materials         |
| CHS             | - | Cross Head Speed                               |
| CNF             | - | Carbon Nanofiber                               |
| CPNC            | - | Clay containing Polymer Nanocomposite          |
| DGEBA           | - | Diglycidal Ether of bisphenol A                |
| DMA             | - | Dynamic Mechanical Analysis                    |
| DSC             | - | Differential scanning calorimetry              |
| $E_F$           | - | Flexural Modulus                               |
| $E_T$           | - | Tensile Modulus                                |
| FRP             | - | Fiber Reinforced Polyester                     |
| $F_s$           | - | Flexural strength                              |
| $G'$            | - | Storage Modulus                                |
| $G''$           | - | Loss modulus                                   |
| GFRPNC          | - | Glass Fiber Reinforced Polyester Nanocomposite |
| MEKP            | - | Methyl ethyl Ketone Peroxide                   |
| MMT             | - | Montmorillonite                                |
| MWCNT           | - | Multi walled Carbon Nanotube                   |
| PLS             | - | Polymer Layered Silicates                      |
| PNC             | - | Polyester Nanocomposite                        |

|                |   |                                |
|----------------|---|--------------------------------|
| PP             | - | Polypropelene                  |
| SEM            | - | Scanning Electron Microscopy   |
| SFRP           | - | Short Fiber Reinforced Plastic |
| T <sub>g</sub> | - | Glass Transition Temperature   |
| TGA            | - | Thermo Gravimetric Analysis    |
| T <sub>s</sub> | - | Tensile Strength               |
| TSS            | - | Time Stress Superposition      |
| TTS            | - | Time Temperature Superposition |
| UTM            | - | Universal Testing Machine      |
| XRD            | - | X-Ray Diffraction              |

# **CHAPTER 1**

## **INTRODUCTION**

Selection of the right material is of paramount importance in any technology. The introduction of composite materials has led to customization of engineering properties of the material. The conventional engineering material, steel, has been substituted by the composite material in many areas in the last three decades. Composites can be defined as materials that consist of two or more chemically and physically different phases separated by a distinct interface. The different phases are combined judiciously to achieve a system with more useful structural or functional properties non-attainable by any of the constituent alone. Composites have emerged as an important class of engineering materials due to their advantages such as low weight, corrosion resistance, high fatigue strength, and faster assembly. They are extensively used as materials in making aircraft structures, electronic packaging to medical equipment, and space vehicle to home building.

Properties of composite materials are strongly influenced by the properties of their constituent materials, distribution and interaction among them. The reinforcement in the system may differ in concentration, distribution and orientation. All these factors may be important in describing the property of composite. Size and size distribution controls the texture of the material. Together with volume fraction, size and size distribution determines the interfacial area which determines the interaction of reinforcement and matrix.

Concentration is usually measured in terms of volume or weight fraction. The concentration distribution is a measure of homogeneity or uniformity of the system. Most materials are developed to improve the properties such as strength, stiffness, toughness and high temperature performance. The strengthening mechanism of composite depends on the geometry and the composition of the reinforcement [1].

There are different types of composite materials available. Composites have been developed using the three types of engineering materials such as metal, ceramic and polymer as matrices. The introduction of nano particles as fillers instead of micro particles in polymer matrix led to the arrival of nanocomposites. The Global consumption of nanocomposites is expected to grow annually by over 20% in the coming years [2].

Unlike other categories of nano particles, the nano layered clays gained wide acceptability as nanoclay. Adding organo clay to polymer matrix improved the hardness as well as mechanical properties. The observed improvement is related to the intercalation of clay platelets. However the presence of internal pores and improper intercalation reduced the hardness as well as mechanical property in some cases [3].

As a matter of fact the easiness of processing, application in different fields especially where extreme climatic conditions happened such as cryogenic condition as well as hot weather, high tech applications such as space purposes and under water applications, polymer matrix composites are in the wake of proving its capability. A lot of researches are going on in the field with different types of matrices, fillers, reinforcements etc. The high performing polymer like epoxies occupy major space in

the literature available on polymer nanocomposites. The high cost and processing difficulties are the hurdle to widen the application. The cost of polyester resin is only about one third of the cost of epoxy resin and if polyester resin can be modified to replace epoxy resin there may be significant cost advantage. General application of any engineering material will be proposed by the performance under tensile load, impact load, flexural load and dynamic mechanical properties, Creep behavior etc. The polymeric material for a prolonged application is a major difficulty. All the polymers, because of aging, get degraded and hence prolonged application is difficult. Hence the creep behavior of the material is very significant to study. A special emphasis is given to tensile creep analysis of the material.

Property enhancement through the addition of small quantity of nanoclay is also very significant to note. Adding more nanoclay will make the process of dispersion more complicate and difficult as well as increase the cost of production. Small quantity of nanoclay draws more attention because of cost effectiveness and processability. Many research papers on the property enhancement of polymer by addition of nanoclay are available. An outline of the studies that initiated present work is described below.

### **1.1 POLYMER MATRIX COMPOSITES (PMC)**

Polymer matrix composites are the most commercially exploited composite. The polymer matrices commonly used are polyester, vinyl ester, epoxy, phenolic, polyimide, polyamide, polypropylene, poly ether ether ketone (PEEK) etc. PMCs are very popular due to their low cost and simple fabrication methods. Use of nano reinforced polymers as structure materials is limited by low level of their mechanical

properties, namely strength, modulus, and impact resistance. Reinforcement of polymers by strong fibrous network permits fabrication of PMCs, which is characterized by a) High specific strength b) High specific stiffness c) High fracture resistance d) Good abrasion resistance e) Good impact resistance f) Good corrosion resistance g) Good fatigue resistance h) Low cost. The main disadvantages of PMCs are its low thermal resistance and high coefficient of thermal expansion.

A polymer composite is made by the combination of a polymer and synthetic or natural inorganic filler. Fillers are employed to improve the desired properties of the polymer or to simply reduce the cost. Polymer composites with improved mechanical, thermal, barriers and fire retardancy properties are widely used in very large quantities in a variety of applications. Conventional fillers such as talc, calcium carbonate, fibers, etc, often requires to use a large amount in the polymer matrix to have significant improvements in the composite properties which may result in some other undesired properties such as brittleness or loss of opacity. Polymer matrix composites (PMCs) are comprised of a variety of short or continuous fibers bound together by an organic polymer matrix. Unlike a ceramic matrix composite (CMC), in which the reinforcement is used primarily to improve the fracture toughness, the reinforcement in a PMC provides high strength and stiffness. The PMC is designed so that the mechanical load to which the structure is subjected to in service is supported by the reinforcement. The function of the matrix is to bond the fibers together and to transfer loads between them. Polymer matrix composites are often divided into two categories: reinforced plastics and advanced composites.

Chief among the advantages of PMCs is their light weight coupled with high stiffness and strength along the direction of the reinforcement. This combination is the basis of their usefulness in aircraft, automobiles, and other moving structures. Other desirable properties include superior corrosion and fatigue resistance compared to metals. However the current PMCs are limited to service temperature below 316 °C, because of the decomposition of matrix at high temperature.

The final properties of composites are influenced by the nature, properties of components and their dimensions. The micro structure of composite and the interfacial interaction between matrix and dispersed phase also have significant influence. The efficiency of property improvement depends strongly on the properties (mechanical) of the filler, the adhesion between matrix and filler and especially on the aspect ratio of the filler. The aspect ratio of the filler is very important and crucial for many properties in composite such as electrical, mechanical and thermal properties. Polymer composites with high aspect ratio of nano-fillers such as platelet clays, carbon nanotubes and nanofibers are very important due to their enhanced properties. Combination of filler nano scale dimension and high aspect ratio with its nano scale dispersion within polymer matrix leads to the significant improvements in the polymer properties at very low filler volume fractions [4].

## **1.2 PARTICULATE FILLED COMPOSITE**

A composite whose reinforcement may be classified as particles is called a particulate filled composite. The dimension of the reinforcement determines its capability of contributing its properties to the composite. The particles and matrix materials in a particulate composite can be any combination of metallic and non metallic materials.

Composites with particles of tungsten, molybdenum, or their carbides in silver and copper materials are widely used for electrical contact applications.

Inorganic fillers are used largely for improving properties of various plastics. Many commercially important elastomers are filled with carbon black or silica to improve strength and abrasion resistance.

The composite properties generally achieved by the traditional micrometer-scale fillers reached a limit because it involves many compromises. Stiffness is traded for toughness, or toughness is obtained at the cost of glass transition temperature. In addition, macroscopic defects due to the discrepancy in the filler fraction often result in the failure of materials. Clay-containing polymeric nanocomposite (CPNC) has several advantages over the polymer matrix composites. The main improvements are in modulus, impact strength, heat resistance, dimensional stability, barrier properties, flame retardancy, optical properties, ion conductivity, and thermal stability.

### **1.3 POLYMER NANOCOMPOSITES**

Nanocomposites constitute a new class of material having nano-scale dispersion, typically 1-100 nm, of the dispersed phase in a given matrix. The outstanding reinforcement of nanocomposites is primarily attributed to the large interfacial area per unit volume or weight of the dispersed phase. A nanocomposite is defined as a composite material in which at least one dimension of at least one component is in the nanometer size scale ( $< 100$  nm). The nanocomposites have actually been used for centuries by the nature. Using natural materials and polymers such as carbohydrates, lipids and proteins, nature makes strong nanocomposites such as bones, shells and wood [5].

Nanocomposites were first referenced as early as 1950, and polyamide nanocomposites were reported as early as 1976. However, it was not until Toyota researchers began a detailed examination of polymer/layered silicate clay mineral composites became more widely studied in both academic and industrial laboratories. The true start of the history of polymer nanocomposites was in 1990 when Toyota first used clay/nylon-6 nanocomposites for Toyota car in order to produce timing belt covers. After that the other automotive applications were implemented by many companies including Mitsubishi, General Motors etc [6].

Polymer nanocomposites have attracted great attention worldwide academically and industrially due to the exhibition of superior properties such as modulus, strength, toughness and barrier far from those of conventional micro composites and comparable with those of metals. However polymer nanocomposites have the added advantages of lower density and ease of processability. In polymer nanocomposites, the filler has at least one dimension in the nanometer scale and its nanoscale dispersion within the polymer matrix leads to the interfacial contacts between the polymer and inorganic filler which provides superior properties than those of polymer phase. When the dimensions of filler particles are decreased to the nano scale, their properties change significantly. This is well-known as “nano-effect”. Studies and modeling using continuum mechanics reveal that the enhanced properties of nanocomposites are strongly dependent on the particular features of the nano filler system, in particular, its content, aspect ratio and the ratio of filler mechanical properties to those of the matrix. The nanoscale is considered where the dimensions of filler particles (diameter), platelets (thickness) or fibers (diameter) are in the size range of 1-100 nm. Figure 1.1 shows different types of nano particles.

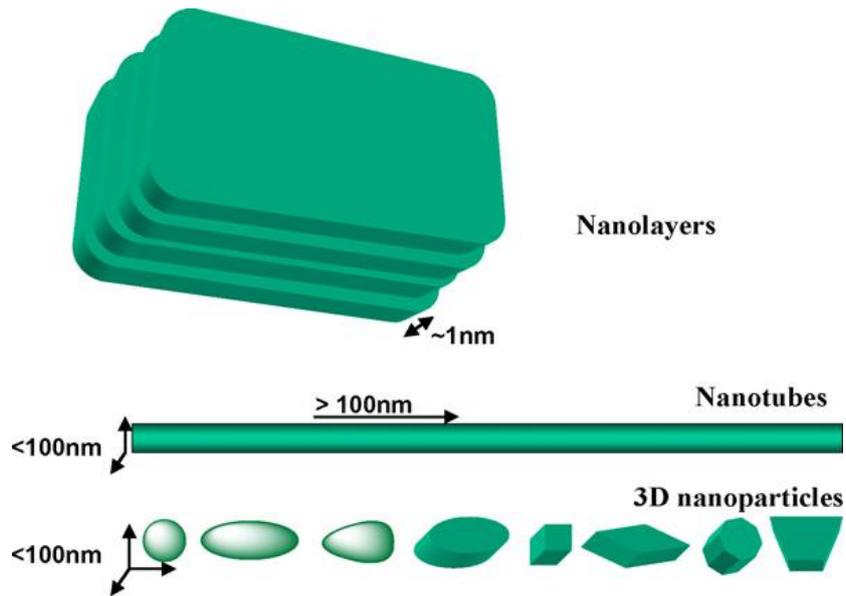


**Figure 1-1** Different types of nanofillers [7]

A broad spectrum of polymer properties can be improved by nanocomposite technology such as mechanical, thermal, barrier, durability, chemical stability, flame retardancy, scratch/wear resistance, biodegradability as well as optical, magnetic and electrical properties [8][9]. The final properties of nanocomposites are determined by the component properties, composition, and micro-structure and interfacial interactions. However it has been established that the properties of nanocomposites are strongly influenced by the dimensions and micro structure of the filler phase. In other words the filler nature has the main effect on the final morphology and properties of the polymer nanocomposite. Clays are one group of nano-fillers which have been widely used for the preparation of polymer nanocomposites. Now there has been a growing interest for the development of polymer/clay nanocomposites due to their dramatically improved properties compared to the conventional filled polymers in a very low fraction of filler addition. Polymer/clay nanocomposites have received intense attention and research interest driven by the unique properties which can

never be obtained by micro size fillers or especially by other nano fillers. The value added properties enhanced without sacrificing pure polymer processability, mechanical properties and light weight, make the clays more and more important in modern polymer industry. Clay minerals are belonging to the main group of silicates with layered structure known as layered silicates.

Polymer nanocomposites consist of a polymeric material (e.g., thermoplastics, thermosets, or elastomers) with reinforcement of nano-particles. Polymer could be incorporated either as the polymeric species itself or via the monomer, which is polymerized in situ to give the corresponding polymer-clay nanocomposite.

Most commonly used nano-particles include:

- Montmorillonite organoclays (MMT)
- Carbon nanofibers (CNFs)
- Polyhedral oligomeric silsesquioxane (POSS)
- Carbon nanotubes {multiwall (MWNTs), small-diameter (SDNTs), single-wall (SWNTs)}
- Nanosilica (N-silica)
- Nanoaluminum oxide ( $\text{Al}_2\text{O}_3$ )
- Nanotitanium oxide ( $\text{TiO}_2$ )

Commonly used polymer, acting as the matrix medium for polymeric nanocomposites include:

- Nylons
- Polyolefin, e.g. polypropylene
- Polystyrene
- Ethylene-vinyl acetate (EVA) copolymer
- Epoxy resin
- Polyester resins
- Polyurethanes
- Polyimides
- Poly ethylene terephthalate (PET)

There are two main challenges in developing nanocomposite materials after the desired polymer has been selected for the purpose. First, the choice of nano-particles requires an interfacial interaction and/or compatibility with the polymer matrix. Second, the processing technique should provide proper uniform dispersion and distribution of nano-particles or nano-particle aggregates within the polymer matrix. In addition, the amount of nano particles added to polymer matrix also plays a significant role in deciding the mechanical properties of the nanocomposites.

The nanoparticles are generally added in very small quantities to result in improved properties. This in turn will result in significant weight reductions particularly in military and aerospace applications, greater strength and increased barrier performance for similar material thickness, whereas, the micro-dimensional particles/additives require much higher loading levels to achieve similar performance.

## 1.4 STRUCTURE OF CLAY PARTICLES

The structure of clay particles is in layers; each layer is composed of two types of structural sheets: octahedral and tetrahedral. The tetrahedral sheet is composed of silicon-oxygen tetrahedra linked to neighboring tetrahedra by sharing three corners, resulting in a hexagonal network. The remaining fourth corner of each tetrahedron forms a part to adjacent octahedral sheet. The octahedral sheet is usually composed of aluminum or magnesium in six-fold coordination with oxygen from the tetrahedral sheet and with hydroxyl. The two sheets together form a layer, and several layers may be joined in a clay crystallite by interlayer cations, Vander Waals force, electrostatic force, or by hydrogen bonding. The elementary structural units are silica tetrahedron and aluminum octahedral. The variety of clay minerals can be described by the arrangement of tetrahedral and octahedral sheets, i.e., 1:1 clay mineral would have one tetrahedral and one octahedral sheet per clay layer; 2:1 clay mineral would contain two tetrahedral sheets and one octahedral sheet sandwiched between the two tetrahedral sheets (montmorillonite is an example of a clay mineral having 2:1 sheet-structure); and 2:1:1 clay minerals are composed of an octahedral sheet adjacent to a 2:1 layer.

One of the main advantages of nano particles is the large surface area to volume ratio which increases the number of particle–matrix interactions, thus increasing the effects on the overall material properties. Surface area of montmorillonite is 750-800 m<sup>2</sup>/g and have high-aspect Ratio: about 100 to 15000[11]. A well dispersed system generally yields more desirable composite properties. Particle agglomerates decrease material performance by the inclusion of voids that act as preferential sites for crack

initiation and failure. Particles, especially in the nano range tend to agglomerate, or cluster, due to the dominant intermolecular Van der Waals interactions between them.

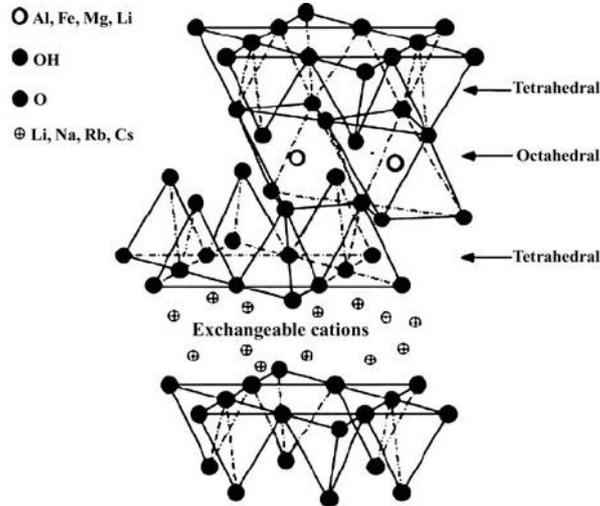


**Figure 1-2** Structure of 2:1 layered silicate [10]

## 1.5 POLYMER NANOCOMPOSITE STRUCTURES

Depending on the nature of the components used (layered silicate, organic cation and polymer matrix) and the method of preparation, three main types of composites may be obtained when layered clay is associated with a polymer as shown in figure 1-3 [15]. When the polymer is unable to intercalate between the silicate sheets, a phase separated composite as shown in figure 1-3(a) is obtained, whose properties stay in the same range as traditional micro composites. Beyond this classical family of composites, two types of nanocomposites can be recovered. Intercalated structure (Figure 1-3(b)) in which a single (and sometimes more than one) extended polymer chain is intercalated between the silicate layers results a well ordered multilayer morphology built up with alternating polymeric and inorganic layers. When the silicate layers are completely and uniformly dispersed in a continuous polymer

matrix, an exfoliated or delaminated structure is obtained (Figure 1-3(c)). While preparing polymer matrix nanocomposites, one of the biggest obstacles is the aggregation tendency of the nano particles. If aggregates remain in the system, the nano particles cannot reinforce the system; sometimes they even worsen the mechanical properties, as less reinforcing particles present and aggregates may act as defect centers; in case of failure, they act sometimes as crack initiators. There are several methods for the proper dispersion of nano particles but they are mostly complicated and require great attention. Materials with very advantageous properties can be prepared by the surface treatment of the nanoparticles and by the improvement of the production technologies [5].

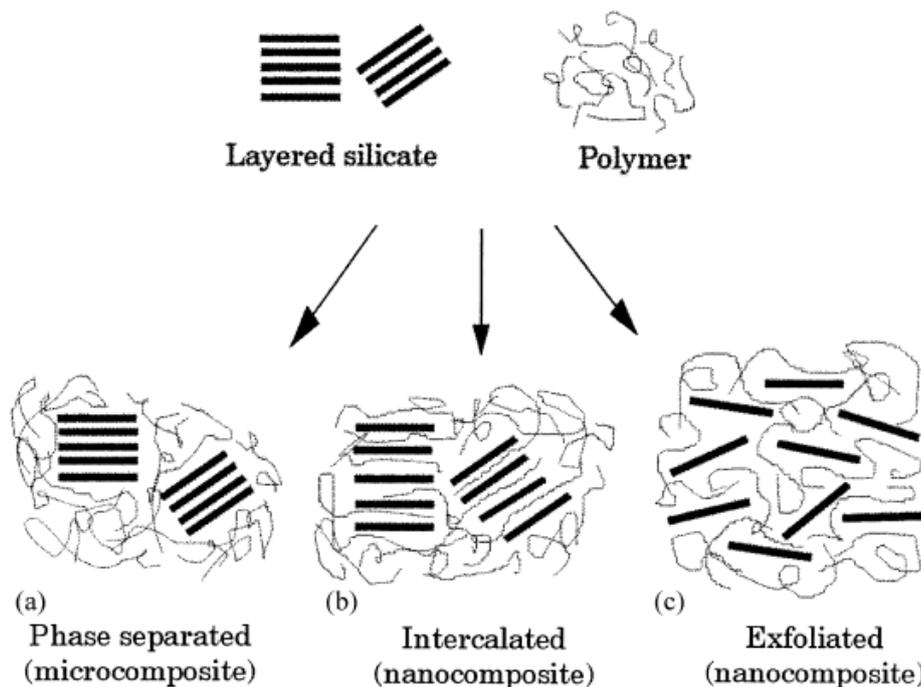


**Figure 1-3** Scheme of different types of composite arising from the interaction of layered silicates and polymers [15]

## 1.6 SYNTHESIS OF POLYMER-CLAY NANOCOMPOSITES

A number of polymer layered silicate (PLS) nanocomposite preparation methods have been reported by many researchers[10][13][15]. The three most common methods to synthesize PLS nanocomposites are intercalation of a suitable monomer and subsequent in situ polymerization, intercalation of polymer from solution, and polymer melt intercalation. In the in situ polymerization method (Figure 1-4), the monomer is used directly as a solubilizing agent for swelling the layered silicate. Subsequent polymerization takes place after combining the silicate layers and monomer, thus allowing formation of polymer chains between the intercalated sheets. The second method involves intercalation of polymer from solution (Figure 1-5). This method requires a suitable solvent that can both solubilize the polymer and swell the silicate layers. When the layered silicate is dispersed within a solution of the polymer, the polymer chains intercalate and displace the solvent within the gallery of the silicate. A PLS nanocomposite is obtained upon the removal of the solvent, either by solvent evaporation or polymer precipitation. The last method, melt intercalation (Figure 1-6), does not require the use of a compatible solvent or suitable monomer. In this method, a polymer and layered silicate mixture is heated under either a batch or continuous shear (in an extruder) above the softening point of the polymer. During the heating process, polymer chains diffuse from the molten polymer into the silicate galleries to form either intercalated or exfoliated depending on the degree of penetration. This method has become the mainstream for the fabrication of PLS nanocomposites in recent years because it is simple, economical, and environment friendly. However, melt mixing seems to be only partially successful since concentrations of exfoliated silicates greater than about 4 wt% have not been possible yet.

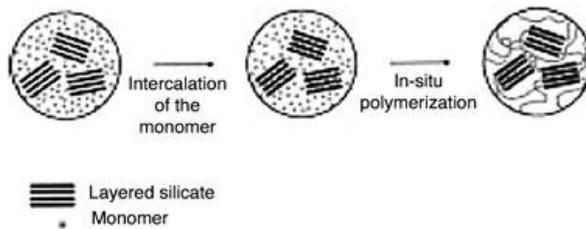


**Figure 1-4** Schematic representation of PLS nanocomposite obtained by insitu polymerization [10]

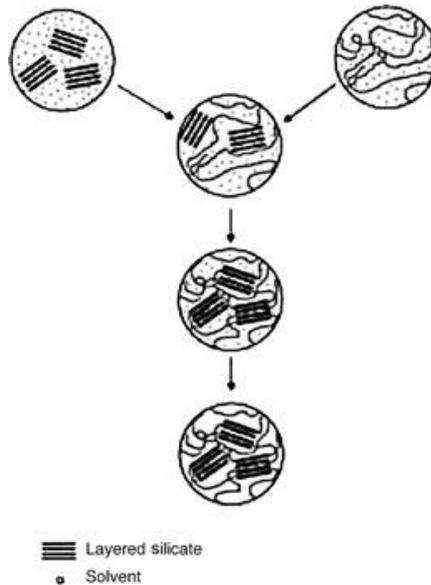


**Figure 1-5** Schematic representation of PLS nanocomposite obtained by intercalation of polymer from solution [10]

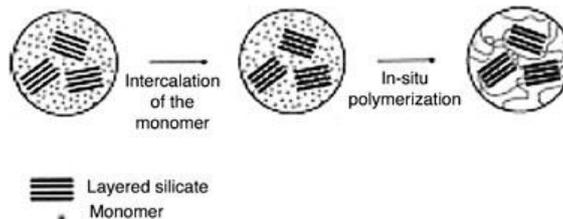


**Figure 1-6** Schematic representation of PLS nanocomposite obtained by direct melt intercalation [10]

## 1.7 PROPERTIES OF POLYMER-BASED NANOCOMPOSITES

Polymer-based nanoparticle nanocomposites were prepared via a range of processes and show their properties improved as compared to pristine polymer. To get better mechanical properties such as the tensile strength, modulus or stiffness, inorganic

material can be added. The mechanical properties of nanocomposites, prepared from various polymers and inorganic particles, did not always improve. In some cases, the properties of nanocomposites decrease by the addition of inorganic particles because of aggregation in polymer matrices. To resolve this difficulty, the load amounts of inorganic particles were optimized with organic material. For structural application at elevated temperatures, the dimensional constancy or low thermal expansion coefficient of these nanocomposites is very important[21.] The high thermal expansion coefficient of neat polymers causes dimensional changes during the molding procedure. Polymer composites have applications such as filled elastomers for damping, electrical insulators, thermal conductors, and high-performance composites for use in automobiles.

Materials with synergistic properties are chosen to create composites with customized properties; for example, high-modulus but brittle carbon fibers are added to low-modulus polymers to create a stiff, lightweight composite with some degree of toughness. Stiffness is traded for toughness, or toughness is obtained at the cost of optical clarity. In addition, macroscopic defects due to regions of high or low volume fraction of filler often lead to breakdown or failure. Recently research and development of nanofilled polymers has increased greatly, for several reasons. First, extraordinary combinations of properties have been observed in some polymer nanocomposites.

In fibrous or particle-reinforced polymer nanocomposites, dispersion of the nanoparticle and adhesion at the particle–matrix interface play crucial roles in determining the mechanical properties of the nanocomposite. Without proper dispersion, the nanomaterial will not offer improved mechanical properties over that of conventional composites, in fact, a poorly dispersed nanomaterial may degrade the

mechanical properties. Additionally, optimizing the interfacial bond between the particle and the matrix, one can tailor the properties of the overall composite, similar to what is done in macrocomposites. For example, good adhesion at the interface will improve properties such as interlaminar shear strength, delamination resistance, and fatigue and corrosion resistance [16][17].

## **1.8 PROPERTY ENHANCEMENT OF POLYMERS BY NANOFILLERS**

Many researchers have experimented with nano particles in polymeric resin for the modification of resin. Mashael et.al reported thermal degradation of nanocomposite prepared with montmorillonites (MMTs). They also analyzed the effect of sonication on preparing the intercalated nanocomposite [22]. Analysis on epoxy-polyester blend reinforced with MMT reported the increase of tensile strength and interlaminar shear strength by the incorporation of MMT. Slight variation in glass transition temperature also resulted from the addition of MMT [23].

The method of mixing clay in polyester resin, curing agents, and curing conditions influence the properties of nanocomposites. The clay-polyester nanocomposites produced using reactive organoclay had better dynamic modulus. The formation mechanism based on fabrication methods has been reported for unsaturated polyester layered silicate nanocomposites [24]. Nano silica fillers in polymer nanocomposite reduced the initial and final degradation temperature as per the research report. Intercalation of polymer chains in silicate layers act as barrier against temperature and show more stability than pristine polymer. The addition of Nano-silica increases thermal resistance of polymer nanocomposites. Improvement in physical properties is reported at higher loading of Nano fillers [25]. The evaluation of the structure-

properties relationship indicated significant potential for nanoclays to control the behavior of thermoplastic- modified epoxy systems [26]. The nano-particles in the epoxy resin decreased the fracture toughness of the composite although the fracture surface was much rougher than that of the epoxy. If the nano-particle reinforced matrix is used for a composite laminate, the interlaminar fracture toughness and the impact characteristic can be improved at the room temperature [27].

A marked improvement in tensile properties was found with increase in organo clay content in the composite. Research on the thermal stability and degradation kinetics of epoxy /MMT nanocomposites reported that epoxy nanocomposites are stable up to 221 °C and undergo one step thermal degradation in the temperature range 221-505°C. It is also observed that the thermal stability of the nanoclay loaded epoxy composites is slightly high as compared to neat epoxy. Introduction of the nanoclay (inorganic) phase into epoxy matrix increases the thermal stability, and affects the total heat of degradation, which suggests a change in the degradation reaction mechanism. The DMA and DSC analysis have shown that  $T_g$  decrease slightly with increasing MMT. SEM has shown that the 1 wt. % MMT particles were dispersed well within the polymeric matrix [28].

With inorganic particle and nanoparticle inclusions, nucleation of crystallization can occur. At the nanodimension scale, the nanoparticle can substitute the absence of primary nuclei; thus competing with the confined crystallization. At higher nanoparticle content, the increased viscosity (decreased chain diffusion rate) can lead to decreased crystallization kinetics. At higher levels of nanoparticle addition, retardation of the crystallization rate has been observed even in those systems where

nucleation was observed at low levels of nanoparticle incorporation. Also nucleation was observed with unmodified clay, whereas the exfoliated clay yielded a reduced crystallization rate [29]. A review of the crystallization behavior of layered silicate clay nanocomposites noted that while nucleation is observed in many systems the overall crystallization rate is generally reduced particularly at higher levels of nanoclay addition [30][31].

Researchers have reported about weak stiffness improvements in the case of epoxy-based nanocomposites when true exfoliated structures were observed. They described a stiffening effect when the montmorillonite is modified by a functionalized organic cation (carboxylic acid or hydroxyl groups) that can interact with the matrix during curing. In thermoplastic-based (intercalated or exfoliated) nanocomposites, the stress at break, which expresses the ultimate strength that the material can bear before break, may vary strongly depending on the nature of the interactions between the matrix and the filler. Exfoliated layers are the main factor responsible for the stiffness improvement, while intercalated particles, having a less important aspect ratio, rather play a minor role [32]. Research report on thermal and mechanical property enhancement of nylon based nanocomposite revealed that clay-based nanocomposites showed better flammability, while the CNF-based nanocomposites showed better mechanical property [5].

## **1.9 NANOCCLAY MODIFIED FIBER REINFORCED POLYMER**

Fiber-reinforced polymer composites now widely used for many engineering applications including structural elements [33]. The addition of fibers to the polymer matrix increases the overall mechanical strength of the composite material as

compared to the neat polymer. The fibers have many advantages such as low density, high specific strength and modulus, relative non abrasiveness, ease of fiber surface modification, and wide availability. Composites of natural fibers and thermoplastics have found applications in many industries, particularly automotive industry. Investigations of Kornmann et. al. [34] reported increase in flexural strength of glass fiber-reinforced polymer composite laminates using nanoclay/epoxy matrix system.

Yuan Xu et. al. [35] investigated the, effect of nanoclay content on flexural strength and fracture toughness of carbon fiber reinforced epoxy/clay nanocomposites. According to them adding some clay can enhance the properties but adding more clay may not guarantee more improvement. This is due to the increase in viscosity of the epoxy on the addition of clay and the augmentation of the amount of air bubbles during the mixing process. Investigation on the effect of adding natural fillers on epoxy and polyester reinforced with glass fiber reported the effect of tensile strength, compressive strength, impact strength, hardness, water absorption etc [82].

Tensile and bending tests performed on nanocomposites showed that with the addition of nanoclay up to 3 wt%, the tensile strength increased and then decreased at a loading of 5 wt%. However the flexural strength increased with addition of nanoclay up to 5 wt%. The hardness of the nanocomposites also increased with increasing nanoclay content. Durability studies conducted on nanocomposites in water and alkaline medium for a period of one month showed degradation in mechanical properties of all specimens [36]. The effectiveness of reinforcement depends on the adhesion between matrix and fiber, so this is a key factor in determining the final properties of the composite material, particularly its mechanical properties [38][39][40].

Conventional static tests such as tensile, bending and impact tests are usually performed to characterize the mechanical properties of composites, because fiber-reinforced thermoplastic composite materials can undergo various types of dynamic stressing during service. Studies on the dynamic mechanical properties of these materials are of great importance. Similar to other properties, dynamic mechanical properties depend on types of fiber, fiber length and orientation, fiber loading, fiber dispersion, and fiber-matrix adhesion [41]. Studies by Amash and Zugenmaier [42] reported an increase in the stiffness and a decrease in the damping with increasing glass fiber content in polypropylene (PP) composites. All composites had storage and loss modulus values higher than those of pure polypropylene, whereas their mechanical loss factor (damping) was lower. Considerable improvement in the storage modulus values is seen when fibers are added whereas their mechanical loss factor (damping) was lower. Glass transition temperature was slightly shifted to lower temperatures in the case of composites as compared with the pure polymer [43].

Studies on epoxy based composite revealed that stress concentration on the individual fibers minimized with the dispersed nanoparticles in the contact region, which consequently protected the polymer matrix in the interfacial regions from the thermal–mechanical failure. This finally led to the gradual removal process of short fibers and the high wear resistance of the composites [11].

Nanoparticles tend to reduce the wear rate of composite by a reduction in the friction. Research reports revealed that the addition of nano-CuO could generally enhance the wear resistance of short fiber-reinforced polyphenylene sulfide [44]. The beneficial effect of nanoparticles was attributed to the development of a thin and uniform transfer film. Addition of nano-  $\text{TiO}_2$  could significantly reduce the friction

coefficient and the wear rate of epoxy composites filled with traditional fillers. Again, the additional nanoparticles proved to be useful in enhancing the wear resistance and reducing the friction of the SFRPs [21].

A significant improvement in tribological performance of short fiber reinforced polymer obtained from nanoparticles was due to their friction reducing abilities. This is because the adhesion between the contact surfaces was reduced with the presence of nanoparticles. Stress concentration on the individual fibers was minimized with the dispersed nanoparticles in the contact region, which consequently protected the polymer matrix in the interfacial regions from the thermal–mechanical failure. This finally led to the gradual removal process of short fibers and the high wear resistance of the composites. Javad et. al. [45] investigated the effects of nanoclay particles on impact and flexural properties of glass fiber-reinforced unsaturated polyester (UP) composites. The performance such as high velocity impact, low velocity impact, hardness and flexural properties were studied. Highest performance in ballistic limit and energy absorption were obtained for specimens containing 1.5 wt % nanoclay. According to Sudirman et. al. [46] silica concentration of 1.0 wt% is the highest concentration that be able to achieve good dispersion in unsaturated polyester resin matrix. Good dispersion of silica strongly creates mechanical properties of composite to be higher. It needs to specify the geometry such as may be described by shape, size and size distribution. The reinforcement in the system may differ in concentration, concentration distribution and orientation. All these factors may be important in describing the property of composite. Together with volume fraction size, size distribution determines the interfacial area which in turn determines the interaction of reinforcement and matrix [47].

Nano scaled silicon dioxide is suggested as a good reinforcing component for GFRP because addition of it shows essential increase in stiffness and damage free range [48]. Addition of nano particle to GFRP laminate increases the mechanical property such as tensile strength and tensile modulus without considerable weight increment.

### **1.10 CREEP BEHAVIOR OF NANOCOMPOSITE**

Time dependent behavior of polymeric composites is having very significant importance in their analysis for engineering applications. Challa and Progelhof [49] investigated the effect of temperature on the creep characteristics of polycarbonate and developed a relationship based on Arrhenius theory to develop creep master curves. Krishnaswamy [50] conducted creep rupture testing on high density polyethylene pipes at various hoop stress levels and temperatures and reported the dependency of density and crystallinity towards failure. Greco et. al. [51] investigated the flexural creep behavior of compression molded glass fiber reinforced polypropylene at various applied stress level. He reported the effect of matrix crystallinity for the improvement in creep properties of glass fiber reinforced polypropylene. Acha et. al. [52] investigated the Relation between interfacial properties and creep deformation. Higher creep resistance was observed for composites with good interfacial bonding which was confirmed by the observation of the composite fractured surfaces. Findley and Khosla [53] conducted creep tests for unreinforced thermoplastics; polyethylene, polyvinyl chloride and polystyrene. Approximation was carried out for the linear viscoelastic region by power law and compared the creep performance by estimating the power law coefficient and power law exponent. Power law model modified by Hadid et. al. [54] used stress–time superposition principle to predict long-term material creep behavior of

injection molded fiber glass reinforced polyamide. Master curves were developed and a perfect superposition of the curves at various stress levels was visualized. Novak [55] used strain energy equivalence theory and developed a creep predictive model to predict the creep behavior of talc filled polypropylene. Banik et. al. [56] reported the improvement in creep resistance due to unidirectional reinforcement for polypropylene composites. Liu et al. [56] used multi-Kelvin element theory and power law functions to predict creep compliance in polyethylene material and compared with the tensile creep experiments. Subramanyan et.al.[58] investigated the influence of reinforced fiber length on the creep performance of thermoplastic composite at various stress levels at room temperature condition. Discontinuous fiber reinforced polypropylene composites were injection molded and their short term flexural creep performance was investigated.

According to studies conducted by Nunenz et. al.[59] on kenaf fiber reinforced composite, it was observed that the creep strain and creep compliance decreased as the fiber content increased. This behavior was expected from the increased rigidity of the composites. Better creep resistance with increase of kenaf loading was also reported by Yanjun [60]. There are three roles of the additives on creep resistance of the composites which can be proposed to explain the experimental observations. The first is the volume effect, where the additives reduced the relative volume of viscoelastic polymer matrix, which was prone to creep. The second is the bridging effect, where the additives sustained part of the stress by connecting to each other. The third is the blocking effect, where the additives interacted with the molecular chains of polymer matrix and blocked them from moving under stress.

Feiyi and Chun developed a creep model for stitched and unstitched woven carbon fiber polymer composite. According to them the stitched woven fiber composite will take more time to creep than the un stitched and found that the shear and the normal stresses have been significantly reduced as a result of stitching. According to them, the enhanced creep resistance of stitched composites can be directly attributed to the reductions in the shear and normal stresses. This highlights that the main mechanism for the significant improvement in creep performance, by stitching, is the significant reduction in the interlaminar stresses [61]. It has been observed that through-thickness stitching the creep resistance of composites can be improved, provided the stitches are aligned in the direction of loading. At a given time, the stress level required to induce the same amount creep strain in stitched composites was about twice that for unstitched composites [62].

Investigation of the creep and dynamic mechanical behavior of natural fiber/epoxy composites using functionalized multi walled carbon nano tube (MWCNT) modified matrix showed that the creep resistance of natural fiber reinforced composites was greatly improved by the addition of MWCNTs [63]. The comparison of the time-displacement data under constant indentation creep load indicates that the addition of MWCNTs results in a noticeable decrease in creep rate, particularly under the conditions of elevated temperature and high nano indentation creep load. This behavior might indicate a failure of the epoxy–MWCNTs interface at high load levels. However, increasing the temperature to a near glass transition did not impact the ability of the MWCNTs to reduce the creep response of the nanocomposites compared to neat epoxy samples [64].

Due to the viscoelastic nature of polymeric materials, the analysis of their long term behavior is essential. For a viscoelastic polymer, the modulus is known to be a function of time at a constant temperature. The modulus is also a function of temperature at a constant time. According to this time-temperature correspondence, long term behavior of a polymer may be measured by two different means. First, experiments for extended periods of time can be carried out at a given temperature, and the response measured directly. This technique becomes increasingly time consuming due to the long response times of many polymers. The second method takes advantage of the principles of time temperature correspondence, wherein experiments are performed over a short time frame at a given temperature, and then repeated over the same time frame at another temperature. The two methods are equivalent according to the principles of time temperature super positioning. The structural applications of polymer matrix composites (PMC) demand lifetimes of 15, 25 and 50 years. However the mechanical properties of these composites have a time dependent nature, i.e. strength and stiffness are time-dependent due to the viscoelasticity of polymers.

Creep behavior of fiber epoxy composite studied by Lubna Ghalib [65] reported that, the effect of time on the strain of the epoxy increases with increase in time at constant temperature. On considering the strain induced in service it is required to take into account not only the stress, but also the time for which it is applied. The strain decreases with increase in the volume percent of the fiber as the composite materials is stiffer and stronger than the polymer matrix and the stiffness increases with increase in the percent of the fiber. It has been shown in the literature that the

polymers filled with exfoliated layered silicate platelets can give an increased creep resistance than unfilled polymers. The effect of moisture on creep behavior of polymer containing nanoparticles is still unclear. Due to moisture absorption, glass transition temperature  $T_g$  can be reduced below the operating temperature and this increases the creep compliance [66]. Studies on the creep behavior of epoxy/clay nano composite described the correlation between the three creep parameters – viscoelastic plus plastic deformation, viscoelastic relaxation and residual (plastic) on creep behavior. All the deformations increase with the increase of filler content to an extent. Therefore, it was confirmed that inclusion of clay nanoparticles to epoxy resin restricts the mobility of polymer chains in dry atmosphere and improves creep resistibility of the polymer, but absorbed moisture drastically plasticized the polymer and changed the creep behavior leading to the increase of creep compliance with the increase of filler content. Particularly, high deformations were observed for the highest filler content in atmosphere with highest humidity which can be explained by additional sliding of silicate nanoparticles within the layered stacks [67].

The present study proposes the modification of polyester resin and reinforced polyester on the tensile creep behavior by the addition of nanoparticles.

### **1.11 BACKGROUND OF PRESENT WORK**

Polymer matrices widely used for research are epoxy, polypropylene, rubber etc. Studies available on polyester/ isophthalic polyester as matrix medium are a meager. The incorporation of a low volume fraction of nano particles can lead to a significant improvement in polymer properties such as tensile strength, elastic modulus, wear

and scratch resistance, electrical and thermal conductivity, thermal and flammability resistance and impact strength. In addition, many polymer nanocomposites can be fabricated and processed using methods similar to those used for standard polymers, which is important from an economic manufacturing point of view. In many cases a significant reduction in cost can be obtained by enhancing the properties of a cheap polymer using inexpensive nanofillers to match the properties of a more expensive polymer. Researchers have focused on the synthesis of new nanocomposites, starting from careful materials selection and process control by either the direct use of an existing technique or by modified and adapted techniques. However, achieving uniform dispersion of the nanoparticles is an important scientific and technological challenge in nanocomposite fabrication. The filler-filler and filler-matrix interactions are important factors affecting the material properties. These factors are highly dependent on the processing method, the polymer matrix and the nanofiller type and content. Various studies have been carried out to investigate the effect of nanoparticle structure, dispersion, interfacial strength, strain rate and processing method on the mechanical performance [12]. In the present work, the effects of nanofiller type and nanofiller content on the mechanical properties, thermal behavior and creep of polyester based nanocomposites have been investigated.

## **1.12 SCOPE AND OBJECTIVES**

Development of new materials necessitates the enhancement of technology innovation. The development of new materials ratifies the application based on different requirements among which cost and processibility are playing important role. The

reinforcement of polymers using fillers is common. Polymer nanocomposites represent a radical alternative to traditional filled polymer compositions. Polymer nanocomposites are obtained by discrete constituents on the order of a few nanometers. Uniform dispersion of these nano sized fillers produces a very large increase of the interfacial area between the nanoparticles and the polymer. The immense internal interfacial area and the nanoscopic dimensions between nanoparticles is relevant [13]. This allowed obtaining multifunctional, high-performance properties much improved with respect to those of traditionally filled polymeric materials. In the past decade polymer/clay nanocomposites have emerged as a new class of materials and attracted considerable interest in research and development worldwide further to reports from the Toyota group on Nylon 6 / clay nanocomposites [14]. There is a large potential associated with the preparation and analysis of nanocomposites filled with a wide spectrum of nanoparticles, which are available commercially, and many others, which can be prepared easily in the laboratory. However, there are limitations in the use of these organoclay-based nanocomposites, especially because of the difficulties in dispersing the filler homogeneously in the matrix and therefore inefficiently increasing the interfacial area.

The analysis of the mechanical properties and thermal properties are very important in the application of these materials in engineering. Performance of the material under different loading conditions and different temperature is of vital importance. Many a material in engineering applications subjected to different temperature conditions and a long period of application in versatile field of requirement signifies the necessity of creep analysis. The limitation in knowing the real performance under real conditions

proposed the estimation of long term performance using theoretical concepts. The structure and morphology of the dispersed nanoparticles, polymer phase and the interface of the nanocomposites, which play the relevant role in understanding the properties of these materials already established by various researchers. The performance of the polyester resin, one of the cheapest resins available, is proposed to be, modified using different nanoclay as well as different quantities of nanoclay especially, Cloisite15A and the reinforcing of these by cheaply available glass fiber mat enunciate the importance of the thesis. The mechanical and thermal characterization of the material will be helpful to identify the applicability.

These can be studied by using various methods of testing such as Tensile test, Impact test, Flexural test, Dynamic mechanical analysis, Thermogravimetric analysis, creep test, Scanning Electron microscopy etc. SEM micrographs will be helpful to analyze the fracture surface and hence an insight in to the mode of failure of the nanocomposite. TGA allows studying the thermal degradation of prepared compositions.

Also the methodology which is adopted for the preparation of nanocomposite is of great importance. This study is focused mainly on the modification and enhancement of the properties of isophthalic polyester as well as glass fiber reinforced polyester using nanoclays in a small quantity and to find the optimum quantity which gives the best balance of proportion.

A fundamental part of this work deals with the characterization of all prepared composites in order to study the effect of the used nano fillers on their polymer matrix.

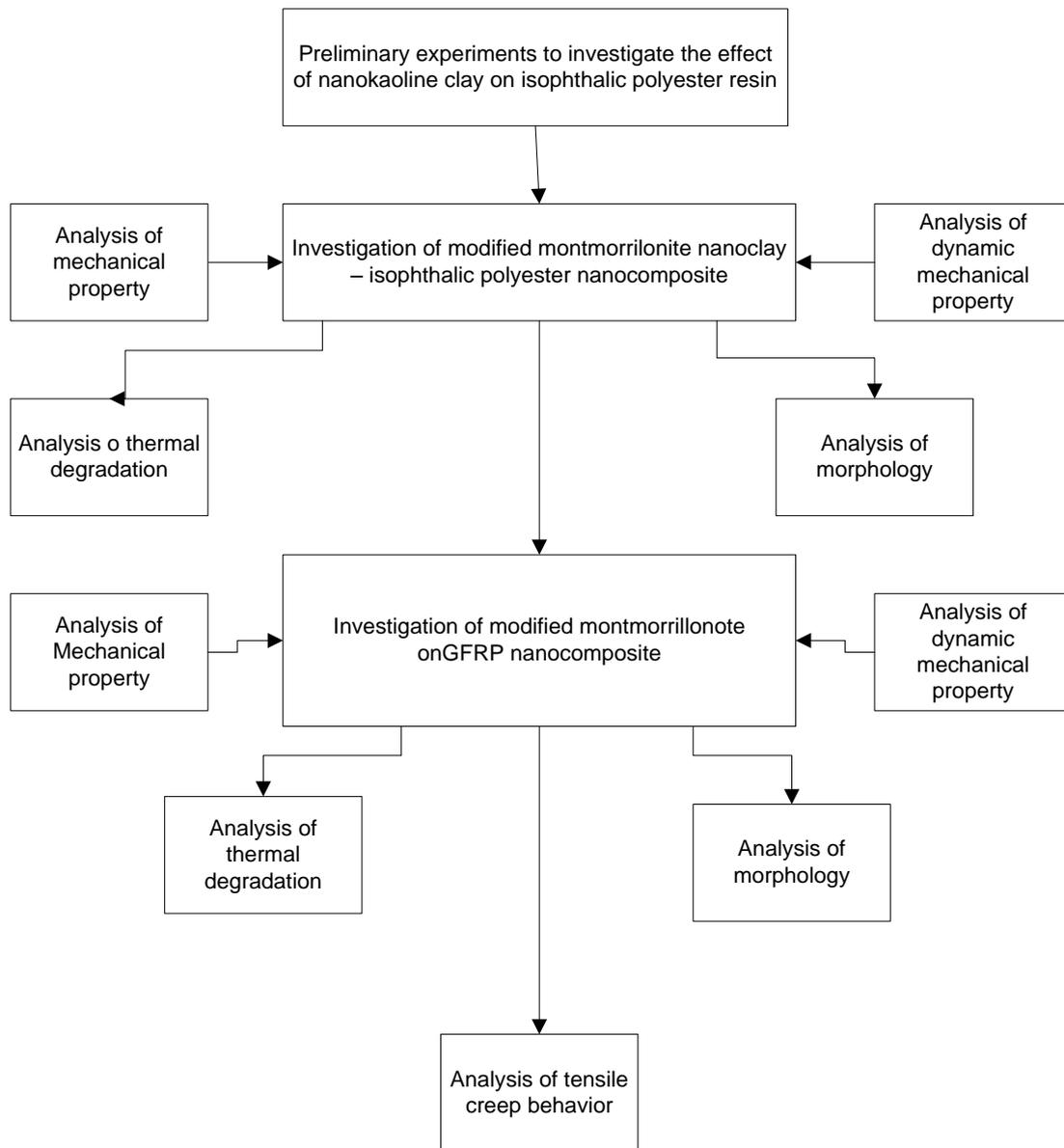


**Figure 1-7** Schematic representation of Methodology adopted for the study

The main objectives of this study are

- Investigate the effect of various nanokaoline clays on polyester for improving its mechanical property for use in high modulus/ high temperature applications.

- Upgrade polyester resin by modified montmorillonite nanoclay and to optimize the quantity of nanoclay for properties such as tensile strength, flexural strength, impact strength and thermal stability
- Investigate the effect of modified nanoclay in glass fiber reinforced polyester (GFRP) and analyze mechanical, thermal, morphological properties of nanomodified GFRP.
- Study the performance of polymer nanocomposite and glass fiber reinforced polymer nanocomposite for a prolonged application under various loads.

Polymer nanocomposite because of its easiness to process, light weight, corrosion resistance, will play a pivoted rule in the field of engineering materials in to the days to come. The requirement of nanofiller in small quantity and significant enhancement of property in many areas such as mechanical, thermal, dynamic mechanical underlines the importance of nanofiller.

Nano particles added in small quantity to polymer when processed to ensure intercalation will modify the polymer to derive the required property improvement.

### **1.13 RESEARCH METHODOLOGY**

The experimental work in the study can be broadly classified in to the following.

- Material processing and preparation
- Mechanical Characterization of nanokaoline clay filled polyester
- Mechanical and thermal Characterization of Cloisite15A filled polyester
- Mechanical and Thermal Characterization of Cloisite15A filled Glass FRP
- Analysis of Tensile Creep behavior

## **CHAPTER 2**

### **EXPERIMENTAL**

#### **2.1 INTRODUCTION**

The materials, equipments and methodologies used in the preparation and characterization of polymer nanocomposites (PNCs) as well as glass fiber reinforced polymer nanocomposites (GFRPNCs) are described in this chapter. Method of casting is used for the preparation of PNCs and hand layup technique is used for the preparation of GFRPNCs. The techniques used for characterization were tensile testing and flexural testing by universal testing machine (UTM), impact testing by Izod impact tester, Dynamic Mechanical Testing by Dynamic mechanical Analyzer (DMA), thermal analysis by Thermogravimetric Analyzer (TGA) and Differential scanning calorimeter. Scanning electron microscopy (SEM) and X-Ray diffraction (XRD) were used to study the nature of fracture surfaces and morphology. Also the tensile creep behavior of the material analyzed by DMA.

#### **2.2 MATERIALS**

The different raw materials used for the preparation of nanocomposites and reinforced nanocomposites with specification/ properties are given below.

##### **2.2.1 Polyester Resin**

Iso type Resins are based on Isophthalic acid. These are generally considered a higher class of resin and a little more costly as compared to general purpose resin. They are not quite as user friendly but have improved engineering parameters such as tensile

strength, flexural strength, impact resistance, and fatigue resistance. Additionally, they will also have much improved water and chemical resistance. The reagents used for the curing action were, methyl Ethyl Ketone Peroxide (MEKP) and Cobalt naphthenate. Styrene monomer used to improve the dispersion of clays in the polymer. The materials were supplied by M/s Sharon Enterprises, Kochi, Kerala.

### 2.2.2 Nanoclay

Nanoclay known as nanokaolinate clay with trade name- Nanocaliber was used for the preliminary investigation. Both modified and unmodified nanokaoline clays were used, which was supplied by English Indian Clays limited, Veli, Thiruvananthapuram

**Table 2-1** Properties of isophthalic polyester

| Sl. No. | Property                    | Units of measure | Nominal |
|---------|-----------------------------|------------------|---------|
| 1       | Tensile strength            | MPa              | 80      |
| 2       | Tensile modulus             | MPa              | 3000    |
| 3       | Flexural strength           | MPa              | 127     |
| 4       | Flexural modulus            | MPa              | 4000    |
| 5       | Heat distortion temperature | oC @ 264 psi     | 107     |
| 6       | Barcol Hardness             | -                | 43      |

Unmodified nanoclay (Nanocaliber-N100) and four different types of surface modified nanoclay such as amino modified (Nanocaliber-N100A), Vinyl modified (Nanocaliber N100V), Dialkyl modified (Nanocaliber -N100Z), and mercapto modified (Nanocaliber-N100M) were used in this study. The surface modification used to obtain better affinity and adhesion towards polymer matrix. The properties of nanokaoline clay are described in given Table 2-2.

**Table 2-2** Properties of nanokaoline clay

| Sl. No. | Property                   | Approximate value          |
|---------|----------------------------|----------------------------|
| 1       | Appearance                 | White/ off white powder    |
| 2       | Average particle size      | 100.5 nm                   |
| 3       | Plate thickness            | < 80 nm                    |
| 4       | pH(100% suspension)        | 6.5 – 7.5                  |
| 5       | Bulk density               | 0.2 to 0.3 g/cc            |
| 6       | Specific surface area(BET) | 28 – 30 m <sup>2</sup> /kg |
| 7       | Oil absorption(g/100g)     | 48 – 50 g/100g             |
| 8       | Moisture                   | <1 w/w %                   |

**Table 2-3** Properties of Cloisite15A

| Sl. No. | Property                | Description       |
|---------|-------------------------|-------------------|
| 1       | Organic modifier        | 2M2HT             |
| 2       | Modifier concentration  | 125 meq/100g clay |
| 3       | Moisture                | < 2%              |
| 4       | Weight loss on ignition | 43%               |
| 5       | Density                 | 1.66 g/cc         |
| 6       | d <sub>001</sub>        | 31.5 Å            |

Further to the first part of investigation with different types of nanokaolinate clays as filler in isophthalic polyester resin, detailed analysis have been carried out with modified Montmorillonite nanoclay, Cloisite15A. Cloisite15A is dimethyl de hydrogenated tallow (2M2HT) quaternary ammonium modified Montmorillonite nanoclay. It is a 2:1 layered silicate belongs to smectite group.

The material was supplied by M/s Southern Clay Products Inc. USA. The properties of the same detailed in Table 2-3. SEM micrograph of Cloisite15A is shown in figure 2-1.

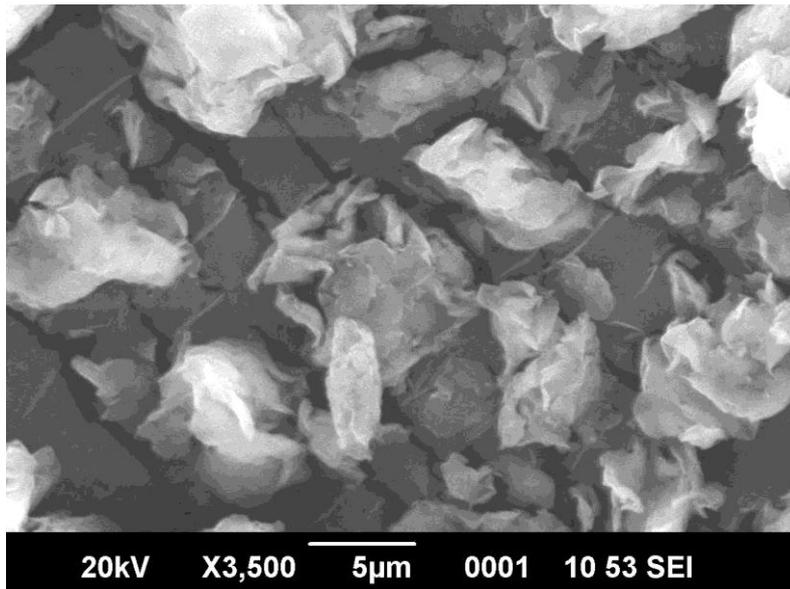


**Figure 2-1** SEM image of modified nanoclay, Cloisite15A

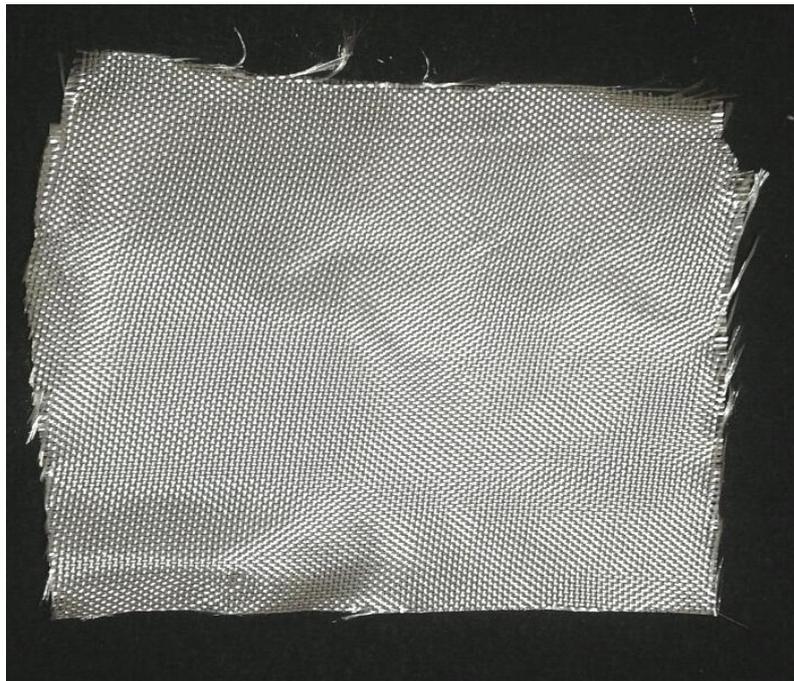


**Figure 2-2** Image of glass fiber mat

### **2.2.3 Glass fiber fabric**

Mil cloth made of E glass fiber has been used as reinforcement. The specification of the same was 200 gsm. It is known as 7Mill cloth commercially. The prime characteristics were dimensional stability, moisture resistance, strength and fire resistance. Samples for the preparation of GFRPNCs were cut out from the cloth in the size 300 mm X 200 mm by means of a scissors. The photograph of the sample used is shown in figure 2-2. The material was supplied by M/s Sharon Enterprises, Kochi, Kerala.

## **2.3 MATERIAL PREPARATION**

Method of casting used for the preparation of specimen of Polyester Nanocomposites (PNCs). A mould prepared from a Teflon sheet having the mold cavities in the shape and size of specimen proposed by ASTM standard for respective cases of testing such as tensile, flexural and impact was used. Hand layup technique was used for the preparation of glass fiber reinforced polyester nanocomposites (GFRPNCs). A ceramic tile with glossy surface is used to support the laying process. A 2” fiber brush specially prepared for FRP laying was used for the preparation. The detailed procedure is given below.

### **2.3.1 Specimen Preparation**

Test specimens for mechanical testing as per ASTM standards were prepared by casting in a mould made of Teflon for polymer nanocomposite. Initially the clay was kept in a microwave oven for 24 hours at a temperature of 80 °C to remove the moisture. For the preparation of polyester/clay nanocomposite, the polyester resin was mixed manually with desired amount of clay by a glass rod and the mixture was stirred well by using mechanical stirrer at a speed of 750 rpm. Then the mix was sonicated in an ultrasonicator for 30 minutes. This was to enhance the dispersion of

nanoclay in the matrix. The ultrasonicator used was probe type with a probe diameter 13 mm, make: Vibra-Cell VCX 750 ultrasonic processor supplied by M/s SONICS & MATERIALS, INC, USA. The photograph of the same is shown in figure 2-3.

During the ultrasonication process the mix was kept in an ice bath to prevent the overheating of the material. The amplitude is set for 50% and sonication cycle was set with vibration time 7 seconds and dwell time 3 seconds. Further to the sonication process, the mixture degassed and cooled in a water bath. Then weighed quantity of reagents such as cobalt naphthenate and methyl ethyl ketone peroxide were added one by one and mixed thoroughly with a glass rod. Then the polyester/nanoclay blend poured in to a Teflon mould prepared for the specimen for tensile test and impact test as per the ASTM standards. Then it kept undisturbed for 24 hrs for proper curing. Specimen prepared by varying the nanoclay content for different percentage by weight of the polyester resin. Similar procedure had been adopted by Mirmohseni et.al. [78]



**Figure 2-3** Ultrasonicator

For the preparation of test specimen for glass fiber reinforced polyester nanocomposite (GFRPNC), the nanoclay was treated and polyester/nanoclay blend prepared following the procedure described above. Further, a hand layup technique was used for the preparation of laminates. A ceramic tile of smooth surface placed over the table is applied with wax as mold releasing agent to facilitate the easy removal of the sample. Then a coat of the mix of polyester and nanoclay prepared is applied over the surface of tile using a brush and a roller is used to provide uniform thickness for the coating applied. Then the first layer of glass fiber mat is placed over the coat of mix. Further the mix was applied again in thin layer by using the brush. The process completed by laying five layers of glass fiber mat. The closed mould was kept under a pressure of  $500 \text{ N/m}^2$  (approximately) for 24 hrs at room temperature. To ensure complete curing the blended nano composite samples were post cured at  $70^\circ\text{C}$  for 1 hr. and the test specimens of required size and shape were cut out of the sample sheet. The specimen have been prepared through same procedure for varying the weight of clay i.e. without clay (pure polyester- 0 % clay), 0.5 % clay, 1 % clay, 1.5 % clay and 2 % clay. A similar procedure has been adopted by Chakradar et.al. [23] To obtain test specimens from the laminates prepared, water jet machining technique was used. The test specimen for tensile test, impact test, flexural test and dynamic mechanical analysis were prepared accordingly.

## **2.4 CHARACTERIZATION TECHNIQUES**

The mechanical, dynamic mechanical, thermal and morphological properties of nanocomposites were determined by standard techniques which are detailed below.

### **2.4.1 Tensile Tests (ASTM D 638, ISO 527-1)**

Tensile elongation and tensile modulus measurements are among the most important indications of strength in a material and are the most widely specified properties of plastic materials.

Tensile test, in a broad sense, is a measurement of the ability of a material to withstand forces that tend to pull it apart and to determine to what extent the material stretches before breaking. Tensile modulus, an indication of the relative stiffness of a material, can be determined from a stress–strain diagram. Different types of plastic materials are often compared on the basis of tensile strength, elongation, and tensile modulus data. Many plastics are very sensitive to the rate of straining and environmental conditions. Therefore, the data obtained by this method cannot be considered valid for applications involving load time scales or environments widely different from this method. This is because the test does not take into account the time dependent behavior of plastic materials

The tensile properties of the samples were determined according to ASTM D638-03 on a Shimadzu Autograph AG-X series universal testing machine. The photograph of the same is in the figure 2-4. Different cross head speeds, 0.5, 5 and 50 mm/min adopted for the experiment. The specimen with overall length 165 mm in the dumbbell shape are held tight by two grips in the jaws of UTM. The tensile strength, maximum strain and tensile modulus were determined. In each case minimum five samples were tested.

Tensile strength is the maximum tensile stress recorded during tensile operation. It corresponds to yield strength if the breaking strength is less than the yield stress. It is measured as the force measured by the load cell at the time of break divided by the original cross sectional area of the sample at the point of minimum cross section. Thus,

$$\text{Tensile stress, } \sigma = \frac{\text{Force}}{\text{Area}}, \text{ unit is N/m}^2 (\text{Pa}) \text{ or MPa}$$



**Figure 2-4** Universal Testing Machine

However the actual/ true stress will be higher than this because the actual area at the time of break is less than the original cross sectional area. True stress is determined by the instantaneous load acting on the instantaneous cross sectional area. True stress is related to the engineering stress, assuming the material volume remains constant.

#### **2.4.2 Impact Tests (ASTM D 4812)**

The impact property of the polymeric materials depends mainly on the toughness of the material. Toughness can be described as the ability of the polymer to absorb applied energy. The molecular flexibility has a great significance in determining the relative brittleness of the material. Impact energy is a measure of toughness, and the impact resistance is the ability of a material to resist breaking (fracture) under a shock-loading.

There are two basically different test methods, namely Izod type and Charpy type. In Izod type testing, the specimen is clamped vertically to a cantilever beam and broken by a single swing of the pendulum released from the fixed distance from the specimen clamp. In the Charpy-type test method, the specimen is supported horizontally and broken by a single swing of the pendulum in the middle. The results are expressed in terms of kinetic energy consumed by the pendulum in order to break the specimen. The breaking energy is the sum of energies needed to deform it, to initiate cracking, to propagate the fracture across it and the energy expended in tossing the broken ends of the specimen.

In this work Izod impact strength (un notched) of the samples of polyester/clay nanocomposite as well as glass fiber reinforced polyester/ clay nanocomposite were determined by using Resil Impactor Junior (CEAST), which is shown in figure 2-5. The specimens were tested on the impact tester having 4J capacity hammer and striking velocity 3.45 m/s. Impact strength expressed in  $\text{kJ/m}^2$ .



**Figure 2-5** Resil impact tester

### **2.4.3 Flexural Tests (ASTM D790M)**

Flexural strength is the ability of the material to resist applied bending forces perpendicular to the longitudinal axis of the specimen. The stresses induced by flexural load are a combination of compressive and tensile stresses and properties are calculated in terms of the maximum stress and strain occurring at the outside surface of the test bar. By the application of flexural load, the upper and lower surface of the specimen under three point bending load subjected to compression and tension, axisymmetric plane subjected to shear load. Thus the specimen subjected to bending and shear or the failure happens when the bending or shear stress reaches critical value.

$$\text{Flexural strength } F_s = \frac{3PL}{2bd^2} \quad (2.1)$$

Where, P- maximum load, b- width of specimen, L- length of span, d- thickness of specimen.

Flexural modulus was also determined. It is the ratio of the stress to the corresponding strain within the elastic limit. The test was carried out in a universal testing machine, Shimadzu Autograph AG-X series.

#### **2.4.4 Scanning Electron Microscopy (SEM)**

Morphology of the fracture surfaces were investigated using SEM [16]. Resolution of smaller objects can be provided from electron microscopy, allowing direct observation of thin specimens, like single polymer crystals, and the electron diffraction patterns. It is carried out in the conditions of temperature well below the room temperature and source of accelerated voltages (higher than the usual 50000 – 100000V) in order to prevent of damage to single polymer crystals. In scanning electron microscopy (SEM), a fine beam electron is scanned across the surface of an opaque specimen. These photons are emitted when the beam hits to surface, then collected to provide a signal used to strengthen the intensity of the electron beam. In the case of nanocomposites, no peaks are observed in X-Ray analysis (XRD) in their disordered state due to lack in structural observation of the layers having large d-spacings. Thus, in such cases, scanning electron microscopy (SEM) yields more accurate results than XRD analysis in characterization.

The SEM micrographs were taken for the fracture surfaces of PNCs and GFRPNCs failed under different load conditions. The analysis was done by using a JEOL Model JSM - 6390LV, scanning electron microscope. The photograph of the same is shown in the figure 2-6.



**Figure 2-6** Scanning Electron Microscope

#### **2.4.5 Dynamic Mechanical Analysis (DMA)**

In dynamic mechanical analysis, DMA, the viscoelastic properties of a material are characterized by applying a sinusoidal deformation to the material at a single or at multiple frequencies, and monitoring the response of the material. Since polymers are viscoelastic materials, i.e. they simultaneously exhibit solid-like and liquid-like properties; they are by definition time-dependent. This means that the response of a viscoelastic material to an imposed deformation will depend on how fast or slow the deformation was applied to the sample. When characterizing a material by DMA, the time of the deformation is the frequency as frequency is the inverse of time (frequency =  $1/\text{time}$ ). Therefore, high frequencies are analogous to short times and low frequencies to long times. DMA is most widely used to measure the glass transition temperature of polymers, because the frequency can have such a significant effect on the temperature at which the glass transition is detected, it is important to report the frequency along with the glass transition temperature.

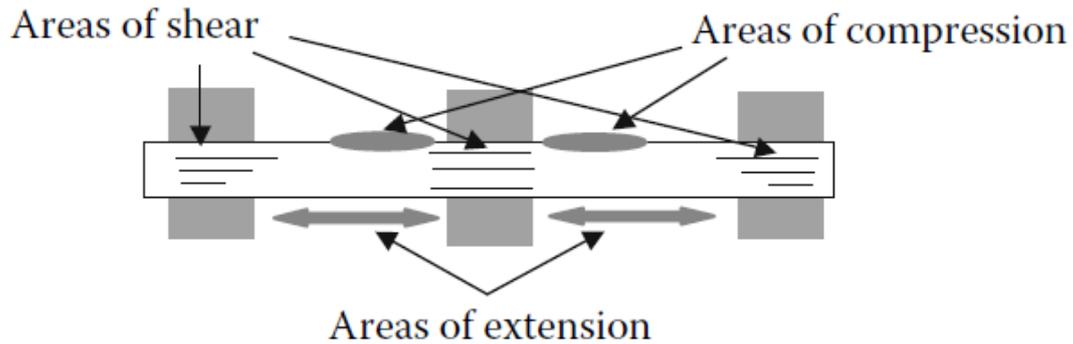


**Figure 2-7** Clamping in dual cantilever mode

According to ISO 6721-1, the storage modulus  $G'$  represents the stiffness of a viscoelastic material and is proportional to the energy stored during a loading cycle. It is roughly equal to the elastic modulus for a single, rapid stress at low load and reversible deformation. In the same ISO standard, the loss modulus  $G''$  is defined as being proportional to the energy dissipated during one loading cycle. It represents, for example, energy lost as heat, and is a measure of vibration energy that has been converted during vibration and that cannot be recovered. The phase angle is the phase difference between the dynamic stress and the dynamic strain in a viscoelastic material subjected to a sinusoidal oscillation. The phase angle is expressed in radians. The loss factor  $\tan\delta$  is the ratio of loss modulus to storage modulus. It is a measure of the energy lost, expressed in terms of the recoverable energy, and represents mechanical damping or internal friction in a viscoelastic system. The loss factor  $\tan\delta$  is expressed as a dimensionless number. A high  $\tan\delta$  value is indicative of a material that has a high, non elastic strain component, while a low value indicates one that is more elastic.

Cantilever fixtures clamp the ends of the specimen in place, introducing a shearing component to the distortion and increasing the stress required for a set displacement. Two types of cantilever fixtures are used: single cantilever and dual cantilever.

Schematic diagram of dual cantilever configuration is shown in Figure 2-7. Moduli from dual cantilever fixtures tend to run 10%–30% different than the same material measured in three-point bending at best. This is due to shearing strain induced by clamping the specimen in place at the ends and center, which makes the sample more difficult to deform [19]. The experiment carried out on DMA Q800 (TA Instruments, New Castle, USA). The photograph of which is shown in figure 2-8.



**Figure 2-8** Dynamic Mechanical Analyzer

#### **2.4.6 X- Ray Diffraction (XRD)**

XRD Analysis was carried out with X Ray Diffractometer, Bruker, D8 AXS advanced model. The photograph of the same is shown in figure 2-9. Cu K $\alpha$  radiation of wavelength  $\lambda = 1.54 \text{ \AA}$  and Ni filter operating at 30 kV and 20 mA was used.



**Figure 2-9 X-Ray Diffractometer**

WAXD is the most useful and suitable technique for the measurement of the d-spacing of ordered immiscible and ordered intercalated polymer layered silicate nanocomposite, but it may be insufficient for distinguishing disorderd and exfoliated material that will not give any peak. When  $d_{001}$  (d spacing ) of the clay in the compsite is equal or lower than the one for the pure clay mineral, an ordinary composite was obtained. On the other hand when the d spacing in the composite is higher than the pure nanoclay, the polymer molecules were positioned between the clay platelets and an intercalated nanocomposite was produced. If the peak corresponding to  $d_{001}$  is not observed in the nanocomposite diffractograms, an exfoliated structure can be expected. The lack of peak may be misinterpreted in case where no peak is seen or the amount of clay was too low to be detected in WAXD analysis.

In this project characterization of both PNCs and GFRPNCs were done by using X-Ray diffractogram.

### **2.4.7 Thermogravimetric Analysis (TGA)**

Thermogravimetric analysis (TGA) is one of the members of the family of thermal analysis techniques which is used to characterize a wide variety of materials. TGA measures the amount and rate (velocity) of change in the mass of a sample as a function of temperature or time in a controlled atmosphere. The measurements are used primarily to determine the thermal and/or oxidative stabilities of materials as well as their compositional properties. The technique can analyze materials that exhibit either mass loss or gain due to decomposition, oxidation or loss of volatiles (such as moisture). It is especially useful for the study of polymeric materials, including thermoplastics, thermosets, elastomers, composites, films, fibers, coatings and paints. TGA measurements provide valuable information that can be used to select materials for certain end-use, predict product performance and improve product quality.

The technique is particularly useful for the measurements such as, thermal stability assessment, compositional analysis, predict the lifetime of polymers under actual service conditions, isothermal measurements at elevated temperatures and measure the time taken for a certain extent of mass loss to occur [20]. The experiment carried out in a TGA Q500, TA instruments, US, the photograph of the same is shown in the figure 2-10. Test samples of weight 5-10 mg, heated up to a temperature of 800 °C at the rate 10 °C/min. The degradation obtained by measuring the periodic weight of the specimen by the instrument automatically. The measurements were taken for both PNCs and GFRPNCs.



**Figure 2-10** Thermogravimetric analyzer

#### **2.4.8 Differential Scanning Calorimetry (DSC)**

Differential scanning calorimetry has been widely applied in the investigation of numerous phenomena occurring during the thermal heating of organoclays and polymer/clay nanocomposites, involving glass transition ( $T_g$ ), melting, crystallization and curing as a function of temperature. The DSC method is one of the most common techniques applied to investigate the  $\alpha$ -transition in polymers and their composites. The  $\alpha$ -transition is related to the Brownian motion of the main chains at the transition from the glassy to the rubbery state and the relaxation of dipoles associated with it. In this study the effect on glass transition temperature because of the incorporation of nano fillers in to polymer were analyzed. The studies were carried out on polyester nanocomposites and glass fiber reinforced polyester nanocomposites. The experiments were carried out using DSC Q2000 (TA Instruments, New Castle, USA). The photograph of the equipment used is shown in figure 2-11. Test specimens weighing 5-6 mg were placed in pans for testing. It heated at the rate 10 °C/min. The

Instrument measures the additional heat flow required to maintain the sample pan at the same temperature as the reference pan.

Heat flow, i.e. heat absorption (endothermic) or heat emission (exothermic) is measured, per unit time for the sample and the result is compared with that of a thermally inert reference. The materials as they undergo changes in chemical and physical properties are detected by transducers, which changes into electrical signals that are collected and analyzed to give thermograms. DSC directly gives recording of heat flow rate against temperature.



**Figure 2-11** Differential Scanning Calorimeter

#### **2.4.9 Creep Test**

Creep behavior is determined to predict the performance under Tensile Creep measurements are made by applying the constant load to a specimen and measuring

its extension as a function of time. The extension measurement can be carried out in several different ways. The simplest way is to make two gauge marks on the tensile specimen and measure the distance between the marks at specified time intervals. The percent creep strain is determined by dividing the extension by initial gauge length and multiplying by 100. The percent creep strain is plotted against time to obtain a tensile creep curve. The test is also carried out at different stress levels and temperatures to study their effect on tensile creep properties.

Two accelerated test methods exist, one using the Time-Temperature Superposition (TTS) principle and the other using the Time-Stress superposition (TSS) principle, which are utilized to generate predictions of long-term creep behavior. TTS relies on the fact that higher temperatures accelerate viscoelastic phenomena within viscoelastic materials, while the basis for TSS is that higher stresses accelerate viscoelastic phenomenon

In this work, tensile creep test results were compiled from tests conducted under identical creep stresses over a range of temperatures. The array of creep curves obtained from these tests were shifted along the time-scale, each by a different factor which correspond to an individual testing temperature, such that they converged to form an extended creep curve at the reference temperature. This extended curve is referred to as the master-curve and it should represent the actual creep behavior at the reference temperature. The analysis was conducted by DMA Q800 TA instrument and using the software, TA analyzer facility of the instrument.

## CHAPTER 3

### ANALYSIS OF ISOPHTHALIC POLYESTER /NANOKAOLINE CLAY NANOCOMPOSITE

#### 3.1 INTRODUCTION

The transition from micro particles to nano particles yields dramatic changes in physical properties. Nano scale materials have a large surface area for a given volume. Since many important chemical and physical interactions are governed by surfaces and surface properties, a nano structured material can have substantially different properties from a larger-dimensional material of the same composition. In the case of particles and fibers, the surface area per unit volume is inversely proportional to material's diameter, thus, smaller the diameter, the greater the surface area per unit volume. Consequent to the property of nanoclay as a reinforcing agent for polymers the significance of the same got increased. Recently, researchers are trying to achieve superior improvement of thermo mechanical property of the polymers by the incorporation of nanoclay. China clay, a traditional name of kaolin, is a mixture of minerals generally containing kaolinite, quartz, mica, feldspar, illite and Montmorillonite [70].

Clay minerals may be divided into four major groups, mainly in terms of the variation in the layered structure. These include the kaolinite group, the Montmorillonite/ smectite group, the illite group, and the chlorite group. The kaolinite group has three members, including kaolinite, dickite, and nacrite, each with a formula of  $\text{Al}_2\text{Si}_2\text{O}_5(\text{OH})_4$ . The formula indicates that the members of this group are polymorphs, means that they have

same formula but differing structures. Each member is composed of silicate sheets ( $\text{Si}_2\text{O}_5$ ) bonded to aluminum oxide/hydroxide layers ( $\text{Al}_2(\text{OH})_4$ ); the two types of layers are tightly bonded. These clays are used as fillers in ceramics, paint, rubber, paper, and plastics. The effect of nanoclay content in the blend on mechanical properties had been investigated. Reinforcing with nano fillers proved the enhancement of mechanical properties of blends without increasing weight, density etc. [71]. Nanoclay acts as a nucleating agent and contributes to rise of the crystallization temperature and reduction of crystal size of matrix of polymer. The ultimate tensile strength and initial modulus of hybrid fibers were found to increase with increasing organoclay content [72]. Tensile strength and modulus found to improve with the addition of 100V, vinyl modified nanokaoline in Polypropylene homo polymer (PP). Also a substantial increase in tensile modulus for the PP/SGF/nanoclay hybrid composite was reported. Researchers also reported the improvement in thermal stability [73]. Studies on the NBR, nanokaoline clay observed an improvement in mechanical properties of the composites from reinforcing with both unmodified and modified nanokaoline clay. Modified clay is found to be better reinforcing filler compared to unmodified clay. The cure rate is increased with the addition of both clays [74].

Over the past 10 years, many other researchers have also attempted to improve the properties of epoxies using nanoclay. The organo clay simultaneously improved both fracture toughness and elastic modulus of the epoxy system without decreasing the compressive strength [76]. Nanocomposites consisting of a polymer and layered silicate remarkably enhanced mechanical and materials properties. The main reason for enhancement of properties in nanocomposites is the greater interfacial interaction between the matrix and layered silicate, compared with conventional filler-reinforced systems [77].

Extensive research works have been conducted with polymer nanocomposite with silica, montmorillonite and many other nanoparticles. However there are only very few literatures are available on nanokaoline clay as reinforcement. The study conducted on the effect of nanokaoline clay particles on the mechanical, morphological and processing features of PS/HDPE blends reported that the incorporation of organo modified nanokaoline clay increase interfacial adhesion with the matrix. Also the tensile strength and tensile modulus, impact strength and flexural strength increase with certain percentage of filler loading [75].

Many researchers have attempted to achieve superior thermo- mechanical properties and barrier properties to the polymers by the incorporation of nanoclay. Here in this chapter an attempt is made to study the variation in the properties of isophthalic polyester by the addition of unmodified nanokaoline clay as well as different types of modified nanokaoline clays.

## **3.2 METHODOLOGY**

### **3.2.1 Raw materials**

The raw materials used were isophthalic polyester resin, reagents such as cobalt naphthenate and methyl ethyl ketone peroxide (MEKP). Isophthalic polyester resin used for matrix. The materials were supplied by Sharon enterprises, Kochi, India. Cobalt naphthenate as accelerator and methyl ethyl ketone peroxide (MEKP) as catalyst were used for the curing of polyester resin. For easiness of processing, the clay was made into dispersion with styrene and then the dispersion was added to the polyester resin for modification.

Four types of nanokaoline clays were used separately for the preparation of four types of nanocomposites. The different nanokaoline clays used are unmodified nanokaoline clay (Nanocaliber N100), amino modified nanokaoline clay (Nanocaliber-N100A), dialkyl modified nanokaoline clay (Nanocaliber N100Z) and mercapto modified nanokaoline clay (Nanocaliber N100M).

### **3.2.2 Material Preparation**

Test specimens for mechanical testing as per ASTM standards were prepared by the method of casting. The procedure used to prepare specimen for the experimentation related to characterization is explained chapter-2. Specimen was prepared for different types of nanokaoline clay such as unmodified, amino modified, dialkyl modified and mercapto modified. The experiment conducted for different proportions of nanokaolineclay such as 1%, 2% and 3% by weight of the polyester resin. The Similar procedure had been adopted by Mirmohseni et.al. [78].

### **3.2.3 Mechanical Characterization**

Tensile test was carried out by a universal testing machine, Schimadzu AGX-I as per ASTM D 638-03. The parameters adopted for tensile tests were cross head speed (CHS) and percentage composition of the filler. Three different cross head speeds (CHS), 0.5 mm/min, 5mm/min and 50 mm/min were selected for the experimentation. Specimen from different samples viz 0% (pure polyester), 1 %, 2 % and 3% nanokaoline clay were prepared. In each case five samples were tested. The impact property was determined by Izod impact test as per ASTM D 4812. Here also

the specimen was prepared from 0%, 1 %, 2% and 3% nanokaoline clay filled nanocomposites. In each category five samples were experimented.

### 3.2.4 Study of Fracture surface

The fracture surface of the specimen analyzed from the SEM micrographs. The SEM micrographs were obtained for 1% and 2% nanokaoline clay filled nanocomposite with filler unmodified nanokaoline clay (N100) and mercapto modified nanokaoline clay (N 100M).

**Table 3-1** Tensile properties of polyester nanocomposite with different type of nanokaoline clay as filler

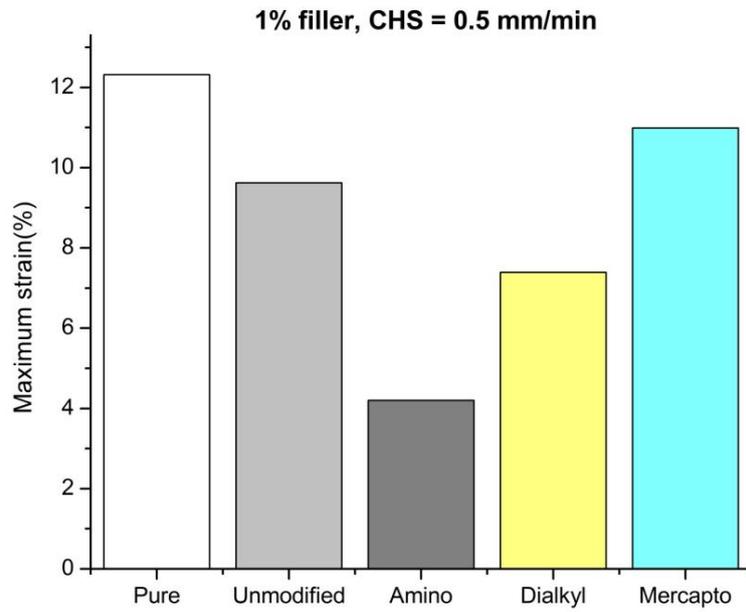
| Nanoclay             | Tensile strength (MPa) | Maximum strain (%) | Tensile modulus (MPa) |
|----------------------|------------------------|--------------------|-----------------------|
| Pure polyester resin | 60.41                  | 12.32              | 1018.99               |
| Unmodified           | 40.59                  | 9.62               | 1078.27               |
| Amino                | 31.25                  | 4.20               | 1045.01               |
| Dialkyl              | 37.78                  | 7.39               | 1210.87               |
| Mercapto             | 55.19                  | 10.99              | 1122.55               |

## 3.3 RESULTS AND DISCUSSION

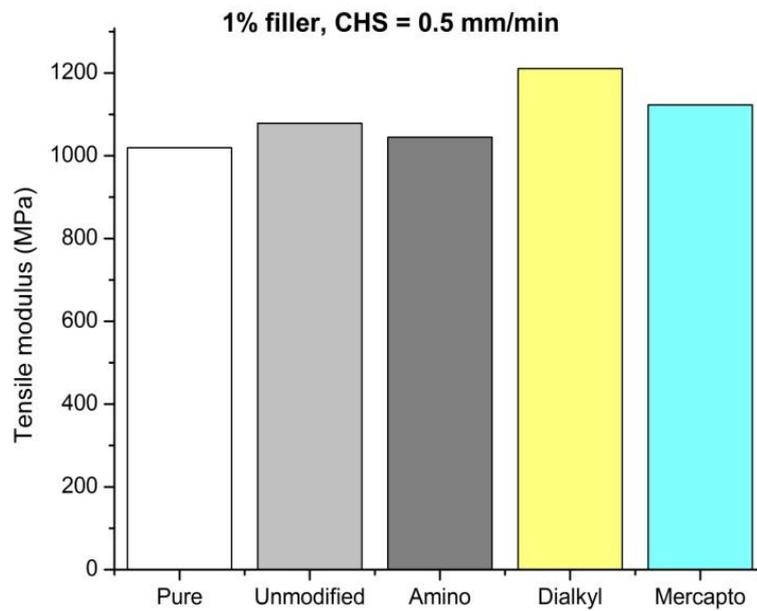
### 3.3.1 Tensile Properties

Table 3-1 gives the result of tensile tests conducted on nanocomposites prepared with different types of nanokaoline clays. Specimen was prepared with unmodified (N100), amino modified (N100A), dialkyl modified (N100Z) and mercapto modified

(N100M) nanokaoline clay with 1% by weight of the resin. Figure 3-1, 3-2 and 3-3 are the bar plots of maximum strain, tensile modulus and tensile strength of nanocomposites formed with various types of clay. The percentage elongation of the nanocomposite decreases with the increase of nanokaoline clay content. That means the strain found to be decrease with the addition of nanokaoline clays to polyester resin. But the strain is lowest for amino modified and dialkyl modified nanokaoline clay filled polyester. For unmodified nanokaoline clay filled sample as well as mercapto modified nanokaoline clay filled samples the percentage strain almost close to that of pure polyester resin. The tensile modulus is high for dialkyl modified nanokaoline filled nanocomposite. Whereas for unmodified, amino modified and mercapto modified nanokaoline filled nanocomposite, there is only a marginal difference in the tensile modulus. Thus about 19% increase in tensile modulus obtained with dialkyl modified nanokaoline clay and 10% increase obtained for mercapto modified nanokaoline clay whereas, for other types of clay the increment is negligibly small. Almost similar trend of variation of percentage strain is observed for tensile strength. No notable increase in tensile strength is obtained from the addition of nanokaoline clay. But the tensile strength decreased to a remarkable extent with the addition of dialkyl and amino modified nanokaoline. The strength as well as modulus is controlled by the nanoclay/ matrix interaction, which will be influenced by the type of modifying agent in the clay. If proper dispersion of the nanoclay is obtained, then the interfacial bonding will be good enough to improve the modulus [13].



**Figure 3-1** Maximum strain under tensile load for polyester nanocomposite with different type of nanokaoline clay as filler



**Figure 3-2** Tensile modulus of polyester nanocomposite with different nanokaoline clay as filler

The result of tensile test conducted on nanocomposite prepared with various types of nanokaoline clays of composition 0, 1, 2 and 3 % weight of polyester resin is represented in table 3-2 to 3-5. The different types of nanokaoline clays used were N 100, N 100A, N 100Z, N 100M. The experiment conducted at Cross head speed (CHS) 0.5, 5 and 50 mm/min. Figure-3-4 to 3-11 gives the graphical plots of tensile properties such as of modulus and strength with percentage weight of filler.

The test results showed an increase in tensile modulus with the addition of nanokaoline clay for the content from 1% to 2% except for the nanofiller, unmodified nanokaoline clay. Even though there is no regular trend available, from the general trend of the graph the tensile strength showed a decrease with the addition of nanoclay. It is because they tend to break early as they become brittle while the nanoclay is added. Also the addition of nanoclay will make the mixture more viscous and increases the possibility for the formation of voids. There is also a possibility for the decrease in homogeneity of the material with the addition of nanoclay and the same is evident from the SEM images in figure 3-17. According to general behavior of adding particles to polymer medium, there is a decrease of tensile strength. This is because the particles in particulate composites place constraints on the plastic deformation of the matrix. Particles are effective in enhancing the stiffness of the material but do not offer much for strengthening [1]. An increase in tensile modulus with the loading speed (CHS) is evident from the results. Maximum tensile modulus obtained at CHS 50 mm/min [76].

At low strain the weak van der Waals force is enough to bond the fillers to polymer, hence the modulus will be high at low strain rate even without good filler matrix interaction due to the transfer of stress between fillers and matrix. However at high

strains, the materials are more brittle and the strength will be low with a low elongation at break. Also without good interaction, the homogeneity of material is low and easy to have crack to break. It may be the reason for the reduced tensile strength at testing speed, 50 mm/min.

From the results, 9% to 14% increase of tensile modulus is obtained with the addition of 1% nanoclay at CHS = 5 mm/min. Only a very little increase is noticed at CHS =50 mm/min. The increase of tensile modulus is marginal with more than 1% nanoclay content and testing speed 0.5 mm/min (low speed) and 50 mm/min (high speed). While we ascertaining adhesion and homogeneity of nanoclay dispersion for the improvement of properties, it happened at 1% nanoclay content. Again N100A, N100Z and N100M (all are modified nanokaoline) respectively shows 16%, 16% and 14% increase in tensile modulus at 1% nanoclay loading, whereas, N100 (unmodified nanokaoline) gives only 9% increase at 1% nanoclay loading. Hence the modified nanokaoline clay can be credited with more compatibility and adhesion with polyester matrix.

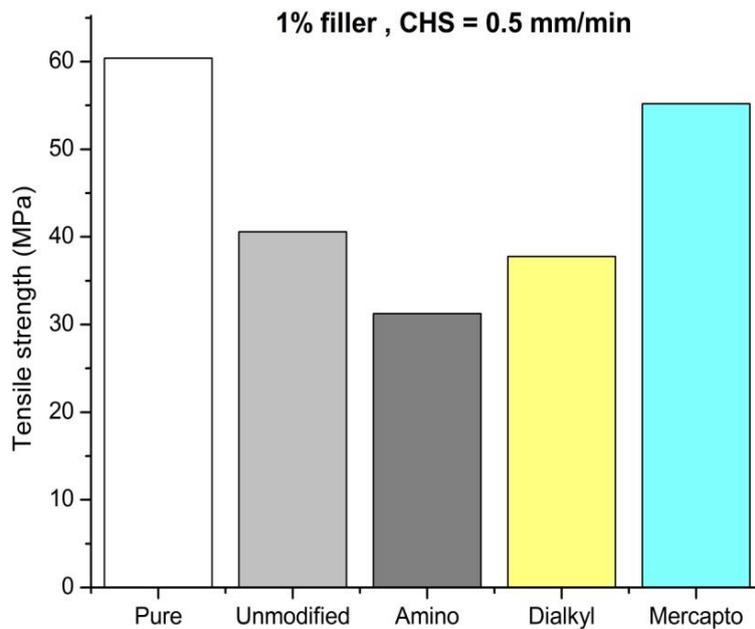


**Figure 3-3** Tensile strength of polyester nanocomposite with different type of nanokaoline clay as filler

**Table 3-2** Tensile properties of polyester nanocomposite with unmodified nanokaoline clay (N100) as filler

| wt.% of nanoclay | CHS= 0.5mm/min         |                       | CHS= 5 mm/min          |                       | CHS= 50 mm/min         |                       |
|------------------|------------------------|-----------------------|------------------------|-----------------------|------------------------|-----------------------|
|                  | Tensile Strength (MPa) | Tensile modulus (MPa) | Tensile Strength (MPa) | Tensile modulus (MPa) | Tensile Strength (MPa) | Tensile modulus (MPa) |
| 0                | 60.41                  | 1018.99               | 58.66                  | 1405.08               | 48.14                  | 1802.67               |
| 1                | 40.59                  | 1078.27               | 39.75                  | 1508.82               | 39.47                  | 1812.62               |
| 2                | 45.73                  | 1162.08               | 44.91                  | 1253.21               | 42.19                  | 1470.82               |
| 3                | 41.64                  | 1070.67               | 42.65                  | 1239.25               | 39.68                  | 1362.67               |

**Table 3-3** Tensile properties of polyester nanocomposite with amino modified nanokaoline clay (N 100A) as filler

| wt.% of nanoclay | CHS= 0.5mm/min         |                       | CHS= 5 mm/min          |                       | CHS= 50 mm/min         |                       |
|------------------|------------------------|-----------------------|------------------------|-----------------------|------------------------|-----------------------|
|                  | Tensile Strength (MPa) | Tensile modulus (MPa) | Tensile Strength (MPa) | Tensile modulus (MPa) | Tensile Strength (MPa) | Tensile modulus (MPa) |
| 0                | 60.41                  | 1018.99               | 58.66                  | 1405.08               | 48.14                  | 1802.67               |
| 1                | 31.25                  | 1045.01               | 29.67                  | 1480.64               | 36.54                  | 1923.32               |
| 2                | 42.66                  | 935.22                | 37.52                  | 1223.35               | 32.49                  | 1418.56               |
| 3                | 40.16                  | 889.97                | 36.39                  | 1217.57               | 32.06                  | 1219.62               |

**Table 3-4** Tensile properties of polyester nanocomposite with dialkyl modified nanokaoline clay (N 100Z) as filler

| wt.% of nanoclay | CHS= 0.5mm/min         |                       | CHS= 5 mm/min          |                       | CHS= 50 mm/min         |                       |
|------------------|------------------------|-----------------------|------------------------|-----------------------|------------------------|-----------------------|
|                  | Tensile Strength (MPa) | Tensile modulus (MPa) | Tensile Strength (MPa) | Tensile modulus (MPa) | Tensile Strength (MPa) | Tensile modulus (MPa) |
| 0                | 60.41                  | 1018.99               | 58.66                  | 1405.08               | 48.14                  | 1802.67               |
| 1                | 37.78                  | 1210.87               | 40.35                  | 1488.15               | 38.64                  | 1975.37               |
| 2                | 45.13                  | 1132.57               | 46.47                  | 1355.19               | 40.73                  | 1599.31               |
| 3                | 42.61                  | 924.93                | 34.69                  | 1145.5                | 34.58                  | 1306.05               |

**Table 3-5** Tensile properties polyester nanocomposite with mercapto modified nanokaoline clay (N 100M) as filler

| wt.% of nanoclay | CHS= 0.5mm/min         |                       | CHS= 5 mm/min          |                       | CHS= 50 mm/min         |                       |
|------------------|------------------------|-----------------------|------------------------|-----------------------|------------------------|-----------------------|
|                  | Tensile Strength (MPa) | Tensile modulus (MPa) | Tensile Strength (MPa) | Tensile modulus (MPa) | Tensile Strength (MPa) | Tensile modulus (MPa) |
| 0                | 60.41                  | 1018.99               | 58.66                  | 1405.08               | 48.14                  | 1802.67               |
| 1                | 55.19                  | 1122.55               | 46.99                  | 1462.05               | 43.43                  | 1876.72               |
| 2                | 41.28                  | 1071.97               | 47.61                  | 1330.29               | 50.14                  | 1421.25               |
| 3                | 39.62                  | 1023.31               | 38.85                  | 1140.07               | 43.49                  | 1194.42               |

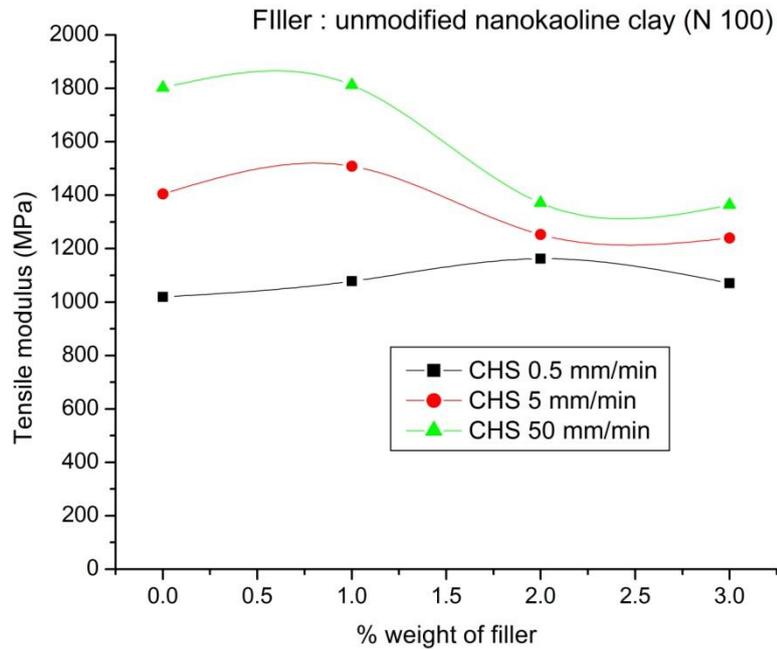


**Figure 3-4** Variation of tensile modulus of polyester nanocomposite with nanoclay (N 100) content at different testing speed

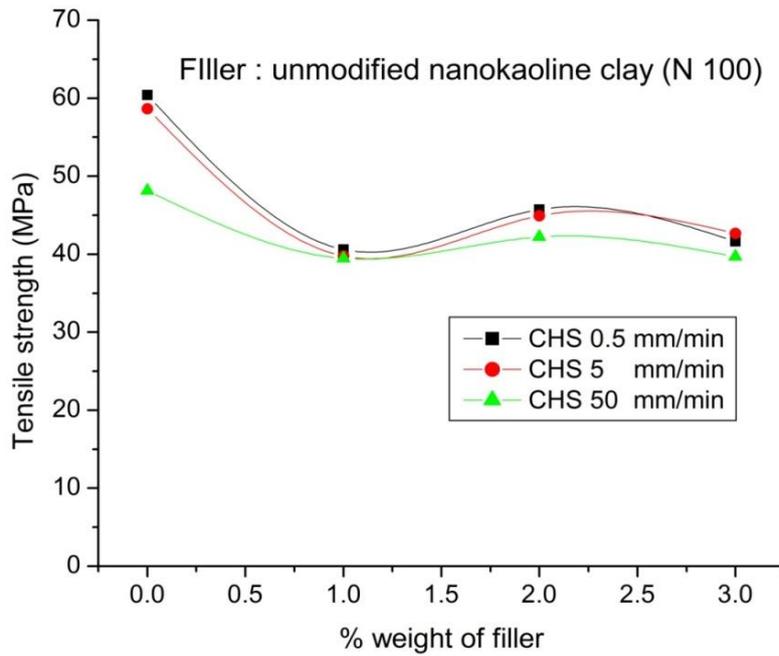


**Figure 3-5** Variation of Tensile strength of polyester nanocomposite with nanoclay (N 100) content at different testing speed

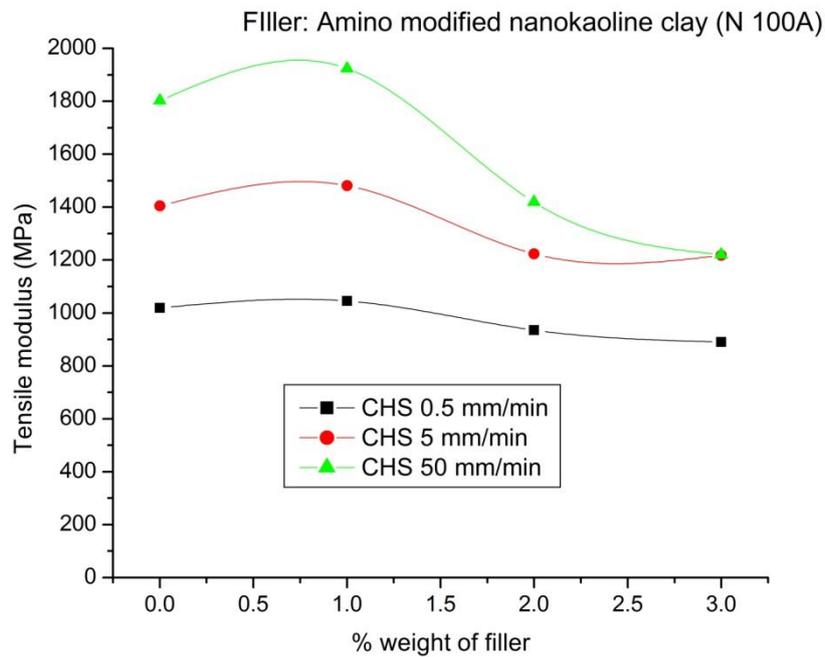


**Figure 3-6** Variation of tensile modulus of polyester nanocomposite with nanoclay (N 100A) content at different testing speed

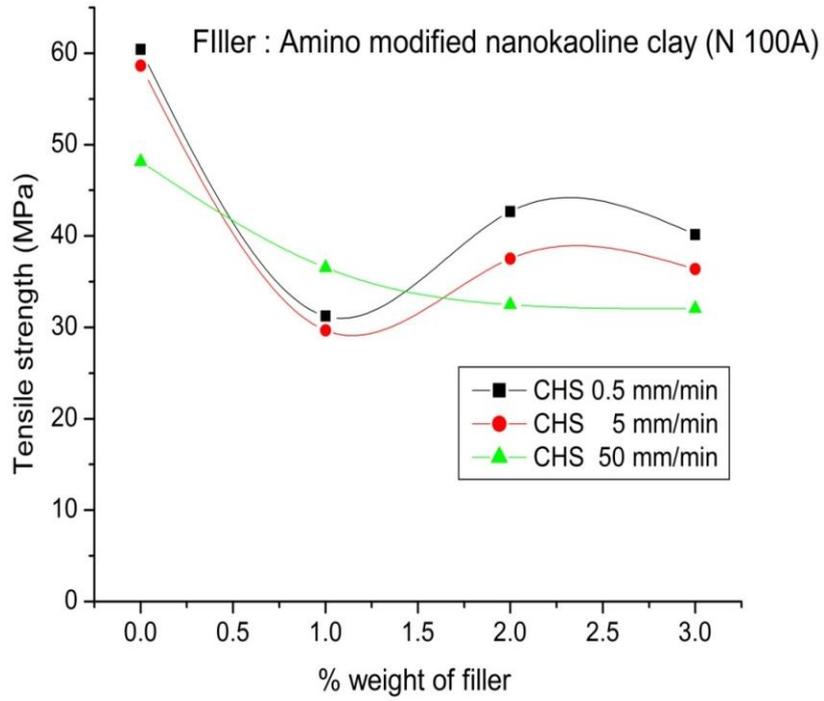


**Figure 3-7** Variation of tensile strength of polyester nanocomposite with nanoclay (N 100A) content at different testing speed

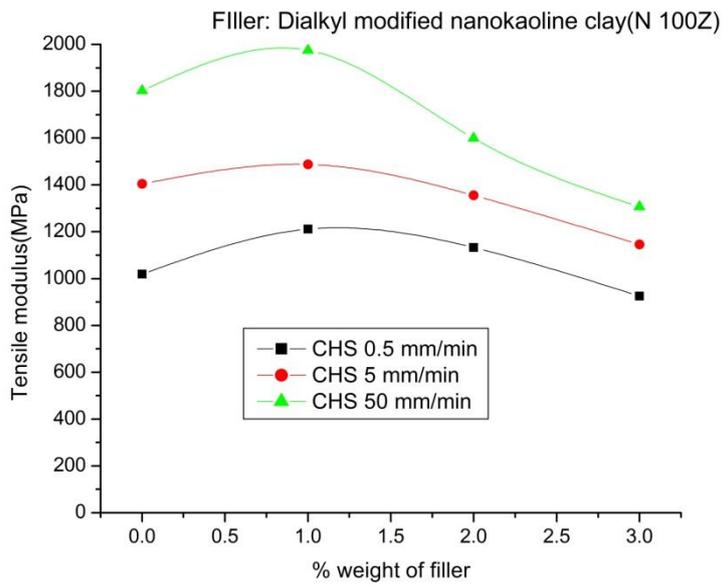


**Figure 3-8** Variation of tensile modulus of polyester nanocomposite with nanoclay (N 100Z) content at different testing speed

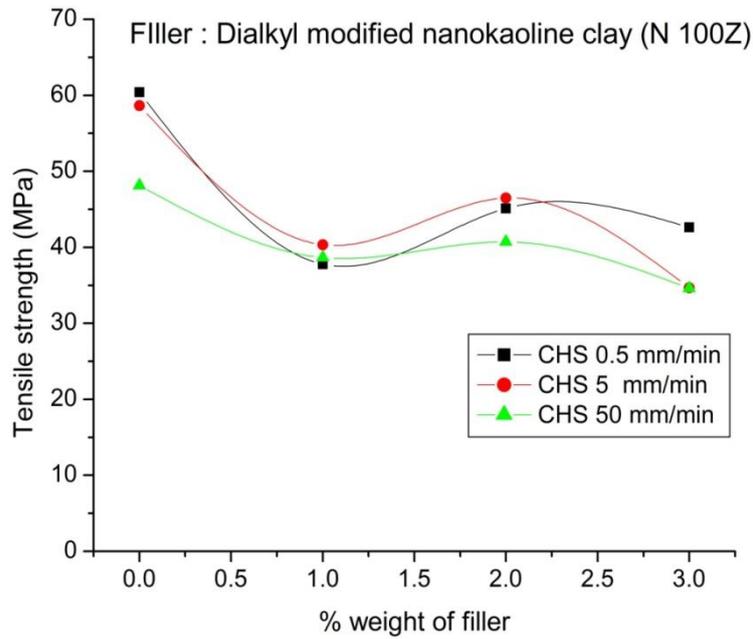


**Figure 3-9** Variation of tensile strength of polyester nanocomposite with nanoclay (N 100Z) content at different testing speed

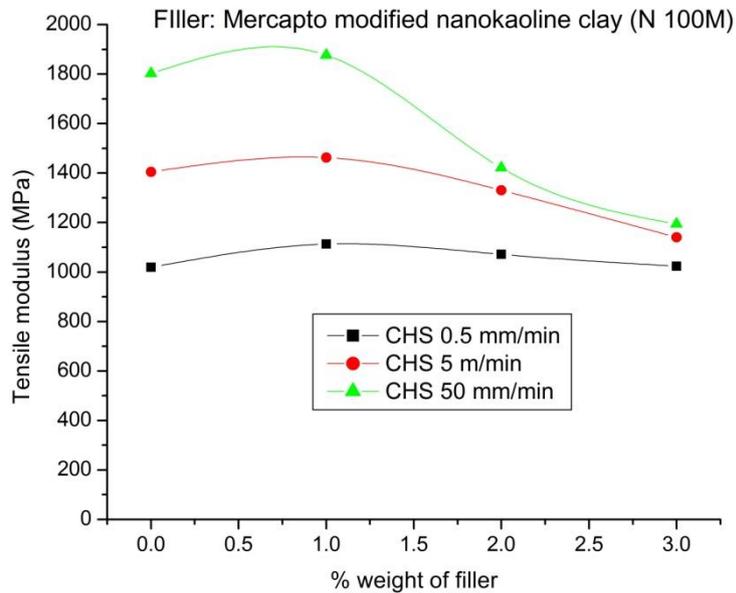


**Figure 3-10** Variation of tensile modulus of polyester nanocomposite with nanoclay (N 100M) content at different testing speed

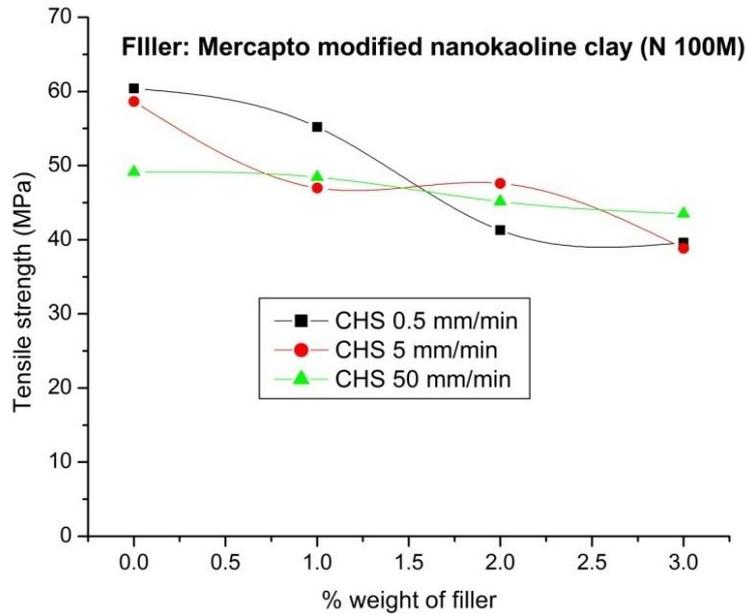


**Figure 3-11** Variation of tensile strength of polyester nanocomposite with nanoclay (N 100M) content at different testing speed

### 3.3.2 Impact Properties

Table 3-6 shows the results of impact test conducted on polymer modified with various types of nanokaoline clays. The percentage weight of nanokaoline clay added to the polyester was 1%. Figure 3-12 shows the bar plot of the data in table 3-6. Nanocomposite with Amino silane modified nanokaoline clay (N 100A) gives the maximum impact strength. A better adhesion can be attributed to the improvement of impact strength. Modified nanoclay gives better compatibility with the matrix material, which also may leads to the capacity of the material to withstand at high impact load. However the impact strength with other type of modified nanokaoline clay as filler not indicated any improvement. The reasons may be the quantity (very small ) of nanoclay added and the difficulty in achieving dispersion.

Table 3-7 to 3-10 shows the results of the impact test conducted on polyester nanocomposite prepared with various types of nanokaoline clays as filler in different percentage weight of composition such as 0,1,2 and 3. The different types of nanoclay used were unmodified nanokaoline (N 100), amino modified nanokaoline (N 100A),

dialkyl modified nanokaoline (N 100Z) and mercapto modified nanokaoline (N 100M). The graphical plots for the respective type of nanokaoline clays as filler are represented in figure 3-13 to 3-16.

**Table 3-6** Variation Impact strength of polyester nanocomposite with different type of nanokaoline clay as filler

| Type of Nanokaoline clay   | Impact strength (kJ/m <sup>2</sup> ) |
|----------------------------|--------------------------------------|
| Pure(pristine)             | 12.27                                |
| Unmodified (N 100)         | 12.45                                |
| Amino modified (N 100A)    | 12.82                                |
| Dialkyl modified (N 100Z)  | 11.98                                |
| Mercapto modified (N 100M) | 10.35                                |

**Table 3-7** Variation of impact strength of polyester nanocomposite with nanoclay (N 100) content

| % weight of nanokaoline clay (Unmodified) | Impact strength(kJ/m <sup>2</sup> ) |
|---|-------------------------------------|
| 0   | 12.27                               |
| 1   | 12.45                               |
| 2   | 11.87                               |
| 3   | 6.66                                |

**Table 3-8** Variation of impact strength of polyester nanocomposite with nanoclay (N 100A) content

| % weight of nanoclay (Amino modified) | Impact strength(kJ/m <sup>2</sup> ) |
|---------------------------------------|-------------------------------------|
| 0                                     | 12.27                               |
| 1                                     | 12.82                               |
| 2                                     | 10.75                               |
| 3                                     | 8.63                                |

**Table 3-9** Variation of impact strength of polyester nanocomposite with nanoclay (N 100Z) content

| % weight of nanoclay (Dialkyl modified) | Impact strength(kJ/m <sup>2</sup> ) |
|---|-------------------------------------|
| 0                                       | 12.27                               |
| 1                                       | 11.98                               |
| 2                                       | 11.85                               |
| 3                                       | 6.84                                |

**Table 3-10** Variation of impact strength of polyester nanocomposite with nanoclay (N 100M) content

| <b>% weight of nanoclay (mercapto)</b> | <b>Impact strength (kJ/m<sup>2</sup>)</b> |
|--|---|
| 0                                      | 12.27                                     |
| 1                                      | 10.35                                     |
| 2                                      | 6.37                                      |
| 3                                      | 4.83                                      |

It is difficult to predict any regular trend for the variation of impact strength with different percentage weight of nanoclay loading. The variation of Impact strength is of zig zag nature. In general the impact strength decreased initially by the addition of 1% clay and the value get increased for 2 % nanoclay filled samples. Further it decreases. No regular trend is evident. Almost similar nature of variation as that of tensile strength is noted for impact strength also. A possibility for the improvement of impact strength with the addition of nanoclay is evident, but the decrease in impact strength while increasing % weight of nanoclay may be due to the formation of voids due to increased viscosity of the material. Also the improper mixing of the clay in the polyester may result in an in homogeneity.

Figure 3-13 and 3-14 shows a marginal improvement in impact strength with the addition of 1% filler when unmodified and amino modified nanokaoline clay as filler. Whereas, for dialkyl modified and mercapto modified nanokaoline clay filled nanocomposite a marginal decrement is indicated. The impact strength of the polymer needs to be improved by the addition of nanoclay which provides adhesion and compatibility. However due to the low percentage weight of filler and difficulty in achieving homogeneous structure, the impact strength showed only a minor change.

In general we cannot state any exact trend of variation of impact properties with different types of nanokaoline clay as filler at 1% filler content or 2 or 3% filler content. Proper dispersion of the filler in the matrix was very difficult to achieve,

which may be the reason for the lack of regular trend in the variation of impact properties. The agglomeration of nanofiller in the resin is evident from SEM micrographs in figure 3-17 and 4-19.

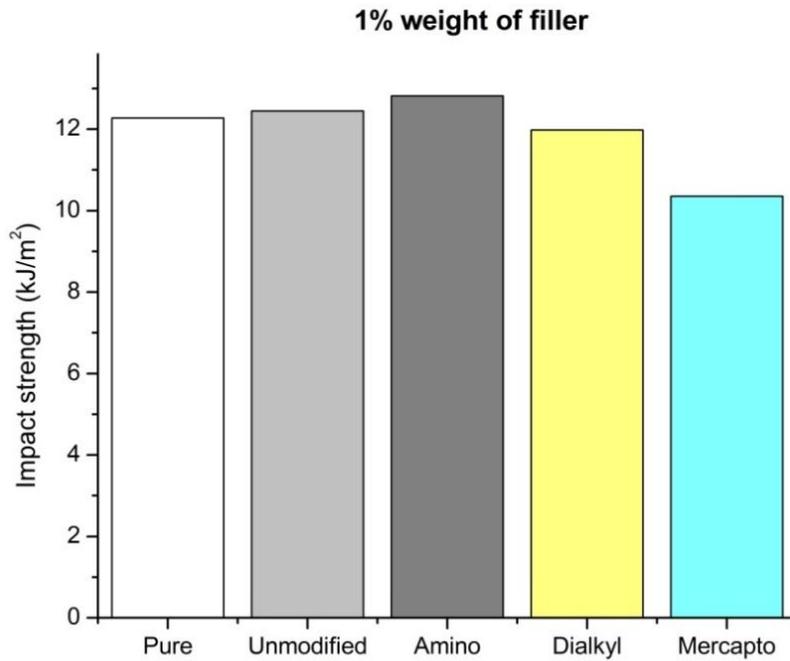


**Figure 3-12** Variation Impact strength of polyester nanocomposite with different type of nanokaoline clay as filler at 1% weight.

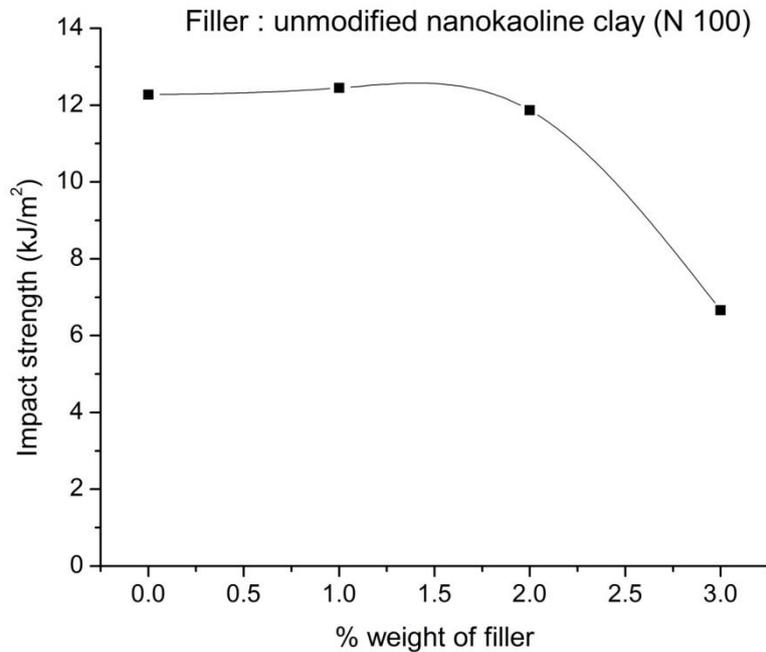


**Figure 3-13** Variation of impact strength of polyester nanocomposite with nanoclay (N 100) content

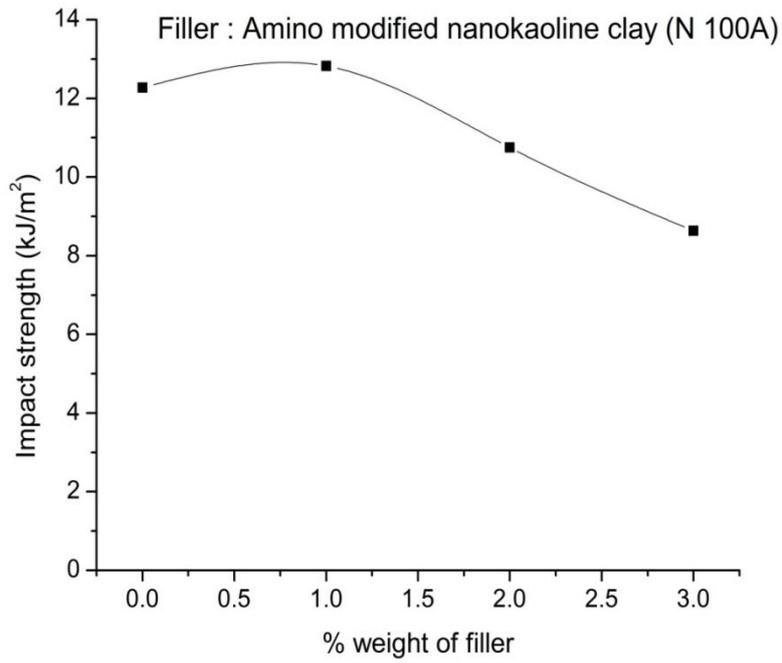


**Figure 3-14** Variation of impact strength of polyester nanocomposite with nanoclay ( N 100A) content

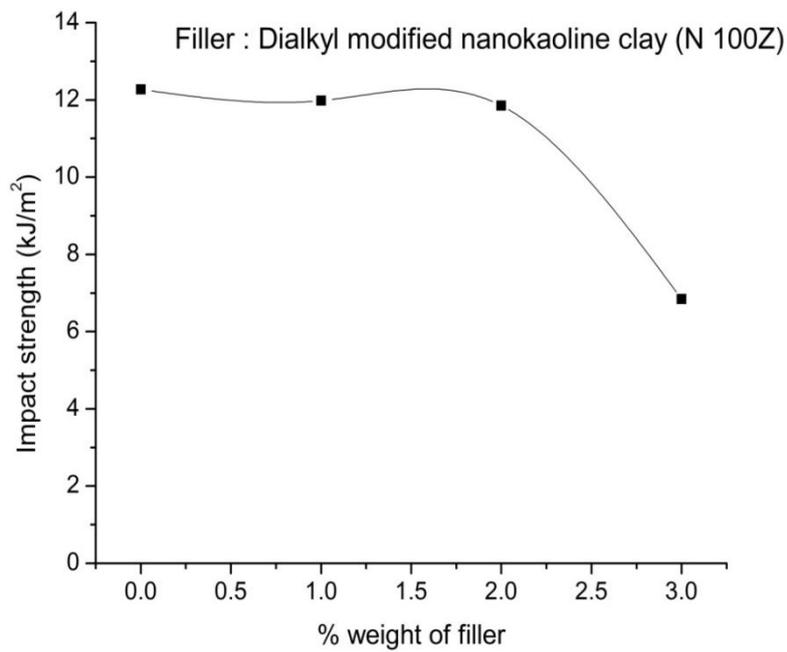


**Figure 3-15** Variation of impact strength of polyester nanocomposite with nanoclay (N 100Z) content

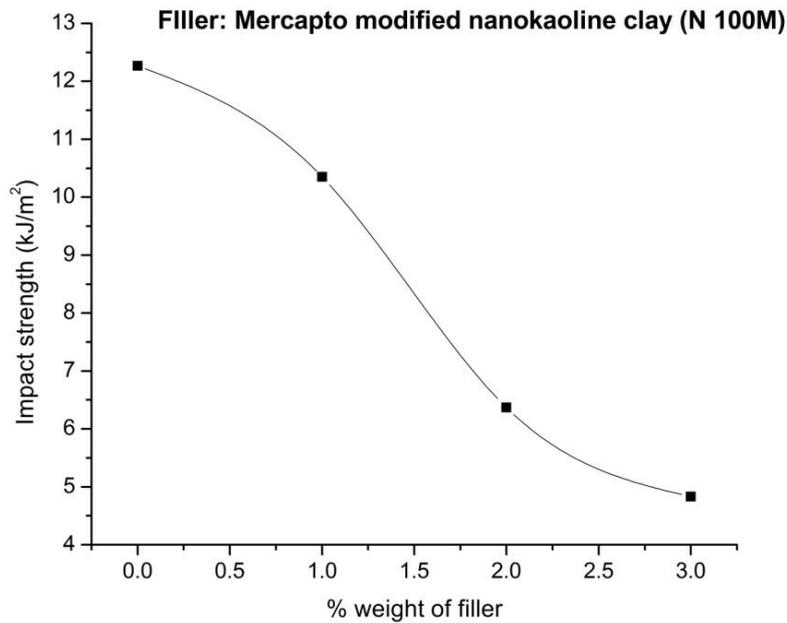


**Figure 3-16** Variation of impact strength of polyester nanocomposite with nanoclay (N 100M) content

### 3.3.3 SEM Analysis

Figure 3-17 (a) to (e) shows the SEM images of the fracture surface of pure polyester and nanokaoline clay filled polyester nanocomposite subjected to tensile test at a loading rate, CHS = 5 mm/min. Formation of voids and in homogeneity due to the non uniform mixing of the clay are evident from the images. The nature of fracture not much influenced by the presence of clay at its variation in quantity as per the images of 1% and 2% nanokaoline clay filled sample. Void formation is more with modified nanokaoline clay as compared to un modified nanokaoline clay. The fracture surface of both 1% and 2% nanoclay filled nanocomposite have a large degree of roughness as compared to the fracture surface of pure polyester. Hence a ductile nature of failure is evident for nanoclay filled sample. An effective and explainable material property change is not clear from the micro graphs of specimen.

However, the irregular nature of variation in mechanical properties such as tensile modulus and impact strength is in agreement with the SEM images. Fracture surface of pure resin indicates a brittle nature of failure as it is smooth.

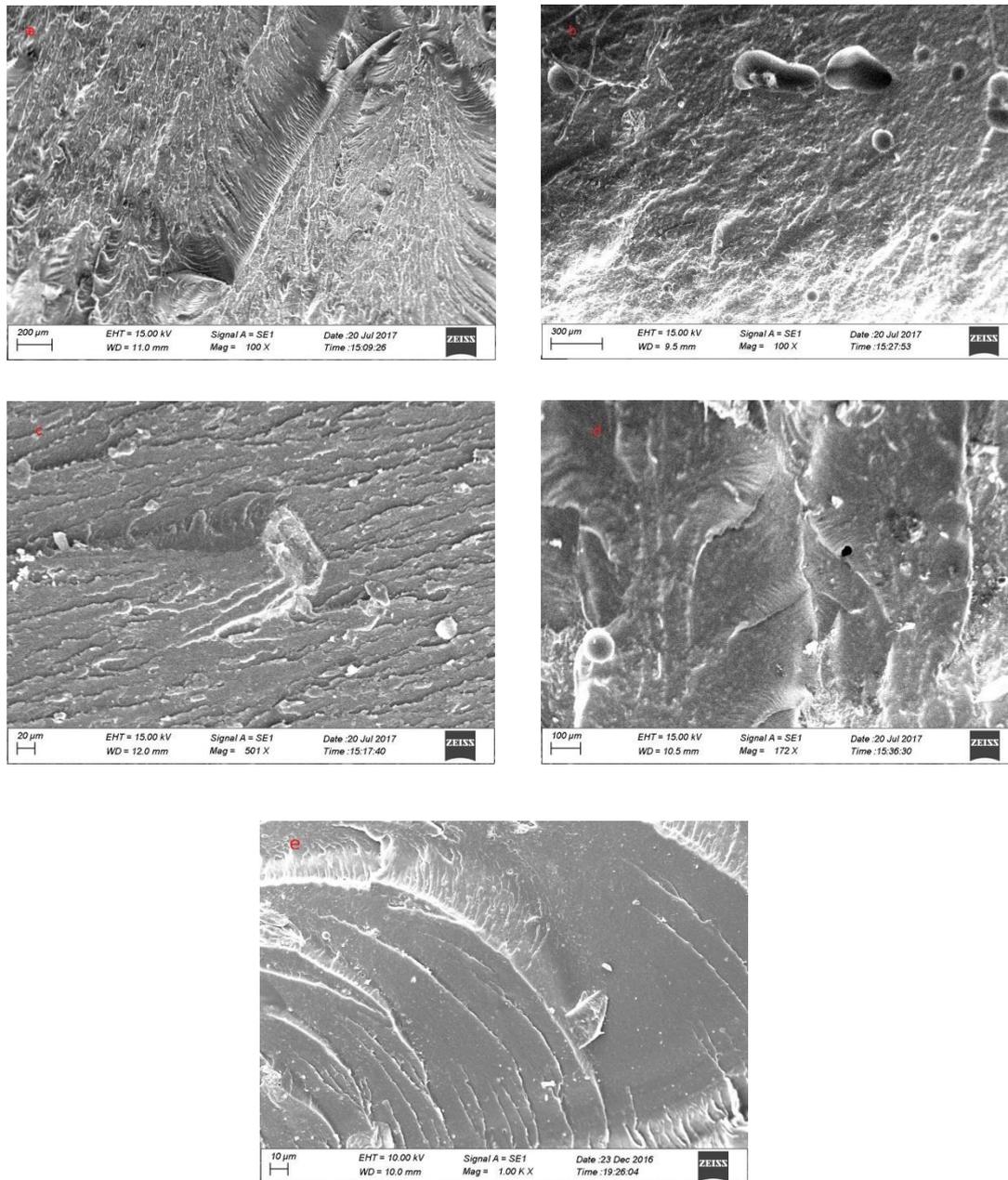


**Figure 3-17** SEM micrographs of fracture surface (a) 1% unmodified nanokaoline filled polyester (b) 1% mercapto modified nanokaoline filled polyester (c) 2% unmodified nanokaoline filled polyester (d) 2% mercapto modified nanokaoline filled polyester and (e) pure polyester

### 3.4 CONCLUSIONS

The following conclusions were drawn from the study of mechanical property variation of isophthalic polyester resin by incorporating unmodified nanokaoline clay and different types of modified nanokaoline clays:

1. The tensile modulus increases with clay content, indicating that the nanoclay reinforces the polyester. It shows 9 to 14 % increase in tensile modulus by adding 1% nanokaoline clay.
2. Nanocomposites with modified clay give higher tensile modulus as compared to nanocomposite with unmodified clay as filler.
3. Impact strength shows only marginal change with the addition of 1% nanoclay, whereas the strength reduced to about 40% by the addition of 2 to 3% nanoclay.
4. Since the improvement is not substantial, no consistent nature of variation is observed for both tensile modulus and impact strength.
5. It is evident from the SEM micrograph the presence of nanoclay induces a ductile nature of failure in the material.

## **CHAPTER 4**

# **MECHANICAL AND THERMAL CHARACTERIZATION OF ISOPHTHALIC POLYESTER-CLOISITE15A NANOCOMPOSITE**

### **4.1 INTRODUCTION**

Modification of isophthalic polyester resin by nanokaoline clay has resulted in modest improvement in mechanical properties (chapter 3). Modified nanokaoline clay gave better improvement as compared to unmodified nanokaoline clay. The modification by dispersion of nanokaoline clay in the polymer medium is observed to be cumbersome due to the agglomeration of nanokaoline clay particles. Hence the continuation of experiments with another filler material is significant from the importance of Composites. Since nano fillers have now emerged as the ultimate reinforcing fillers [79][80], more investigations are very relevant with new nanofillers. Modification of polyester resin with Cloisite15A, a modified montmorillonite is proposed.

Polymers filled with Montmorillonite (MMT) clay have attracted significant interest in recent years. Homogeneous dispersion of the nanoclay in the polymers is the most serious challenge and the main step in the synthesis of nanocomposites. Depending on the physical state of the polymer, different processing methods are used, such as in situ polymerization, high shear mixing, three-roll milling, and twin screw extrusion. Mohan et.al.[81] investigated rheology and curing characteristics of epoxy/clay nanocomposites. Improvements in the interlaminar fracture toughness and flexural strength by the addition of nanoclays to polymer have been reported by researchers.

About 38% improvement in flexural strength by the addition of 2 phr nanoclay to epoxy matrix had been reported. However, adding more clay (4 phr) leads to a drop in flexural strength. That means adding some clay can enhance the properties but adding more clay may not guarantee improvement. This is due to the increase in viscosity of the polymer on the addition of the clay and the augmentation of the amount of air bubbles during the mixing process [35].

Studies on clay added polymer indicate that the increase in the fracture surface area due to crack deflection is the major toughening mechanism in the clay/epoxy nanocomposite. When the clay particles are intercalated into the resin the potential toughening effect improved significantly as the fracture surface area becomes larger. It has been suggested that the exfoliated structure mainly leads to an improved modulus, while the remaining stacked structure of intercalated clay platelets is the key to improve toughness [83][84][85][86].

Improvement in the stress intensity factor noticed with nanoclay content for DGEBA-MMT clay composite with modified and unmodified MMT. The improvement in the elastic modulus was also reported but the failure strength and strain decreased [87]. Fracture toughness is a critical mechanical property which characterizes the resistance of a material to crack propagation. Improvement of fracture toughness and tensile strength by the addition of clay to polymer resin were reported by many researchers. But the impact strength has been decreased [88][89]. The improvement of tensile strength, elongation at break and shore D hardness of epoxy nanocomposite were also reported [90].

Studies on epoxy/ABS/ TiO<sub>2</sub> system proved that the impact and tensile strengths of the hybrid having similar TiO<sub>2</sub> content were increased with increasing ABS content to 4% and decreased with higher loadings. For specimens with similar ABS content, the impact and tensile strengths were increased with increasing TiO<sub>2</sub> content up to 6% and decreased at higher loadings. Thus the combination of layered and particulate nanofillers had synergistic effect on impact and tensile strengths of the epoxy polymer [97]. Generally the impact strength may increase by the presence of fibers. The presence of filler can impede crack growth due to the possibility of imposing a greater tendency for plastic deformation in the matrix [94]. Studies on the effect of fly ash on polypropylene reported the enhancement of flexural property [95].

Polyester resin is one of the most used thermosetting polymers. Its application in many fields is restricted by the brittleness. The increasing demand for a high performing material can be met by the performance improvement of an easily available low cost polymer such as polyester. The cost of raw material, quantity of the material as well as the processing method adopted will be the factors which control the cost of the product material.

In this chapter isophthalic polyester resin, which is of low cost as compared to epoxy and similar resin, is proposed to be modified using modified montmorillonite nanoclay. Properties such as tensile modulus, flexural modulus, impact strength, dynamic mechanical properties such as storage modulus, loss modulus and damping ratio, thermal stability etc. are proposed to be investigated. The behavior of the fracture surface under tensile load is also proposed to be examined using SEM.

## **4.2 METHODOLOGY**

The methodology adopted for the analysis of polyester- Cloisite15A nanocomposites at various filler content is described below in detail.

### **4.2.1 Raw materials**

Isophthalic polyester resin was used as the matrix material, cobalt naphthenate was used as the accelerator and methyl ethyl ketone peroxide (MEKP) as the catalyst. For easiness of processing, the clay was made into dispersion with styrene and then the dispersion was added to the polyester resin for modification. Cloisite15A, quaternary ammonium modified montmorillonite used as the nanofiller.

### **4.2.2 Specimen Preparation**

Test specimens for mechanical testing as per ASTM standards were prepared by casting. The mould made of Teflon sheet has mould cavities, which were shaped according the size and shape of specimen for different mechanical tests. The detailed procedure for the specimen preparation is described in chapter-2.

Specimen have been prepared for the nanoclay content 0%, 0.5%, 1%, 1.5% and 2% by weight of the polyester resin. Similar procedure had been adopted by Mirmohseni et.al. [78] Specimens for DMA were also prepared by casting. Samples with pure polyester and nanocomposite with nanofiller of percentage weight 0.5, 1, 1.5 and 2 were prepared.

### 4.2.3 Mechanical Characterization

The mechanical properties from tensile, flexural and impact tests obtained for analysis. Tensile test was carried out by a universal testing machine. The parameters considered for the tensile test were cross head speed (CHS) and percentage composition of the filler. For finding the effect of loading rate three test speeds: 0.5 mm/min, 5mm/min and 50 mm/min were used. The experiment was conducted for five specimens on each category viz pure polyester (0% Cloisite15A), 0.5 %, 1%, 1.5 % and 2 % filler incorporated samples. A photograph of the casted specimen used for tensile test is shown in figure 4-1

The impact property was determined by Izod impact test. Here the specimens were prepared by the method of casting. Samples of pure polyester, 0.5 % Cloisite15A filled, 1 % Cloisite15A filled, 1.5 % Cloisite15A filled and 2 % Cloisite15A filled nanocomposites were tested. The photograph of the specimen is shown in figure 4-2. Five samples of each category were experimented.



**Figure 4-1** specimen prepared for tensile test

The specimen prepared by the method of casting was used for flexural test. The photograph of the casted specimen is shown in figure 4-3. The test was carried out on universal testing machine for the loading rate, i.e. Cross Head Speed (CHS) 0.5 mm/min, 5 mm/min and 50 mm/min. The experiment was conducted on 5 specimens prepared under identical condition from each category.



**Figure 4-2** specimen prepared for impact test

#### **4.2.4 Dynamic Mechanical Analysis**

The specimens were prepared by casting in the size 63.5 mm length, 12 mm width and 3.3 to 4 mm thicknesses. Samples with various filler content such as 0%, 0.5%, 1%, 1.5% and 2% Cloisite15A were prepared. The specimen was mounted in dual cantilever mode in dynamic mechanical analyzer. The experiment was conducted at an oscillating frequency of 1 Hz, 10 Hz and 100 Hz. Measurements were done for each case separately in the temperature range from room temperature to 140°C at a heating rate, 2 °C/min. The signals are automatically used to determine the dynamic storage modulus ( $G'$ ), loss modulus ( $G''$ ) and the damping factor ( $\tan\delta$ ), which were plotted as a function of temperature. The  $\tan\delta$  peak was taken as the glass transition temperature ( $T_g$ ) of the tested samples.



**Figure 4-3** specimen prepared for flexural test

#### **4.2.5 Thermal Analysis**

Thermogravimetric analysis (TGA) measures weight changes in a material as a function of temperature (or time) under a controlled atmosphere. Its principle uses include measurement of a material's thermal stability, filler content in polymers,

moisture and solvent content, and the percent composition of components in a compound. TGA data obtained was the variation of weight and derived weight with respect to temperature. The Thermogravimetric analysis (TGA) was carried out on TGA Q500 instrument. The tests have been carried out in the temperature range from 0 to 800 °C in air. Specimen with and without nanoclay as filler i.e. pure polyester (0 % nanoclay), 0.5 % nanoclay, 1 % nanoclay, 1.5 % nanoclay and 2 % nanoclay were subjected to Thermogravimetric analysis.

Thermograms from differential scanning calorimetry were also obtained for nanocomposites with different filler content. The thermograms indicating the variation of heat flow with temperature is plotted. The DSC studies were carried out using DSC Q2000 Instrument. Test specimens weighing 5-10 mg are placed in pans for testing. It was heated at the rate 10 °C/min. The Instrument measures the additional heat flow required to maintain the sample pan at the same temperature as the reference pan. Thermograms of nanocomposites with different filler content viz pure polyester (0 % nanoclay), 0.5 % nanoclay, 1 % nanoclay, 1.5 % nanoclay and 2 % nanoclay were subjected to analysis.

#### **4.2.6 Study of Fracture surface**

SEM micrographs of fracture surface of polymer nanocomposites were obtained for the analysis. Tests were carried out with fracture surface of pure polyester and nanocomposites of different filler content such as 1% and 2% Cloisite15A, subjected to tensile loading at testing speed 5 mm/min to study the performance under loading. The SEM images obtained for the fracture surface of impact tested specimen. As a characterization technique and to examine the intercalation/exfoliation of clays in the

nanocomposite, X-Ray Diffractograms were taken to study the morphology of the nanocomposite.

**Table 4-1** Tensile properties of polyester nanocomposite with filler content (% weight of Cloisite15A) at different testing speed

| % weight of filler (Cloisite15A) | CHS = 0.5 mm/min       |                       | CHS = 5 mm/min         |                       | CHS = 50 mm/min        |                       |
|----------------------------------|------------------------|-----------------------|------------------------|-----------------------|------------------------|-----------------------|
|                                  | Tensile Strength (MPa) | Tensile Modulus (MPa) | Tensile Strength (MPa) | Tensile Modulus (MPa) | Tensile Strength (MPa) | Tensile Modulus (MPa) |
| 0                                | 59.48                  | 1018.99               | 57.24                  | 1605.59               | 49.51                  | 2002.67               |
| 0.5                              | 47.44                  | 1148.41               | 49.95                  | 2091.86               | 44.80                  | 2507.14               |
| 1                                | 42.05                  | 1239.53               | 37.97                  | 2109.53               | 39.06                  | 2192.19               |
| 1.5                              | 34.09                  | 1132.45               | 32.95                  | 1917.10               | 39.40                  | 1869.80               |
| 2                                | 35.10                  | 1059.17               | 35.60                  | 1672.11               | 28.76                  | 1674.86               |

**Table 4-2** Variation of impact strength of polyester nanocomposite with filler content (% weight of Cloisite15A)

| % weight of filler (Cloisite15A) | Impact strength (kJ/m <sup>2</sup> ) |
|----------------------------------|--------------------------------------|
| 0                                | 13.56                                |
| 0.5                              | 15.52                                |
| 1                                | 16.36                                |
| 1.5                              | 15.37                                |
| 2                                | 14.92                                |

## 4.3 RESULTS AND DISCUSSION

### 4.3.1 Tensile Test

Figure 4-4 shows the graphical plot of experimental values from tensile test indicated in Table 4-1. The tensile modulus improves with increase in clay content, reaches a

maximum value and thereafter decreases. The value of tensile modulus increases by 15 to 25 % at a nanoclay content of 0.5 to 1 % by weight of resin for different testing speed i.e. 0.5 mm/min, 5 mm/min as well as 50 mm/min. The maximum value is noticed with clay content of 0.5 to 1 wt%. Further increase in the nanoclay content resulted in the decrease of tensile modulus. This is due to the reason that, at lower percentage weight of filler, it will be dispersed properly in the polyester and will act as a reinforcing agent. However, at higher filler content the proper mixing of the filler in the polyester medium becomes too difficult because of the increase in viscosity of the mix, which will cause agglomeration of the clay platelets and also create more voids. Consequently there is the possibility for decrease in value of tensile modulus at higher filler content. The maximum tensile modulus of the material is obtained at maximum testing speed as expected. The nanoclay content above 1% is found not appreciable as the tensile modulus decreases. The improved modulus up to 1% nanoclay loading can be directly ascribed to the stiffening effect of clay fillers since the clay has higher modulus than polyester. However, the limited improvement in some cases may be related to the microstructures formed under the present processing conditions. Also at increased level of clay content the decrease of stiffness can be attributed to the improper dispersion, agglomeration of clay platelets and formation of voids, which is evident from the SEM images [87].

The tensile modulus shows the maximum value at higher loading rate i.e. Cross Head Speed, CHS = 50 mm/min, as compared to other loading rate, which is an indication of the improved performance of the material under impact load rather than gradually applied load.

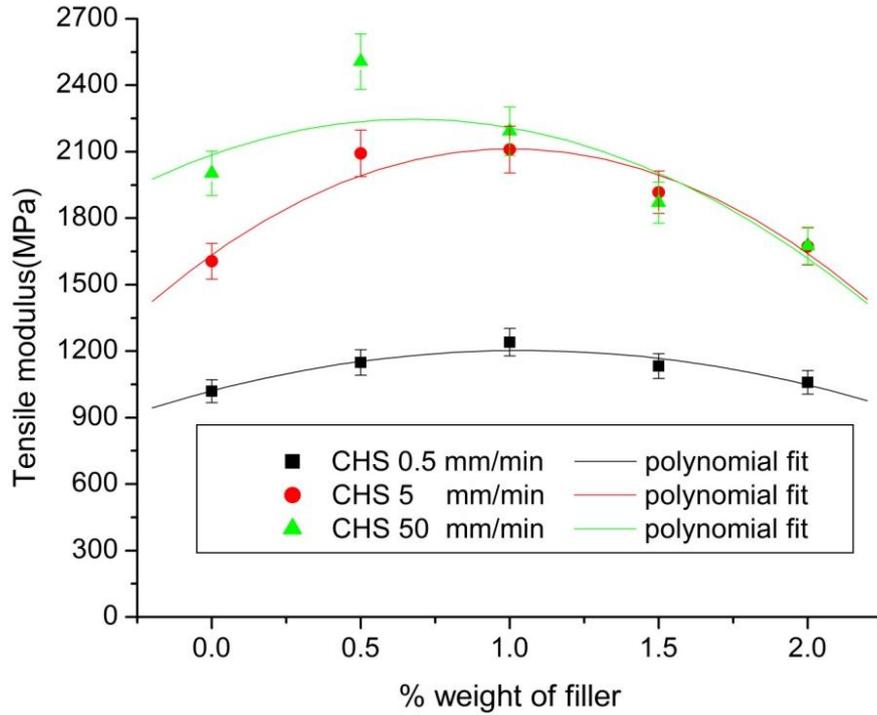


**Figure 4-4** Variation of tensile modulus of polyester nanocomposite with filler content (% weight of Cloisite15A) at different testing speeds

**Table 4-3** Variation of flexural properties of polyester nanocomposite with filler content (% weight of Cloisite15A) at different testing speeds

| % weight of filler (Cloisite15A) | CHS = 0.5 mm/min          |                            | CHS = 5 mm/min            |                            | CHS = 50 mm/min           |                            |
|----------------------------------|---------------------------|----------------------------|---------------------------|----------------------------|---------------------------|----------------------------|
|                                  | Flexural modulus in (MPa) | Flexural Strength in (MPa) | Flexural modulus in (MPa) | Flexural Strength in (MPa) | Flexural modulus in (MPa) | Flexural Strength in (MPa) |
| 0                                | 3829.42                   | 79.28                      | 4032.05                   | 78.68                      | 4375.76                   | 69.45                      |
| 0.5                              | 4639.18                   | 68.44                      | 4875.72                   | 71.56                      | 4877.10                   | 62.84                      |
| 1                                | 5116.62                   | 63.77                      | 5323.97                   | 67.74                      | 5325.57                   | 61.99                      |
| 1.5                              | 5299.09                   | 68.78                      | 5585.54                   | 62.81                      | 5635.61                   | 63.46                      |
| 2                                | 5733.91                   | 66.39                      | 5874.23                   | 67.49                      | 6035.12                   | 60.64                      |

The value of tensile modulus obtained is high for CHS 5 mm/min and 50 mm/min as compared to CHS 0.5 mm/min. The effect of the addition of filler in polyester resin for its improvement in tensile modulus is much more evident in high loading rate as

compared to low loading rate. The nature of loading at low CHS is gradually applied and leads to a ductile mode of failure for the composite. But a sudden application load during the CHS 5 mm/min and 50 mm/min induce a brittle nature of failure with undue delay in loading. Consequently the tensile modulus was found to be high for high testing speed.

### **4.3.2 Impact Test**

Table 4-2 indicates the experimental results of impact test. The impact strength is found to increase significantly from 13.56 kJ/m<sup>2</sup> for pure polyester resin to 16.36 kJ/m<sup>2</sup> by the incorporation of 1 wt% Cloisite15A, while the impact strength decreased for higher filler loading. Figure 4-5 shows the variation of impact strength with filler content. It increased to about 15 and 20 % with the addition of 0.5 and 1 wt% nanoclay. However the trend is found decreasing for the nanoclay loading above 1%. The reduced strength at higher wt% may be caused due to the weakening of the clay matrix interface because of the improper dispersion and agglomeration. Also with increase of clay content there is the possibility for the formation of voids due to the improper dispersion, which also causes the weakening of interface, makes the crack formation easy and hence the reduction of impact strength [88]. The brittle nature of failure is evident from the SEM image of the fracture surface indicated in figure 4-22 for the nanoclay added polyester. As compared to the SEM images of the neat resin sample, the fracture surface of nanocomposite appeared to have a large degree of roughness [117]. Unlike the tensile loading, the failure mode will be brittle under impact loading, which also may contribute to reduced impact strength at high filler content.

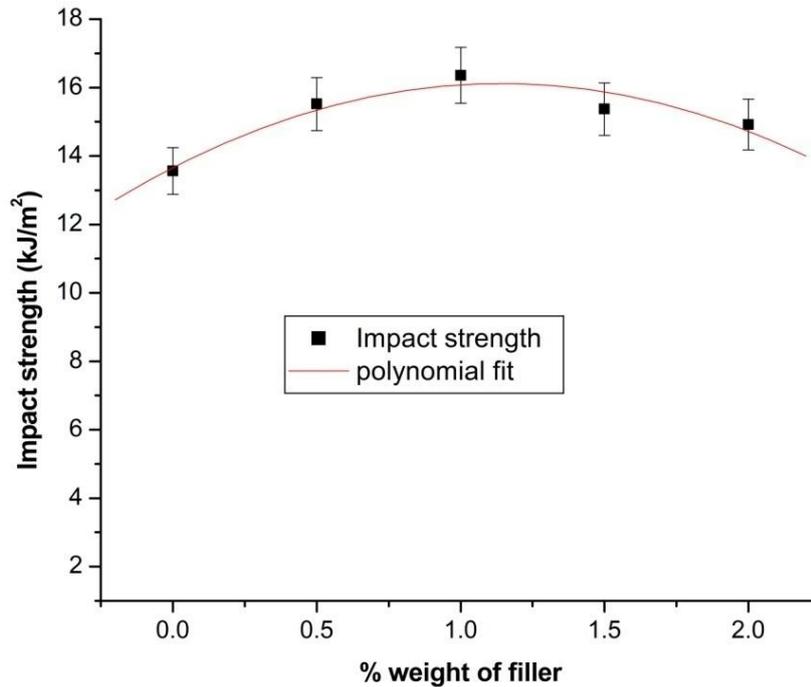


**Figure 4-5** Variation of impact strength of polyester nanocomposite with filler content (% weight of Cloisite15A)

### 4.3.3 Flexural Test

The graphical plot of flexural test results is shown in figure 4-6. The flexural modulus shows a continuous improvement with increase in clay content as in the case of tensile modulus for CHS 0.5 mm/min and 50 mm/min. However there is a short fall of flexural modulus for nanocomposite with 1.5 % filler content at loading rate, CHS = 5 mm/min. The flexural strength decreased with increase of filler content. A maximum of 79.28 MPa is observed for pure polyester and minimum of 60.64 MPa obtained for 2 % filler content. The flexural modulus increases for smaller filler concentration whereas at higher filler concentration i.e. to 2% by weight of filler content it does not show as much as increase in its value for 0.5% filler content. At smaller particle content the interaction of the particle with the matrix will be higher

and the agglomeration will be less which will be responsible for the high flexural modulus value. However, at high filler content the possibility for the agglomeration reduces the strength and stiffness [95][112]. The interfacial adhesion may be improved due to the dispersion of nanoclay, which may restrict the mobility of the matrix at the interface. Also the reinforcement efficiency show strong dependence on dispersion of nanoparticles. Well-dispersed nanoparticles can effectively enhance the comprehensive properties of nanocomposites [92]. The flexural modulus shows about 21 to 35 % increase by the addition of 1% nanoclay and 35 to 50% increase by the addition of 2% nanoclay.

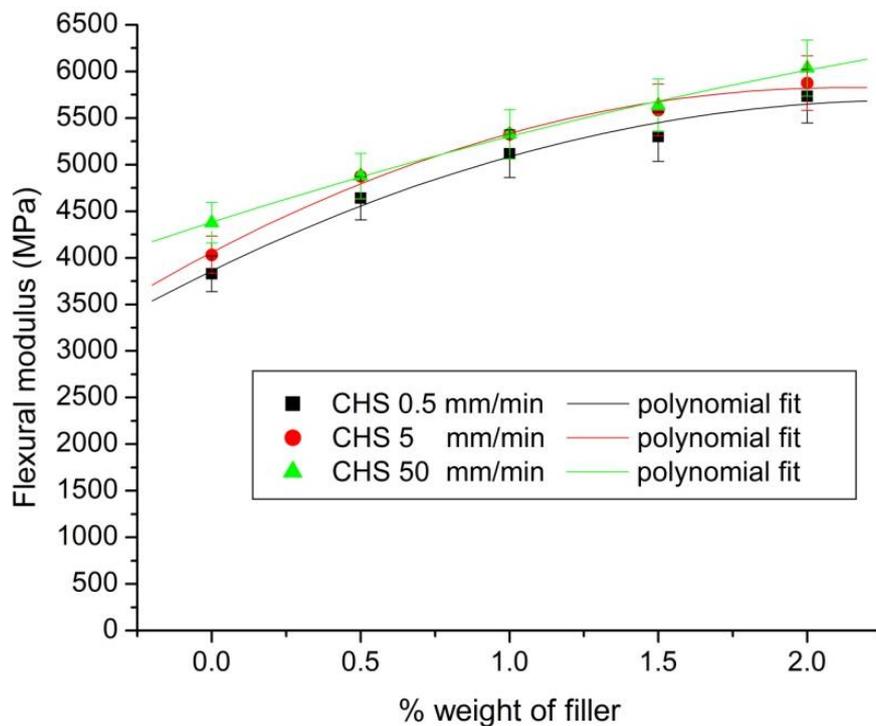


**Figure 4-6** Variation of flexural modulus of polyester nanocomposite with filler content (% weight of Cloisite15A) at different testing speeds

The physical interference of particles in the polymer matrix restricts the elongation at break and an increase of modulus. Unlike the impact loading, the ductile nature of failure during flexural loading may be the reason for the sustainability with the hike of flexural modulus. For a solid conclusion more analysis is required.

#### **4.3.4 Dynamic Mechanical Analysis**

In Dynamic Mechanical Analysis, the sample is subjected to a sinusoidal mechanical vibration. Here the experiment is conducted at frequency 1 Hz, 10 Hz and 100 Hz. Dynamic mechanical characteristics were studied from storage modulus, loss modulus and damping factor. The detailed discussion about each is given below.

#### **Storage Modulus of Nanocomposite**

Figures 4-7 to 4-9 show the graphical plot of storage modulus ( $G'$ ) as a function of temperature for the pure polyester resin and nanocomposite with different weight percentages of nanoclay. Even though there is no consistent change of storage modulus with increase of clay content, 1% nanoclay filled sample shows high value of storage modulus for 10 Hz and 100 Hz frequencies. 1.5% Cloisite15A filled nanocomposite also shows a value almost near to maximum for 1Hz frequency. In all the three frequencies, i.e. 1, 10 and 100 Hz as well as at various temperature ranges it has become evident that 1 or 1.5 % Cloisite15A filled nanocomposites dominate with maximum value of storage modulus. The storage modulus is low for 2% nanoclay filled samples for all the three frequencies as well as various temperature ranges. The stiffness effects introduced by nanoclay enable the composite to retain high storage modulus with 1 or 1.5 % nanoclay filled samples [95]. However, the effect is not predominant for samples with 2%

nanoclay as the non uniform distribution of clay particles due to agglomeration which leads to uneven variation of mechanical reinforcement effect which increases with the nanoclay content [97]. The storage modulus is high for frequency 100 Hz as compared to 1 Hz and 10 Hz for the sample with 1 % nanoclay. This is an indication of the increase in the stiffness with the addition of nanoclay.

The comparison of storage modulus shows that by the addition of clay there is an increase of storage modulus initially, but the value decreases with further increase of clay content. About 35 to 40% increase in the storage modulus reported at room temperature but the difference is very small when the temperature approaches to glass transition temperature,  $T_g$ . The initial increase can be attributed to the property of the clay to act as reinforcement to some extent. But further addition may create agglomeration of clay particles, which reduces the strength. Up to 75°C there is only a very little change in the storage modulus. After that the rate of decrease in storage modulus is high. This is due to the weakening of intermolecular bonding in the polymeric matrix with the increase of temperature.

It can be seen that , the initial value of storage modulus is high for each sample at the ambient temperature due to the fact that, at this stage the molecules are in the frozen state, therefore they retain high stiffness properties in the glassy condition.  $G'$  is high when the molecular movement is limited or restricted and it consequently will cause the storage of mechanical energy. The stiffening effect is more remarkable at lower temperature. This phenomenon is explained by the mismatch in coefficient of thermal expansion between the matrix and inorganic fillers, which might allow better stress transfer between matrices and fillers at low temperatures [96]. The pattern of

decrement in the storage modulus value with the increasing temperature is due to the fact that, the matrix reaches its softening point and there by reduces the elastic response of the material.

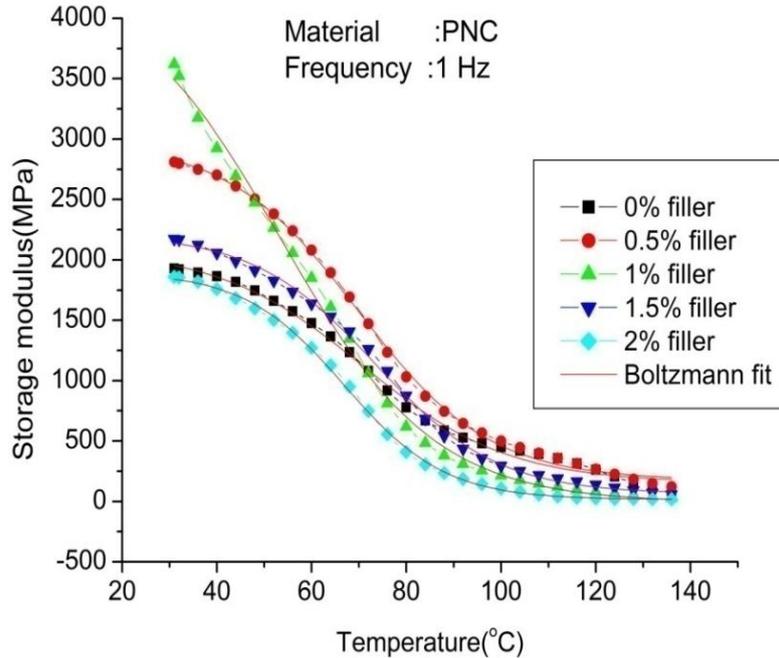


**Figure 4-7** Variation of storage modulus of polyester nanocomposite with temperature for different filler (Cloisite15A) content at frequency 1 Hz

As the temperatures approaches the glass transition temperature region, around 90 °C, there is a large drop in the storage modulus values. This indicates the phase transition from the rigid glassy state, where the molecular motions are restricted to a flexible rubbery state, where the molecular chains have greater freedom to move. When the polymer and its composites are heated above their T<sub>g</sub>, an increase in free volume occurs followed by an increase in molecular mobility [97]. Under this situation, the chain segments gradually align with the applied force. When this occurs, the storage modulus G' decreases. It is also observed that the curves tend to converge to that of pure Polyester at higher temperature i.e. above 120 °C, which means the nanoclay could not play any significant role in storage modulus at high temperature.

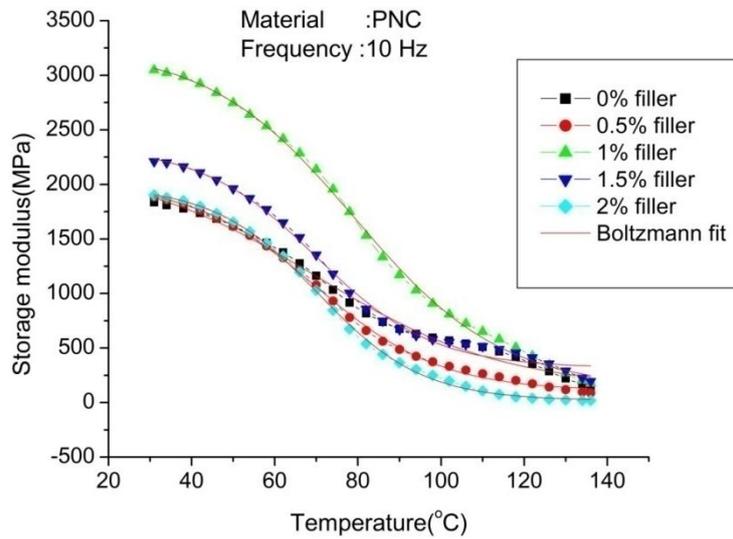


**Figure 4-8** Variation of storage modulus of polyester nanocomposite with temperature for different filler (Cloisite15A) content at frequency 10 Hz

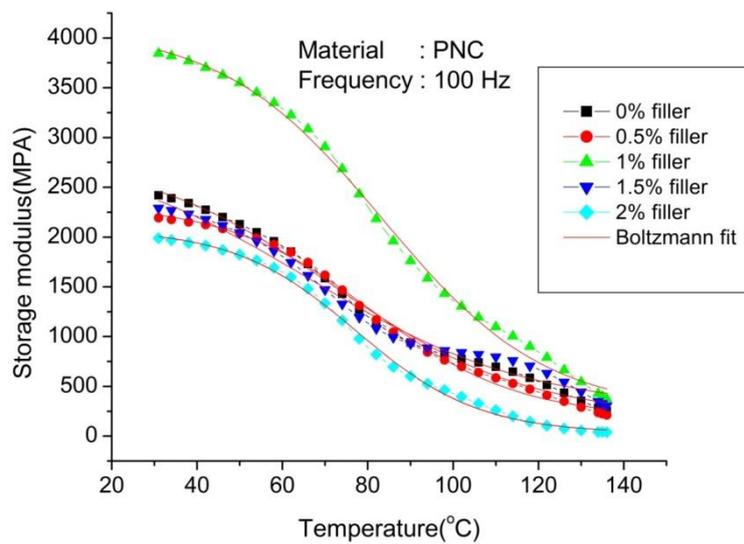


**Figure 4-9** Variation of storage modulus of polyester nanocomposite with temperature for different filler (Cloisite15A) content at frequency 100 Hz

## Loss Modulus of Nanocomposite

Figure 4-10 to 4-12 shows the graphical plot of loss modulus ( $G''$ ) with temperature for various specimens of nanocomposite prepared by varying the composition of nanoclay. The experimental results at frequency 1 Hz, 10 Hz and 100 Hz are obtained. No consistent nature can be interpreted for the variation of Loss modulus at various temperature levels. The peak values of loss modulus are observed around 80 to 90 °C for all the frequencies 1Hz, 10 Hz and 100 Hz. There is an increased rate for the decrease of loss modulus after the peak for nanocomposite as compared to pure resin. The rate of decrease of loss modulus is more for 2% nanoclay filled sample as compared to other samples. Approximately 38% hike in loss modulus can be observed at the glass transition region by the incorporation of 1% Cloisite15A to the resin. There is an increase in the amplitude of loss modulus pattern for the samples with 0.5 and 1.5 % clay, which is an indication of the increased amount of amorphous part in that sample [98]. This indicates higher viscosity as a result of the molecular movement restriction due to the presence of the fillers. Thus, higher the nanoclay content, the higher the viscosity, which at the end requires higher needs for energy dissipation. Secondly it can be concluded that the inclusion of nanoclay shows negligible effect to the peak temperature of loss modulus. The transition peak shown in  $G''$  is around 85 to 90°C.

The  $G''$  peak reached maximum value near the  $T_g$  and then decreases with the increase of temperature. The temperature range from 85 to 90°C represent a transition region from the glassy state to a rubbery state [96][97]. Above the transition temperature, the  $G''$  curve dropped gradually indicating the increase of the flow of the chain movement, thus reducing the viscosity.

The slight decrease in the  $T_g$  could be ascribed to the presence of a limited amount of unreacted polyester resin, that can have some plasticization effect, while the reduction of the height of the relaxation processes can be related to the non-dissipative nature of the filler, which reduces the viscoelastic response of the composite. The interfacial losses will be very small when the matrix/filler interfacial bonding is good. The increased interfacial adhesion leads to an overall increase in the elastic modulus, which is reflected in the plot of storage modulus [113].

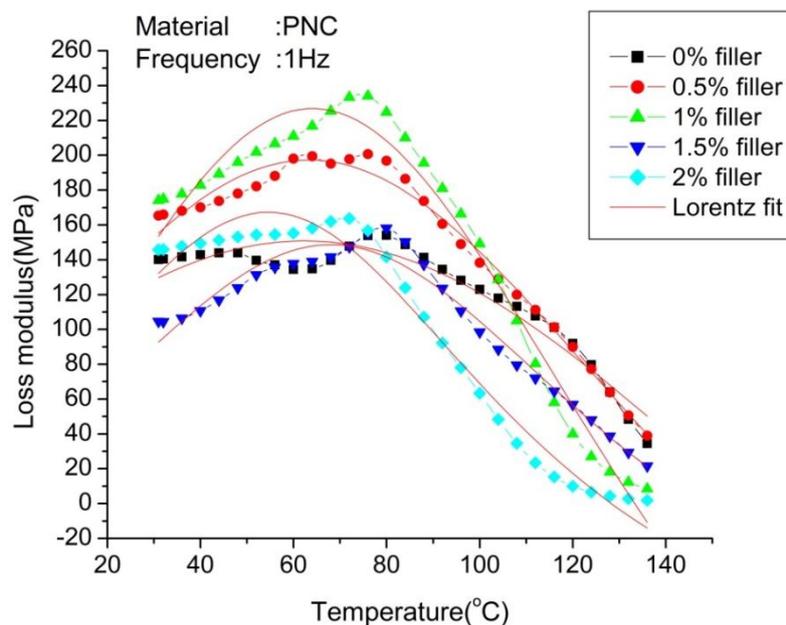


**Figure 4-10** Variation of loss modulus of polyester nanocomposite with temperature for different filler (Cloisite15A) content at frequency 1 Hz

As temperature continues to increase above the glass transition molecular frictions are reduced, less energy is dissipated and the loss modulus again decreases. This higher temperature decrease in loss modulus results in a peak in loss modulus in the glass transition region. The glass transition region is special because it is a transition in molecular response revealed as a change in properties.

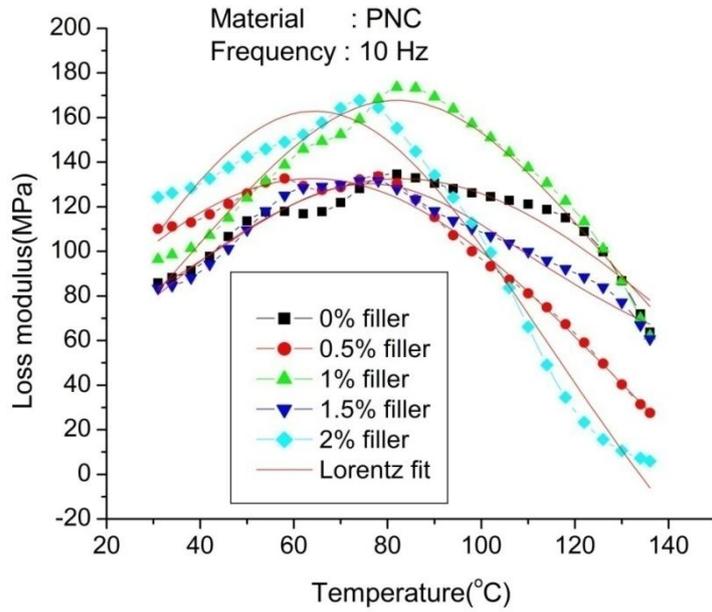


**Figure 4-11** Variation of loss modulus of polyester nanocomposite with temperature for different filler (Cloisite15A) content at frequency 10 Hz

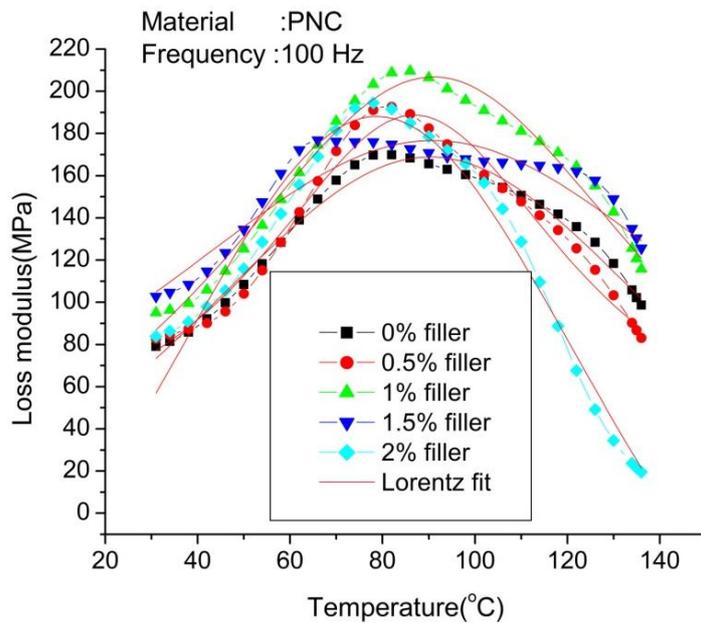


**Figure 4-12** Variation of loss modulus of polyester nanocomposite with temperature for different filler (Cloisite15A) content at frequency 100 Hz

### **Damping Factor ( $\tan\delta$ / $\tan\delta$ )**

Figures 4-13 to 4-15 describe the variation of damping factor,  $\tan\delta$  with temperature for different nanocomposites, obtained from the experiments conducted at frequency 1Hz, 10Hz and 100 Hz. The trend of variation obtained was similar to that of loss modulus. The value of  $\tan\delta$  indicates the relative importance of both viscous and elastic behaviors of materials, whereby  $\tan\delta < 1$  exhibits more elastic behavior and may behave like solid, while  $\tan\delta > 1$  exhibits more viscous behavior and behaves more like liquid [97]. It is evident from the figure that, the range of  $\tan\delta$  is  $< 1$ , which exhibits that the fabricated composites behave like a solid. The 2% Cloisite15A filled nanocomposite showed a markedly higher damping than the pure polyester. Whereas, only a minor increase in  $\tan\delta$  value is obtained for other composition except in the case of frequency 1 Hz. This indicates more viscoelastic energy dissipation with the presence of nanoclay. From the damping factor curves,  $T_g$  of the composites can be determined by the  $\tan\delta$  peak temperature. It can be seen that there is no significant shift in glass transition temperature,  $T_g$  with nanoclay content. The peak for each curve falls at the same temperature range or only a slight variation was recorded. This phenomenon may be contributed by extremely low percentages of clay which used for the nanocomposites. The  $\tan\delta$  value of pure polyester is approximately 0.5 and on increasing the filler  $\tan\delta$  values increase up to 0.75 in different cases.

Generally we can conclude that, the filler can induce damping of vibrations due to scattering and assist in dissipation of energy within the matrix. The temperature at which maximum damping occurs (Glass Transition ' $T_g$ ') same for all nanocomposites

except for 2% nanoclay filled sample. A similar trend is obtained for 1% nanoclay filled sample at frequency 1 Hz. The same can be observed from the  $\tan \delta$  plot for 1% and 2% Cloisite15A filled sample at different frequencies.

The maximum value for  $\tan \delta$  observed at 1Hz frequency. Thus the damping property will be dominated at low frequency loading, where the storage modulus reported low value.

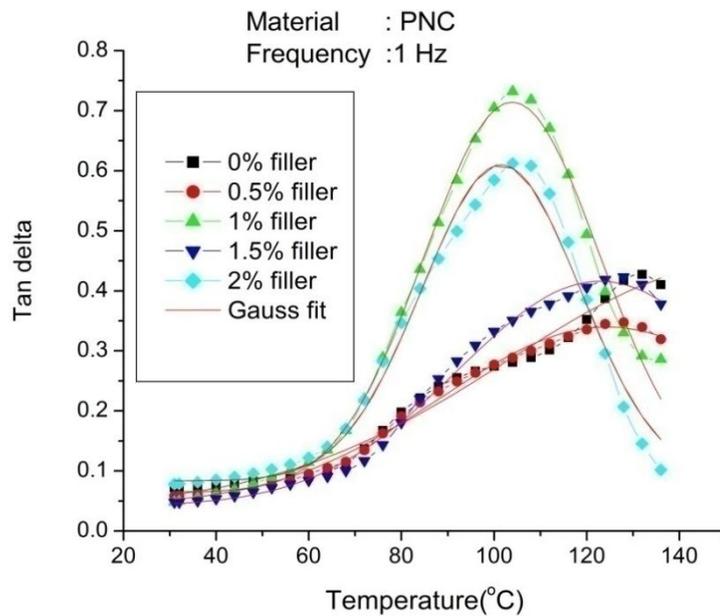


**Figure 4-13** Variation of  $\tan \delta$  of polyester nanocomposite with temperature for different filler (Cloisite15A) content at frequency 1 Hz

There is a shift in the  $\tan \delta$  peak towards lower temperature with the increase of nanoclay content. This can be explained on the basis of variation in the cross linking density. Researchers reported that the variation in the cross linking resulted from the inclusion of nanoparticles, creates an increase in the glass transition temperature ( $T_g$ ) at low cross-link density and a decrease in  $T_g$  at higher cross-link densities. Moreover, increasing cross-link density leads to an increased network disruption due to the presence of nanoparticle obstacles in densely connected network [116].

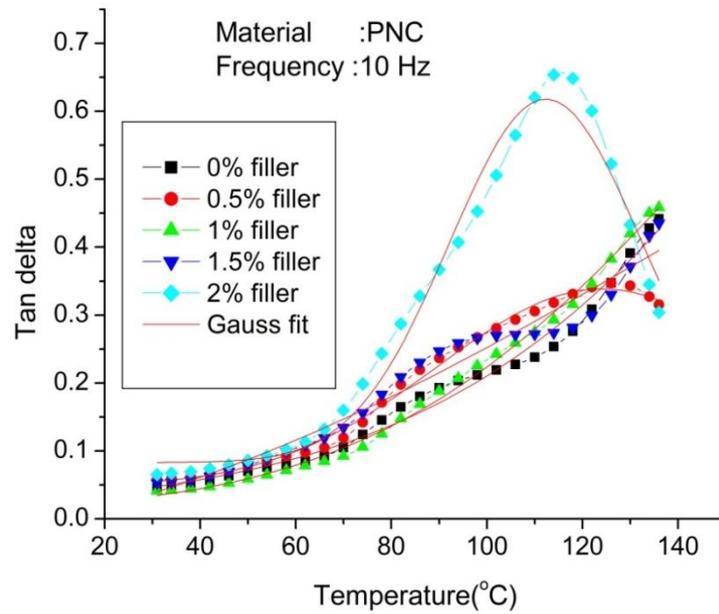


**Figure 4-14** Variation of  $\tan\delta$  of polyester nanocomposite with temperature for different filler (Cloisite15A) content at frequency 10 Hz

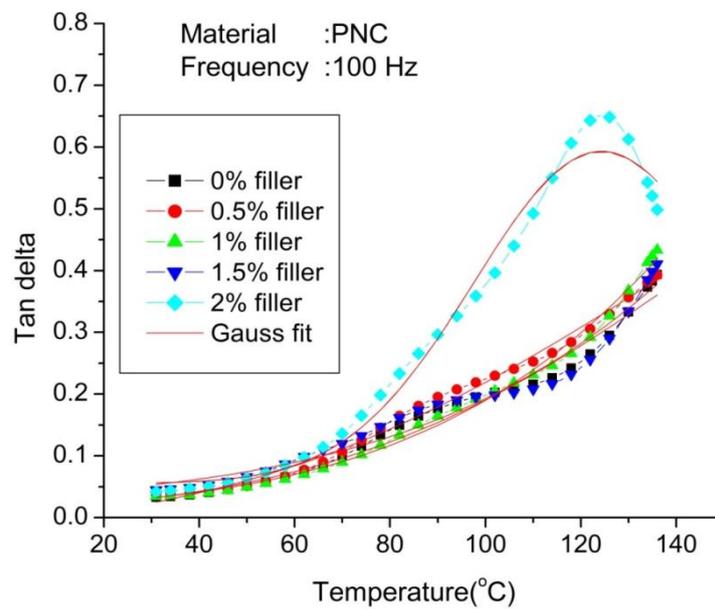


**Figure 4-15** Variation of  $\tan\delta$  of polyester nanocomposite with temperature for different filler (Cloisite15A) content at frequency 100 Hz

**Table 4-4** Values of parameters A,B ,C and regression coefficient of the mathematical model obtained from polynomial fit for mechanical properties.

| Parameters     | Tensile modulus     |                   |                    | Flexural modulus    |                   |                    | Impact strength |
|----------------|---------------------|-------------------|--------------------|---------------------|-------------------|--------------------|-----------------|
|                | CHS = 0.5<br>mm/min | CHS = 5<br>mm/min | CHS = 50<br>mm/min | CHS = 0.5<br>mm/min | CHS = 5<br>mm/min | CHS = 50<br>mm/min |                 |
| A              | -172.40             | -477.80           | -401.70            | -298.53             | -370.47           | -97.74             | -1.90           |
| B              | 357.70              | 947.41            | 44.90              | 1490.84             | 1619.77           | 1010.92            | 4.31            |
| C              | 1020                | 1648.89           | 2107.46            | 3880.60             | 4074.23           | 4385.52            | 13.68           |
| R <sup>2</sup> | 0.906               | 0.919             | 0.762              | 0.982               | 0.933             | 0.998              | 0.902           |

**Table 4-5** Values of parameters and regression coefficient of the mathematical model obtained from Boltzmann fit for storage modulus at different testing frequencies.

| Parameters  | 1Hz            |                |                |       |                | 10Hz           |                |                |       |                | 100 Hz         |                |                |       |                |
|-------------|----------------|----------------|----------------|-------|----------------|----------------|----------------|----------------|-------|----------------|----------------|----------------|----------------|-------|----------------|
|             | A <sub>1</sub> | A <sub>2</sub> | X <sub>0</sub> | dx    | R <sup>2</sup> | A <sub>1</sub> | A <sub>2</sub> | X <sub>0</sub> | dx    | R <sup>2</sup> | A <sub>1</sub> | A <sub>2</sub> | X <sub>0</sub> | dx    | R <sup>2</sup> |
| 0% filler   | 2066.04        | 155.08         | 70.88          | 15.32 | 0.965          | 21.86          | 127.02         | 70.04          | 22.58 | 0.993          | 2809           | 185.22         | 71.91          | 22.81 | 0.994          |
| 0.5% filler | 2983.97        | 177.36         | 69.78          | 13.83 | 0.998          | 2023.02        | 105.82         | 69.89          | 14.33 | 0.998          | 2333.48        | 188.9          | 80.95          | 17.21 | 0.997          |
| 1% filler   | 4364.30        | -10.54         | 53.441         | 16.15 | 0.997          | 3258           | 126.37         | 79.19          | 17.68 | 0.998          | 4108.82        | 243.06         | 83.56          | 19.02 | 0.998          |
| 1.5% filler | 2216.41        | 62.33          | 73.43          | 12.89 | 0.990          | 2348.99        | 318.19         | 70.05          | 13.91 | 0.994          | 2914.17        | 261.24         | 66.066         | 26.04 | 0.983          |
| 2% filler   | 1901.17        | 15.256         | 66.99          | 10.59 | 0.993          | 1986.33        | 18.14          | 70.38          | 12.54 | 0.990          | 2082.06        | 28.03          | 77.34          | 14.30 | 0.998          |

**Table 4-6** Values of parameters and regression coefficient of the mathematical model obtained from Lorentz fit for loss modulus at different testing frequencies.

| Parameters  | 1Hz     |       |        |           |       | 10Hz    |       |        |           |       | 100 Hz  |       |        |           |       |
|-------------|---------|-------|--------|-----------|-------|---------|-------|--------|-----------|-------|---------|-------|--------|-----------|-------|
|             | $y_0$   | $x_c$ | W      | A         | $R^2$ | $y_0$   | $x_c$ | W      | A         | $R^2$ | $y_0$   | $x_c$ | W      | A         | $R^2$ |
| 0% filler   | -460.28 | 62.37 | 331.50 | 318233.46 | 0.928 | -226.25 | 82.71 | 251.59 | 141815.25 | 0.919 | -83.85  | 9.23  | 151.96 | 60333.79  | 0.979 |
| 0.5% filler | -292.68 | 63.32 | 211.09 | 162482.21 | 0.985 | -256.91 | 63.99 | 237.94 | 145987.65 | 0.992 | 13.93   | 86.80 | 83.85  | 23027.63  | 0.972 |
| 1% filler   | -369.95 | 64.11 | 176.69 | 165648.58 | 0.973 | -116.10 | 81.95 | 155.52 | 69353.43  | 0.963 | -36.64  | 91.02 | 121.94 | 46638.67  | 0.978 |
| 1.5% filler | -128.61 | 68.02 | 147.12 | 63976.72  | 0.969 | 13.37   | 76.01 | 110.95 | 20389.97  | 0.965 | -35.14  | 90.94 | 167.46 | 55732.03  | 0.882 |
| 2% filler   | -125.76 | 54.57 | 127.83 | 58851.30  | 0.972 | -243.52 | 64.43 | 169.71 | 108346.88 | 0.975 | -253.80 | 78.76 | 147.06 | 102084.98 | 0.970 |

**Table 4-7** Values of parameters and regression coefficient of the mathematical model obtained from Gaussian fit for tandelta ( $\tan\delta$ ) at different testing frequencies

| Parameters  | 1Hz   |        |        |       |       | 10Hz   |        |        |         |       | 100 Hz |        |        |         |       |
|-------------|-------|--------|--------|-------|-------|--------|--------|--------|---------|-------|--------|--------|--------|---------|-------|
|             | $y_0$ | $x_c$  | W      | A     | $R^2$ | $y_0$  | $x_c$  | W      | A       | $R^2$ | $y_0$  | $x_c$  | W      | A       | $R^2$ |
| 0% filler   | 0.039 | 153.69 | 100.71 | 51.17 | 0.980 | 0.013  | 353.04 | 214.33 | 863.69  | 0.986 | 0.0009 | 231.68 | 159.82 | 147.52  | 0.979 |
| 0.5% filler | 0.043 | 124.34 | 71.26  | 26.49 | 0.995 | 0.048  | 124.08 | 68.89  | 25.13   | 0.995 | -0.033 | 220.67 | 171.18 | 146.22  | 0.992 |
| 1% filler   | 0.064 | 103.91 | 37.91  | 30.87 | 0.994 | 0.009  | 221.89 | 142.33 | 165.95  | 0.996 | 0.004  | 353.44 | 205.28 | 1007.04 | 0.994 |
| 1.5% filler | 0.041 | 122.88 | 61.24  | 28.75 | 0.995 | -0.110 | 255.05 | 243.85 | 249.002 | 0.964 | 0.021  | 393.91 | 232.98 | 1206.49 | 0.963 |
| 2% filler   | 0.083 | 101.51 | 34.19  | 22.57 | 0.984 | 0.082  | 112.35 | 40.199 | 26.97   | 0.982 | 0.055  | 124.33 | 53.36  | 35.98   | 0.965 |

#### 4.3.5 Model Analysis

Mathematical equations were obtained for the mechanical and dynamic mechanical behavior of the material by comparing with the standard models available in the software, Origin 6.1. Polynomial fit found to be the best for the Mechanical properties such as tensile modulus, Flexural modulus and Impact strength. Boltzmann model, Lorentz model and Gaussian model were used respectively for the analysis of Dynamic Mechanical behaviors such as Storage modulus, Loss modulus and Damping factor ( $\tan\delta$ ).

##### Model for Tensile Modulus

The mathematical expression obtained by fitting the experimental data from tensile tests conducted for various polyester nanocomposites at different testing speed (CHS) to polynomial function is

$$E_T = Ax^2 + Bx + C \quad (4.1)$$

Where,  $E_T$  is the tensile modulus (TM) and “ $x$ ” is the percentage weight of filler.  $A$ ,  $B$  and  $C$  are parameters which depend on the loading condition i.e. CHS. From the above equation, tensile modulus is found to vary with percentage weight of filler and the loading condition, i.e. whether the load applied is gradual (CHS 0.5 mm/min), sudden (CHS 5 mm/min) or impact nature (CHS 50 mm/min). The numerical values of  $A$ ,  $B$  and  $C$  are as shown in Table 4-4. The value of regression coefficient  $R^2$ , also indicated in the table for respective cases. The regression coefficient is above 0.9 except for CHS 50 mm/min. The polynomial fit is selected because of the value of  $R^2$ ,

is high for polynomial fit out of the different models such as exponential fit, logarithmic fit, sigmoidal fit were compared. The tensile modulus peaks at about 0.5 to 1 % weight of filler as per the model. The tensile modulus is maximum when the filler 1% for CHS =0.5 mm/min. For CHS=5 mm/min the tensile modulus peaks when filler 0.75% and for CHS =50 mm/min, the tensile modulus maximum when filler 0.5%. Hence the trend from experimental values is in agreement with the model.

### **Model for Impact Strength**

Similar to tensile test results, the experimental data from impact test were also found to be agreeing with polynomial function which was used to fit the data. The mathematical model obtained is given in equation 4.2. Thus the variation of impact strength of the PNCs is

$$Y_i = Ax^2 + Bx + C \quad (4.2)$$

Where  $Y_i$  is the impact strength and  $x$  is the percentage weight of filler. The value of non dimensional parameters A, B and C are tabulated in Table-4.4. From the model, the value of impact strength found varies with the percentage weight of filler. Again the value of non dimensional parameters depends on the percentage weight of filler. Thus from the factors considered, the impact strength varies with percentage weight of filler.

### Model for Flexural Modulus

The variation of Flexural modulus with the percentage weight of filler as well as the loading condition i.e. CHS can be modeled to obtain the mathematical expressions

$$E_F = Ax^2 + Bx + C \quad (4.3)$$

Where, 'E<sub>F</sub>' is the flexural modulus and  $x$  is the percentage weight of filler. A, B and C are non dimensional parameters which depends on the two variables considered, that are the loading condition and percentage weight of filler for analysis. Thus the flexural modulus found to be varying with percentage weight of filler and the loading condition, i.e. whether the load applied is gradual (CHS: 0.5 mm/min), sudden (CHS 5 mm/min) or impact nature (CHS 50 mm/min). The numerical values of the parameters A, B and C is as shown Table 4-4

### Model for Storage Modulus

The experimental results obtained from the Dynamic Mechanical Analysis of the Polymer Nanocomposites were compared with Boltzmann model. The storage modulus data, plotted compared with Boltzmann model as shown in figure- 4.7, 4.8 and 4.9 respectively for the conditions 1Hz, 10Hz and 100Hz frequencies. The Boltzmann model obtained for the storage modulus is

$$G' = \frac{A_1 - A_2}{1 + e^{\frac{(x-x_c)}{dx}}} + A_2 \quad (4.4)$$

Where,  $G'$  gives the storage modulus corresponds to the temperature,  $x$ .  $A_1$  and  $A_2$  are lower and upper limit,  $x_c$  – centre value and  $dx$  is constant depends on the iteration

time. The values obtained for the parameters are tabulated in Table 4-5. The storage modulus depends on the temperature and the non dimensional parameters depend on the frequency and percentage weight of filler. Hence the storage modulus was found to be a function of temperature, percentage weight of filler, frequency etc.

### **Model for Loss Modulus**

The experimental results obtained for loss modulus from dynamic mechanical analysis plotted in figure 4-10, 4-11 and 4-12 respectively for the conditions such as , frequency 1 Hz, 10 Hz and 100 Hz. and found fit for Lorentz model

$$G'' = y_0 + \frac{2A}{\pi} \times \frac{w}{4(x-x_c)^2 + w^2} \quad (4.5)$$

Where,  $y_0$ ,  $A$ ,  $x_c$  and  $w$  are the various non dimensional parameters of the model, whose values are tabulated in Table 4-6. According to the model, the loss modulus  $G''$  is a function of temperature and influenced by the parameters, which depends on the frequency and percentage weight of filler.

### **Model for Damping Factor ( $\tan\delta$ )**

The experimental results obtained for damping factor plotted in figure 4-13, 4-14 and 4-15 were found fit for Gaussian model while compared. The mathematical model obtained with coefficient of regression  $R^2 = 0.95$  is

$$\tan \delta = y_0 + \frac{A}{w\sqrt{\pi/2}} e^{-\frac{2(x-x_c)^2}{w^2}} \quad (4.6)$$

Where,  $y_0$ ,  $w$ ,  $A$ ,  $x_c$  are parameters of the model tabulated in Table 4-7. Here also as in the case of storage modulus and loss modulus which were used to compare with Boltzmann model and Lorentz model respectively, the Gaussian model describes the relation between damping factor( $y$ ) and temperature( $x$ ). The damping factor was found varying with temperature, frequency and percentage weight of filler.

#### **4.3.6 X- Ray Diffraction**

The polymer /clay nanocomposite can be divided in to three types- immiscible, intercalated and exfoliated composites. Of the first case there is no separation of clay platelets. Thus wide angle X- ray scan of the composite is expected to look like that of nanoclay. Generally such scans are made over a low range of angles,  $2\theta$ . In the second case exact peak will be obtained with a shift as compared to pure nanoclay. In the third case there is no exact, but a broad peak or flat which is different from the latter two was obtained.

Often X-ray scans of polymer nanocomposites show a peak reminiscent of the organoclay peak but shifted to lower  $2\theta$  or larger d-spacing condition. The peak shift indicates that the gallery has expanded and the polymer chains intercalated in to the gallery. Figure 4-16 and 4-17 are respectively the XRD pattern of pure nanoclay (Cloisite15A) and 1% Cloisite15A filled nanocomposite. The nanoclay shows the peak at  $2.92^\circ$ ,  $4.41^\circ$  and  $7.12^\circ$ . There is no sharp peak for the polymer nanocomposite but a small peak with a shift to left of small intensity can be observed. Also a broad peak at around  $2\theta = 7^\circ$  for the PNC is there. Thus we cannot mark any exact peak function for the nanocomposite. So the possibility for the exfoliation rather than

intercalation can be interpreted. Altogether we can predict the exfoliation together with intercalation from the pattern.

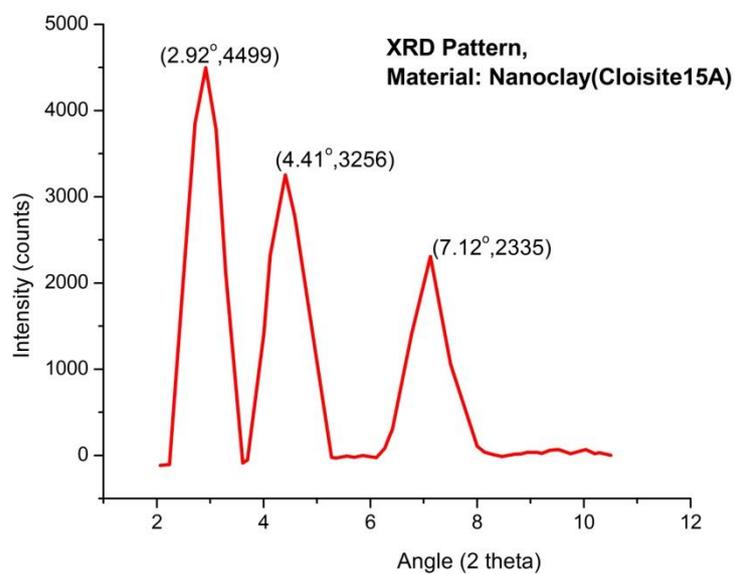


**Figure 4-16** XRD Pattern of pure nanoclay (Cloisite15A)

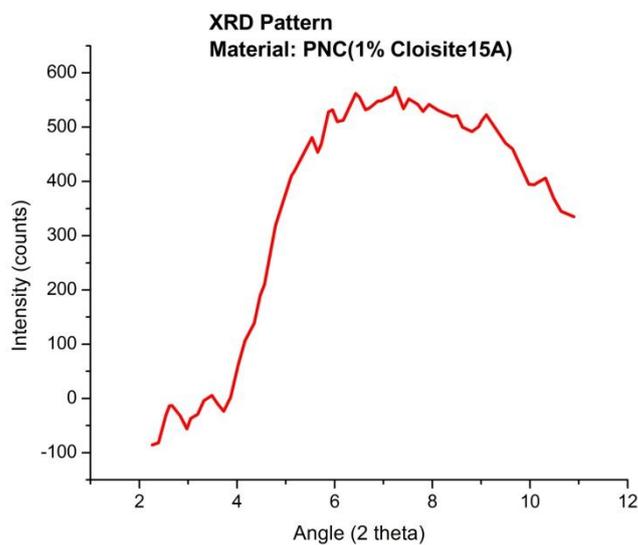


**Figure 4-17** XRD Pattern of PNC (1% Cloisite15A)

#### 4.3.7 Thermogravimetric Analysis

Figures 4-18 and 4-19 illustrate the variation of percentage weight loss and percentage differential weight with increase of temperature from room temperature to 800 °C for five different samples, i.e. 0, 0.5, 1, 1.5, 2 wt. % nanoclay blended nanocomposites. For all blends, weight loss was constant up to 150°C and then decomposition started at around 150 to 200°C. A notable variation in the degradation temperature is not evident from the curve with variation in the clay content. However, a minor variation is found which may be due to the variation in the presence of moisture content. The degradation continues with the same trend up to 320 °C with a weight loss of approximately 10%. The second phase of degradation starts at around 320 °C. Weight loss was constant for different nanoclay filled sample, which is around 65% over a temperature range from 320 °C to 400 °C. The existence of inorganic materials in polymer matrix generally, enhances the thermal stability of the nanocomposite. The weight-loss vs temperature curve showed that the residue left beyond 400°C for nanocomposite is in line with the inorganic material content of each sample which is almost zero.

The analysis of the DMA and TGA results recommends the applicability of the nano composite at elevated temperature. This property enhancement obtained at very low percentage of filler is most desirable thing. The addition of filler has no significant effect on the degradation temperature of the polymer pointing to the fact that the thermal stability of the material is not much affected by the addition of nanofiller, Cloisite15A.

Although Cloisite15A has ammonium salt and organic content, both have the catalytic effect, which will have a tendency to decrease the thermal stability. There exists some

inorganic hydrated cations in the aluminosilicate interlayer of organo modified MMT because the sodium gallery cations of montmorillonite cannot entirely be exchanged during organic modification by alkyl ammonium salts and some inorganic hydrated cations e.g.  $Al^{3+}$  or  $Mg^{2+}$  exist in the octahedral structure of montmorillonite which can be not substituted by ionic exchange. So interlayer water residing between the aluminosilicate sheets gradually evolve between 200-500 °C. Interlayer water and hydroxyl group of the aluminosilicate sheets in Organo modified MMT can catalyze thermal decomposition of polymer composite by transesterification reaction. However in the present study only a small decrease in thermal stability is observed with the addition of Cloisite15A since only a very small quantity of nanoclay (less than 3%) is used.[114][115]

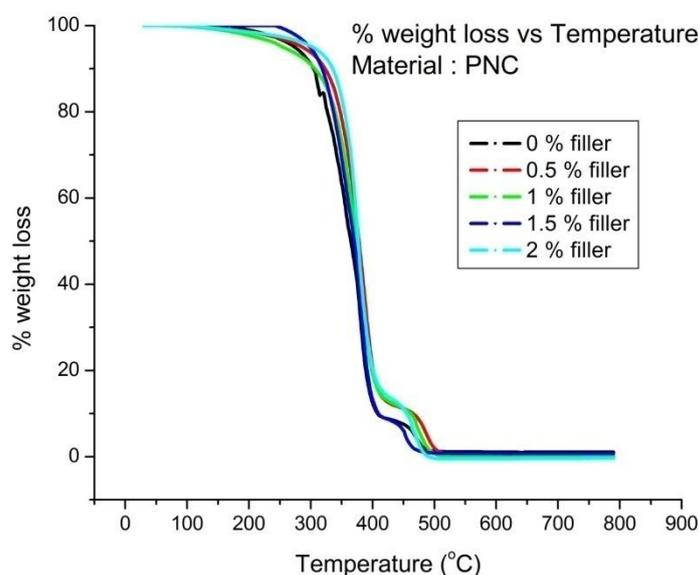


**Figure 4-18** TGA thermogram of PNC, variation of % weight loss with temperature at different filler (Cloisite15A) contents

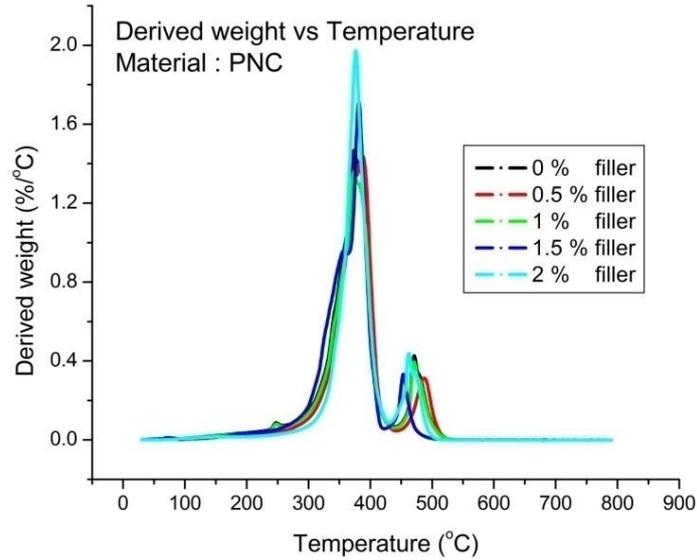


**Figure 4-19** TGA thermogram of PNC, variation of % derived weight with temperature at different filler (Cloisite15A) contents

#### 4.3.8 Differential Scanning Calorimetry

The DSC curves are used to measure the glass transition temperature ( $T_g$ ). The DSC curve of the different nanocomposite samples obtained from first heating cycle is shown in figure 4-20. Glass transition temperatures of all nanocomposites were almost the same or only a marginal variation with the sample without nanofiller. This small increase in the  $T_g$  of all the nanocomposite can be attributed to the mixing of nanofiller. This can be explained by the existence of strong interactions between clay and the polyester matrix, which limits the movement of the polyester chain segments. This leads to an increase in the  $T_g$  of the polyester nanocomposites, which is a typical effect for the inclusion of nanofiller (montmorillonite) in a polymer system.  $T_g$  increases from  $78.36^\circ\text{C}$  (resin) to  $82.15^\circ\text{C}$  by the addition 1% Cloisite15A. This effect was typically ascribed to the confinement of intercalated polymers within the silicate galleries that prevents the segmental motions of the polymer chains. The links between polymeric chains and

the silicate surface may be the reason behind the changes in the glass transition temperature. The restricted relaxation behavior for the polymer nanocomposites with intercalated and exfoliated silicates primarily depended on the exfoliation extent of the layered silicates and on the interaction strength between the silicate surfaces and the polymer macromolecules. The exfoliation as well as intercalation is evident from the XRD results described. Hence the increase of  $T_g$  of the nanocomposites as function of nanoclay content observed in this study may be because of the limited segment mobility from the increased clay content [111].

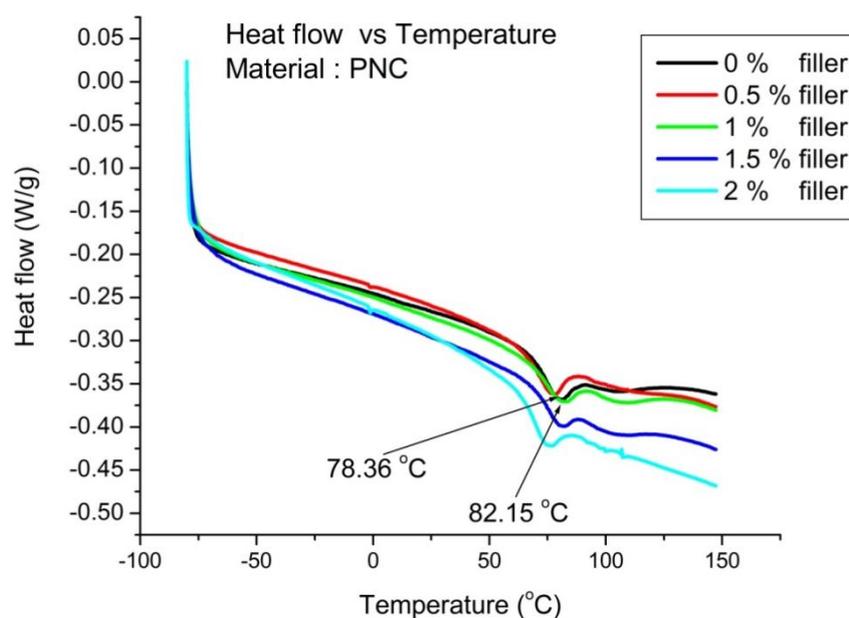


**Figure 4-20** DSC curves of PNC at different filler (Cloisite15A) content.

#### 4.3.9 SEM Analysis

Images obtained from the Scanning Electron Microscopy of various samples are as shown in Figures 4-21(a) to (d). As compared to the SEM images of the neat resin sample, the fracture surface of nanocomposite appeared to have a large degree of roughness. That means the morphology of the fracture surface is significantly

modified by the nanoclay. This rough fracture surface can be explained by the crack deflection and the continual crack propagation occurring on two slightly different fracture planes. This would be due to the presence of large quantity of nanoclay.

More curved patterns were observed throughout the whole crack surface. This indicated that nanofillers could increase the toughness of the matrix. This toughness mechanism could be explained by energy dissipation during the pullout of nanolayers in the composites [117]. Fracture surface in pure polyester resin showed a brittle nature of failure under load, whereas the sample with 1% nanoclay showed a ductile nature of failure. However the nature of failure of the sample with 2% nanoclay cannot be classified exactly as brittle or ductile. Agglomeration of clay particles results a non uniform mixing and hence the modification of the polymer does not effect, which may be the reason for certain region indicated in the diagram reflects a brittle nature of failure in 2% nanoclay filled sample.

Figure 4-22(a) and (b) shows the fracture surface formed from impact loading of the specimen with 0% nanoclay and 1% nanoclay. The fracture surface of 1% nanoclay filled sample have large degree of roughness in the surface similar to that of 1% nanoclay filled specimen, which tested for tensile properties. Thus similar to the failure under tensile load the presence of nanoclay induced a ductile nature for the fracture during the impact loading.

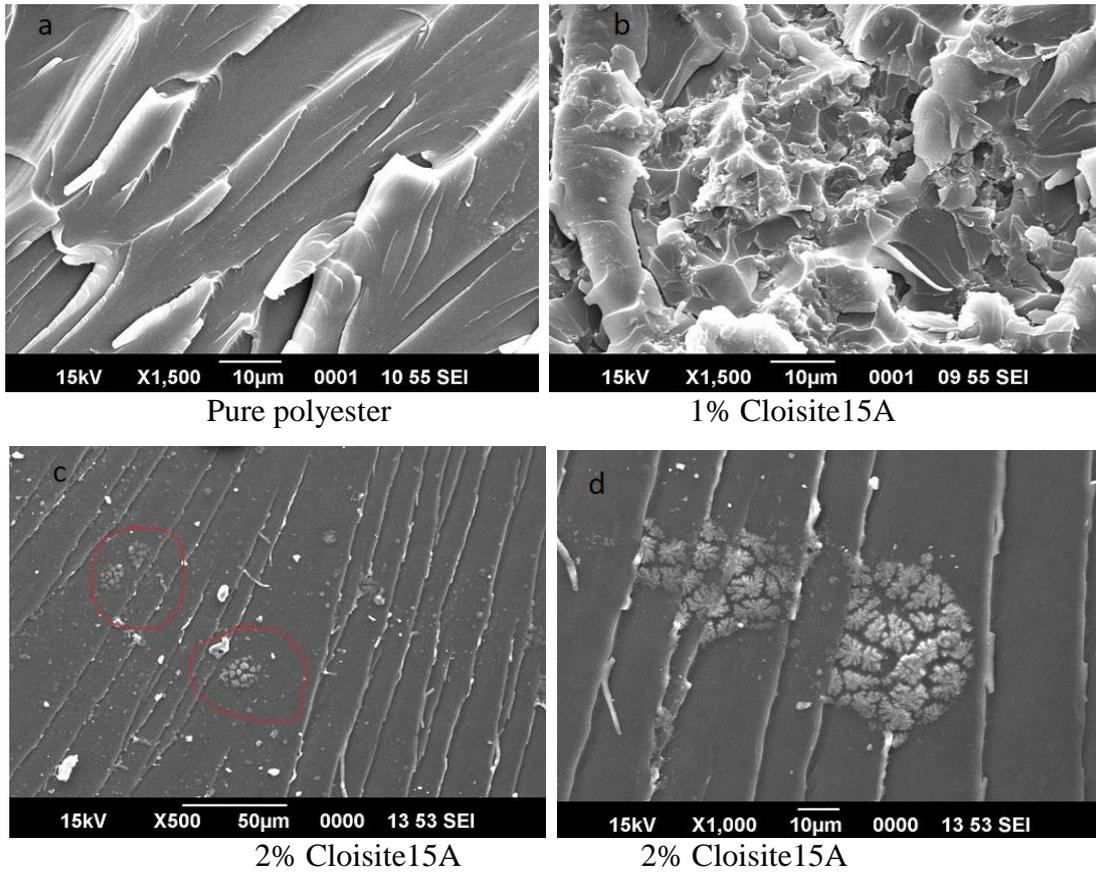


**Figure 4-21** SEM images of (a) pure polyester, (b) 1% nanoclay filled polyester, (c) 2% nanoclay filled polyester (d) 2% nanoclay filled polyester magnified view

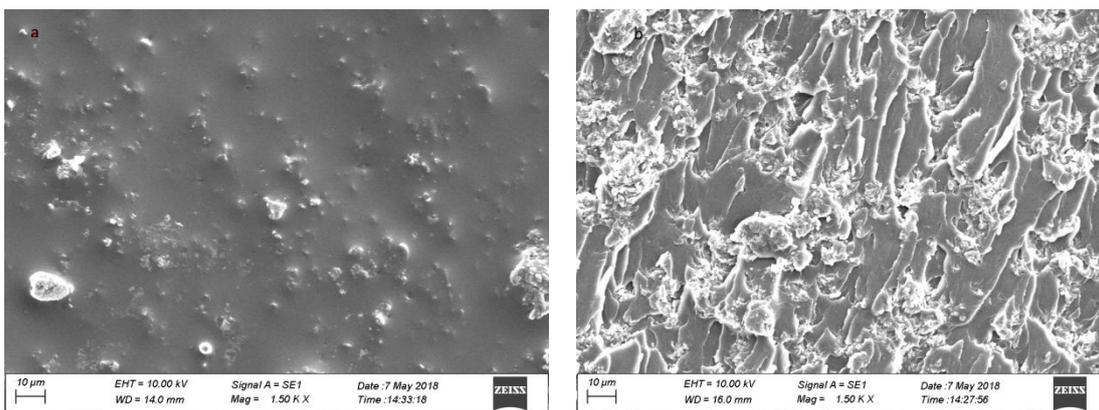


**Figure 4-22** SEM images of (a) pure polyester, (b) 1% nanoclay filled polyester of the fracture surface after impact test

#### 4.3.10 Statistical Analysis

The experimental data obtained for mechanical, dynamic mechanical and thermal property were subjected to statistical analysis by the method of ANOVA. The significance of the experimental data has been analyzed in terms of the parameter for analysis.

#### Tensile Modulus

The data obtained from the tensile test subjected to statistical analysis by the method of two factor ANOVA without replication. The data obtained show the variation of tensile modulus with percentage weight of filler and testing speed (Cross Head Speed, CHS). The ANOVA table obtained from the analysis is given as table-4-8.

**Table 4-1** Statistical analysis, Tensile modulus

| <i>SUMMARY</i>     | <i>Count</i> | <i>Sum</i> | <i>Average</i> | <i>Variance</i> |
|--------------------|--------------|------------|----------------|-----------------|
| % weight of filler | 25           | 25         | 1              | 0.521           |
| CHS 0.5 mm/min     | 25           | 25357.718  | 1014.309       | 16130.753       |
| CHS 5 mm/min       | 25           | 39111.847  | 1564.474       | 242403.873      |
| CHS 50 mm/min      | 25           | 46221.548  | 1848.862       | 251036.246      |

| ANOVA                      |             |           |             |          |                |               |
|----------------------------|-------------|-----------|-------------|----------|----------------|---------------|
| <i>Source of Variation</i> | <i>SS</i>   | <i>df</i> | <i>MS</i>   | <i>F</i> | <i>P-value</i> | <i>F crit</i> |
| % weight of filler         | 6135045.76  | 24        | 255626.91   | 3.020    | 0.000159       | 1.67          |
| CHS mm/min                 | 49786723.50 | 3         | 16595574.50 | 196.054  | 1.47E-34       | 2.73          |
| Error                      | 6094667.67  | 72        | 84648.16    |          |                |               |
| Total                      | 62016436.92 | 99        |             |          |                |               |

From the ANOVA table critical value obtained for the percentage weight of filler is 1.67. the significant value obtained for the corresponding case is 0.000159 is less than the cut off value 0.05, so the null hypothesis ( no significant difference between the percentage weight of filler in terms of tensile modulus) is rejected. Hence there is significant difference for the condition percentage weight of filler in terms of tensile

modulus. Thus it can be concluded from the analysis of the experimental data, that the percentage weight of filler significantly affects the tensile modulus.

The critical value reported to be 2.73 in terms of cross head speed, CHS. The significant value obtained is 1.47E-34, which is less than the cut off value 0.05. Here also the null hypothesis ( there is no significant difference between the cross head speed in terms of tensile modulus) is rejected. Hence there is significant difference between CHS in terms of tensile modulus. A conclusion similar to the case of percentage weight of filler can be reached. The testing speed significantly affects the tensile modulus.

### Impact Strength

The experimental data obtained in impact test were analyzed by single factor ANOVA. The data represent the variation of impact strength with percentage weight of filler. The ANOVA table obtained from the statistical analysis is represented in table 4-9.

**Table 4-2** Statistical analysis, Impact strength

| <i>Groups</i>                     | <i>Count</i> | <i>Sum</i> | <i>Average</i> | <i>Variance</i> |                |               |
|-----------------------------------|--------------|------------|----------------|-----------------|----------------|---------------|
| % weight of filler                | 26           | 26         | 1              | 0.5             |                |               |
| Impact strength kJ/m <sup>2</sup> | 26           | 394.86     | 15.18          | 3.32            |                |               |
| ANOVA                             |              |            |                |                 |                |               |
| <i>Source of Variation</i>        | <i>SS</i>    | <i>df</i>  | <i>MS</i>      | <i>F</i>        | <i>P-value</i> | <i>F crit</i> |
| Between Groups                    | 2616.6       | 1          | 2616.60        | 1367.48         | 55E-38         | 4.034         |
| Within Groups                     | 95.67        | 50         | 1.91           |                 |                |               |
| Total                             | 2712.28      | 51         |                |                 |                |               |

The statistical analysis report of impact test in table 4-9 indicated that the significant value reported to be 55E-38, which is less than the cut off value 0.05. So the null hypothesis (There is no significant difference between the percentage weight of filler in terms of impact strength.) is rejected. Hence there is significant difference between

percentage weights of filler in terms of impact strength. So it can be concluded that the percentage weight of filler significantly influences impact strength of the material. The average value of % weight of filler is 1 and impact strength is 5.54 kJ/m<sup>2</sup>.

### Flexural Modulus

The statistical analysis of the flexural test results by the method of two factor ANOVA without replication is reported in table 4-10. The experimental data obtained show the variation of flexural modulus with percentage weight of filler and testing speed, CHS. Critical value is 1.67 for the percentage weight of filler. The significant value is reported to be  $p = 3.12E-09$ , which is less than the cut off value 0.05. So the null hypothesis (there is no significant difference between the percentage weights of filler in terms of flexural modulus) is rejected. Hence there is significant effect for the percentage weight of filler in terms of flexural modulus. Thus it can be concluded that the variation of flexural modulus significantly influenced by the percentage weight of filler.

**Table 4-3** Statistical analysis, Flexural modulus

| <i>Summary</i>             | <i>Count</i> | <i>Sum</i> | <i>Average</i> | <i>Variance</i> |                |               |
|----------------------------|--------------|------------|----------------|-----------------|----------------|---------------|
| % weight of filler         | 25           | 25         | 1              | 0.520833        |                |               |
| CHS 0.5 mm/min             | 25           | 123195.9   | 4927.836       | 619928.7        |                |               |
| CHS 5 mm/min               | 25           | 127457.6   | 5098.304       | 591085.2        |                |               |
| CHS 50 mm/min              | 25           | 132145.9   | 5285.835       | 380270.1        |                |               |
| ANOVA                      |              |            |                |                 |                |               |
| <i>Source of Variation</i> | <i>SS</i>    | <i>df</i>  | <i>MS</i>      | <i>F</i>        | <i>P-value</i> | <i>F crit</i> |
| % weight of filler         | 25172919     | 24         | 1048872        | 5.801143        | 3.12E-09       | 1.67          |
| CHS mm/min                 | 4.9E+08      | 3          | 1.63E+08       | 903.1186        | 5.02E-57       | 2.73          |
| Error                      | 13017909     | 72         | 180804.3       |                 |                |               |
| Total                      | 5.28E+08     | 99         |                |                 |                |               |

The critical value reported to be 2.731 in terms of CHS. Since the significant value  $p=5.02E-57$  which is less than the cut off value 0.05, the null hypothesis is rejected. That means, there is significant difference between CHS in terms of flexural modulus. Thus the variation of flexural modulus is significantly influenced by CHS.

### Dynamic Mechanical Property

Statistical analysis of data obtained for storage modulus; by the method of two factor ANOVA without replication is reported in table 4-11. The critical value is reported to be 1.12 for % weight of filler and 2.61 for frequency. The significant value for percentage weight of filler is reported as  $2E-205$ , which is less than the cut off value 0.05. Hence there is significant difference between % weights of filler in terms of storage modulus. That means there is significant effect for the percentage weight of filler in terms of storage modulus or the storage modulus is significantly influenced by the percentage weight of filler.

**Table 4-4** Statistical analysis, Storage modulus

| <i>Summary</i>     | <i>Count</i> | <i>Sum</i> | <i>Average</i> | <i>Variance</i> |
|--------------------|--------------|------------|----------------|-----------------|
| % weight of filler | 530          | 530        | 1              | 0.500945        |
| Frequency 1 hz     | 530          | 511710.8   | 965.49         | 744956.7        |
| Frequency 10 hz    | 530          | 553796.1   | 1044.89        | 599085.9        |
| Frequency 100 hz   | 530          | 731078.4   | 1379.39        | 813102.5        |

| <b>ANOVA Report</b>        |           |           |           |          |                |               |
|----------------------------|-----------|-----------|-----------|----------|----------------|---------------|
| <i>Source of Variation</i> | <i>SS</i> | <i>df</i> | <i>MS</i> | <i>F</i> | <i>P-value</i> | <i>F crit</i> |
| % weight of filler         | 8.05E+08  | 529       | 1521423   | 7.179655 | 2E-205         | 1.12          |
| Frequency                  | 5.58E+08  | 3         | 1.86E+08  | 877.3499 | 0              | 2.61          |
| Error                      | 3.36E+08  | 1587      | 211907.5  |          |                |               |
| Total                      | 1.7E+09   | 2119      |           |          |                |               |

Also regarding the frequency of vibration connected with the application of dynamic load on the specimen, the significant value is  $p=0$ , which also is less than the cut off value 0.05. Hence the frequencies also have significant effect on the variation of storage modulus. Thus the storage modulus is significantly influenced by the testing frequency. The average value of storage modulus is 965.49, 1044.89 and 1379.39 respectively for frequency 1Hz, 10Hz and 100 Hz.

**Table 4-5** Statistical analysis, Thermal degradation

| <i>Summary</i> |              |            |                |                 |
|----------------|--------------|------------|----------------|-----------------|
| <i>Group</i>   | <i>Count</i> | <i>Sum</i> | <i>Average</i> | <i>Variance</i> |
| Temperature    | 761          | 312010     | 410            | 48323.5         |
| 0% filler      | 761          | 34699.5    | 45.59          | 2165.43         |
| 0.5% filler    | 761          | 34957.71   | 45.93          | 2077.93         |
| 1% filler      | 761          | 33994.81   | 44.67          | 2060.26         |
| 1.5% filler    | 761          | 34421.34   | 45.23          | 2206.46         |
| 2% filler      | 761          | 33501.16   | 44.02          | 2061.07         |

**ANOVA Report**

| <i>Source of Variation</i> | <i>SS</i>   | <i>df</i> | <i>MS</i>   | <i>F</i> | <i>P-value</i> | <i>F crit</i> |
|----------------------------|-------------|-----------|-------------|----------|----------------|---------------|
| Between Groups             | 84446087.76 | 5         | 16889217.55 | 1720.61  | 0              | 2.21          |
| Within Groups              | 44759949.48 | 4560      | 9815.77     |          |                |               |
| Total                      | 129206037.2 | 4565      |             |          |                |               |

**CORRELATION**

|             | <i>Temperature</i> | <i>0% filler</i> | <i>0.5% filler</i> | <i>1% filler</i> | <i>1.5% filler</i> | <i>2% filler</i> |
|-------------|--------------------|------------------|--------------------|------------------|--------------------|------------------|
| Temperature | 1                  |                  |                    |                  |                    |                  |
| 0% filler   | -0.911             | 1                |                    |                  |                    |                  |
| 0.5% filler | -0.915             | 0.999            | 1                  |                  |                    |                  |
| 1% filler   | -0.919             | 0.998            | 0.999              | 1                |                    |                  |
| 1.5% filler | -0.906             | 0.995            | 0.997              | 0.998            | 1                  |                  |
| 2% filler   | -0.911             | 0.993            | 0.995              | 0.997            | 0.999              | 1                |

**Thermal Degradation**

Statistical analysis of the data obtained for TGA by the method of single factor ANOVA is reported in table 4-12. The critical value is reported to be 2.21. The

significant value is  $p = 0$ , which is less than the cut off value 0.05. So the null hypothesis (there is no significant difference between the percentage weight of filler in terms of % weight loss or thermal degradation) is rejected. Hence it can be concluded that there is significant effect for the percentage weight of filler in terms of weight loss (thermal degradation). The statistical analysis of the same data by the method of correlation is also reported in the table. There exists good correlation among the percentage weight of filler in terms of thermal degradation.

#### **4.4 CONCLUSIONS**

Different types of Polyester-cloisite15A nanocomposites were prepared by varying the percentage weight of Cloisite15A in isophthalic polyester resin. Mechanical characteristics were determined using tensile test, impact test and flexural test. Dynamic mechanical behavior was determined using DMA and thermal stability of the material was evaluated using Thermogravimetric Analysis. Morphology of fracture surface under tensile load was analyzed using scanning electron microscopy. The following conclusions can be drawn from the study:

1. The tensile modulus appreciably improves by the incorporation of small quantity of Cloisite15A (1 and 1.5%). However, the tensile modulus is low for nanocomposite with 2% Cloisite15A compared to other proportions of weight evaluated. The perfect intercalation of nanoclay cannot be achieved for it. It is possible only with low volume fraction, which provides stiffening effect and improvement in property through perfect dispersion. Also the high value for tensile modulus is reported with CHS 50 mm/min compared to 0.5 and 5 mm/min.

2. The tensile modulus is found to increase to about 15 to 25% with addition of 1% nanoclay
3. The impact strength increases with increase in clay content. The maximum value is obtained with a nearly 1.5% clay content and further addition of the nanoclay decreases the impact strength. It shows an increase of 15 to 20 % by the addition of 1 to 1.5% nanoclay.
4. The flexural modulus reported an increase of 21 to 35% by the addition of 1% nanoclay and 35 to 50% improvement by the addition of 2% nanoclay.
5. From the Dynamic Mechanical Analysis, the maximum value for the storage modulus was obtained for nanocomposite with 1% nanoclay. 35 to 40 % increase in storage modulus was reported at room temperature. The Loss modulus attains maximum value at the temperature range 85 to 90 °C for all samples.
6. Thermogravimetric analysis showed that the thermal degradation starts at around 320°C for the pure polyester and the composites.
7. DSC results indicate that there is no notable change in glass transition temperature by the addition of nanoclay.
8. SEM images of fracture surface showed that the addition of nanoclay to polyester changed the nature of failure of the material from brittle to ductile. Also the agglomeration of clay particles is evident from the SEM image of 2% Cloisite15A filled sample.

## **CHAPTER 5**

# **MECHANICAL AND THERMAL CHARACTERIZATION OF GLASS FIBER REINFORCED POLYESTER NANOCOMPOSITE**

### **5.1 INTRODUCTION**

Fiber-reinforced polymer composites are one of the most widely used composite materials. The addition of fibers to the polymer matrix significantly increases the overall mechanical strength of the composite material as compared to the neat polymer. The fibers have many advantages such as low density, high specific strength and modulus, relative non abrasiveness, ease of fiber surface modification and wide availability. Composites of natural fibers and thermoplastics have found applications in many industries, particularly automotive industry. Many investigations have already been done in this field to improve the wear resistance, strength, hardness etc. especially by nano particle addition.

Tensile and bending tests performed on nanocomposites show that with the addition of nanoclay up to 3 wt%, the tensile strength increase and then decrease at a loading of 5 wt%. However, the flexural strength increased with addition of nanoclay up to 5 wt%. The hardness of the nanocomposites also increased with increasing nanoclay content. Researchers have attempted to improve the properties of epoxy composites by adding nanoclay [37]. The effectiveness of reinforcement essentially depends on the adhesion between matrix and fiber. This is the key factor in determining the final properties of the composite material, particularly its mechanical properties [47].

Conventional static tests such as tensile, bending and impact tests are usually performed to characterize the mechanical properties of composites. The property enhancement depends fiber surface treatment, adhesion between fiber and matrix. The fiber-reinforced thermoplastic composite materials can undergo various types of dynamic stressing during service. Similar to other properties, dynamic mechanical properties depends on type of fiber, fiber length and orientation, fiber loading, fiber dispersion and fiber-matrix adhesion [100]. Cho and Bahadur [101] reported that the addition of nano-CuO could generally enhance the wear resistance of short fiber-reinforced polyphenylene sulfide. Adhesion between the contact surfaces is reduced in the presence of nanoparticles. Stress concentration on the individual fibers was minimized with the dispersed nanoparticles in the contact region, which consequently protect the polymer matrix in the interfacial regions from the thermal–mechanical failure. This finally led to the gradual removal process of short fibers and the high wear resistance of the composites. Javad et. al. [45] investigated the effects of nanoclay particles on impact and flexural properties of glass fiber-reinforced unsaturated polyester (UP) composites. The performance such as high velocity impact, low velocity impact, hardness and flexural properties were studied. Highest performance in ballistic limit and energy absorption were obtained for specimens containing 1.5 wt % nanoclay. Silica concentration of 1.0 wt% expressed as the highest concentration that be able to achieve good dispersion in unsaturated polyester resin matrix which is mentioned in chapter1. Good dispersion of silica strongly creates mechanical properties of composite to be higher. The geometry described by shape, size and size distribution then the reinforcement in the system, its concentration, concentration distribution and orientation. All these factors may be important in describing the property of composite.

Addition of nano particle to GFRP laminate increases the mechanical property such as tensile strength and tensile modulus without considerable weight increment. But the tensile behavior at high strain rate is not as good as at low strain rate according to studies. This extra reinforcement increases the above considered mechanical properties. Basically composite material especially FRP are brittle in nature. Filler content also increases the brittleness, not considerably. It is proven that nano filler can compensate the weak mechanical properties of GFRP exhibited by the polymer. But its tensile behavior at higher strain rate is not satisfactory as compared to that in low strain rate [48].

The present study proposes concentrating on the analysis of the effect of nano filler (Cloisite15A) on the polyester reinforced with glass fiber mat. Effect of varying the percentage weight of nano filler on mechanical, thermo mechanical and thermal degradation are proposed to be investigated.

## **5.2 METHODOLOGY**

The methodology adopted for the characterization of glass fiber reinforced polymer nanocomposite is described below.

### **5.2.1 Raw materials**

Isophthalic polyester resin was used as matrix. Cobalt naphthenate and methyl ethyl ketone peroxide (MEKP) were used as curing reagents. Styrene was used to improve the processability and for ease of attaining dispersion of nanoclay in to the polyester matrix. Cloisite15A is used as the nanofiller. The glass fiber fabric used for reinforcement was 7Mil cloth with specification 200 gsm,

### **5.2.2 Specimen Preparation**

Polyester/Cloisite15A blend was prepared by following the procedure described in chapter-2. Then the blend so obtained was used for the preparation of Glass Fiber Reinforced Polyester Nanocomposite (GFRPN) through hand layup technique. A smooth ceramic tile was used as the plane surface for laying the sheets. Initially the tile was placed over a rigid plane surface. The tile surface was applied with wax as mold releasing agent to facilitate the easy removal of the sample after solidification. Then a coat of the Polyester /Cloisite15A blend was applied over the tile surface using a brush and a roller is applied over the surface to get a coat of uniform thickness. Then the first layer of glass fiber mat was placed over the coat of mix. Further the mix was again applied as a thin layer over the glass fiber mat using the brush. The process has been repeated to obtain five layers of glass fiber mat laid properly. The closed mould was kept under a load of 3 kg for 24 hrs at room temperature. To ensure complete curing, the blended nano composite samples were post cured at 70°C for 1 hr. and the test specimens of required size were cut out from the sample sheet by water jet machining. The specimen have been prepared through the same procedure for different concentration of nanoclay i.e. without nanoclay (pure polyester- 0 % nanoclay), 0.5 % nanoclay, 1 % nanoclay, 1.5 % nanoclay and 2 % nanoclay. A similar procedure was adopted by Chakradar et.al. [23]

### **5.2.3 Mechanical Characterization**

Specimen for the tensile test has been prepared in dumbbell shape as per dimensions proposed by ASTM D 638-03 standard. In each case, five samples were tested and the average values were reported. The samples were loaded in tension at cross-head

speeds of 0.5 mm/min, 5mm/min and 50 mm/min to determine their tensile behavior. The experiment carried out on a universal testing machine. Impact strength of the blended nanocomposites was measured using an Izod impact tester. The samples for impact test were made according to specification proposed by ASTM D 4812 -99. The experiment carried out at ambient conditions using pendulum impact tester. In each case, five identical samples were tested and their average load at first deformation was tabulated [23].

#### **5.2.4 Dynamic Mechanical Analysis**

The specimen for DMA was obtained from GFRPNCs sheet made by hand layup technique having thickness approximately 1 mm. The specimen of size: length 63.5 mm and width 12 mm were prepared as proposed by machine standard. Water jet machining used to cut out specimen from the sheet. The specimen was held in dual cantilever mode for the experiment. In the DMA, the samples were subjected to an oscillating frequency of 1 Hz, 10 Hz and 100 Hz. Measurements were done for each frequency separately in the temperature range from room temperature to 140°C at a heating rate of 2 °C/min. The signals were automatically used to determine the dynamic storage modulus ( $G'$ ), loss modulus ( $G''$ ) and the damping factor ( $\tan\delta$ ), which were plotted as a function of temperature. The  $\tan\delta$  peak was taken as the glass transition temperature ( $T_g$ ) of the test samples [97]. The DMA Q 800, TA instruments described in chapter-2 used for the conduct of experiment.

### **5.2.5 Thermal Analysis**

The Thermogravimetric analysis (TGA) was carried out on TA Instrument Q500. The tests have been carried out in the temperature range from room temperature to 800 °C in air. Specimen with and without nanoclay as filler i.e. pure polyester (0 % nanoclay), 0.5 % nanoclay, 1 % nanoclay, 1.5 % nanoclay and 2 % nanoclay were subjected to thermo gravimetric analysis.

Differential scanning calorimetry was also used to study the thermal behavior. Thermograms of reinforced nanocomposites with different filler content viz pure polyester (0 % nanoclay), 0.5 % nanoclay, 1 % nanoclay, 1.5 % nanoclay and 2 % nanoclay were subjected to analysis.

### **5.2.6 Study of Fracture surface**

SEM micrographs were obtained for the fracture surface of reinforced polymer nanocomposites for the analysis. Fracture surface of specimen subjected to tensile test as well as impact tests were used for SEM analysis. GFRPNCs with various filler content, which subjected to tensile loading at 5 mm/min and 50 mm/min were taken to study the nature of fracture surface under slow loading and rapid loading. Impact tested specimens were analyzed for various filler content.

In order to analyze the morphology of the specimen, X-Ray diffractograms were obtained for the pure nanoclay and GFRPNC. It was done to determine the morphology, to understand the filler distribution and its interactions with the polymer matrix.



**Figure 5-1** Specimen for tensile test



**Figure 5-2** Specimen for flexural test

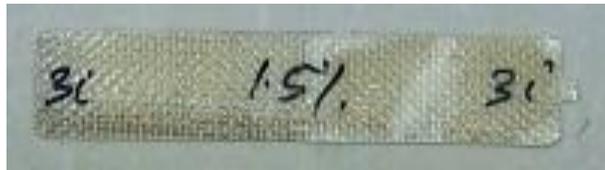


**Figure 5-3** Specimen for impact test

**Table 5-1** Variation of Tensile properties of glass fiber reinforced polyester nanocomposite (GFRPNC) with filler content at different testing speed

| % weight of filler (Cloisite15A) | CHS = 0.5 mm/min       |                       | CHS = 5 mm/min         |                       | CHS = 50 mm/min        |                       |
|----------------------------------|------------------------|-----------------------|------------------------|-----------------------|------------------------|-----------------------|
|                                  | Tensile strength (MPa) | Tensile Modulus (MPa) | Tensile strength (MPa) | Tensile Modulus (MPa) | Tensile strength (MPa) | Tensile modulus (MPa) |
| 0                                | 167.71                 | 5669.44               | 159.46                 | 4911.38               | 215.24                 | 4265.44               |
| 0.5                              | 176.47                 | 6695.34               | 217.58                 | 6699.28               | 246.29                 | 6912.96               |
| 1                                | 194.58                 | 6342.61               | 234.40                 | 6035.96               | 239.82                 | 6470.92               |
| 1.5                              | 181.17                 | 4525.09               | 219.70                 | 5195.31               | 217.28                 | 5578.55               |
| 2                                | 143.07                 | 3830.52               | 190.18                 | 4004.06               | 202.22                 | 4761.58               |

**Table 5-2** Variation of Impact strength of glass fiber reinforced polyester nanocomposite (GFRPNC) with filler content

| <b>% wt. of filler (Cloisite15A)</b> | <b>Impact strength (kJ/m<sup>2</sup>)</b> |
|--------------------------------------|---|
| 0                                    | 76.13                                     |
| 0.5                                  | 81.40                                     |
| 1                                    | 90.79                                     |
| 1.5                                  | 80.89                                     |
| 2                                    | 80.66                                     |

### **5.3 RESULTS AND DISCUSSION**

#### **5.3.1 Tensile Test**

Mechanical properties obtained from the tensile test and impact test were analyzed. Table 5-1 shows the results of tensile test conducted at different testing speeds, CHS (Cross Head Speed) 0.5 mm/min, 5 mm/min and 50 mm/min. The results are plotted in figures 5-4 and 5-5 respectively for the tensile modulus and tensile strength with respect to percentage weight of nanoclay.

From the experimental results the tensile modulus is high for 0.5 and 1% nanoclay filled sample as compared to sample without filler. However, there is a decrease in tensile modulus value with further addition of nanoclay in to the polymer matrix. An improvement of 10 to 40 % in the value of tensile modulus is obtained by the addition of 0.5 to 1% nanoclay, Cloisite15A. The modulus is maximum for testing speed 50 mm/min as compared to 0.5 mm/min and 5 mm/min. Adding nanoclay improves the stiffness of the polymer and the general trend indicate the capacity of the material to withstand under impact load. However, when the percentage weight of nanoclay goes above 1%, tensile

modulus starts decreasing, which means that 1% is the optimum percentage weight of nanoclay for best properties. That means more nanoclay may not guarantee any improvement in property. At higher volume of nanoclay loading the dispersion is poor due to agglomeration of clay, which will be resulted from a weak interface due to the presence of non homogeneity in the matrix medium. Again due to increased viscosity of the clay/polyester mix, the possibility for the formation of voids is more when the clay content is high. From the experimental results improvement in tensile modulus is noticed with the addition of nanoclay [82].

Maximum tensile strength is obtained at CHS 50 mm/min than 0.5 and 5 mm/min. The stiffness as well as the strength at high loading rate is an indication of the improved tensile behavior as well as impact behavior. This can be ascribed to the improved adhesion between fiber and matrix from the addition of nanoclay. Also there is an improvement in the stiffness with the addition of nanoclay to the matrix, which ultimately may contribute to the decrease of fiber pullout due to improved adhesion and hence improved modulus and strength. Decreased fiber pull out due to the presence of nanofiller is evident from the SEM image of GFRPNC illustrated in figure 5-24.

The exfoliation of nanoclay, which is evident from the XRD pattern in figure 5-16, may be contributed to the improved interfacial adhesion between fiber and matrix. This ultimately reduced the fiber pull out and hence the tensile strength and modulus got improved [91]. However, at higher filler content the agglomeration resulted into the stress concentration, poor filler matrix adhesion and hence lack of stress transfer

capability of fillers. The agglomerated nanoclay due to improper dispersion resulted in to a non homogeneous matrix medium and stress concentration.

According to the experimental result tensile modulus showed an increase of 11% at CHS=0.5 mm/min with the addition of 1% Cloisite15A, 22% increase at CHS=5 mm/min and 51% increase at CHS=50 mm/min. Tensile strength shows an improvement of 16% at CHS = 0.5 mm/min, 45% at CHS = 5 mm/min and 11% at CHS = 50 mm/min.

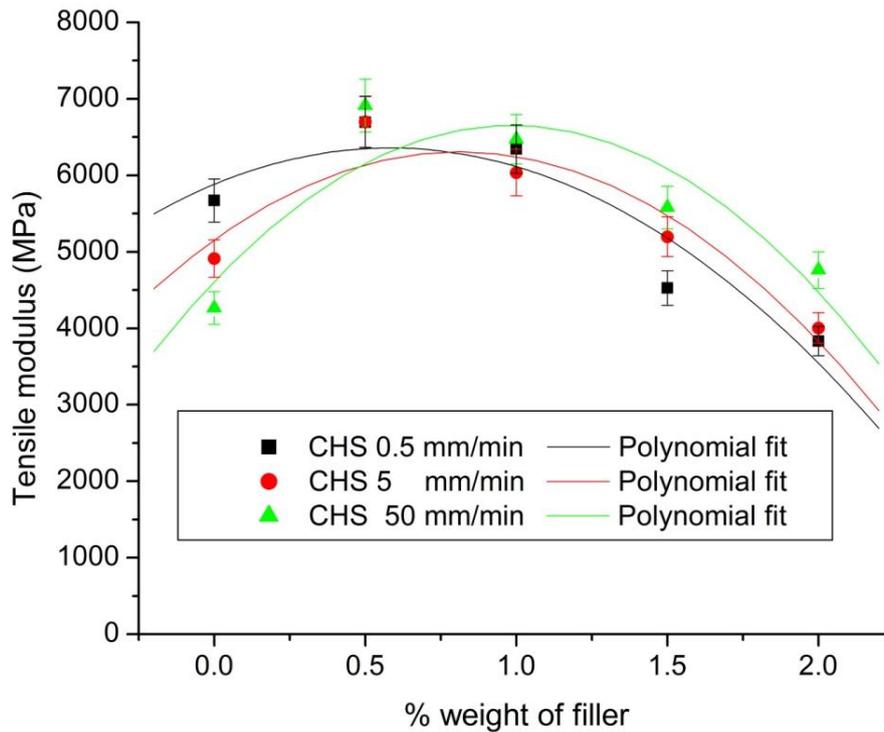


**Figure 5-4** Variation of tensile modulus of glass fiber reinforced polyester nanocomposite with filler content (% weight of Cloisite15A) at different testing speeds

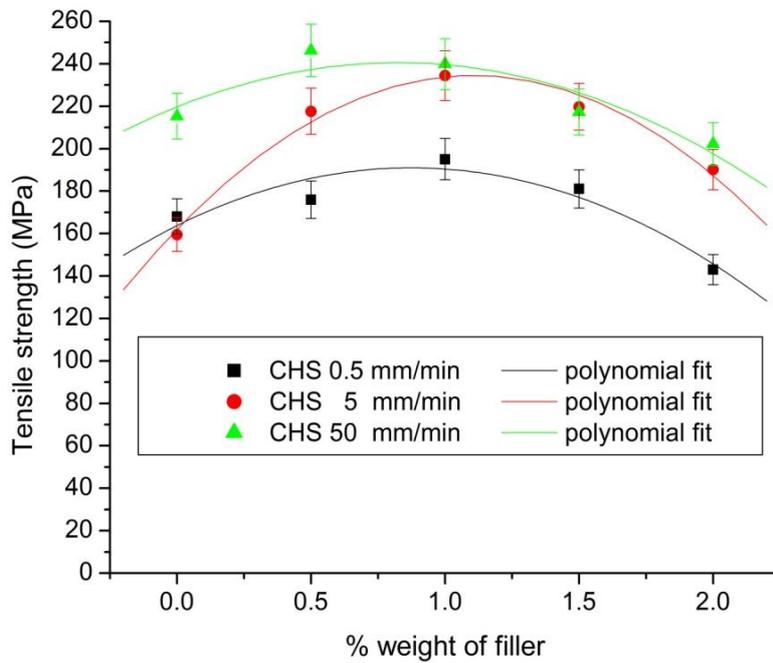


**Figure 5-5** Variation of tensile strength of glass fiber reinforced polyester nanocomposite with filler content (% weight of Cloisite15A) at different testing speeds

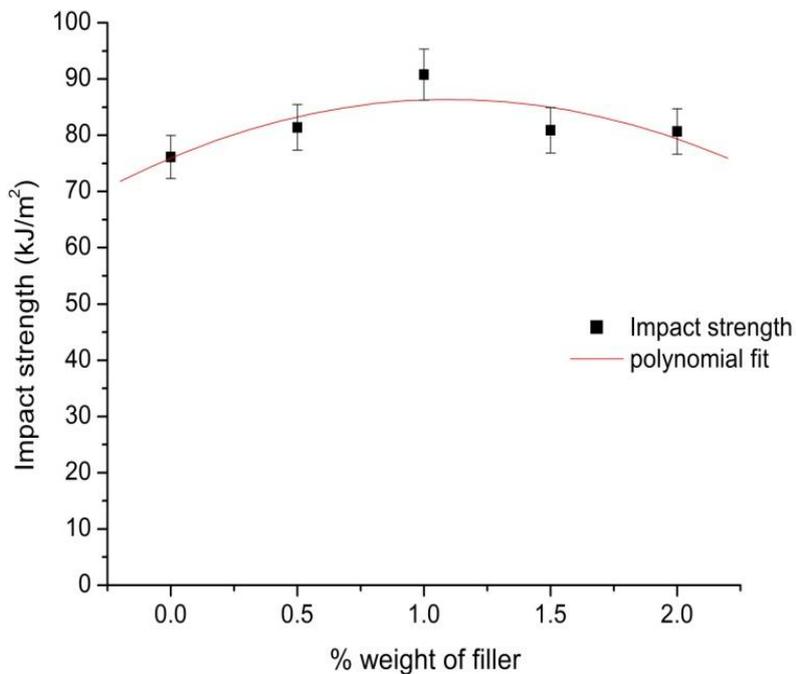


**Figure 5-6** Variation of impact strength of glass fiber reinforced polyester nanocomposite with filler content (% weight of Cloisite15A)

### 5.3.2 Impact Test

The experimental data from Impact test is tabulated in table 5-2 for the specimen prepared with different percentage weight of Cloisite15A such as 0.5, 1, 1.5 and 2. Figure 5-6, the graphical plot, illustrated the variation of impact strength. It can be observed from the graph that, the impact strength increases with addition of nanoclay in to the polyester matrix. This trend continues up to 1% nanofiller. Further addition of nanoclay causes to decrease the impact strength, but only to a limited extent. But the improvement noticed is nearly 18 % with the addition of 1% nanoclay. Studies have also revealed the improvement of inter laminar shear strength by the addition of nanoclay to polymer. This may be contributed to the enhancement of impact strength [45][91]. However, the imperfections due to non homogeneous mixing of nanoclay at large percentage weight may be the reason for decrease in impact strength at higher loading.

SEM micrographs of the fracture surface of specimen used to conduct impact test are shown in figure 5-27. There is no notable difference in the morphology of the fracture surface of pure polyester resin as matrix and Cloisite15A filled polyester as matrix. Since the quantity of nanoclay added is only 1%, it may not result any notable improvement in the stiffness and hence the impact strength.

Inhomogeneous dispersion of nanoparticles may be responsible for the decrease of impact strength for filler content 2% as the presence of excessive nanoparticles makes uniform dispersion difficult or even impossible. Generally the nanoparticles function in two ways: (1) serving as a binding agent to modify the morphological structure of the matrix and (2) acting as stress concentrators to promote cavitation at the particle–

polymer boundaries. The possibility for the latter may prevail in most cases, which may be the reason for the decrease of impact strength [92].

### **5.3.3 Dynamic Mechanical Analysis**

The Dynamic mechanical behavior was studied by experiment conducted in a DMA Q800 apparatus (TA Instruments, New Castle, USA). It measures the modulus (stiffness) and damping (energy dissipation) properties of materials. The polymer sample is subjected to an oscillating stress and the resulting strain is recorded continuously. The ratio of dynamic stress to dynamic strain is the complex modulus,  $G^*$ , which can be resolved into the storage modulus,  $G'$ , and the loss modulus,  $G''$ . The storage modulus represents the ability of a material to store energy for every oscillation and it is related to the stiffness of the material. The loss modulus represents the heat dissipated by the material due to its molecular motions and this reflects the damping characteristics of the polymer.

The specimen has been taken from nano clay modified polyester reinforced with 200 gsm glass fiber mat. The polyester resin was modified with 1% and 2 % Cloisite15A for different types of specimen. Pure polyester (0% filler) reinforced with 200 gsm glass fiber mat was also used for analysis. The glass transition temperature of the specimen was obtained from the experiment conducted in the Tg run mode of DMA. Dual cantilever configuration was used for clamping the specimen. The experiment was conducted for frequencies 1 Hz, 10 Hz and 100 Hz for the temperature range from room temperature to 140 °C.

## Storage Modulus of Reinforced Nanocomposite

Figures 5-7, 5-8 and 5-9 are the plots of the storage modulus ( $G'$ ) as a function of temperature for the GFRPNCs with different weight percentage of nano clay respectively for the testing frequencies: 1Hz, 10 Hz and 100 Hz. Even though there is no consistent change of storage modulus with increase of clay content, nanocomposite with 1% nanoclay gave highest value for storage modulus. This trend is evident for all the three frequencies 1, 10 and 100 Hz as well as at various temperature ranges. The stiffness effects introduced by nanoclay enable the composite to sustain high storage modulus value.[102] The mechanical reinforcement effect is increasing with the nanoclay content. The storage modulus is high at a frequency 100 Hz as compared to 1 Hz and 10 Hz.

As can be seen, the initial value of storage modulus is high for each sample at the ambient temperature due to the fact that, at this stage the molecules are in the frozen state, therefore they retain high stiffness properties in the glassy condition.  $G'$  is higher when the molecular movement is limited or restricted and it consequently will cause the storage of mechanical energy to be increased similar to that of PNCs described in chapter-4. The stiffening effect was more remarkable at lower temperature due to the mismatch in coefficient of thermal expansion between the matrix and inorganic fillers, which might allow better stress transfer between matrices and fillers at low temperatures [103]. The pattern of decrement in the storage modulus value with the increasing temperature is due to the softening of matrix and gradually being shifted from elastic to viscoelastic nature.

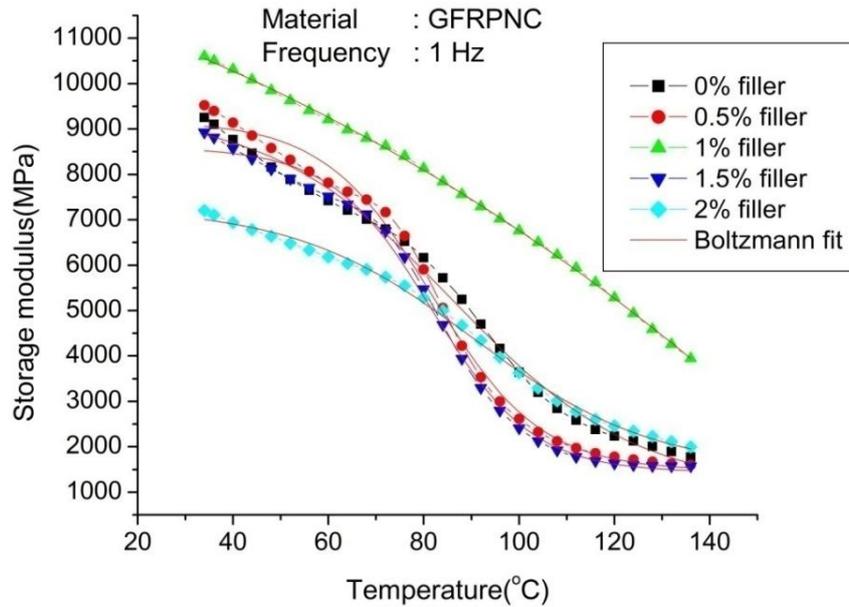


**Figure 5-7** Variation of storage modulus of Glass Fiber Reinforced Polyester Nanocomposite with temperature for different filler (Cloisite15A) content at frequency 1Hz

As the temperatures approaches the glass transition temperature region, there is a large drop in the storage modulus values, indicating the phase transition from the rigid glassy state where the molecular motions are restricted to a flexible rubbery state in which the molecular chains have greater freedom to move. When the polymer and its composites are heated above their  $T_g$ , an increase in free volume typically occurs followed by an increase in molecular mobility [99]. Under this situation, the chain segments gradually align with the applied force. When this occurs, the storage modulus  $G'$  decreases. It is also observed that the curves tend to converge to that of pure polyester when approaching the melting temperature of polymer. This convergence at higher temperature explains the successful exploitation of Glass fiber mat as reinforcement

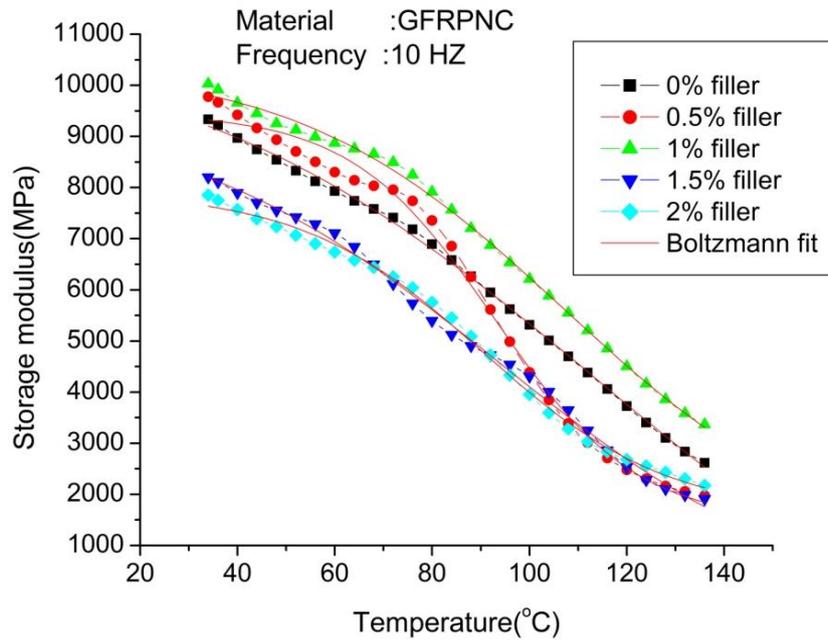


**Figure 5-8** Variation of storage modulus of glass fiber reinforced polyester nanocomposite with temperature for different filler (Cloisite15A) content at frequency 10 Hz

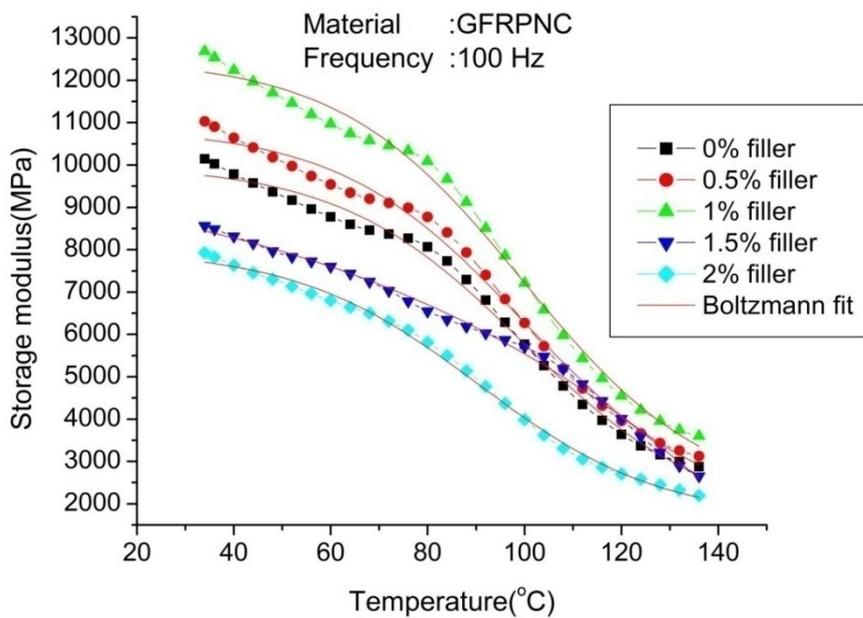


**Figure 5-9** Variation of storage modulus of glass fiber reinforced polyester nanocomposite with temperature for different filler (Cloisite15A) content at frequency 100 Hz

## Loss Modulus of Reinforced Nanocomposite

Figures 5-10, 5-11 and 5-12 illustrate the variation of loss modulus ( $G''$ ) with temperature for frequencies 1Hz, 10 Hz and 100 Hz respectively. We cannot interpret any consistent variation for the loss modulus with nanoclay addition. Here the trend is almost similar to that of storage modulus. But there is an increase in the amplitude of loss modulus pattern for the samples with 0.5 and 1.5 % clay, which is an indication of the increased amount of amorphous part in that sample [102]. This indicates higher viscosity as a result of the molecular movement restriction due to the presence of the fillers. Thus, higher the clay content, higher the viscosity, which at the end requires higher needs for energy dissipation. Secondly it can be concluded that the inclusion of nanoclay showed negligible effect to the peak temperature of loss modulus. The peak was not significantly shifted with regard to the effect of different wt. % of clay loading. This indicates that the inclusion of clay may not significantly affect the relaxation behavior of Polyester FRP. The relaxation transition peak  $G''$  is around 85 to 90°C. The  $G''$  peak reaches a maximum value near the  $T_g$  and then decreases sharply with the increasing temperature.

The temperature range from 85 to 90°C represents a transition region from the glassy state to a rubbery state [37]. Above the transition temperature, the  $G''$  curve drops gradually indicating higher chain movement, thus reducing the viscosity. Any how we can predict a more complex structural relaxation for the nanocomposites. The relaxation is attributed to the chain mobility of the polymer. The degree of adhesion to the fiber affects the molecular mobility which will be enhanced by the presence of

nanoclay; however in this case the low volume fraction of the nanofiller did not have any notable impact in inducing interfacial bonding.

The loss modulus is a measure of energy dissipation, though as a modulus it is hardness or stiffness of a material. Upon heating storage modulus is decreasing but loss modulus increases first because of the increase in molecular friction up to the rubbery state. Around 30% increase in loss modulus for the nanocomposite as compared to neat GFRP is reported.

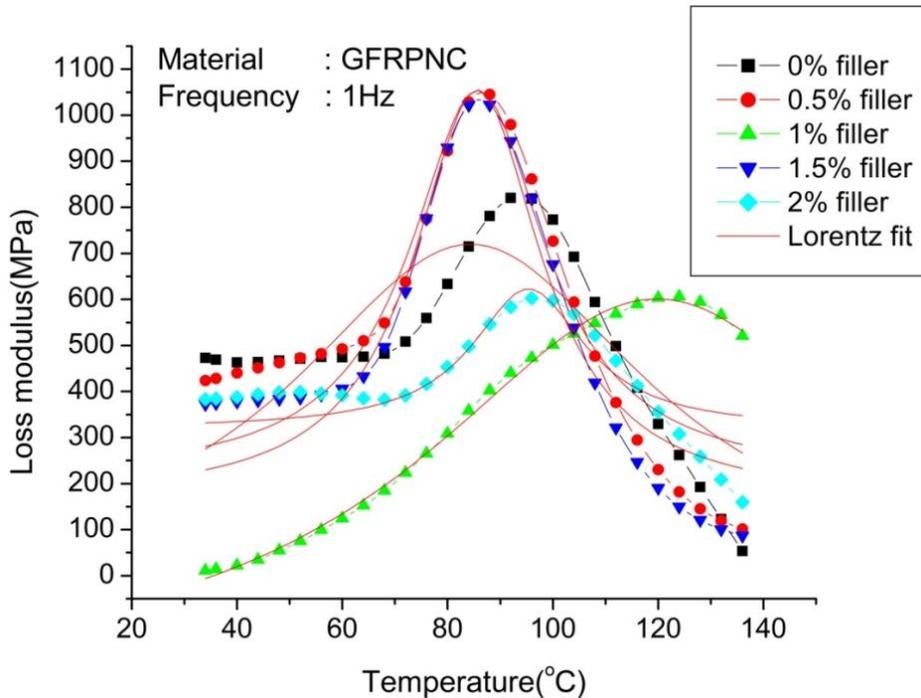


**Figure 5-10** Variation of Loss modulus of glass fiber reinforced polyester nanocomposite with temperature for different filler (Cloisite15A) content at frequency 1 Hz

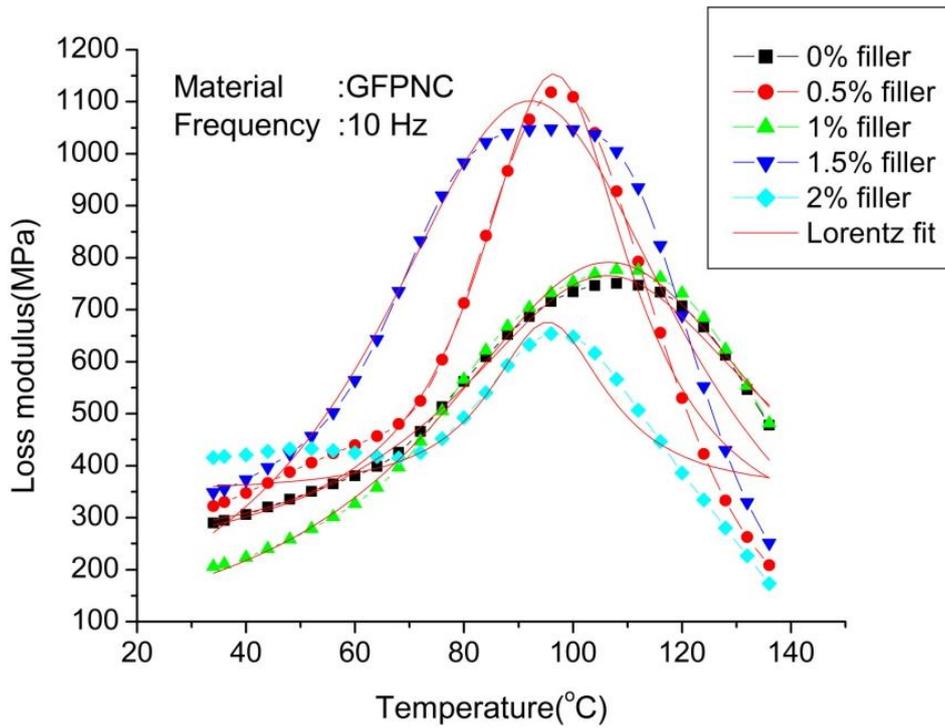


**Figure 5-11** Variation of Loss modulus of glass fiber reinforced polyester nanocomposite with temperature for different filler (Cloisite15A) content at frequency 10 Hz

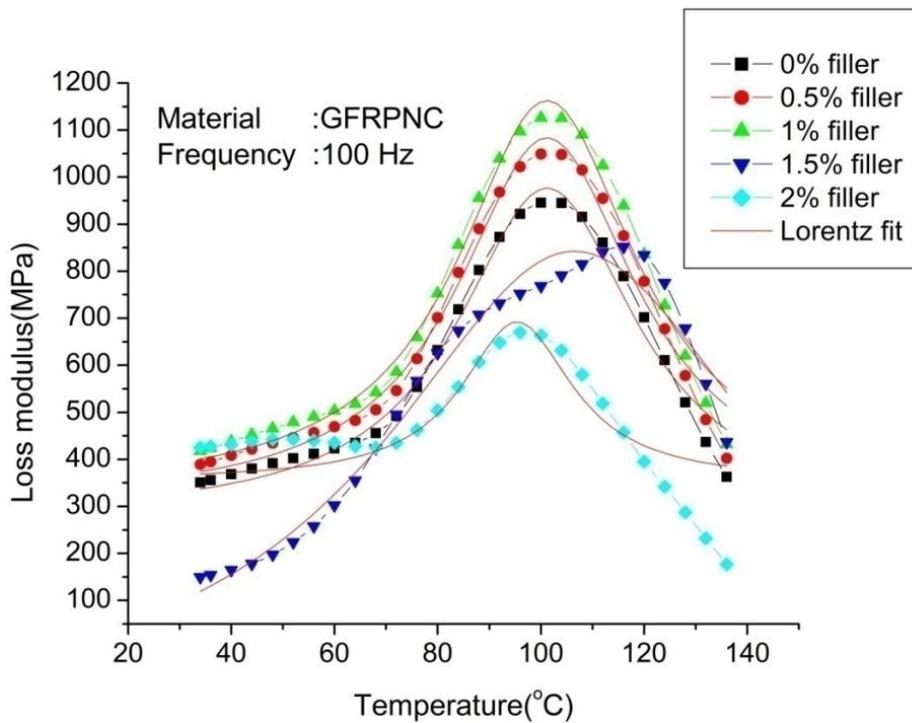


**Figure 5-12** Variation of Loss modulus of glass fiber reinforced polyester nanocomposite with temperature for different filler (Cloisite15A) content at frequency 100 Hz

## Damping Factor ( $\tan\delta$ )

Figures 5-13, 5-14 and 5-15 describe the variation of  $\tan\delta$  with temperature for different nanocomposite.  $\tan\delta$  indicates the relative importance of both viscous and elastic behaviors of materials,  $\tan\delta < 1$  exhibits more elastic behavior where the composite behaves like solid, while  $\tan\delta > 1$  exhibits more viscous behavior where the composite behaves more like liquid [103]. It is also observed that 0.5, 1 and 1.5 % Cloisite15A filled nanocomposite show a slightly higher damping than the pure polyester FRP. This indicates more viscoelastic energy dissipation [99]. From the damping factor curves,  $T_g$  of the composites can be determined by the  $\tan\delta$  peak temperature. It can be seen that there is no significant shift in glass transition temperature  $T_g$  with nanoclay content. The maximum peak for each curve is more or less at the same  $T_g$  temperature. This phenomenon may be due to the low percentages of nanoclay.

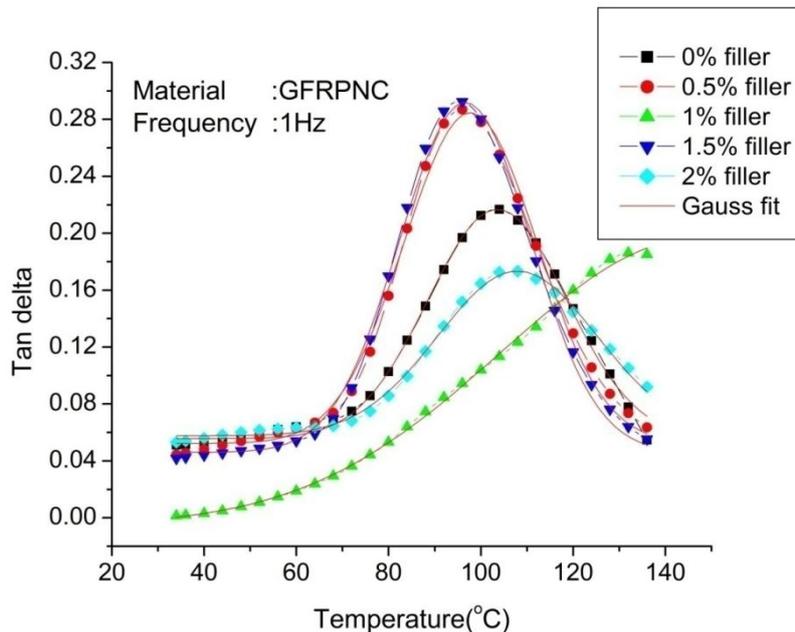


**Figure 5-13** Variation of  $\tan\delta$  of glass fiber reinforced polyester nanocomposite with temperature for different filler (Cloisite15A) content at frequency 1 Hz

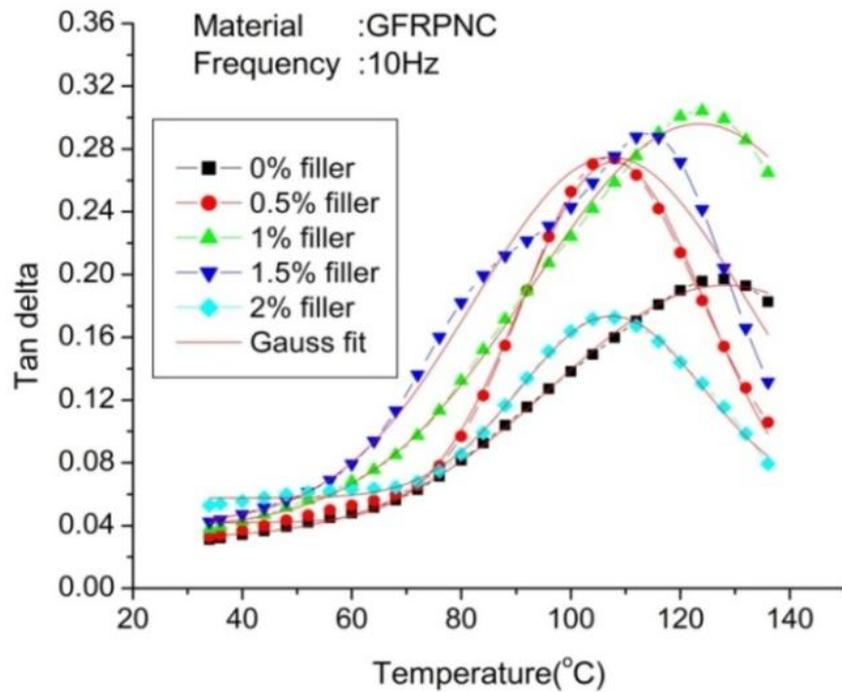


**Figure 5-14** Variation of  $\tan\delta$  of glass fiber reinforced polyester nanocomposite with temperature for different filler (Cloisite15A) content at frequency 10 Hz

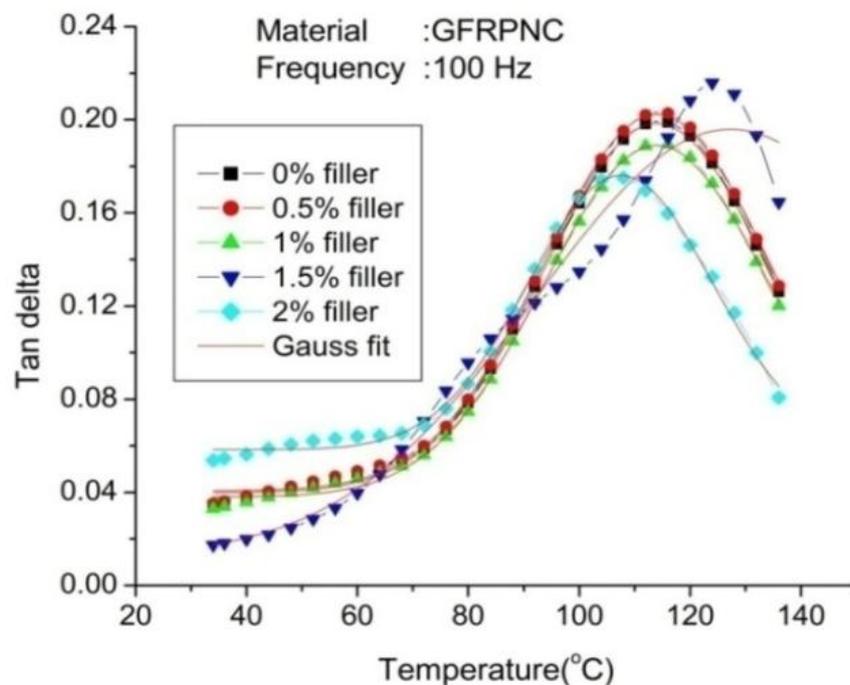


**Figure 5-15** Variation of  $\tan\delta$  of glass fiber reinforced polyester nanocomposite with temperature for different filler (Cloisite15A) content at frequency 100 Hz

### 5.3.4 Model Analysis

Mathematical equations were obtained for the mechanical and dynamic mechanical behavior of the material by comparing the standard models available in the software, Origin6.1. Polynomial fit found to be the best fit among the different models used to compare the Mechanical properties such as tensile modulus, tensile strength and impact strength. The experimental values in respective cases were found in agreement with the model so that a regression coefficient ( $R^2$ ), close to 0.9 in most cases is obtained. Similarly Boltzmann model, Lorentz model and Gaussian model were found fit respectively for the experimental values of Dynamic mechanical properties: storage modulus, loss modulus and damping factor. Here also the coefficient of regression was close to 0.9. Detailed analysis is given below for respective cases.

**Table 5-3** Values of parameters A, B, C and regression coefficient of mathematical model obtained from polynomial fit for mechanical properties.

| Parameters | Tensile modulus  |               |               | Tensile strength |              |               | Impact strength |
|------------|------------------|---------------|---------------|------------------|--------------|---------------|-----------------|
|            | CHS = 0.5 mm/min | CHS =5 mm/min | CHS=50 mm/min | CHS= 0.5 mm/min  | CHS=5 mm/min | CHS=50 mm/min |                 |
| A          | -1401            | -1754         | -2108         | -35.71           | -59.09       | -30.94        | -8.65           |
| B          | 1633             | 2842          | 4148          | 62.43            | 130.88       | 50.87         | 19.01           |
| C          | 5881             | 5156          | 4612          | 163.74           | 162.00       | 219.71        | 75.94           |
| $R^2$      | 0.875            | 0.878         | 0.693         | 0.785            | 0.979        | 0.849         | 0.632           |

#### Model for Tensile Modulus

The mathematical expression obtained from the experimental results of tensile modulus for different testing speed (Cross Head Speed, CHS) is

$$E_T = Ax^2 + Bx + C \quad (5.1)$$

where,  $E_T$  is the tensile modulus (TM) and “ $x$ ” the percentage weight of filler. A, B and C are parameters which depend on the Cross Head Speed. Thus the Tensile modulus varies with percentage weight of filler and the loading condition, i.e. whether the load is applied gradually (CHS 0.5 mm/min), suddenly (CHS 5 mm/min) or impact mode (CHS 50 mm/min). The numerical values of constants A, B and C are given in table 5-3. From the curves the maximum value for tensile modulus obtained at percentage weight of filler 0.5, 0.75 and 1 respectively for testing speed 0.5, 5 and 50 mm/min.

The variation of tensile strength with the percentage weight of filler as well as the loading condition i.e. CHS can be expressed in the form of a mathematical equation given below,

$$\sigma_T = Ax^2 + Bx + C \quad (5.2)$$

where, ‘ $\sigma_T$ ’ is the tensile strength and  $x$  is the percentage weight of filler. A, B and C are non parameters which depends on the variables considered, such as loading condition and percentage weight of filler. Thus the tensile strength is found to vary with percentage weight of filler and the loading condition, i.e. whether the load applied is gradual (CHS: 0.5 mm/min/ 5 mm/min), sudden (CHS 50 mm/min) .

### **Model for Impact Strength**

The variation of impact strength of the GFRPNCs can be mathematically represented by the following equation.

$$Y_i = Ax^2 + Bx + C \quad (5.3)$$

where ‘ $Y_i$ ’ is the impact strength and  $x$  is the percentage weight of filler. The value of non dimensional parameters A, B and C are tabulated as in Table-5.3, which depend on the percentage weight of filler.

### **Model for Storage Modulus**

The experimental results obtained for the storage modulus from the Dynamic Mechanical Analysis of the GFRPNCs were compared with Boltzmann model as shown in figures 5-7, 5-8 and 5-9 respectively for the conditions 1Hz, 10Hz and 100Hz frequencies. The mathematical equation for the Boltzmann model which found agreeing with the experimental data is given by,

$$G' = \frac{A_1 - A_2}{1 + e^{\frac{(x-x_c)}{dx}}} + A_2 \quad (5.4)$$

where  $G'$  is the storage modulus, which corresponds to the temperature,  $x$  and  $A_1$  and  $A_2$  are lower and upper limit,  $x_c$  centre value and  $dx$  is constant depends on the iteration time. The values obtained for the above parameters are tabulated in Table5-4. The storage modulus depends on the temperature and the non dimensional parameters depend on the frequency and percentage weight of filler. Hence the storage modulus is found to be a function of temperature, percentage weight of filler, frequency etc.

### **Model for Loss modulus**

The experimental results obtained for loss modulus at various filler content from dynamic mechanical analysis are plotted in figures 5-10, 5-11 and 5-12 and the best fit is found to be Lorentz model. The mathematical equation for the same is given below.

$$G'' = y_0 + \frac{2A}{\pi} \times \frac{w}{4(x-x_c)^2 + w^2} \quad (5.5)$$

where,  $y_0$ ,  $A$ ,  $x_c$  and  $w$  are the various non dimensional parameters of the model, whose values are tabulated in Table 5-5. According to the model, the loss modulus ' $G''$ ' is a function of temperature and influenced by the parameters, which depends on the frequency and percentage weight of filler.

#### **Model for Damping Factor ( $\tan\delta$ )**

The experimental results obtained for damping factor plotted in figures 5-13, 5-14 and 5-15, are found in agreement with the Gaussian model. The mathematical equation for the same is given as,

$$y = y_0 + \frac{A}{w\sqrt{\pi/2}} e^{-\frac{2(x-x_c)^2}{w^2}} \quad (5.6)$$

where  $y_0$ ,  $w$ ,  $A$ ,  $x_c$  are parameters of the model tabulated in Table 5-6. In the case of storage modulus and loss modulus which confirmed to the Boltzmann model and Lorentz model respectively, the Gaussian model describes the relation between damping factor and temperature. The damping factor is found to vary with temperature, frequency and percentage weight of filler.

The obtained experimental values are in close agreement with the selected model according to the  $R^2$  value, which substantiate the regression analysis.

**Table 5-4** Values of parameters in Boltzmann model for storage modulus of GFRPNCs

| Parameters<br>→ | 1Hz            |                |                |        |                | 10Hz           |                |                |       |                | 100 Hz         |                |                |       |                |
|-----------------|----------------|----------------|----------------|--------|----------------|----------------|----------------|----------------|-------|----------------|----------------|----------------|----------------|-------|----------------|
|                 | A <sub>1</sub> | A <sub>2</sub> | X <sub>0</sub> | dx     | R <sup>2</sup> | A <sub>1</sub> | A <sub>2</sub> | X <sub>0</sub> | dx    | R <sup>2</sup> | A <sub>1</sub> | A <sub>2</sub> | X <sub>0</sub> | dx    | R <sup>2</sup> |
| 0% filler       | 9402.85        | 1047.70        | 86.11          | 19.31  | 0.993          | 11011.41       | -2564.13       | 114.16         | 42.81 | 0.998          | 10004.48       | 1616.88        | 99.61          | 18.91 | 0.993          |
| 0.5% filler     | 9173.21        | 1472.46        | 81.83          | 11.36  | 0.994          | 9459.73        | 1451.40        | 92.67          | 14.64 | 0.993          | 10879.87       | 1758.35        | 99.61          | 18.91 | 0.993          |
| 1% filler       | 16073.88       | -9541.04       | 276.32         | 109.90 | 0.998          | 10432.97       | 839.78         | 106.96         | 27.40 | 0.997          | 12505.60       | 2021.1         | 99.69          | 18.91 | 0.993          |
| 1.5% filler     | 8594.53        | 1437.32        | 81.75          | 10.52  | 0.996          | 9610.57        | -394.51        | 93.36          | 32.96 | 0.996          | 10218.81       | -33989.08      | 235.60         | 63.52 | 0.996          |
| 2% filler       | 7277.77        | 1479.41        | 90.54          | 18.80  | 0.997          | 7932.77        | 1612.55        | 90.53          | 18.80 | 0.997          | 8005.64        | 1627.34        | 90.53          | 18.80 | 0.997          |

**Table 5-5** Values of parameters in Lorentzian model for loss modulus of GFRPNCs

| Parameters<br>→ | 1Hz     |        |        |           |       | 10Hz   |        |       |           |       | 100 Hz  |        |       |           |       |
|-----------------|---------|--------|--------|-----------|-------|--------|--------|-------|-----------|-------|---------|--------|-------|-----------|-------|
|                 | $y_0$   | $x_c$  | W      | A         | $R^2$ | $y_0$  | $x_c$  | W     | A         | $R^2$ | $y_0$   | $x_c$  | W     | A         | $R^2$ |
| 0% filler       | -25.23  | 84.36  | 82.78  | 96917.17  | 0.626 | 173.51 | 106.28 | 69.68 | 64846.44  | 0.993 | 273.69  | 101.20 | 42.27 | 46691.13  | 0.979 |
| 0.5% filler     | 209.60  | 85.75  | 31.42  | 41713.59  | 0.856 | 232.35 | 96.48  | 34.01 | 49232.76  | 0.956 | 303.59  | 101.20 | 42.27 | 51792.13  | 0.979 |
| 1% filler       | -248.39 | 119.76 | 108.34 | 144614.35 | 0.997 | 18.78  | 106.55 | 78.38 | 95152.23  | 0.995 | 325.82  | 101.20 | 42.27 | 55584.68  | 0.979 |
| 1.5% filler     | 162.03  | 85.66  | 39.61  | 41513.35  | 0.901 | -31.37 | 92.12  | 70.16 | 124871.57 | 0.948 | -159.13 | 106.51 | 90.16 | 141966.21 | 0.974 |
| 2% filler       | 318.76  | 95.37  | 26.27  | 12567.15  | 0.686 | 345.85 | 95.37  | 26.27 | 13635.35  | 0.686 | 354.14  | 95.37  | 26.27 | 13962.11  | 0.686 |

**Table 5-6** Values of parameters in Gaussian model for  $\tan\delta$  of GFRPNCs

| Parameters<br>→ | 1Hz    |        |       |       |       | 10Hz  |        |       |       |       | 100 Hz |        |       |       |       |
|-----------------|--------|--------|-------|-------|-------|-------|--------|-------|-------|-------|--------|--------|-------|-------|-------|
|                 | $y_0$  | $x_c$  | W     | A     | $R^2$ | $y_0$ | $x_c$  | W     | A     | $R^2$ | $y_0$  | $x_c$  | W     | A     | $R^2$ |
| 0% filler       | 0.056  | 103.58 | 30.07 | 6.08  | 0.994 | 0.032 | 128.20 | 62.58 | 12.65 | 0.998 | 0.039  | 113.97 | 40.62 | 8.07  | 0.998 |
| 0.5% filler     | 0.052  | 97.77  | 28.65 | 8.41  | 0.993 | 0.042 | 107.77 | 33.69 | 9.71  | 0.997 | 0.040  | 113.97 | 40.62 | 8.23  | 0.998 |
| 1% filler       | -0.005 | 147.38 | 85.55 | 21.69 | 0.998 | 0.038 | 128.51 | 60.56 | 19.58 | 0.998 | 0.038  | 113.97 | 40.60 | 7.69  | 0.998 |
| 1.5% filler     | 0.045  | 96.62  | 28.45 | 8.77  | 0.995 | 0.041 | 107.27 | 49.95 | 14.64 | 0.974 | 0.012  | 127.39 | 70.26 | 16.17 | 0.978 |
| 2% filler       | 0.057  | 107.93 | 34.55 | 5.01  | 0.996 | 0.057 | 107.46 | 33.29 | 4.84  | 0.996 | 0.058  | 107.46 | 33.29 | 4.91  | 0.996 |

### 5.3.5 X-Ray Diffraction

Figure 5-16 shows the XRD pattern of GFRPNC with 1% Cloisite15A. Similar to the pattern of PNC described in chapter-4, here also no exact peak identified, but peaks with low intensity can be observed, which indicate the occurrence of exfoliated platelets from the entry of polymeric chains and partial intercalation. A broad peak is visible with the pattern at around  $2\theta = 7^\circ$ . A similar broad peak obtained for the PNC also. Thus we cannot identify any exact peak function for the nanocomposite. So the possibility for the intercalation is rare, but the exfoliation of clay platelets by the entry of polymer chains can be confirmed. Thus altogether the indicated trend of pattern substantiated the exfoliation together with intercalation.

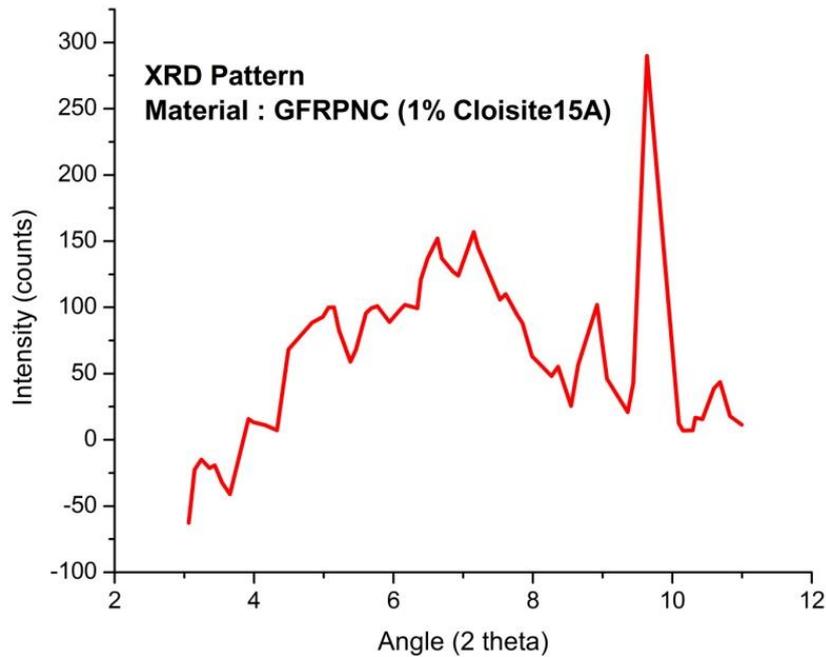
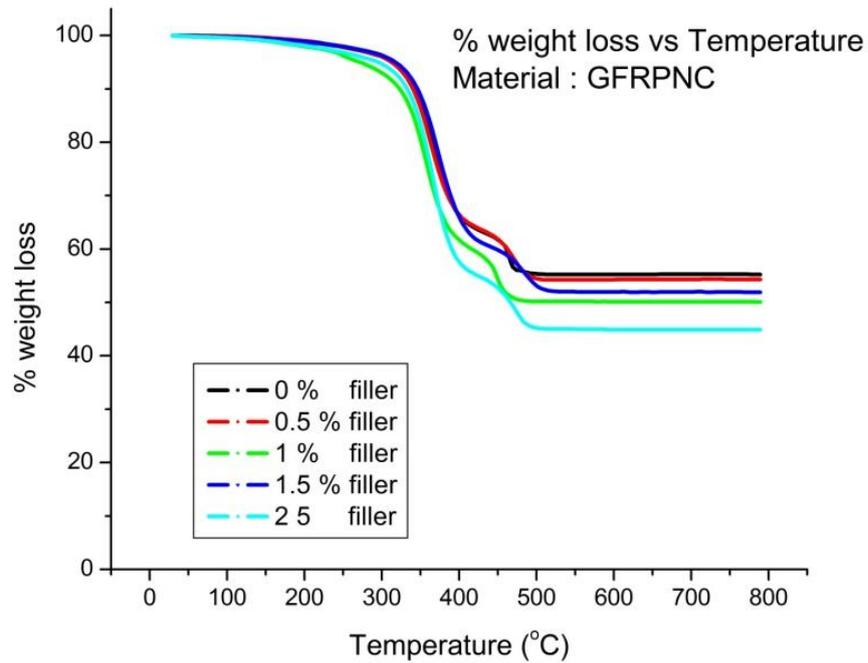


**Figure 5-16** XRD pattern of GFRPNC (1% Cloisite15A)

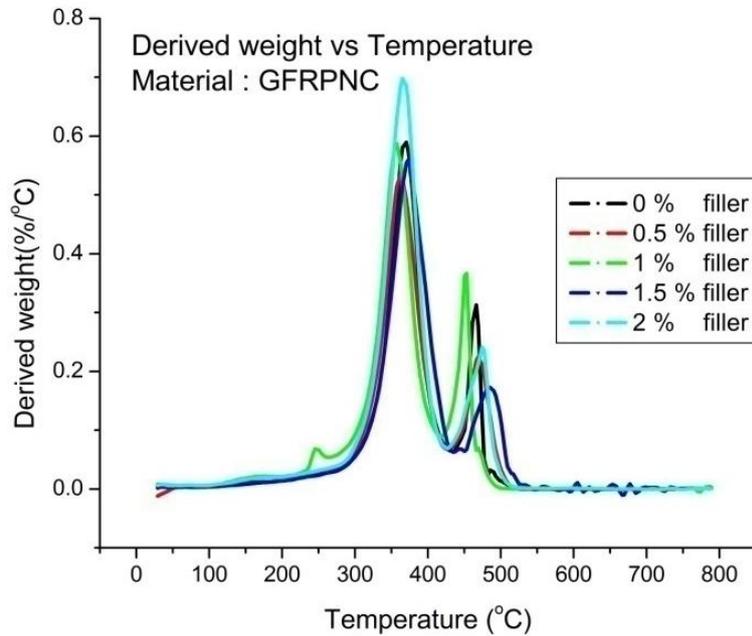
### 5.3.6 Thermogravimetric Analysis

Figure 5-17 and 5-18 illustrate the variation of percentage weight loss and percentage differential weight with increase of temperature of the composite from room temperature to 800 °C of five different samples, prepared by varying the percentage weight of filler (nanoclay) i.e. with 0, 0.5, 1, 1.5, 2 wt. % nanoclay. In the nanocomposites, the curing rate increased with increase of nanoclay loading when compared to the pure polyester FRP. For all blends weight loss is constant up to 150°C and then decomposition starts at around 150 to 200°C. Any remarkable variation in the degradation temperature is not evident from the curve with variation in the quantity of nanoclay content. However, a minor variation is evident which may be due to the variation in the presence of moisture content. The degradation continues with the same trend up to 320 °C with a weight loss of 10%. The second phase of degradation starts at around 320 °C weight losses were constant for different clay filled sample, which is around 25%.

It is clear that, the decomposition temperature of the nanocomposite shifts towards higher temperature indicates improved thermal stability of the polymer up to 2 wt. % clay. The existence of inorganic materials in polymer matrix, generally, enhances the thermal stability of the nanocomposite. The weight-loss temperature curve shows that the residue left beyond 400°C is in line with the inorganic material content of each sample [97]. The degradation begins at approximately 150–200 °C and ends at approximately 300 °C, and the mass loss is 10%. These losses can be attributed to the thermal degradation of the alkyl tails ( $-\text{CH}_2$ ) and ammonium heads ( $-\text{N}(\text{CH}_3)_3$ ) [104]



**Figure 5-17** Variation of % weight loss of glass fiber reinforced polyester nanocomposite with temperature for different filler (Cloisite15A) content



**Figure 5-18** Variation of % derived weight of glass fiber reinforced polyester nanocomposite with temperature at different filler (Cloisite15A) content

### 5.3.7 Differential Scanning Calorimetry

Similar to the analysis of PNCs described in chapter 4, from the DSC curves, the glass transition temperature ( $T_g$ ), was measured. The DSC curves of different GFRPNCs are shown in figure 5-18. Glass transition temperature of all nanocomposites is almost the same or only marginally different from sample without nanofiller. This may be due to the presence of very low quantity of nanofiller. Previous studies revealed an increase in the  $T_g$  from the incorporation of nanofiller in to polyester medium due to the existence of strong interactions between clay and the polyester matrix, which limits the movement of the polyester chain segments. This leads to an increase in the  $T_g$  of the polyester nanocomposites, which is a typical effect for the inclusion of nanofiller (Cloisite15A) in a polymer system. A similar nature of variation in heat flow was observed for PNCs is repeated for GFRPNCs. However the variation in  $T_g$  due to the addition of nanoclay is nearly  $1^\circ\text{C}$ . There is no significant effect contributed by the clay as the major stiffness contribution from reinforcement already happened. [111].

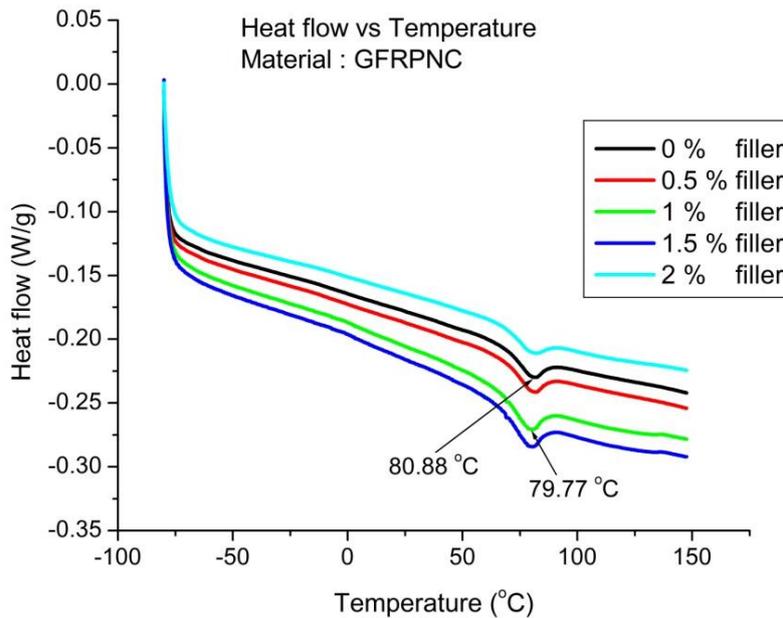


**Figure 5-19** DSC curves of glass fiber reinforced polyester nanocomposite at different filler (Cloisite15A) content

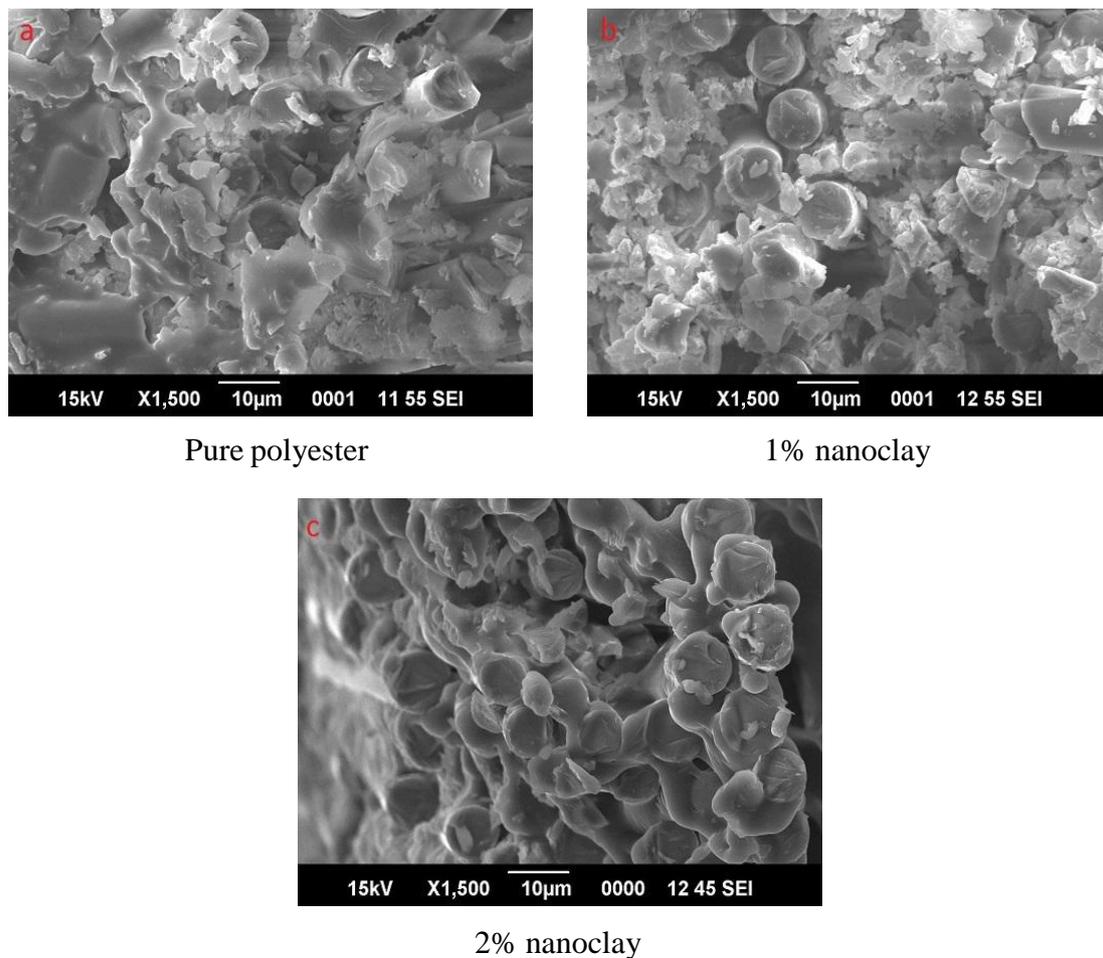
### 5.3.8 SEM Analysis

Examination of fracture surfaces can be used to derive information related to interfacial property and mode of involved dissipation of materials. SEM micrographs of sheared cross section of pure polyester GFRP, 1% nanoclay filled GFRPNC, 2 % nanoclay filled GFRPNC are as shown in figure 5-20 (a) to (c). Figure 5-21 to 5-26 show the fracture surface of 0% nanoclay filled GFRPNC, 1% nanoclay filled GFRPNC and 2% nanoclay filled GFRPNC at testing speed CHS 5 mm/min and 50 mm/min.

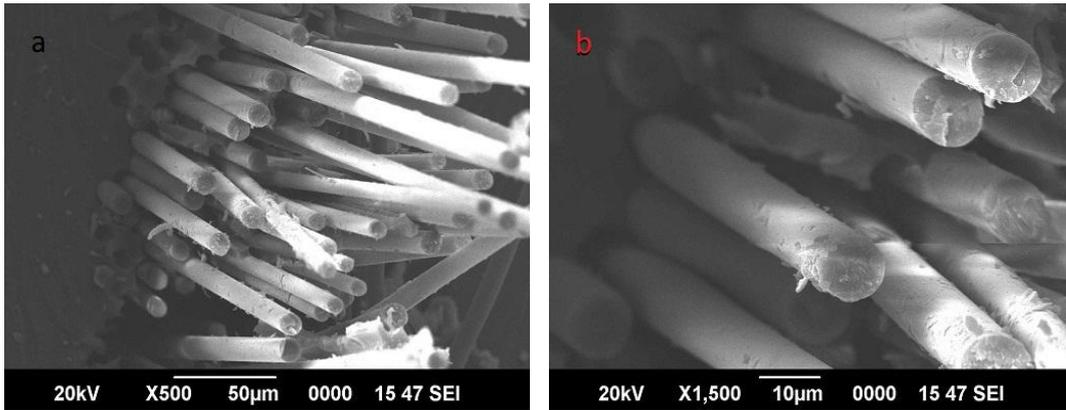
It is clear from the figure 5-21 and 5-22 that, the fracture surface for the 0% nanoclay filled GFRP break at testing speed 0.5 mm/min and 50 mm/min, the fiber pullout is maximum for CHS 50 mm/min. The SEM of 1% nanoclay filled sample shown in figure 5-23 and 5-24 respectively for CHS 5 mm/min and CHS 50 mm/min indicates lower level of fiber pullout as compared to 0% nanoclay filled sample. The neat blend sample shows failure from brittle fracture. From the figure for 1% clay filled GFRPNC it can be observed from the fracture surface, that brittle fracture changes to ductile fracture due to addition of clay particles. Referring to figure 5-25 and 5-26, the specimen with 2% nanoclay, the fiber pull out is not as much as in specimen with 0% nanoclay. The agglomerated clay particles can also be seen in the figure. The high stress concentrations caused by the agglomerated particles might affect the mechanical properties, which result in reduced strength by initiating early failure in the sample with 2% clay.

Figure 5-27, shows the SEM image of the fracture surface of specimen with 0% nanoclay and 1% nanoclay subjected to impact test. A randomly oriented fiber can be observed in the specimen with 0% Cloisite15A, whereas, an orderly arrangement of the fiber is visible in the image of the specimen with 1% nanoclay. The presence of nanoclay contributes an adhesion with the fiber surface, so that the failure will be elapsd.

Generally the incorporation of nanoclay to polyester matrix supports the property enhancement as per the SEM results.



**Figure 5-20** SEM images of fracture surfaces, (a) pure polyester, GFRP (b) 1% nanoclay filled GFRPNC (c) 2% nanoclay filled GFRPNC



**Figure 5-21** Fracture surface of 0% Cloisite15A filled sample under tensile load of CHS 5 mm/min

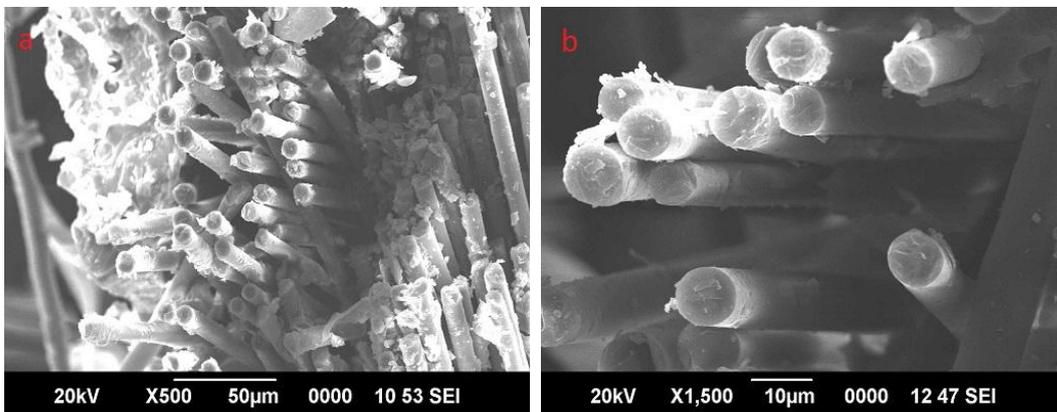


**Figure 5-22** Fracture surface of 0% Cloisite15A filled sample under tensile load of CHS 50 mm/min

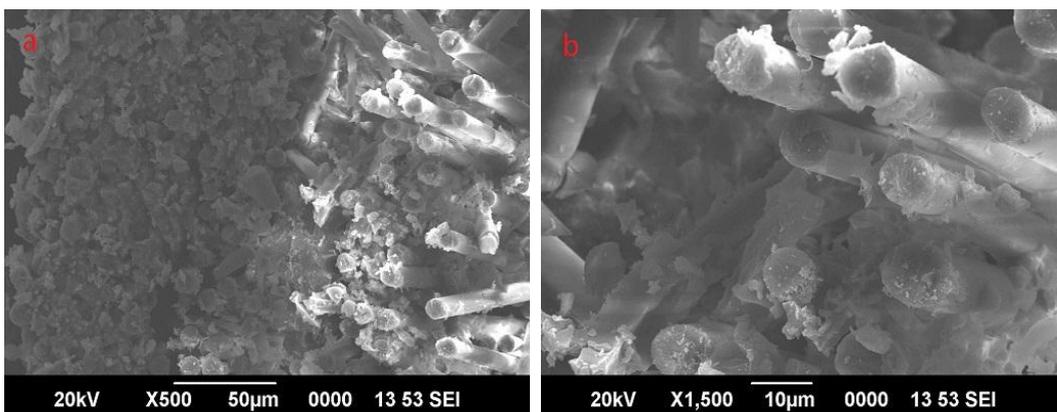


**Figure 5-23** Fracture surface of 1% Cloisite15A filled sample under tensile load of CHS 5 mm/min

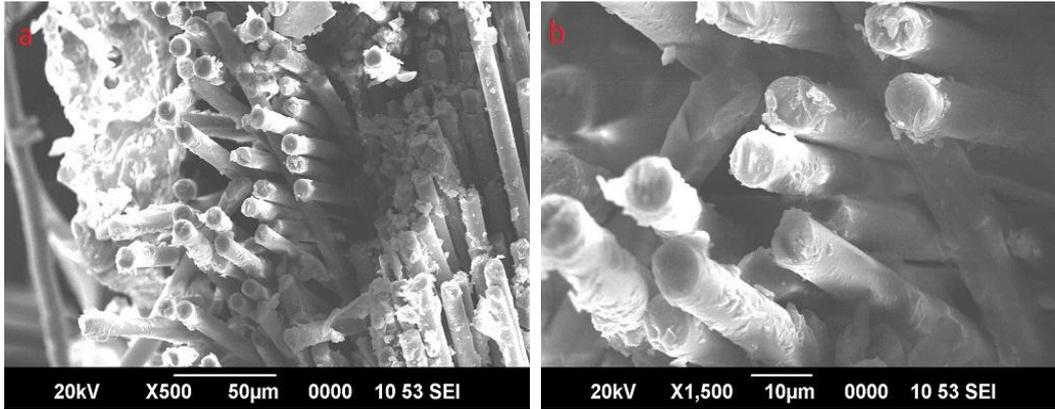


**Figure 5-24** Fracture surface of 1% Cloisite15A filled sample under tensile load of CHS 50 mm/min

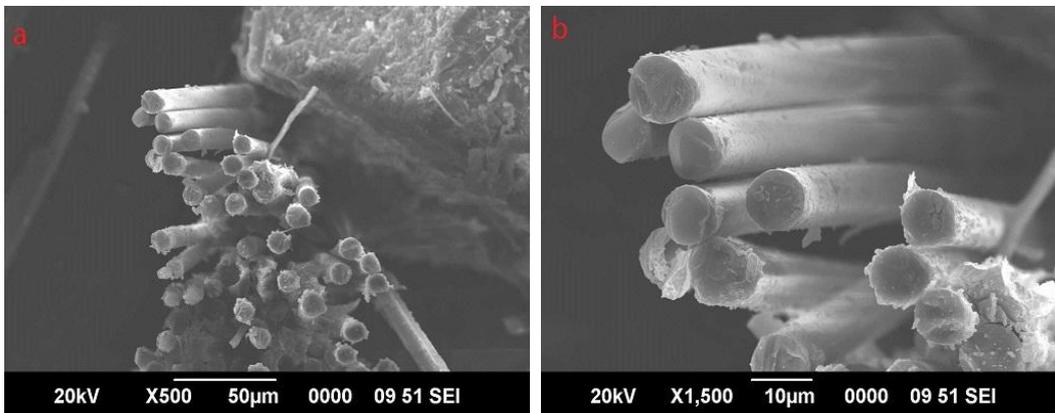


**Figure 5-25** Fracture surface of 2% Cloisite15A filled sample under tensile load of CHS 5 mm/min

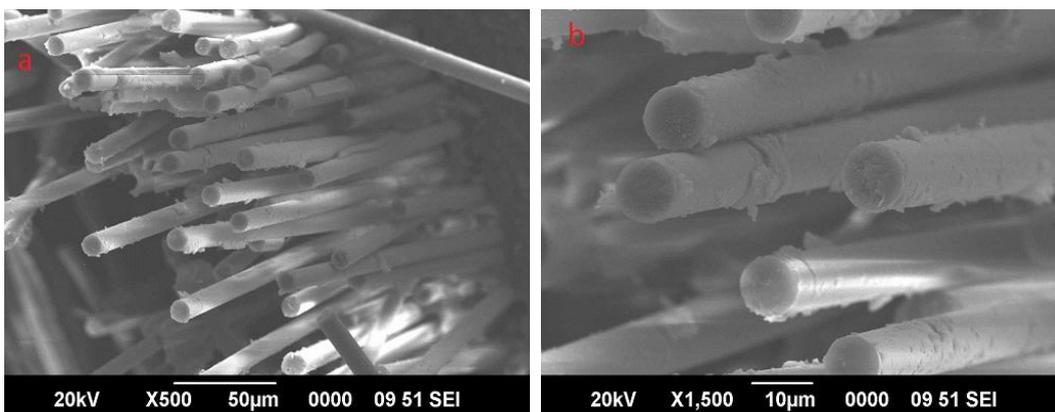


**Figure 5-26** Fracture surface of 2% Cloisite15A filled sample under tensile load of CHS 50 mm/min

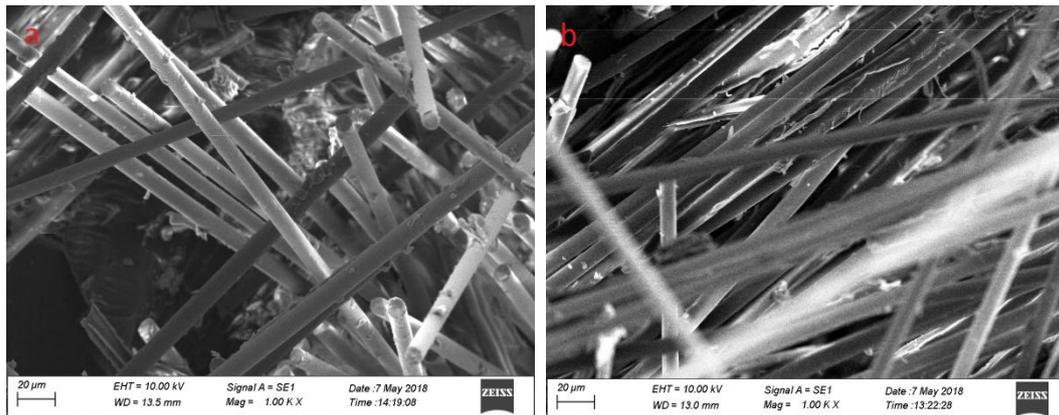


**Figure 5-27** Fracture surface of impact tested specimen with (a) 0% Cloisite15A, (b) 1% Cloisite15A

### 5.3.9 Statistical Analysis

The experimental data obtained from mechanical testing, dynamic mechanical analysis and thermal analysis were subjected to statistical analysis to check the significance of the data. Method of ANOVA used for the same.

#### Tensile Modulus

The details from statistical analysis conducted by the method of two factor ANOVA without replication on experimental results obtained from tensile test is reported in table 5-7.

From the table of ANOVA, the significant value is observed to be 0.0091 for percentage weight of filler with the reported critical value 3.26. Since the significant value is less than the cutoff value 0.05, the null hypothesis (there is no significant difference between the percentage weights of filler in terms of tensile modulus) is rejected. Thus there is a significant difference between the five conditions based on percentage weight of filler in terms of tensile modulus. It signifies an effect on the tensile modulus from the addition of nanoclay in the polyester resin. From the table, when the filler content 0.5%, the highest mean tensile modulus is 5077.02 MPa,

followed by 1% filler content, tensile modulus 4712.62 MPa. The least mean tensile modulus 3149.54 MPa reported for 2% filler.

**Table 5-7** Statistical analysis, Tensile modulus

| <i>SUMMARY</i> | <i>Count</i> | <i>Sum</i> | <i>Average</i> | <i>Variance</i> |
|----------------|--------------|------------|----------------|-----------------|
| 0 % filler     | 5            | 14846.26   | 3711.56        | 6451775.01      |
| 0.5% filler    | 5            | 20308.08   | 5077.02        | 11464139.40     |
| 1% filler      | 5            | 18850.49   | 4712.62        | 9899694.86      |
| 1.5 % filler   | 5            | 15300.45   | 3825.11        | 6687321.35      |
| 2% filler      | 4            | 12598.15   | 3149.54        | 4566534.53      |
| CHS 0.5 mm/min | 4            | 27062.99   | 5412.59        | 1466743         |
| CHs 5 mm/min   | 4            | 26845.98   | 5369.19        | 1079281.63      |
| CHS 50 mm/min  | 4            | 27989.49   | 5597.89        | 1241700.81      |

| <b>ANOVA Report</b>        |           |           |           |          |                |               |
|----------------------------|-----------|-----------|-----------|----------|----------------|---------------|
| <i>Source of Variation</i> | <i>SS</i> | <i>df</i> | <i>MS</i> | <i>F</i> | <i>P-value</i> | <i>F crit</i> |
| % weight of filler         | 9838321   | 4         | 2459580.2 | 5.56     | 0.0091         | 3.26          |
| CHS mm/min                 | 111895812 | 3         | 37298604  | 84.24    | 2.49E-08       | 3.49          |
| Error                      | 5312583   | 12        | 442715.25 |          |                |               |
| Total                      | 127046716 | 19        |           |          |                |               |

In a similar manner based on the variation of CHS, the significant value is observed to be 2.49E-08 with a reported critical value of 3.49. The significant value is less than the cut off value 0.05. Therefore there is a significant effect for CHS in terms of tensile modulus. The maximum mean value of tensile modulus is 5597.89 MPa for CHS 50 mm/min. whereas the minimum value is 5369.19 MPa reported for CHS 5 mm/min.

## Impact Strength

Statistical analysis conducted on the data obtained from Impact test by the method of single factor ANOVA. The details of analysis reported in Table 5-8.

**Table 5-8** Statistical analysis, Impact strength

| <i>Groups</i>                       | <i>Count</i> | <i>Sum</i> | <i>Average</i> | <i>Variance</i> |
|-------------------------------------|--------------|------------|----------------|-----------------|
| % weight of filler                  | 5            | 5          | 1              | 0.63            |
| Impact strength(kJ/m <sup>2</sup> ) | 5            | 418.39     | 83.68          | 35.37           |

ANOVA Report

| <i>Source of Variation</i> | <i>SS</i> | <i>df</i> | <i>MS</i> | <i>F</i> | <i>P-value</i> | <i>F crit</i> |
|----------------------------|-----------|-----------|-----------|----------|----------------|---------------|
| Between Groups             | 17089.71  | 1         | 17089.71  | 949.54   | 1.34E-09       | 5.32          |
| Within Groups              | 143.98    | 8         | 17.99     |          |                |               |
| Total                      | 17233.7   | 9         |           |          |                |               |

The significant value obtained as per the analysis is 1.34E-09 with a reported critical value of 5.32. Since the significant value is less than the cut off value 0.05, the null hypothesis (There is no significant difference between percentage weights of filler in terms of impact strength) is rejected and it can be concluded that there is significant difference between percentage weight of filler in terms of impact strength. Addition of filler plays a significant role in the impact strength of the material.

## Dynamic Mechanical Property

Table 5-9 describes the report of the statistical analysis of the storage modulus. The significant value is reported to be 6.8E-205 for the percentage weight of filler. Since the significant value is less than the cut off value 0.05, the values obtained are significant in terms of storage modulus. Thus there is significant relation between percentage weights

of filler in terms of storage modulus. Regarding frequency, the significant value is 0, which is less than the cut off value 0.05. Hence a significant relation exists between testing frequencies in terms of storage modulus in this case also.

**Table 5-9** Statistical analysis, Storage modulus

Anova: Two-Factor Without Replication

| <i>SUMMARY</i>     | <i>Count</i> | <i>Sum</i> | <i>Average</i> | <i>Variance</i> |
|--------------------|--------------|------------|----------------|-----------------|
| % weight of filler | 515          | 515        | 1              | 0.500973        |
| Frequency 1 Hz     | 515          | 2820118    | 5475.958       | 6887898         |
| Frequency 10 Hz    | 515          | 3040600    | 5904.078       | 5149567         |
| Frequency 100 Hz   | 515          | 3536608    | 6867.199       | 5788210         |

ANOVA Report

| <i>Source of Variation</i> | <i>SS</i> | <i>df</i> | <i>MS</i> | <i>F</i> | <i>P-value</i> | <i>F crit</i> |
|----------------------------|-----------|-----------|-----------|----------|----------------|---------------|
| % weight of filler         | 6.51E+09  | 514       | 12666477  | 7.365    | 6.8E-205       | 1.124         |
| Frequency                  | 1.48E+10  | 3         | 4.94E+09  | 2870.189 | 0              | 2.611         |
| Error                      | 2.65E+09  | 1542      | 1719733   |          |                |               |
| Total                      | 2.4E+10   | 2059      |           |          |                |               |

**Thermal Degradation**

The table describes the report of statistical analysis done for the data obtained by TGA in terms of percentage loss weight (Thermal degradation). The significant value obtained is 0, which is less than cut off value 0.05. Hence there is a significant relation exists between the percentage weight of filler in terms of thermal degradation. But the plot of the experimental result, temperature vs % weight loss in figure 5-16 indicated no noticeable variation in thermal degradation of different nanocomposites with variation in filler content. The correlation of the data is also checked and the report is given below the ANOVA table. The report indicated that good correlation exists between the data for different percentage weight of filler in terms of thermal degradation (% weight loss).

**Table 5-10** Statistical analysis, Thermal degradation

**Anova: Single Factor**

| <i>Groups</i> | <i>Count</i> | <i>Sum</i> | <i>Average</i> | <i>Variance</i> |
|---------------|--------------|------------|----------------|-----------------|
| Temperature   | 766          | 315209     | 411.5          | 48960.17        |
| 0% filler     | 766          | 57644.92   | 75.254         | 407.685         |
| 0.5% filler   | 766          | 57324.03   | 74.836         | 421.360         |
| 1% filler     | 766          | 54749.62   | 71.475         | 487.739         |
| 1.5% filler   | 766          | 56650.15   | 73.956         | 466.099         |
| 2% filler     | 766          | 53067.79   | 69.279         | 606.415         |

**ANOVA Report**

| <i>Source of Variation</i> | <i>SS</i> | <i>df</i> | <i>MS</i> | <i>F</i> | <i>P-value</i> | <i>F crit</i> |
|----------------------------|-----------|-----------|-----------|----------|----------------|---------------|
| % weight of filler         | 73178545  | 5         | 14635709  | 1710.13  | 0              | 2.216         |
| Within Groups              | 39282341  | 4590      | 8558.244  |          |                |               |
| Total                      | 1.12E+08  | 4595      |           |          |                |               |

**Correlation**

|             | <b>0% filler</b> | <b>0.5% filler</b> | <b>1% filler</b> | <b>1.5% filler</b> | <b>2% filler</b> |
|-------------|------------------|--------------------|------------------|--------------------|------------------|
| 0% filler   | 1                |                    |                  |                    |                  |
| 0.5% filler | 0.9996           | 1                  |                  |                    |                  |
| 1% filler   | 0.9975           | 0.9980             | 1                |                    |                  |
| 1.5% filler | 0.9990           | 0.9989             | 0.9948           | 1                  |                  |
| 2% filler   | 0.9996           | 0.9998             | 0.9985           | 0.9984             | 1                |

## 5.4 CONCLUSIONS

Mechanical and thermal properties of nanocomposite have been studied. The following conclusions can be drawn from the study.

1. Highest Tensile modulus and tensile strength were obtained at 0.5 to 1 % nanoclay content. 11 to 50 % improvement in tensile modulus was obtained by the addition of 1% nanoclay. The modulus value for 1.5% and 2% nanoclay filled samples were low.
2. The impact strength also peaked at about 1% nanoclay content.
3. Storage modulus was the highest at about 1% nanoclay filled samples. From the  $\tan\delta$  vs temperature curve the Glass Transition temperature,  $T_g$  was found to be in the range 95 to 110 °C. But from DSC curves the  $T_g$  was found at the range 79 to 81 °C.
4. There was no notable variation in thermal stability by the addition of nano filler. The degradation started at 320 °C for all samples irrespective of the filler content.
5. The DSC results indicate that there is no notable change in  $T_g$  value with the incorporation of nano filler. A drop of approximately 1°C can be observed by the incorporation of 1% nanofiller.
6. The SEM micrographs of fracture surface indicate that pure polyester composite fails under a brittle mode, whereas the addition of nanoclay promotes a ductile nature in the failure. Also there is a slight reduction in fiber pullout by the presence of nanoclay is evident.

## **CHAPTER 6**

### **TENSILE CREEP BEHAVIOR OF NANOCOMPOSITE**

#### **6.1 INTRODUCTION**

Polymer nanocomposites, have gained wide acceptability as an alternative to conventional polymer composites in many applications. Polymer systems are widely used because of their light weight, design flexibility, easy processability and other desirable features [106]. Polymer materials exhibit time dependent behavior. The strain induced; when a load applied and the stress induced when a strain is applied are functions of time. The stress-strain-time relationship, or constitutive law, can be determined by loading a polymer specimen with constant stress (creep) or constant strain (stress relaxation).

When polymer material is subjected to a constant load, it deforms continuously. The initial strain is roughly predicted by its stress-strain modulus. The material will continue to deform slowly with time indefinitely or until rupture. The primary region is the early stage of loading when the creep rate decreases rapidly with time. Then it reaches a steady state which is called the secondary creep stage followed by a rapid increase (tertiary stage) and fracture. This phenomenon of deformation under load with time is called creep.

Creep resistance is an important property for polymeric materials. It is one of the principal properties of natural fiber reinforced polymer composites for many applications such as aerospace, biomedical and civil engineering [107]. However, it is often impractical to test long-term creep behavior directly with experiment because of

the extremely long time required. Thus, predicting the creep behavior of polymers using short-term testing has gained considerable attention. One of the most useful extrapolation techniques is time-temperature superposition (TTS). It can be used to predict long-term creep behavior of certain polymers by shifting the curves from tests at different temperatures horizontally along a logarithmic time axis to generate a single curve known as the master curve. Thus, a long-term experiment can be replaced by shorter tests at higher temperatures. The shifting distance is called shift factor. The materials for which TTS holds are called thermorheologically simple materials and the rest are called thermorheologically complex materials. The influence of high temperature and long time has similar effect on the polymer material. With shifting the single creep curves (measured at different testing temperatures) together to a selected reference temperature, a master curve can be created. This time-temperature superposition method is able to predict the long-term properties of the material from short time creep tests at higher temperature [56][108][109]. The relation between temperature and the shift factor can generally be described by the Arrhenius Equation. Long term creep estimations, based on master curves and heuristic relations are used to provide information on the given small loads and help designers to a limited extent in dimensioning a given product to its whole life span knowing the forces, environment and in estimating the expected failure time of the part even though it does not provide information on failure deformation or life span.

There are two superposition principles, which are important in predicting creep behavior of plastic materials under various test conditions. The first of these is the Boltzmann Superposition Principle, which describes the response of a material to

different loading. It states that the response of a material to a given load is independent of the response of the material to any load, which is already on the material. The deformation of a specimen is directly proportional to the applied stress, when all deformations are compared to equivalent times. It is only valid in linear viscoelastic region. For the case of creep, the total strain may be expressed by

$$\varepsilon(t) = \int_{-\alpha}^t D(t-\tau) d\sigma(\tau) \quad (6.1)$$

Where  $D(t) = 1/E(t)$  is the compliance function, which is a characteristic of the polymer at a given temperature and initial stress. The second is the Time Temperature superposition Principle, which describes the equivalence of time and temperature. It used Williams-Landel-Ferry (WLF) equation in glass transition region and Arrhenius model outside the glass transition region.

The WLF equation is:

$$\log a_T = \frac{-C_1(T - T_{\text{ref}})}{C_2 + (T - T_{\text{ref}})} \quad (6.2)$$

$a_T$  horizontal (time) shift factor ,

$C_1$  and  $C_2$  are constants,

$T_{\text{ref}}$  reference temperature(K)

$T$  temperature at which test is performed

Arrhenius equation is: 
$$\log a_T = \frac{Ea}{R} \left( \frac{1}{T} - \frac{1}{T_{\text{ref}}} \right) \quad (6.3)$$

$Ea$  is the activation energy ,

$R$  is the universal gas constant,

$T_{\text{ref}}$  is the reference temperature(K),

$T$  is the temperature at which test is performed

The creep behavior of fiber reinforced composites depends strongly on stress, temperature, void content, and fiber loading [51]. It was concluded, that creep resistance decreases if temperature or stress rises. Several investigations on the influence of adhesion and density of composites on the creep behavior have already been done and found that with the increase in consolidation (lower void content), the resistance to creep increases [108][110].

Here in this chapter, the dynamic mechanical behavior of the polymer nanocomposites and glass fiber reinforced polymer nanocomposite on frequency sweep mode i.e. at constant temperature for different frequencies were proposed to analyze. The tensile creep behavior of both PNCs and GFRPNCs were also proposed to be analyzed.

## **6.2 METHODOLOGY**

### **6.2.1 Raw materials**

Raw materials used for the preparation of nanocomposite were, isophthalic polyester resin as the matrix material, cobalt naphthenate as the accelerator and methyl ethyl ketone peroxide (MEKP) as the catalyst. The clay was made into dispersion with styrene and then the dispersion was added to the polyester resin for modification. Cloisite15A, quaternary ammonium modified montmorillonite was used as the nano filler. 200 gsm glass fiber mat was used for the reinforcement of polyester matrix.

### **6.2.2 Specimen Preparation**

The procedure for the preparation of polymer nanocomposites and glass fiber reinforced polymer nanocomposites are described in the previous chapters. Same procedure is followed here also. For the PNCs, the specimen similar to that used for impact test illustrated in figure 4-2 was prepared for the dynamic mechanical analysis in frequency sweep mode. Similarly for the analysis of GFRPNCs in frequency sweep mode, the specimen similar to that illustrated in figure 5-3 was prepared. The specimen were prepared with 0%, 1% and 2% nanoclay, Cloisite15A, for both PNCs and GFRPNCs. The specimen used for the analysis of tensile creep behavior is explained under section 6.2.3. the size and shape of the specimen for the same was proposed by the machine standard.

### **6.2.3 Creep Study**

Tensile creep behavior of the material has been studied by using the DMA Q800 apparatus (TA Instruments, New Castle, USA). The specimen of PNC was prepared by casting in a mould which was specially prepared with a cavity of size 25 mm X 4 mm and 2.5 mm depth in a thick Teflon sheet. The specimen of GFRPNC for the test was cut out of the GFRP sheet in the size: length 25 mm, width 4 mm, thickness 1 mm. The experiment was conducted for the samples with 0 wt%, 1wt% and 2 wt% Cloisite15A as filler for both polyester nanocomposite and glass fiber reinforced polyester nanocomposite. The test was conducted at constant stress of 1MPa and 2MPa each separately at a reference temperature 30 °C (approximated to room temperature) for GFRPNCs. However, the conduct of the test for PNCs was very difficult as the specimen get stick to the support while subjected temperature for a long time. So the experiment for PNCs was limited to a constant stress 1 MPa.

The creep performance is commonly represented by creep compliance  $J(t) = \varepsilon(t)/\sigma$ , where  $\varepsilon(t)$  is creep strain and  $\sigma$  is applied stress [68].

In order to investigate the dynamic mechanical behavior of the material at constant temperature for different frequency it has been analyzed by the method of frequency sweep. The experiment was conducted for frequencies 0.5 Hz, 1.1 Hz, 2.3 Hz, 5.5 Hz, 12 Hz, 23 Hz and 50 Hz by the method of frequency sweep in the temperature ramp mode for the temperature range from room temperature to 140°C at an increment of 5°C. The different frequency conditions mentioned were applied for 5 minutes at isothermal condition. The experiment was conducted for 0%, 1% and 2% nanoclay filled samples. This experiment is helpful to determine the variation in the viscoelastic properties of the material due to the change in frequency of the stress.

## **6.3 RESULTS AND DISCUSSION**

### **6.3.1 Dynamic Mechanical Analysis in frequency sweep**

The results obtained from the analysis of dynamic mechanical behavior of PNCs from experiment conducted by frequency sweep test for the frequencies: 0.5, 1.1, 2.3, 5, 10.8, 23.2, 50 Hz are as given in table 6-1 to 6-3. The variation of storage modulus with temperature is plotted in figure 6-1 to 6-3, which describe the decrease of storage modulus with temperature and increase of storage modulus with frequency. Also the storage modulus curves for different frequency line converge to a single curve as temperature approaches to 140°C. When the temperature reaches to about 100 °C the storage modulus reduced to zero.

The loss modulus for 0%, 1% and 2% nanofilled PNCs are plotted in figure 6-4 to 6-6. The loss modulus peak is observed around 70 to 80 °C for various frequencies. The loss modulus curves for various frequencies converge to a single point for temperature at around 40 °C. The loss modulus initially increases with temperature following the general trend for the nanocomposite with 1% and 2% filler, whereas for pure polyester, the increase is not as much as for nanocomposite. A similar trend of variation as that of loss modulus is indicated by  $\text{Tan}\delta$  (Figure 6-7 to 6-9). The peak is obtained at around 100 to 120 °C. There is a shift for the peak towards higher temperature for 1% nanoclay filled sample which may be due to the slight change in glass transition temperature. Also a clear peak is observed for 1% nanoclay filled PNC.

After glass transition range there is a large drop of loss modulus value for low frequency lines and comparatively small drop for high frequency lines. The trend is more clear and gradual for 1% nanoclay filled sample. On the other hand a systematic variation of loss modulus as well as storage modulus is evident in 1% nanoclay filled sample. A similar trend as that of loss modulus is followed for damping factor  $\text{tan}\delta$ . An increase in stiffness at lower weight percentage of filler can be concluded from the trend of these curves. At a lower percentage level of filler the stiffness of the material increases with increase of filler content. For high percentage of filler, the agglomeration of clay particles leads to non uniform mixing, which will contribute to the decrease of stiffness.

**Table 6-1** Dynamic mechanical properties at various frequencies for neat resin (polyester)

| Temperature (°C) — 0% | Frequency = 0.5 Hz     |                     |           | 1.1 Hz                 |                     |           | 2.3 Hz                 |                     |           | 5 Hz                   |                     |           | 10.8 Hz                |                     |           | 23.2 Hz                |                     |           | 50 Hz                  |                     |           |
|-----------------------|------------------------|---------------------|-----------|------------------------|---------------------|-----------|------------------------|---------------------|-----------|------------------------|---------------------|-----------|------------------------|---------------------|-----------|------------------------|---------------------|-----------|------------------------|---------------------|-----------|
|                       | Storage Modulus in MPa | Loss Modulus in MPa | Tan Delta | Storage Modulus in MPa | Loss Modulus in MPa | Tan Delta | Storage Modulus in MPa | Loss Modulus in MPa | Tan Delta | Storage Modulus in MPa | Loss Modulus in MPa | Tan Delta | Storage Modulus in MPa | Loss Modulus in MPa | Tan Delta | Storage Modulus in MPa | Loss Modulus in MPa | Tan Delta | Storage Modulus in MPa | Loss Modulus in MPa | Tan Delta |
| 36                    | 2120                   | 152                 | 0.07      | 2188                   | 153                 | 0.07      | 2254                   | 153                 | 0.07      | 2325                   | 152                 | 0.07      | 2394                   | 150                 | 0.06      | 2461                   | 146                 | 0.06      | 2528                   | 141                 | 0.06      |
| 46                    | 1881                   | 151                 | 0.08      | 1939                   | 152                 | 0.08      | 1996                   | 153                 | 0.08      | 2062                   | 155                 | 0.08      | 2130                   | 157                 | 0.07      | 2197                   | 158                 | 0.07      | 2268                   | 160                 | 0.07      |
| 56                    | 1554                   | 147                 | 0.09      | 1613                   | 149                 | 0.09      | 1670                   | 152                 | 0.09      | 1737                   | 155                 | 0.09      | 1806                   | 158                 | 0.09      | 1875                   | 162                 | 0.09      | 1950                   | 167                 | 0.09      |
| 66                    | 1187                   | 150                 | 0.13      | 1245                   | 153                 | 0.12      | 1302                   | 156                 | 0.12      | 1370                   | 160                 | 0.12      | 1443                   | 164                 | 0.11      | 1515                   | 170                 | 0.11      | 1594                   | 176                 | 0.11      |
| 76                    | 790                    | 151                 | 0.19      | 853                    | 153                 | 0.18      | 913                    | 156                 | 0.17      | 983                    | 161                 | 0.16      | 1058                   | 166                 | 0.16      | 1134                   | 173                 | 0.15      | 1215                   | 182                 | 0.15      |
| 86                    | 517                    | 127                 | 0.25      | 574                    | 131                 | 0.23      | 629                    | 137                 | 0.22      | 693                    | 143                 | 0.21      | 761                    | 151                 | 0.20      | 831                    | 160                 | 0.19      | 908                    | 170                 | 0.19      |
| 96                    | 330                    | 101                 | 0.31      | 378                    | 108                 | 0.29      | 426                    | 116                 | 0.27      | 482                    | 124                 | 0.26      | 543                    | 134                 | 0.25      | 607                    | 144                 | 0.24      | 678                    | 155                 | 0.23      |
| 106                   | 203                    | 72.9                | 0.36      | 238                    | 82.3                | 0.35      | 276                    | 91.8                | 0.33      | 322                    | 103                 | 0.32      | 373                    | 114                 | 0.31      | 429                    | 125                 | 0.29      | 492                    | 138                 | 0.28      |
| 116                   | 111                    | 42.8                | 0.38      | 132                    | 51.5                | 0.39      | 155                    | 60.7                | 0.39      | 185                    | 72                  | 0.39      | 222                    | 84.5                | 0.38      | 264                    | 97.8                | 0.37      | 314                    | 112                 | 0.36      |
| 126                   | 61.2                   | 19.9                | 0.32      | 70.5                   | 25.3                | 0.36      | 81.7                   | 31.7                | 0.39      | 97.5                   | 40.2                | 0.41      | 118                    | 50.7                | 0.43      | 143                    | 62.7                | 0.44      | 176                    | 76.7                | 0.44      |
| 136                   | 41.6                   | 8.33                | 0.20      | 45.5                   | 11.1                | 0.24      | 50.3                   | 14.5                | 0.29      | 57.4                   | 19.4                | 0.34      | 67.1                   | 25.8                | 0.38      | 79.8                   | 33.9                | 0.42      | 97.5                   | 44.2                | 0.45      |
| 140                   | 37.9                   | 5.82                | 0.15      | 40.5                   | 7.89                | 0.19      | 43.9                   | 10.5                | 0.24      | 49                     | 14.2                | 0.29      | 55.9                   | 19.2                | 0.34      | 65.3                   | 25.7                | 0.39      | 78.6                   | 34.1                | 0.43      |

**Table 6-2** Dynamic mechanical properties at various frequencies for 1% Cloisite15A filled PNC

| Temperature (°C)—1% | Frequency = 0.5 Hz    |                    | 1.1 Hz                |                    | 2.3 Hz                |                    | 5 Hz                  |                    | 10.8 Hz               |                    | 23.2 Hz               |                    | 50 Hz                 |                    |           |      |       |       |      |       |       |      |
|---------------------|-----------------------|--------------------|-----------------------|--------------------|-----------------------|--------------------|-----------------------|--------------------|-----------------------|--------------------|-----------------------|--------------------|-----------------------|--------------------|-----------|------|-------|-------|------|-------|-------|------|
|                     | Storage Modulus (MPa) | Loss Modulus (MPa) | Storage Modulus (MPa) | Loss Modulus (MPa) | Storage Modulus (MPa) | Loss Modulus (MPa) | Storage Modulus (MPa) | Loss Modulus (MPa) | Storage Modulus (MPa) | Loss Modulus (MPa) | Storage Modulus (MPa) | Loss Modulus (MPa) | Storage Modulus (MPa) | Loss Modulus (MPa) | Tan Delta |      |       |       |      |       |       |      |
| 32                  | 2205                  | 139.7              | 0.06                  | 134.3              | 2328                  | 130.2              | 0.06                  | 2388               | 127.1                 | 0.05               | 2441                  | 124.8              | 0.05                  | 2496               | 123.2     | 0.05 | 2547  | 123.4 | 0.05 | 2547  | 123.4 | 0.05 |
| 42                  | 1964                  | 153.3              | 0.08                  | 151.2              | 2081                  | 149.5              | 0.07                  | 2146               | 147.2                 | 0.07               | 2209                  | 144.7              | 0.07                  | 2270               | 142.8     | 0.06 | 2333  | 142.2 | 0.06 | 2333  | 142.2 | 0.06 |
| 52                  | 1594                  | 160.8              | 0.10                  | 163.3              | 1718                  | 166.9              | 0.10                  | 1791               | 170.2                 | 0.10               | 1868                  | 172.9              | 0.09                  | 1943               | 175.4     | 0.09 | 2024  | 177.8 | 0.09 | 2024  | 177.8 | 0.09 |
| 62                  | 1086                  | 173.2              | 0.16                  | 179                | 1212                  | 185.4              | 0.16                  | 1291               | 191.2                 | 0.15               | 1377                  | 197.2              | 0.15                  | 1463               | 204       | 0.14 | 1557  | 211.3 | 0.14 | 1557  | 211.3 | 0.14 |
| 72                  | 514.5                 | 165                | 0.33                  | 173.6              | 652.5                 | 182                | 0.28                  | 736.4              | 191.9                 | 0.26               | 826.6                 | 202                | 0.25                  | 918.7              | 212.4     | 0.23 | 1019  | 223.7 | 0.22 | 1019  | 223.7 | 0.22 |
| 82                  | 214.8                 | 108.3              | 0.51                  | 124.4              | 323                   | 139.8              | 0.44                  | 392.8              | 156.4                 | 0.40               | 470.9                 | 172.6              | 0.37                  | 554.9              | 188.1     | 0.34 | 647.8 | 203.6 | 0.32 | 647.8 | 203.6 | 0.32 |
| 92                  | 84.71                 | 55.63              | 0.66                  | 71.43              | 145.6                 | 88.13              | 0.61                  | 191.1              | 108                   | 0.57               | 247.3                 | 128.9              | 0.53                  | 313                | 149.9     | 0.49 | 390.3 | 171   | 0.44 | 390.3 | 171   | 0.44 |
| 102                 | 33.06                 | 20.14              | 0.60                  | 28.32              | 54.73                 | 38.5               | 0.70                  | 73.91              | 52.77                 | 0.72               | 101                   | 70.64              | 0.71                  | 137.2              | 91.41     | 0.68 | 185.3 | 115.2 | 0.63 | 185.3 | 115.2 | 0.63 |
| 112                 | 18.39                 | 6.385              | 0.34                  | 9.3                | 24.97                 | 13.23              | 0.52                  | 31.06              | 19.36                 | 0.61               | 40.28                 | 28.17              | 0.69                  | 53.84              | 40.18     | 0.74 | 74.16 | 56.38 | 0.76 | 74.16 | 56.38 | 0.76 |
| 122                 | 14.27                 | 2.153              | 0.15                  | 3.205              | 16.47                 | 4.661              | 0.28                  | 18.55              | 6.99                  | 0.37               | 21.74                 | 10.47              | 0.48                  | 26.54              | 15.52     | 0.58 | 33.98 | 22.94 | 0.67 | 33.98 | 22.94 | 0.67 |
| 132                 | 12.91                 | 0.819              | 0.06                  | 1.213              | 13.71                 | 1.784              | 0.13                  | 14.49              | 2.73                  | 0.19               | 15.73                 | 4.18               | 0.26                  | 17.71              | 6.311     | 0.35 | 20.79 | 9.452 | 0.45 | 20.79 | 9.452 | 0.45 |
| 140                 | 12.38                 | 0.447              | 0.04                  | 0.62               | 12.79                 | 0.885              | 0.07                  | 13.17              | 1.344                 | 0.10               | 13.77                 | 2.075              | 0.15                  | 14.78              | 3.153     | 0.21 | 16.33 | 4.632 | 0.28 | 16.33 | 4.632 | 0.28 |

**Table 6-3** Dynamic mechanical properties at various frequencies for 2% Cloisite15A filled PNC

| Temperature in °C—<br>2% | 0.5 Hz                 |                     |           | 1.1 Hz                 |                     |           | 2.3 Hz                 |                     |           | 5 Hz                   |                     |           | 10.8 Hz                |                     |           | 23.2 Hz                |                     |           | 50 Hz                  |                     |           |
|--------------------------|------------------------|---------------------|-----------|------------------------|---------------------|-----------|------------------------|---------------------|-----------|------------------------|---------------------|-----------|------------------------|---------------------|-----------|------------------------|---------------------|-----------|------------------------|---------------------|-----------|
|                          | Storage Modulus in MPa | Loss Modulus in MPa | Tan Delta | Storage Modulus in MPa | Loss Modulus in MPa | Tan Delta | Storage Modulus in MPa | Loss Modulus in MPa | Tan Delta | Storage Modulus in MPa | Loss Modulus in MPa | Tan Delta | Storage Modulus in MPa | Loss Modulus in MPa | Tan Delta | Storage Modulus in MPa | Loss Modulus in MPa | Tan Delta | Storage Modulus in MPa | Loss Modulus in MPa | Tan Delta |
| 32                       | 2069                   | 114.8               | 0.06      | 2130                   | 110.6               | 0.05      | 2173                   | 111.1               | 0.05      | 2224                   | 111.4               | 0.05      | 2274                   | 112.5               | 0.05      | 2324                   | 115.1               | 0.05      | 2359                   | 122.7               | 0.05      |
| 42                       | 1913                   | 118.1               | 0.06      | 1961                   | 117.3               | 0.06      | 2007                   | 116.7               | 0.06      | 2058                   | 116.3               | 0.06      | 2109                   | 116.6               | 0.06      | 2159                   | 118.1               | 0.05      | 2212                   | 121.7               | 0.06      |
| 52                       | 1673                   | 131.4               | 0.08      | 1725                   | 132                 | 0.08      | 1775                   | 133.3               | 0.08      | 1833                   | 134.4               | 0.07      | 1893                   | 135.2               | 0.07      | 1952                   | 136.5               | 0.07      | 2013                   | 138.9               | 0.07      |
| 62                       | 1373                   | 134.6               | 0.10      | 1424                   | 137.9               | 0.10      | 1474                   | 141.8               | 0.10      | 1535                   | 145.9               | 0.10      | 1599                   | 150.5               | 0.09      | 1665                   | 155.9               | 0.09      | 1736                   | 161.8               | 0.09      |
| 72                       | 941.9                  | 153                 | 0.16      | 997.6                  | 154.7               | 0.16      | 1054                   | 157.2               | 0.15      | 1122                   | 161.4               | 0.15      | 1193                   | 166.5               | 0.14      | 1266                   | 172.9               | 0.14      | 1346                   | 180.6               | 0.13      |
| 82                       | 586.5                  | 140.8               | 0.24      | 647.8                  | 144.4               | 0.22      | 706.3                  | 148.9               | 0.21      | 775                    | 154.8               | 0.20      | 846.9                  | 161.7               | 0.19      | 920.5                  | 169.7               | 0.19      | 1000                   | 179.1               | 0.18      |
| 92                       | 363                    | 114.1               | 0.32      | 417.3                  | 122                 | 0.29      | 471.5                  | 129.6               | 0.28      | 534.8                  | 138.5               | 0.26      | 602.1                  | 147.8               | 0.25      | 673                    | 157.7               | 0.24      | 750                    | 168.5               | 0.23      |
| 102                      | 236.5                  | 88.44               | 0.38      | 280.7                  | 98.62               | 0.35      | 327                    | 108.5               | 0.33      | 381.9                  | 119.6               | 0.31      | 441.7                  | 131                 | 0.30      | 506.6                  | 142.7               | 0.28      | 578                    | 155.3               | 0.27      |
| 112                      | 137.3                  | 59.46               | 0.44      | 166.3                  | 69.84               | 0.42      | 198.3                  | 80.56               | 0.41      | 238.8                  | 93.01               | 0.39      | 285.9                  | 106.3               | 0.38      | 338.8                  | 120.2               | 0.36      | 399.7                  | 135                 | 0.34      |
| 122                      | 64.26                  | 28.71               | 0.44      | 77.82                  | 36.29               | 0.46      | 93.87                  | 44.82               | 0.48      | 116.3                  | 55.88               | 0.48      | 144.8                  | 68.86               | 0.48      | 179.3                  | 83.34               | 0.47      | 222.2                  | 99.57               | 0.45      |
| 132                      | 34.46                  | 11.05               | 0.32      | 39.52                  | 14.68               | 0.37      | 45.85                  | 19.21               | 0.41      | 55.19                  | 25.67               | 0.46      | 67.97                  | 34.11               | 0.50      | 84.9                   | 44.62               | 0.52      | 107.8                  | 57.75               | 0.54      |
| 140                      | 26.09                  | 5.024               | 0.19      | 28.37                  | 6.853               | 0.24      | 31.26                  | 9.185               | 0.29      | 35.63                  | 12.66               | 0.35      | 41.76                  | 17.45               | 0.42      | 50.2                   | 23.82               | 0.47      | 62.19                  | 32.35               | 0.52      |

**Table 6-4** Dynamic mechanical properties at various frequencies for 0% Cloisite15A filled GFRPNC

| Temperature (°C) | Frequency = 0.5 Hz    |                    |           | 1.1 Hz                |                    |           | 2.3 Hz                |                    |           | 5 Hz                  |                    |           | 10.8 Hz               |                    |           | 23.2 Hz               |                    |           | 50 Hz                 |                    |           |
|------------------|-----------------------|--------------------|-----------|-----------------------|--------------------|-----------|-----------------------|--------------------|-----------|-----------------------|--------------------|-----------|-----------------------|--------------------|-----------|-----------------------|--------------------|-----------|-----------------------|--------------------|-----------|
|                  | Storage Modulus (MPa) | Loss Modulus (MPa) | Tan Delta | Storage Modulus (MPa) | Loss Modulus (MPa) | Tan Delta | Storage Modulus (MPa) | Loss Modulus (MPa) | Tan Delta | Storage Modulus (MPa) | Loss Modulus (MPa) | Tan Delta | Storage Modulus (MPa) | Loss Modulus (MPa) | Tan Delta | Storage Modulus (MPa) | Loss Modulus (MPa) | Tan Delta | Storage Modulus (MPa) | Loss Modulus (MPa) | Tan Delta |
| 33               | 8517                  | 522                | 0.06      | 8776                  | 499                | 0.06      | 9008                  | 475                | 0.05      | 9233                  | 450                | 0.05      | 9436                  | 430                | 0.05      | 9638                  | 418                | 0.04      | 9849                  | 411                | 0.04      |
| 43               | 8219                  | 494                | 0.06      | 8446                  | 477                | 0.06      | 8657                  | 460                | 0.05      | 8870                  | 441                | 0.05      | 9068                  | 424                | 0.05      | 9265                  | 411                | 0.04      | 9474                  | 408                | 0.04      |
| 53               | 7867                  | 486                | 0.06      | 8089                  | 472                | 0.06      | 8295                  | 457                | 0.06      | 8507                  | 442                | 0.05      | 8707                  | 428                | 0.05      | 8908                  | 416                | 0.05      | 9120                  | 412                | 0.05      |
| 63               | 7592                  | 525                | 0.07      | 7832                  | 509                | 0.07      | 8056                  | 496                | 0.06      | 8288                  | 481                | 0.06      | 8507                  | 467                | 0.05      | 8729                  | 455                | 0.05      | 8958                  | 453                | 0.05      |
| 73               | 7038                  | 652                | 0.09      | 7316                  | 629                | 0.09      | 7569                  | 609                | 0.08      | 7840                  | 588                | 0.08      | 8102                  | 569                | 0.07      | 8362                  | 551                | 0.07      | 8631                  | 544                | 0.06      |
| 83               | 6129                  | 757                | 0.12      | 6463                  | 736                | 0.11      | 6770                  | 717                | 0.11      | 7095                  | 696                | 0.1       | 7409                  | 674                | 0.09      | 7718                  | 654                | 0.08      | 8036                  | 646                | 0.08      |
| 93               | 5142                  | 805                | 0.16      | 5521                  | 810                | 0.15      | 5877                  | 810                | 0.14      | 6257                  | 800                | 0.13      | 6626                  | 785                | 0.12      | 6991                  | 764                | 0.11      | 7370                  | 761                | 0.1       |
| 100              | 4465                  | 769                | 0.17      | 4843                  | 810                | 0.17      | 5211                  | 835                | 0.16      | 5617                  | 847                | 0.15      | 6019                  | 846                | 0.14      | 6421                  | 835                | 0.13      | 6846                  | 836                | 0.12      |
| 103              | 4210                  | 729                | 0.17      | 4571                  | 784                | 0.17      | 4933                  | 823                | 0.17      | 5338                  | 849                | 0.16      | 5748                  | 860                | 0.15      | 6162                  | 857                | 0.14      | 6604                  | 864                | 0.13      |
| 113              | 3524                  | 539                | 0.15      | 3798                  | 623                | 0.16      | 4095                  | 702                | 0.17      | 4455                  | 777                | 0.17      | 4847                  | 838                | 0.17      | 5269                  | 880                | 0.17      | 5747                  | 919                | 0.16      |
| 123              | 3166                  | 335                | 0.11      | 3334                  | 409                | 0.12      | 3528                  | 490                | 0.14      | 3779                  | 584                | 0.15      | 4079                  | 681                | 0.17      | 4432                  | 771                | 0.17      | 4867                  | 867                | 0.18      |
| 133              | 3056                  | 194                | 0.06      | 3149                  | 241                | 0.08      | 3260                  | 297                | 0.09      | 3408                  | 373                | 0.11      | 3595                  | 463                | 0.13      | 3837                  | 564                | 0.15      | 4175                  | 686                | 0.16      |
| 140              | 3062                  | 136                | 0.04      | 3125                  | 165                | 0.05      | 3198                  | 204                | 0.06      | 3296                  | 259                | 0.08      | 3423                  | 331                | 0.1       | 3594                  | 419                | 0.12      | 3855                  | 534                | 0.14      |

**Table 6-5** Dynamic mechanical properties at various frequencies for 1% Cloisite15A filled GFRPNC

| Temperature (°C) | Frequency = 0.5 Hz    |                    |           | 1.1 Hz                |                    |           | 2.3 Hz                |                    |           | 5 Hz                  |                    |           | 10.8 Hz               |                    |           | 23.2 Hz               |                    |           | 50 Hz                 |                    |           |
|------------------|-----------------------|--------------------|-----------|-----------------------|--------------------|-----------|-----------------------|--------------------|-----------|-----------------------|--------------------|-----------|-----------------------|--------------------|-----------|-----------------------|--------------------|-----------|-----------------------|--------------------|-----------|
|                  | Storage Modulus (MPa) | Loss Modulus (MPa) | Tan Delta | Storage Modulus (MPa) | Loss Modulus (MPa) | Tan Delta | Storage Modulus (MPa) | Loss Modulus (MPa) | Tan Delta | Storage Modulus (MPa) | Loss Modulus (MPa) | Tan Delta | Storage Modulus (MPa) | Loss Modulus (MPa) | Tan Delta | Storage Modulus (MPa) | Loss Modulus (MPa) | Tan Delta | Storage Modulus (MPa) | Loss Modulus (MPa) | Tan Delta |
| 32               | 8285                  | 345                | 0.04      | 8458                  | 339                | 0.04      | 8618                  | 329                | 0.04      | 8777                  | 319                | 0.04      | 8925                  | 311                | 0.03      | 9076                  | 304                | 0.03      | 9243                  | 302                | 0.03      |
| 42               | 7940                  | 334                | 0.04      | 8096                  | 333                | 0.04      | 8244                  | 329                | 0.04      | 8401                  | 327                | 0.04      | 8553                  | 322                | 0.04      | 8709                  | 316                | 0.04      | 8881                  | 313                | 0.04      |
| 52               | 7565                  | 333                | 0.04      | 7718                  | 331                | 0.04      | 7862                  | 329                | 0.04      | 8016                  | 329                | 0.04      | 8169                  | 329                | 0.04      | 8330                  | 330                | 0.04      | 8508                  | 332                | 0.04      |
| 62               | 7249                  | 357                | 0.05      | 7416                  | 352                | 0.05      | 7573                  | 348                | 0.05      | 7736                  | 345                | 0.04      | 7895                  | 345                | 0.04      | 8066                  | 346                | 0.04      | 8255                  | 349                | 0.04      |
| 72               | 7054                  | 453                | 0.06      | 7258                  | 437                | 0.06      | 7449                  | 426                | 0.06      | 7646                  | 415                | 0.05      | 7834                  | 409                | 0.05      | 8031                  | 405                | 0.05      | 8248                  | 401                | 0.05      |
| 82               | 6561                  | 575                | 0.09      | 6807                  | 546                | 0.08      | 7031                  | 526                | 0.07      | 7265                  | 508                | 0.07      | 7490                  | 494                | 0.07      | 7717                  | 482                | 0.06      | 7962                  | 472                | 0.06      |
| 92               | 5832                  | 653                | 0.11      | 6119                  | 630                | 0.1       | 6380                  | 611                | 0.1       | 6655                  | 593                | 0.09      | 6919                  | 577                | 0.08      | 7184                  | 563                | 0.08      | 7464                  | 548                | 0.07      |
| 102              | 5051                  | 673                | 0.13      | 5357                  | 669                | 0.13      | 5641                  | 663                | 0.12      | 5946                  | 656                | 0.11      | 6244                  | 648                | 0.1       | 6545                  | 638                | 0.1       | 6864                  | 624                | 0.09      |
| 112              | 4283                  | 629                | 0.15      | 4578                  | 651                | 0.14      | 4862                  | 669                | 0.14      | 5177                  | 681                | 0.13      | 5495                  | 690                | 0.13      | 5822                  | 693                | 0.12      | 6170                  | 688                | 0.11      |
| 122              | 3600                  | 506                | 0.14      | 3843                  | 554                | 0.14      | 4091                  | 599                | 0.15      | 4382                  | 643                | 0.15      | 4693                  | 681                | 0.15      | 5026                  | 710                | 0.14      | 5395                  | 727                | 0.14      |
| 132              | 3155                  | 340                | 0.11      | 3319                  | 394                | 0.12      | 3497                  | 450                | 0.13      | 3720                  | 515                | 0.14      | 3975                  | 581                | 0.15      | 4269                  | 642                | 0.15      | 4618                  | 693                | 0.15      |
| 140              | 2990                  | 225                | 0.08      | 3097                  | 269                | 0.09      | 3218                  | 319                | 0.1       | 3374                  | 380                | 0.11      | 3563                  | 451                | 0.13      | 3795                  | 526                | 0.14      | 4089                  | 599                | 0.15      |



**Table 6-7** Creep compliance of PNCs at stress 1MPa

| Time (s) | Creep compliance(1/Pa) |           |           |
|----------|------------------------|-----------|-----------|
|          | 0% filler              | 1% filler | 2% filler |
| 7.1811   | 1.14E-09               | 8.77E-10  | 1.04E-09  |
| 33.446   | 1.29E-09               | 1.11E-09  | 1.33E-09  |
| 66.694   | 1.37E-09               | 1.17E-09  | 1.49E-09  |
| 136.51   | 1.48E-09               | 1.25E-09  | 1.76E-09  |
| 217.92   | 1.57E-09               | 1.31E-09  | 1.95E-09  |
| 465.66   | 1.75E-09               | 1.43E-09  | 2.25E-09  |
| 733.57   | 1.86E-09               | 1.51E-09  | 2.42E-09  |
| 1243.9   | 2.01E-09               | 1.63E-09  | 2.60E-09  |
| 2069.2   | 2.20E-09               | 1.76E-09  | 2.85E-09  |
| 2952.7   | 2.38E-09               | 1.88E-09  | 3.09E-09  |
| 3990.6   | 2.53E-09               | 2.01E-09  | 3.29E-09  |
| 6130.7   | 2.91E-09               | 2.20E-09  | 3.64E-09  |
| 10606    | 3.40E-09               | 2.49E-09  | 4.12E-09  |
| 14467    | 3.83E-09               | 2.70E-09  | 4.54E-09  |
| 24098    | 4.31E-09               | 3.10E-09  | 5.16E-09  |
| 36068    | 4.79E-09               | 3.44E-09  | 5.62E-09  |
| 48825    | 5.20E-09               | 3.76E-09  | 6.14E-09  |
| 63475    | 5.50E-09               | 4.02E-09  | 6.56E-09  |
| 98129    | 6.44E-09               | 4.59E-09  | 7.53E-09  |
| 1.43E+05 | 7.38E-09               | 5.15E-09  | 8.53E-09  |
| 2.06E+05 | 8.39E-09               | 5.86E-09  | 9.48E-09  |
| 2.49E+05 | 8.90E-09               | 6.24E-09  | 9.86E-09  |
| 3.37E+05 | 9.55E-09               | 6.93E-09  | 1.07E-08  |
| 4.86E+05 | 1.06E-08               | 7.83E-09  | 1.09E-08  |
| 6.29E+05 | 1.17E-08               | 8.56E-09  | 1.34E-08  |
| 8.40E+05 | 1.31E-08               | 9.53E-09  | 1.48E-08  |
| 1.21E+06 | 1.50E-08               | 1.09E-08  | 1.69E-08  |
| 1.74E+06 | 1.77E-08               | 1.23E-08  | 1.90E-08  |
| 2.26E+06 | 1.96E-08               | 1.34E-08  | 2.08E-08  |
| 3.26E+06 | 2.30E-08               | 1.53E-08  | 2.34E-08  |
| 6.70E+06 | 3.38E-08               | 2.00E-08  | 2.86E-08  |
| 1.20E+07 | 6.65E-08               | 2.47E-08  | 3.53E-08  |

**Table 6-8** Creep strain of PNCs at stress 1MPa

| Time (s) | Creep strain |           |           |
|----------|--------------|-----------|-----------|
|          | 0% filler    | 1% filler | 2% filler |
| 7.1811   | 1.14E-03     | 8.77E-04  | 1.04E-03  |
| 33.446   | 1.29E-03     | 1.11E-03  | 1.33E-03  |
| 66.694   | 1.37E-03     | 1.17E-03  | 1.49E-03  |
| 136.51   | 1.48E-03     | 1.25E-03  | 1.76E-03  |
| 217.92   | 1.57E-03     | 1.31E-03  | 1.95E-03  |
| 465.66   | 1.75E-03     | 1.43E-03  | 2.25E-03  |
| 733.57   | 1.86E-03     | 1.51E-03  | 2.42E-03  |
| 1243.9   | 2.01E-03     | 1.63E-03  | 2.60E-03  |
| 2069.2   | 2.20E-03     | 1.76E-03  | 2.85E-03  |
| 2952.7   | 2.38E-03     | 1.88E-03  | 3.09E-03  |
| 3990.6   | 2.53E-03     | 2.01E-03  | 3.29E-03  |
| 6130.7   | 2.91E-03     | 2.20E-03  | 3.64E-03  |
| 10606    | 3.40E-03     | 2.49E-03  | 4.12E-03  |
| 14467    | 3.83E-03     | 2.70E-03  | 4.54E-03  |
| 24098    | 4.31E-03     | 3.10E-03  | 5.16E-03  |
| 36068    | 4.79E-03     | 3.44E-03  | 5.62E-03  |
| 48825    | 5.20E-03     | 3.76E-03  | 6.14E-03  |
| 63475    | 5.50E-03     | 4.02E-03  | 6.56E-03  |
| 98129    | 6.44E-03     | 4.59E-03  | 7.53E-03  |
| 1.43E+05 | 7.38E-03     | 5.15E-03  | 8.53E-03  |
| 2.06E+05 | 8.39E-03     | 5.86E-03  | 9.48E-03  |
| 2.49E+05 | 8.90E-03     | 6.24E-03  | 9.86E-03  |
| 3.37E+05 | 9.55E-03     | 6.93E-03  | 0.010698  |
| 4.86E+05 | 0.010556     | 7.83E-03  | 0.010895  |
| 6.29E+05 | 0.011719     | 8.56E-03  | 0.013385  |
| 8.40E+05 | 0.01311      | 9.53E-03  | 0.014769  |
| 1.21E+06 | 0.014999     | 0.010919  | 0.016874  |
| 1.74E+06 | 0.017658     | 0.012342  | 0.019013  |
| 2.26E+06 | 0.019558     | 0.013393  | 0.020788  |
| 3.26E+06 | 0.022978     | 0.015256  | 0.023362  |
| 6.70E+06 | 0.033793     | 0.019979  | 0.028598  |
| 1.20E+07 | 0.06646      | 0.024666  | 0.035343  |

**Table 6-9** Creep compliance of GFRPNCs at stress 1MPa

| Time (seconds) | Creep compliance $j(t)$ (1/Pa) |           |           |
|----------------|--------------------------------|-----------|-----------|
|                | 0% filler                      | 1% filler | 2% filler |
| 5.02           | 2.02E-10                       | 1.51E-10  | 1.82E-10  |
| 16.76          | 2.48E-10                       | 1.50E-10  | 1.86E-10  |
| 33.26          | 2.61E-10                       | 1.47E-10  | 1.89E-10  |
| 69.80          | 2.70E-10                       | 1.47E-10  | 1.91E-10  |
| 148.82         | 2.77E-10                       | 1.47E-10  | 1.95E-10  |
| 272.63         | 2.84E-10                       | 1.47E-10  | 1.98E-10  |
| 523.68         | 2.88E-10                       | 1.48E-10  | 2.01E-10  |
| 822.14         | 2.92E-10                       | 1.51E-10  | 2.04E-10  |
| 1303.10        | 2.97E-10                       | 1.55E-10  | 2.10E-10  |
| 2216.50        | 3.04E-10                       | 1.59E-10  | 2.15E-10  |
| 3149.80        | 3.10E-10                       | 1.63E-10  | 2.17E-10  |
| 5514.60        | 3.17E-10                       | 1.67E-10  | 2.20E-10  |
| 8261.90        | 3.21E-10                       | 1.69E-10  | 2.23E-10  |
| 10970          | 3.27E-10                       | 1.71E-10  | 2.25E-10  |
| 15627          | 3.36E-10                       | 1.72E-10  | 2.28E-10  |
| 22005          | 3.49E-10                       | 1.73E-10  | 2.35E-10  |
| 33265          | 3.65E-10                       | 1.73E-10  | 2.48E-10  |
| 56683          | 3.90E-10                       | 1.72E-10  | 2.71E-10  |
| 80825          | 4.05E-10                       | 1.70E-10  | 2.86E-10  |
| 1.17E+05       | 4.24E-10                       | 1.67E-10  | 3.04E-10  |
| 1.84E+05       | 4.48E-10                       | 1.64E-10  | 3.25E-10  |
| 2.81E+05       | 4.75E-10                       | 1.62E-10  | 3.58E-10  |
| 3.97E+05       | 5.00E-10                       | 1.65E-10  | 3.83E-10  |
| 5.54E+05       | 5.27E-10                       | 1.73E-10  | 4.25E-10  |
| 8.77E+05       | 5.69E-10                       | 1.82E-10  | 4.62E-10  |
| 1.15E+06       | 5.96E-10                       | 1.90E-10  | 4.97E-10  |
| 2.17E+06       | 6.60E-10                       | 2.00E-10  | 5.60E-10  |
| 2.75E+06       | 6.86E-10                       | 2.03E-10  | 5.95E-10  |
| 3.99E+06       | 7.32E-10                       | 2.06E-10  | 6.47E-10  |
| 8.27E+06       | 8.37E-10                       | 2.10E-10  | 7.26E-10  |
| 1.20E+07       | 9.05E-10                       | 2.14E-10  | 7.61E-10  |
| 1.72E+07       | 9.75E-10                       | 2.18E-10  | 7.95E-10  |
| 2.49E+07       | 1.05E-09                       | 2.22E-10  | 8.12E-10  |
| 5.88E+07       | 1.22E-09                       | 2.37E-10  | 8.49E-10  |
| 8.21E+07       | 1.29E-09                       | 2.44E-10  | 8.60E-10  |
| 1.03E+08       | 1.33E-09                       | 2.54E-10  | 8.68E-10  |
| 1.82E+08       | 1.44E-09                       | 2.72E-10  | 8.92E-10  |
| 2.19E+08       | 1.47E-09                       | 2.81E-10  | 8.98E-10  |
| 2.90E+08       | 1.52E-09                       | 2.94E-10  | 9.04E-10  |
| 3.56E+08       | 1.56E-09                       | 3.03E-10  | 9.07E-10  |
| 4.47E+08       | 1.61E-09                       | 3.11E-10  | 9.11E-10  |
| 5.55E+08       | 1.65E-09                       | 3.24E-10  | 9.13E-10  |
| 7.05E+08       | 1.69E-09                       | 3.36E-10  | 9.18E-10  |
| 1.05E+09       | 1.74E-09                       | 3.49E-10  | 9.24E-10  |
| 1.75E+09       | 1.79E-09                       | 3.78E-10  | 9.32E-10  |
| 3.10E+09       | 1.85E-09                       | 4.06E-10  | 9.43E-10  |
| 4.59E+09       | 1.89E-09                       | 4.25E-10  | 9.49E-10  |
| 6.17E+09       | 1.92E-09                       | 4.40E-10  | 9.52E-10  |
| 9.62E+09       | 1.95E-09                       | 4.59E-10  | 9.61E-10  |
| 1.68E+10       | 1.97E-09                       | 4.88E-10  | 9.78E-10  |

**Table 6-10** Creep strain of GFRPNCs at stress 1MPa

| Time (seconds) | Creep strain (%) |           |           |
|----------------|------------------|-----------|-----------|
|                | 0% filler        | 1% filler | 2% filler |
| 5.02           | 2.02E-04         | 1.51E-04  | 1.82E-04  |
| 16.76          | 2.48E-04         | 1.50E-04  | 1.86E-04  |
| 33.26          | 2.61E-04         | 1.47E-04  | 1.89E-04  |
| 69.80          | 2.70E-04         | 1.47E-04  | 1.91E-04  |
| 148.82         | 2.77E-04         | 1.47E-04  | 1.95E-04  |
| 272.63         | 2.84E-04         | 1.47E-04  | 1.98E-04  |
| 523.68         | 2.88E-04         | 1.48E-04  | 2.01E-04  |
| 1303           | 2.97E-04         | 1.55E-04  | 2.10E-04  |
| 2216           | 3.04E-04         | 1.59E-04  | 2.15E-04  |
| 5514           | 3.17E-04         | 1.67E-04  | 2.20E-04  |
| 10970          | 3.27E-04         | 1.71E-04  | 2.25E-04  |
| 15627          | 3.36E-04         | 1.72E-04  | 2.28E-04  |
| 22005          | 3.49E-04         | 1.73E-04  | 2.35E-04  |
| 33265          | 3.65E-04         | 1.73E-04  | 2.48E-04  |
| 56683          | 3.89E-04         | 1.72E-04  | 2.71E-04  |
| 80825          | 4.05E-04         | 1.70E-04  | 2.85E-04  |
| 1.17E+05       | 4.24E-04         | 1.67E-04  | 3.04E-04  |
| 1.84E+05       | 4.48E-04         | 1.63E-04  | 3.25E-04  |
| 2.81E+05       | 4.75E-04         | 1.62E-04  | 3.58E-04  |
| 3.97E+05       | 5.00E-04         | 1.65E-04  | 3.83E-04  |
| 8.77E+05       | 5.69E-04         | 1.82E-04  | 4.62E-04  |
| 1.15E+06       | 5.96E-04         | 1.90E-04  | 4.97E-04  |
| 2.75E+06       | 6.86E-04         | 2.03E-04  | 5.94E-04  |
| 3.99E+06       | 7.32E-04         | 2.06E-04  | 6.47E-04  |
| 8.27E+06       | 8.37E-04         | 2.10E-04  | 7.26E-04  |
| 1.20E+07       | 9.04E-04         | 2.14E-04  | 7.61E-04  |
| 1.72E+07       | 9.75E-04         | 2.18E-04  | 7.95E-04  |
| 3.65E+07       | 1.13E-03         | 2.28E-04  | 8.33E-04  |
| 5.88E+07       | 1.22E-03         | 2.36E-04  | 8.49E-04  |
| 8.21E+07       | 1.29E-03         | 2.44E-04  | 8.60E-04  |
| 1.03E+08       | 1.33E-03         | 2.54E-04  | 8.68E-04  |
| 3.56E+08       | 1.56E-03         | 3.03E-04  | 9.07E-04  |
| 4.47E+08       | 1.61E-03         | 3.11E-04  | 9.11E-04  |
| 5.55E+08       | 1.65E-03         | 3.24E-04  | 9.13E-04  |
| 7.05E+08       | 1.69E-03         | 3.35E-04  | 9.18E-04  |
| 1.38E+09       | 1.76E-03         | 3.62E-04  | 9.27E-04  |
| 3.10E+09       | 1.85E-03         | 4.05E-04  | 9.43E-04  |
| 4.59E+09       | 1.89E-03         | 4.25E-04  | 9.49E-04  |
| 6.17E+09       | 1.92E-03         | 4.40E-04  | 9.52E-04  |
| 9.62E+09       | 1.95E-03         | 4.59E-04  | 9.61E-04  |
| 1.68E+10       | 1.97E-03         | 4.88E-04  | 9.78E-04  |

**Table 6-11** Creep compliance of GFRPNCs at stress 2 MPa

| Time (seconds) | Creep compliance $j(t)$ (1/Pa) |           |           |
|----------------|--------------------------------|-----------|-----------|
|                | 0% filler                      | 1% filler | 2% filler |
| 6.38           | 1.84E-10                       | 6.67E-11  | 7.20E-11  |
| 31.57          | 2.06E-10                       | 8.03E-11  | 1.13E-10  |
| 52.99          | 2.11E-10                       | 8.54E-11  | 1.19E-10  |
| 92.80          | 2.16E-10                       | 8.89E-11  | 1.29E-10  |
| 122.64         | 2.20E-10                       | 9.02E-11  | 1.34E-10  |
| 148.17         | 2.23E-10                       | 9.06E-11  | 1.36E-10  |
| 182.64         | 2.28E-10                       | 9.18E-11  | 1.41E-10  |
| 231.09         | 2.32E-10                       | 9.27E-11  | 1.44E-10  |
| 280.06         | 2.36E-10                       | 9.30E-11  | 1.47E-10  |
| 384.08         | 2.42E-10                       | 9.33E-11  | 1.52E-10  |
| 543.97         | 2.51E-10                       | 9.36E-11  | 1.57E-10  |
| 786.54         | 2.65E-10                       | 9.45E-11  | 1.65E-10  |
| 857.31         | 2.70E-10                       | 9.50E-11  | 1.68E-10  |
| 1230           | 2.82E-10                       | 9.63E-11  | 1.79E-10  |
| 1478           | 2.90E-10                       | 9.70E-11  | 1.83E-10  |
| 1677           | 2.95E-10                       | 9.75E-11  | 1.88E-10  |
| 2136           | 3.07E-10                       | 9.87E-11  | 1.97E-10  |
| 2563           | 3.16E-10                       | 9.96E-11  | 2.05E-10  |
| 3077           | 3.24E-10                       | 1.01E-10  | 2.14E-10  |
| 3848           | 3.36E-10                       | 1.01E-10  | 2.23E-10  |
| 4205           | 3.41E-10                       | 1.02E-10  | 2.30E-10  |
| 4593           | 3.44E-10                       | 1.02E-10  | 2.33E-10  |
| 5758           | 3.59E-10                       | 1.04E-10  | 2.48E-10  |
| 6391           | 3.66E-10                       | 1.05E-10  | 2.56E-10  |
| 7672           | 3.77E-10                       | 1.06E-10  | 2.70E-10  |
| 11330          | 3.96E-10                       | 1.08E-10  | 2.98E-10  |
| 14352          | 4.09E-10                       | 1.10E-10  | 3.10E-10  |
| 18207          | 4.23E-10                       | 1.14E-10  | 3.29E-10  |
| 21037          | 4.30E-10                       | 1.16E-10  | 3.35E-10  |
| 24325          | 4.39E-10                       | 1.19E-10  | 3.44E-10  |
| 35222          | 4.66E-10                       | 1.26E-10  | 3.69E-10  |
| 38226          | 4.73E-10                       | 1.28E-10  | 3.78E-10  |
| 44401          | 4.83E-10                       | 1.31E-10  | 3.91E-10  |
| 61633          | 5.11E-10                       | 1.34E-10  | 4.11E-10  |
| 80243          | 5.39E-10                       | 1.37E-10  | 4.33E-10  |
| 1.29E+05       | 5.76E-10                       | 1.39E-10  | 4.60E-10  |
| 1.54E+05       | 5.86E-10                       | 1.41E-10  | 4.70E-10  |
| 1.86E+05       | 5.96E-10                       | 1.43E-10  | 4.84E-10  |
| 3.61E+05       | 6.41E-10                       | 1.55E-10  | 5.37E-10  |
| 4.34E+05       | 6.55E-10                       | 1.58E-10  | 5.52E-10  |
| 5.23E+05       | 6.65E-10                       | 1.62E-10  | 5.73E-10  |
| 7.56E+05       | 6.94E-10                       | 1.70E-10  | 6.07E-10  |
| 1.09E+06       | 7.18E-10                       | 1.77E-10  | 6.35E-10  |
| 1.57E+06       | 7.42E-10                       | 1.86E-10  | 6.61E-10  |
| 2.72E+06       | 8.91E-10                       | 1.99E-10  | 6.96E-10  |
| 3.93E+06       | 9.84E-10                       | 2.08E-10  | 7.15E-10  |
| 5.31E+06       | 1.03E-09                       | 2.20E-10  | 7.38E-10  |

**Table 6-12** Creep strain of GFRPNCs at stress 2 MPa

| Time (seconds) | Creep strain (%) |           |           |
|----------------|------------------|-----------|-----------|
|                | 0% filler        | 1% filler | 2% filler |
| 6.3823         | 3.67E-04         | 1.33E-04  | 1.44E-04  |
| 31.572         | 4.12E-04         | 1.61E-04  | 2.26E-04  |
| 52.997         | 4.21E-04         | 1.71E-04  | 2.39E-04  |
| 92.809         | 4.32E-04         | 1.78E-04  | 2.58E-04  |
| 122.64         | 4.40E-04         | 1.80E-04  | 2.68E-04  |
| 148.17         | 4.46E-04         | 1.81E-04  | 2.72E-04  |
| 182.64         | 4.56E-04         | 1.84E-04  | 2.82E-04  |
| 231.09         | 4.64E-04         | 1.85E-04  | 2.88E-04  |
| 280.06         | 4.71E-04         | 1.86E-04  | 2.94E-04  |
| 384.08         | 4.84E-04         | 1.87E-04  | 3.03E-04  |
| 543.97         | 5.02E-04         | 1.87E-04  | 3.14E-04  |
| 698.16         | 5.22E-04         | 1.89E-04  | 3.24E-04  |
| 786.54         | 5.30E-04         | 1.89E-04  | 3.30E-04  |
| 857.31         | 5.39E-04         | 1.90E-04  | 3.35E-04  |
| 1478.2         | 5.79E-04         | 1.94E-04  | 3.66E-04  |
| 1677.6         | 5.90E-04         | 1.95E-04  | 3.75E-04  |
| 2136.5         | 6.14E-04         | 1.97E-04  | 3.94E-04  |
| 2563.7         | 6.31E-04         | 1.99E-04  | 4.10E-04  |
| 3077.5         | 6.48E-04         | 2.01E-04  | 4.28E-04  |
| 3848.3         | 6.72E-04         | 2.02E-04  | 4.46E-04  |
| 4205.2         | 6.83E-04         | 2.04E-04  | 4.59E-04  |
| 4593.5         | 6.88E-04         | 2.04E-04  | 4.66E-04  |
| 5758.2         | 7.18E-04         | 2.07E-04  | 4.96E-04  |
| 6391.2         | 7.31E-04         | 2.09E-04  | 5.13E-04  |
| 7672.9         | 7.53E-04         | 2.11E-04  | 5.41E-04  |
| 11330          | 7.92E-04         | 2.16E-04  | 5.95E-04  |
| 11911          | 7.99E-04         | 2.17E-04  | 6.00E-04  |
| 14352          | 8.18E-04         | 2.20E-04  | 6.21E-04  |
| 18207          | 8.46E-04         | 2.28E-04  | 6.58E-04  |
| 21037          | 8.59E-04         | 2.32E-04  | 6.71E-04  |
| 24325          | 8.79E-04         | 2.37E-04  | 6.88E-04  |
| 35222          | 9.32E-04         | 2.53E-04  | 7.39E-04  |
| 38226          | 9.47E-04         | 2.56E-04  | 7.55E-04  |
| 44401          | 9.67E-04         | 2.61E-04  | 7.83E-04  |
| 61633          | 1.02E-03         | 2.68E-04  | 8.21E-04  |
| 78793          | 1.07E-03         | 2.73E-04  | 8.54E-04  |
| 80243          | 1.08E-03         | 2.74E-04  | 8.65E-04  |
| 1.29E+05       | 1.15E-03         | 2.79E-04  | 9.19E-04  |
| 1.54E+05       | 1.17E-03         | 2.82E-04  | 9.40E-04  |
| 1.86E+05       | 1.19E-03         | 2.87E-04  | 9.69E-04  |
| 4.34E+05       | 1.31E-03         | 3.17E-04  | 1.10E-03  |
| 5.23E+05       | 1.33E-03         | 3.24E-04  | 1.15E-03  |
| 7.56E+05       | 1.39E-03         | 3.41E-04  | 1.21E-03  |
| 1.09E+06       | 1.44E-03         | 3.54E-04  | 1.27E-03  |
| 1.57E+06       | 1.48E-03         | 3.71E-04  | 1.32E-03  |
| 3.93E+06       | 1.97E-03         | 4.17E-04  | 1.43E-03  |
| 5.31E+06       | 2.05E-03         | 4.40E-04  | 1.48E-03  |

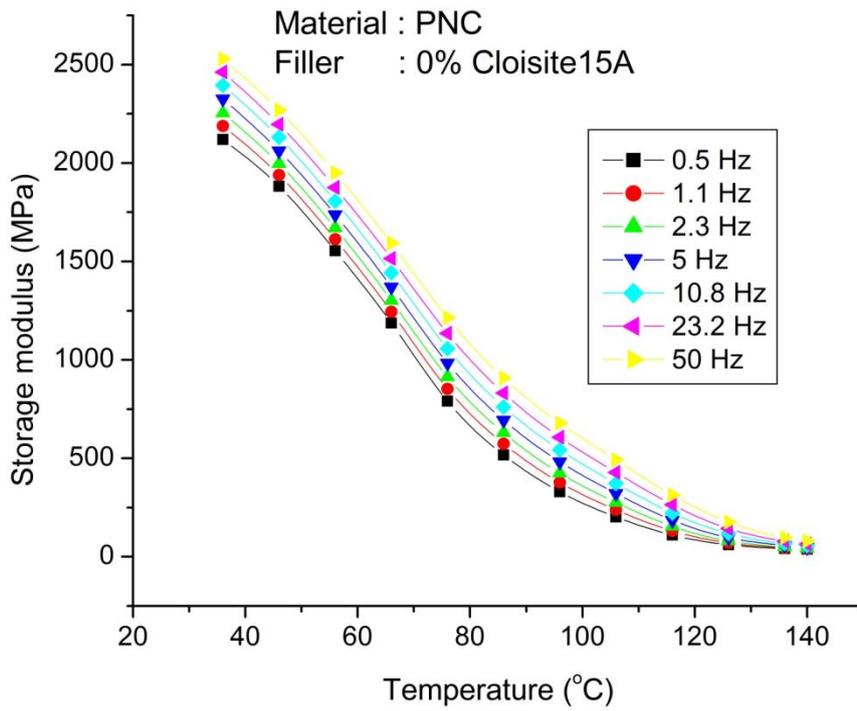


**Figure 6-1** Variation of storage modulus with temperature for different frequencies at filler content 0%

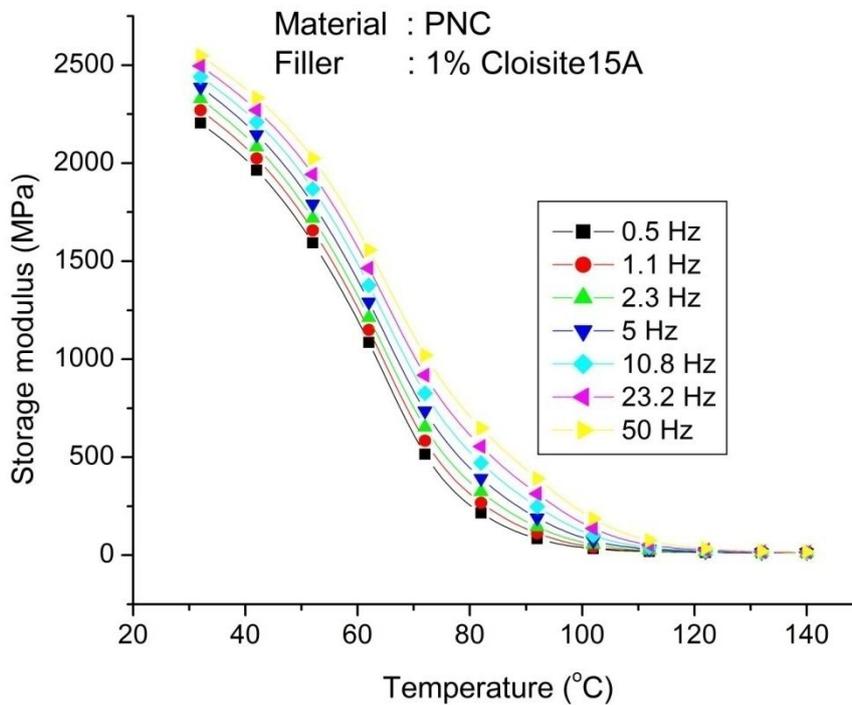


**Figure 6-2** Variation of storage modulus with temperature for different frequencies at filler content 1%

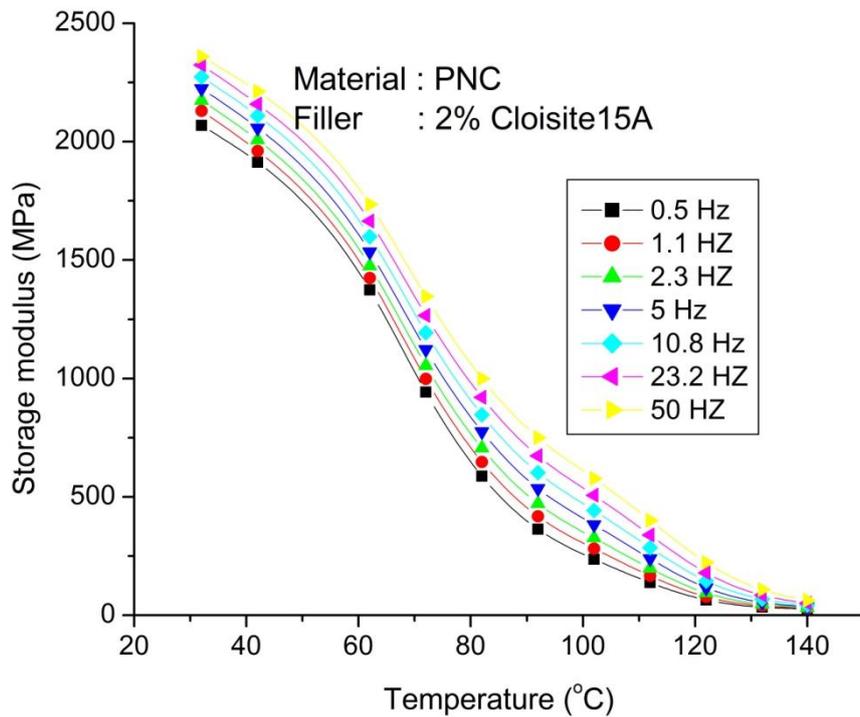


**Figure 6-3** Variation of storage modulus with temperature for different frequencies at filler content 2%

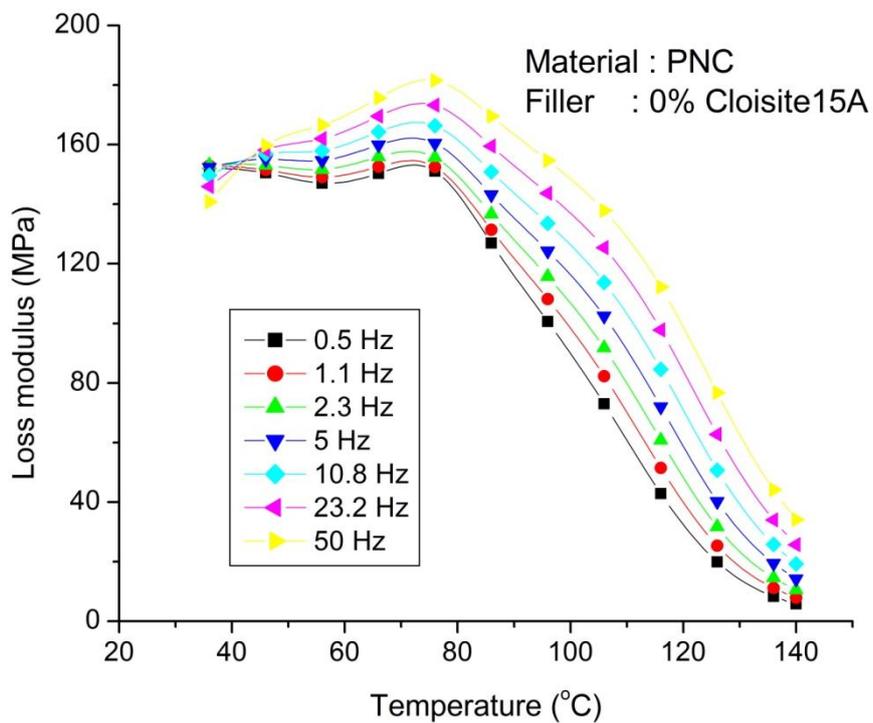


**Figure 6-4** Variation of loss modulus with temperature for different frequencies at filler content 0%

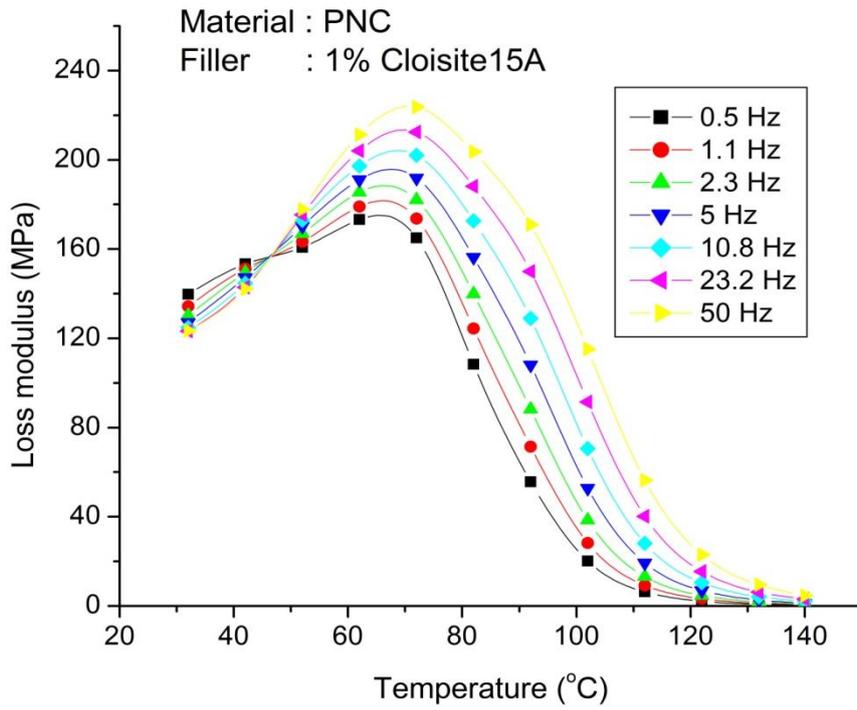


**Figure 6-5** Variation of loss modulus with temperature for different frequencies at filler content 1%

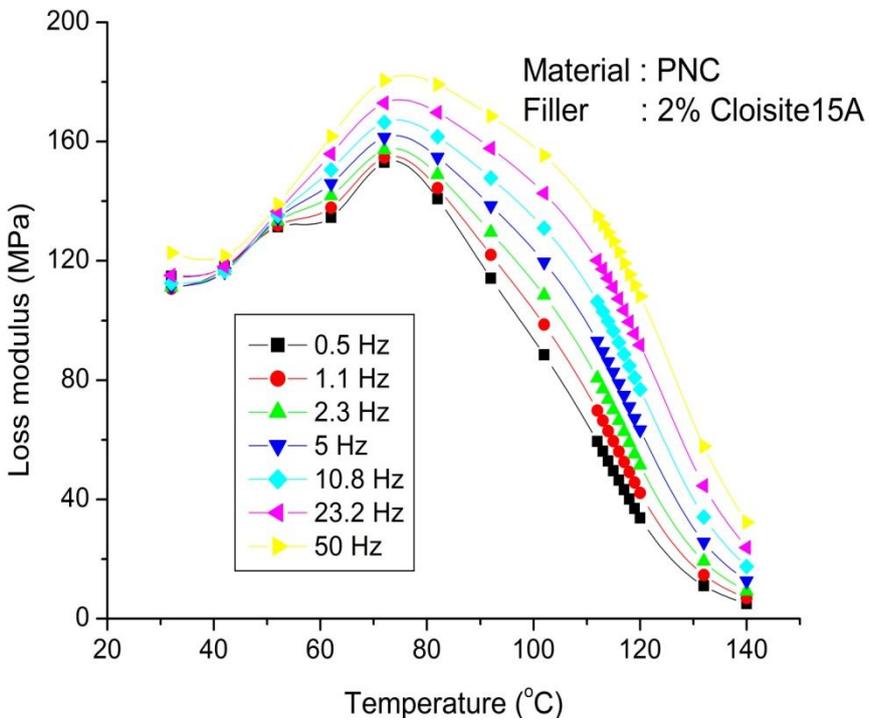


**Figure 6-6** Variation of loss modulus with temperature for different frequencies at filler content 2%

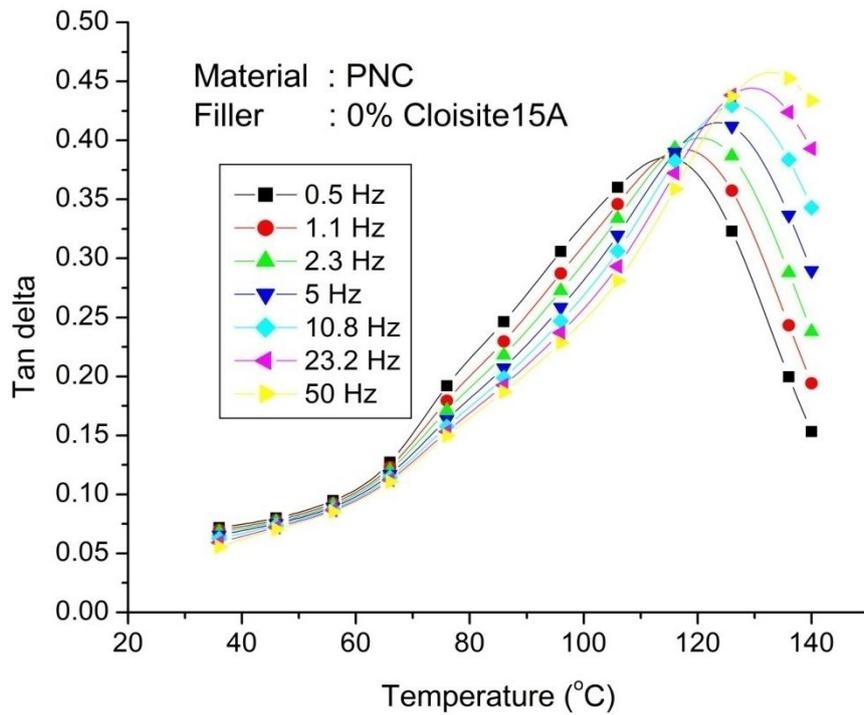


**Figure 6-7** Variation of tandelta with temperature for different frequencies at filler content 0%

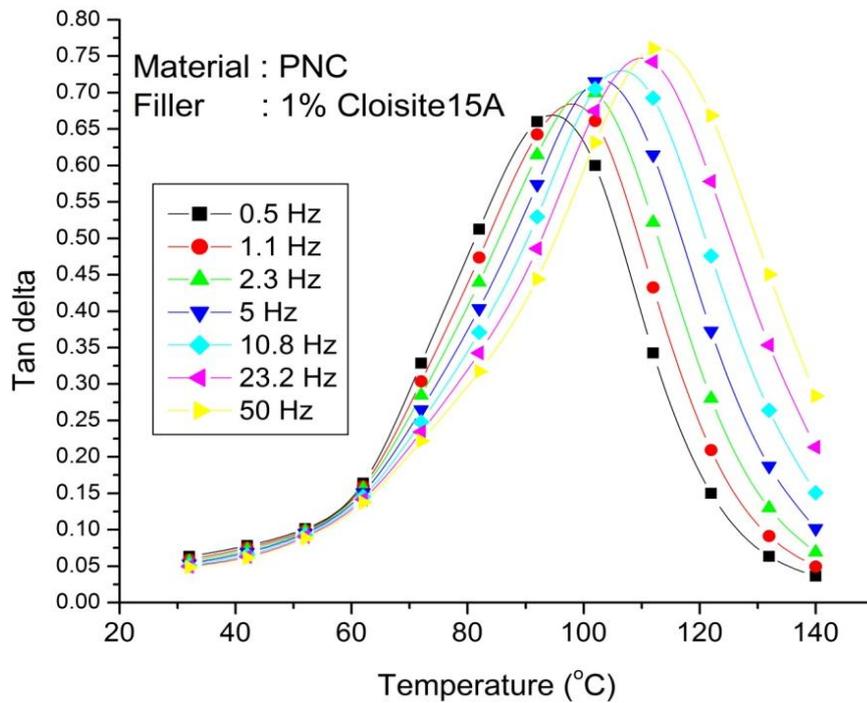


**Figure 6-8** Variation of tan delta with temperature for different frequencies at filler content 1%

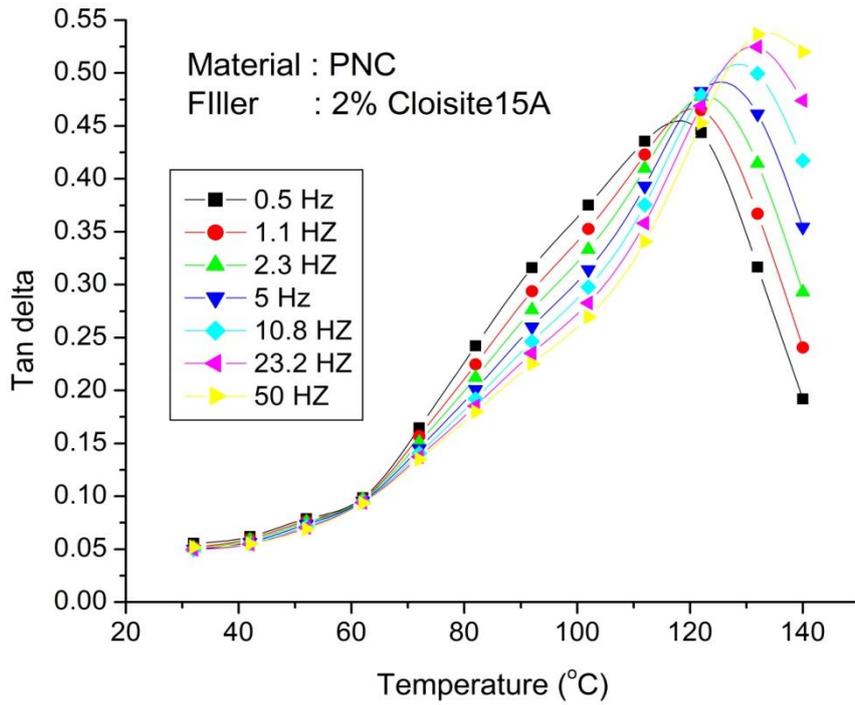


**Figure 6-9** Variation of tandelta with temperature for different frequencies at filler content 2%

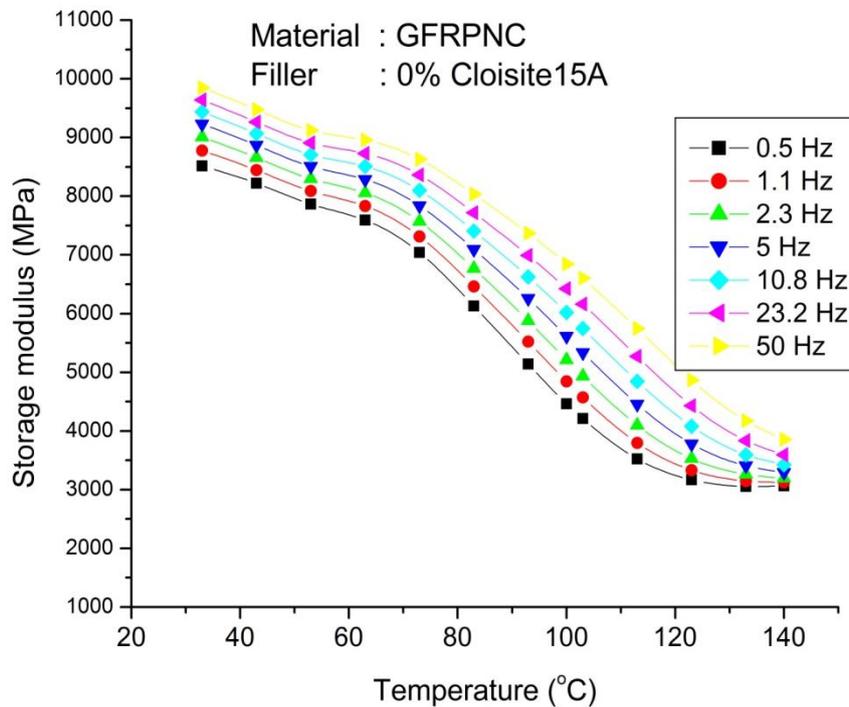


**Figure 6-10** Variation of storage modulus with temperature for different frequencies at filler content 0%

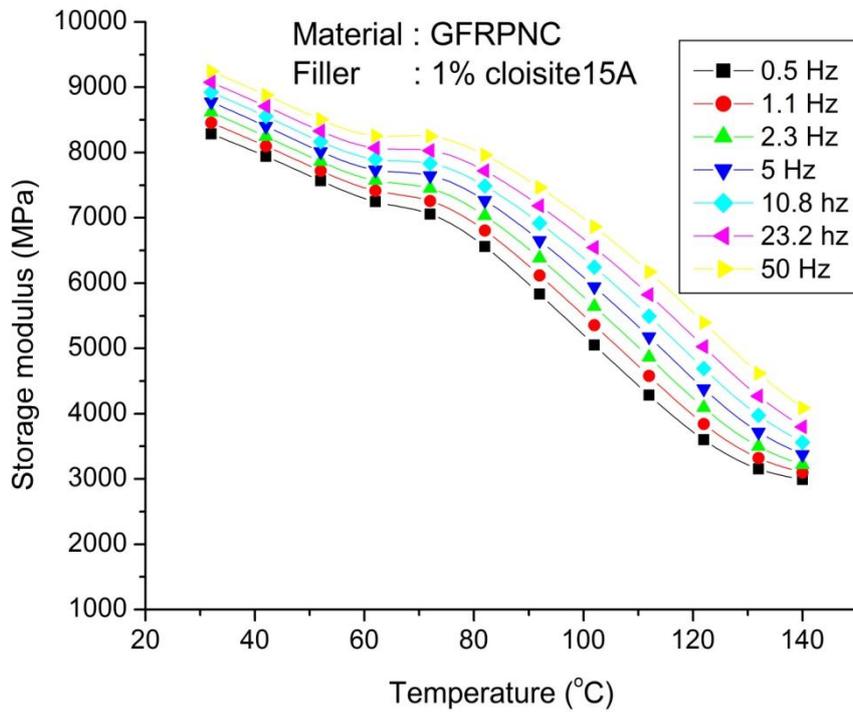


**Figure 6-11** Variation of storage modulus with temperature for different frequencies at filler content 1%

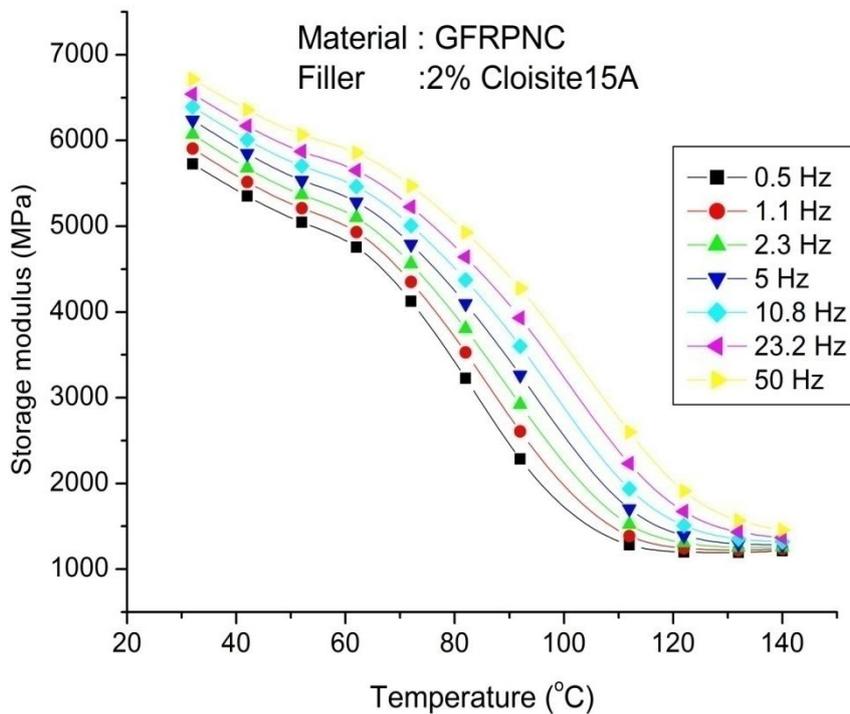


**Figure 6-12** Variation of storage modulus with temperature for different frequencies at filler content 2%

The effect of clay reinforcement on loss modulus and  $\tan\delta$  of Polyester/Nanoclay nanocomposite can be seen from figure 4-10 to 4-15. The loss modulus is less, for pure polyester (0% filler at frequency 1 Hz, 10 Hz and 100 Hz as compared to nanoclay filled sample. The reduced value of loss modulus for the nanocomposite at low frequency is an indication of reduced energy dissipation. The average value of glass transition temperature,  $T_g$  for different wt. % of Cloisite15A is in the range 100 – 120 °C. There is a markedly high increment in the  $T_g$  value with 1% filler. However, the addition of Cloisite15A did not significantly change the glass transition temperature of the GFRP nanocomposite except that for 1% clay filled condition as special case. For the nanocomposite with 1% filler, due to complete exfoliation of the clay in to resin, the molecular mobility may be restricted at high temperature and hence the increase in  $T_g$ . whereas for 2% filled samples the  $T_g$  is low as compared to 1% filled samples. Here due to the increased percentage of clay the absence of entanglement surrounding the nanoclay, the effect due to surface modifiers, un reacted resin plasticization, and a lower cross-link density have been attributed to the decrease in  $T_g$  [28].

$\tan\delta$  increases with the increase of filler weight percentage. Various mechanisms like matrix viscoelasticity, filler/filler interfacial friction, etc., could increase the damping capacity of the polymer composite materials. However, the molecular motion at room temperature is frozen, and this may not contribute to the damping mechanisms. At  $T_g$ , the  $\tan\delta$  value is higher for nanocomposite with 1% filler at 10 Hz frequency indicating the viscous damping because of the segmental motion in the polymer. This increase in the damping factor can be attributed to the restriction to the molecular

movements of nano filler, which caused reduction in the matrix viscoelasticity. However, this did not agree with the samples with 1% and 2 % nano filler [28][69].

The curves plotted with experimental results from frequency sweep mode at frequencies 0.5 Hz, 1.1 Hz, 2.3 Hz, 5 Hz, 10.8 Hz, 23.2 Hz and 50 Hz , shown in figure 6-1 to 6-9 for polyester nanocomposites and figure 6-10 to 6-18 for reinforced polyester nanocomposite in general describe the effect of nano filler under continuous loading. It is observed that the storage modulus increases first and reaches a stable condition with the increase of frequency. The change in the nature of curve reaches the limiting value corresponding to the peak of loss modulus curve as well as tan ( $\delta$ ). The peak of damping coefficient curve shifts slightly to higher frequency range with the addition of nano filler. This is a clear indication of the damping nature of nano composite.

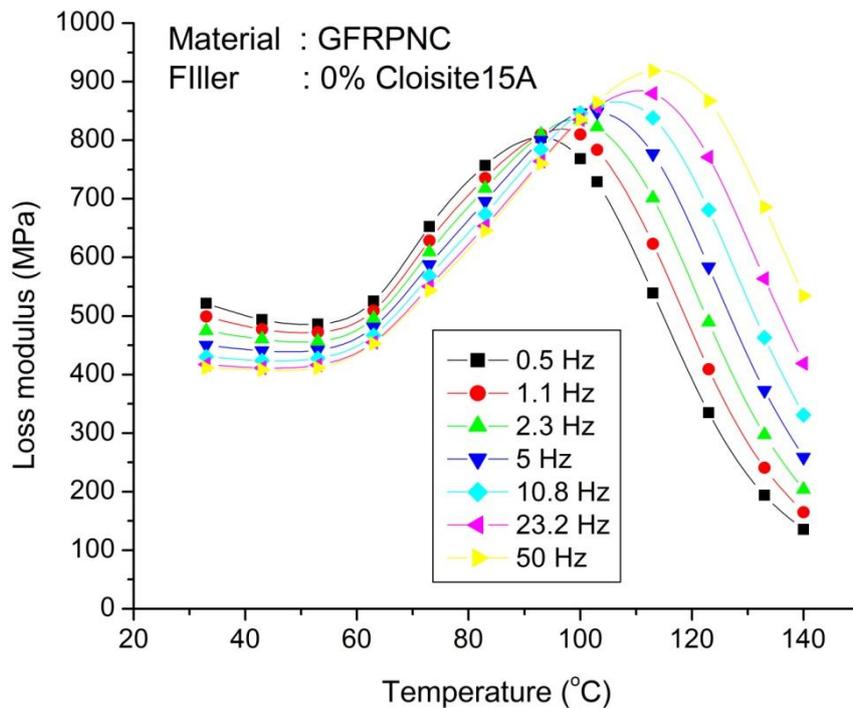


**Figure 6-13** Variation of loss modulus with temperature for different frequencies at filler content 0%

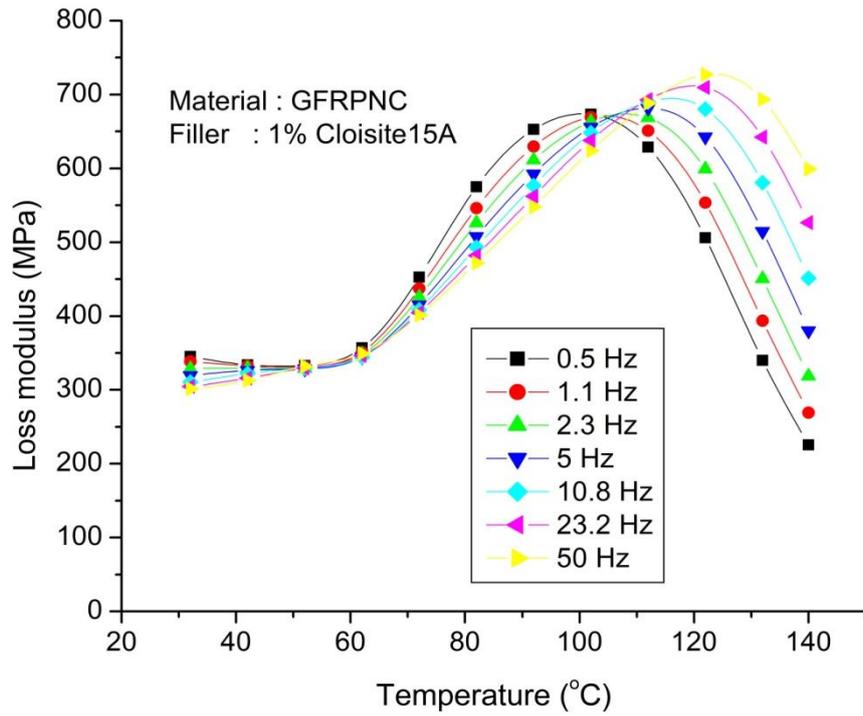


**Figure 6-14** Variation of loss modulus with temperature for different frequencies at filler content 1%

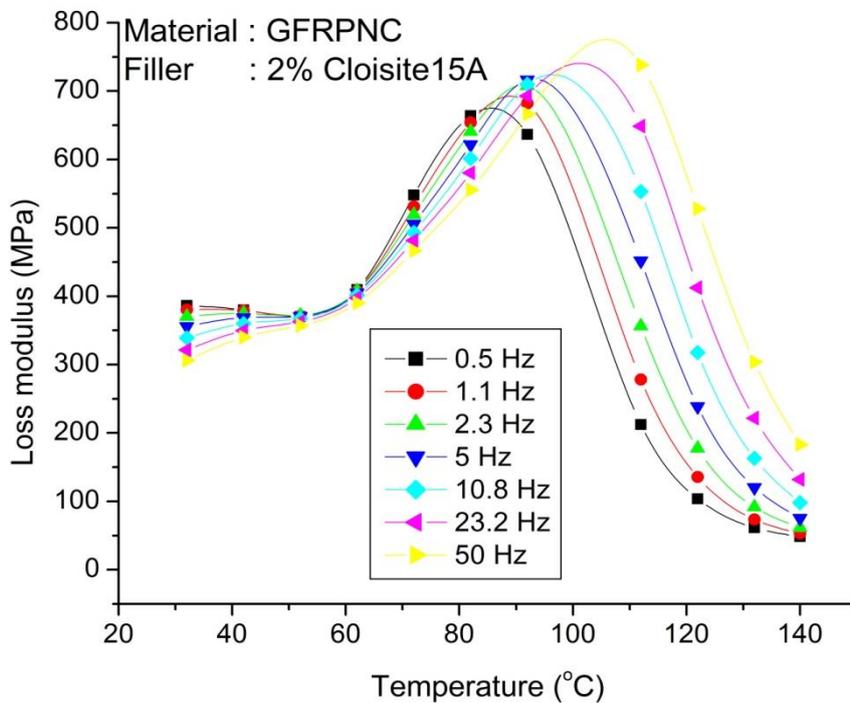


**Figure 6-15** Variation of loss modulus with temperature for different frequencies at filler content 2%

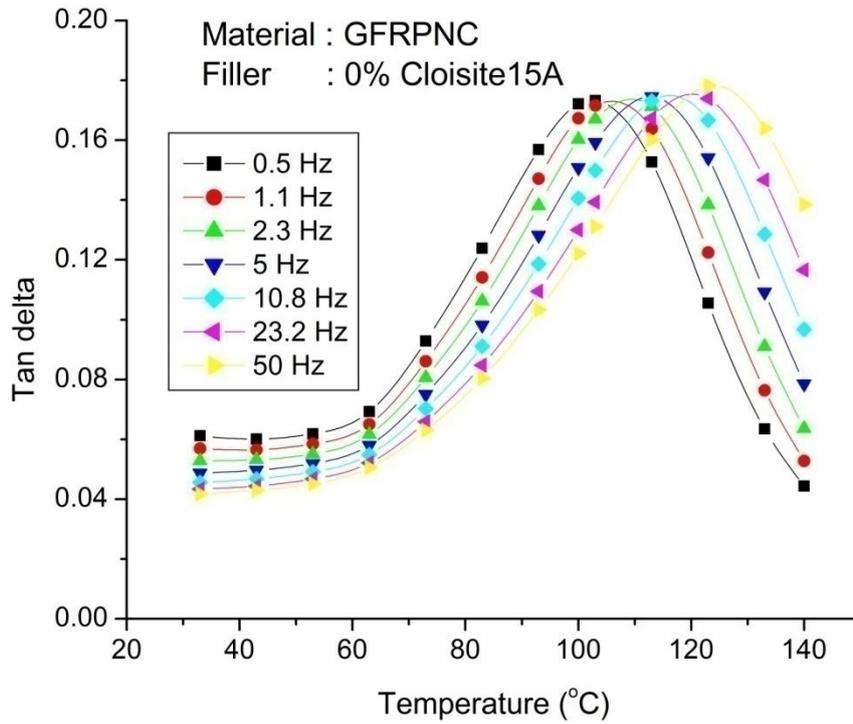


**Figure 6-16** Variation of tandelta with temperature for different frequencies at filler content 0%

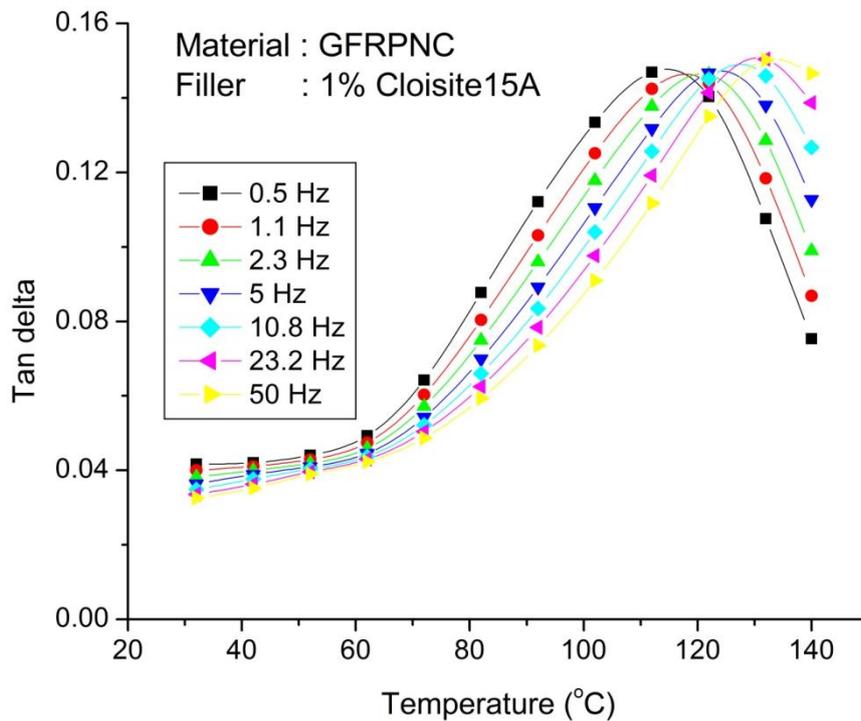


**Figure 6-17** Variation of tandelta with temperature for different frequencies at filler content 1%

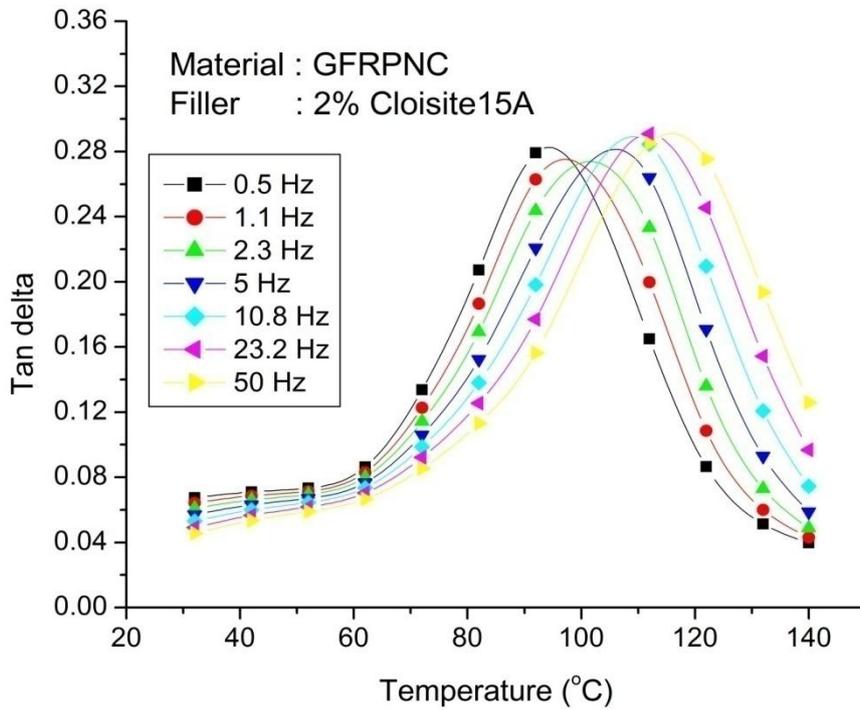


**Figure 6-181** Variation of tandelta with temperature for different frequencies at filler content 2%

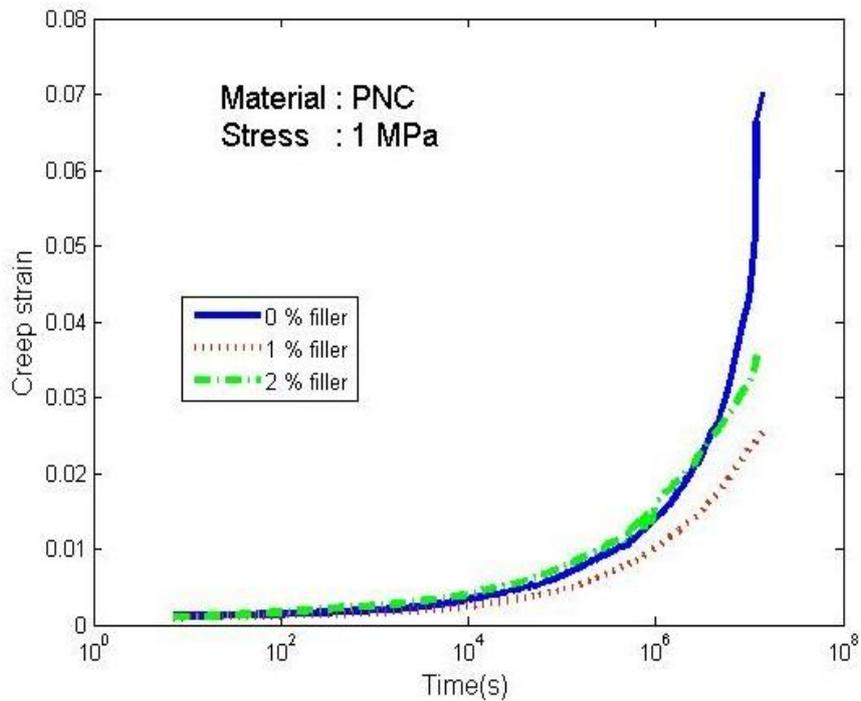


**Figure 6-19** Variation of tensile creep strain with time for different filler (Cloisite15A) content at stress 1MPa for PNC

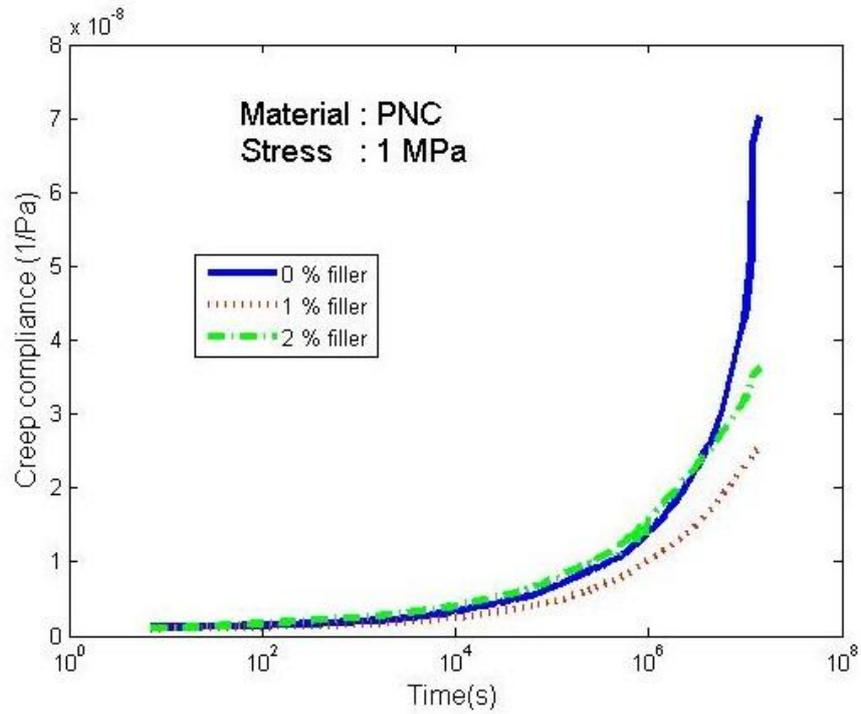


**Figure 6-20** Variation of tensile creep compliance with time for different filler (Cloisite15A) content at stress 1MPa for PNC

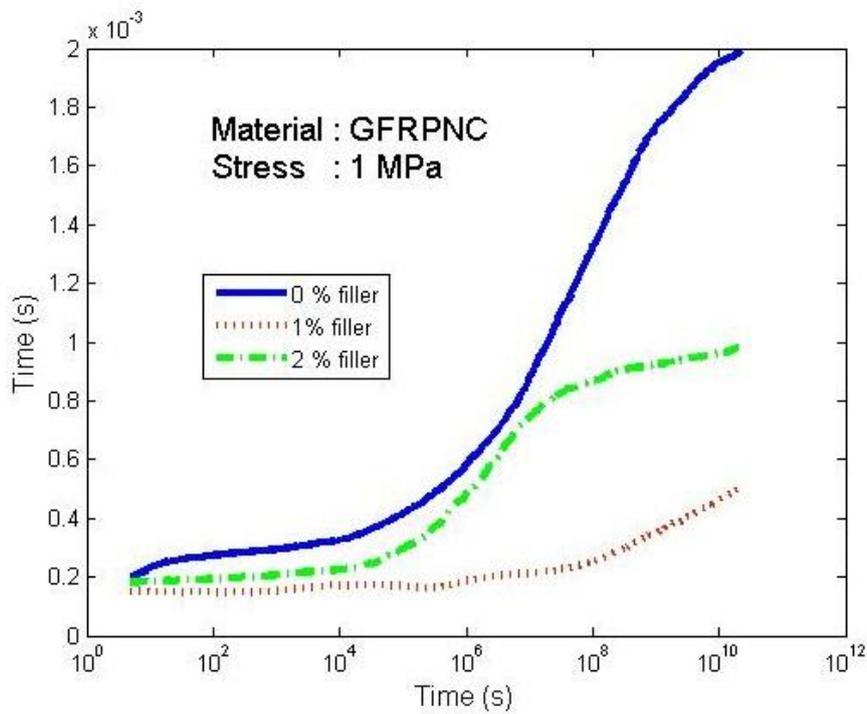


**Figure 6-21** Variation of tensile creep strain with time for different filler (Cloisite15A) content at stress 1MPa for GFRPNC

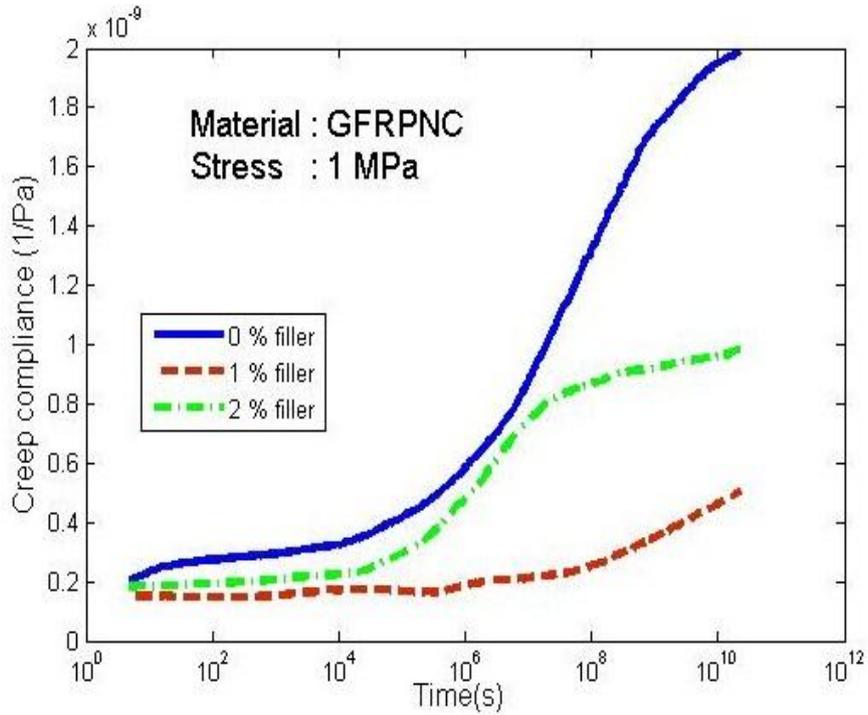


**Figure 6-22** Variation of tensile creep compliance with time for different filler(Cloisite15A) content at stress 1MPa of GFRPNC

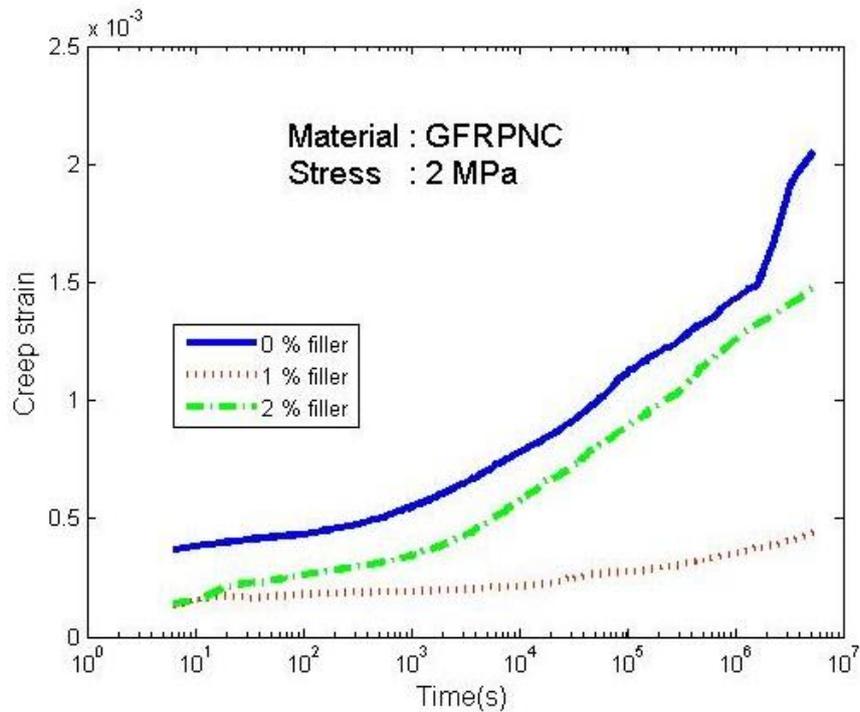


**Figure 6-23** Variation of tensile creep strain with time for different filler (Cloisite15A) content at stress 2 MPa for GFRPNC

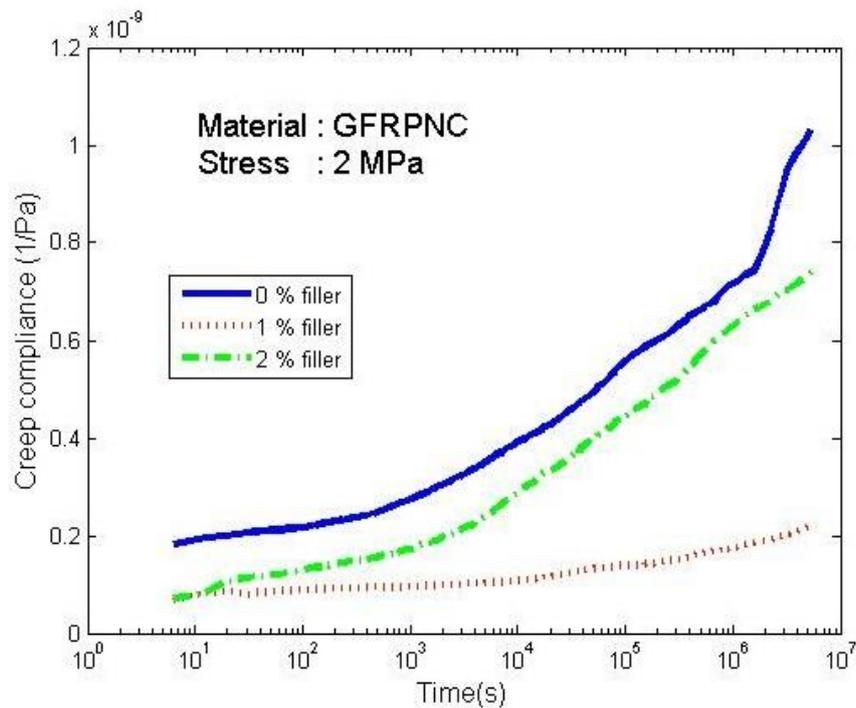


**Figure 6-242** Variation of tensile creep compliance with time for different filler (Cloisite15A) content at stress 2MPa for GFRPNC.

### 6.3.2 Creep data Analysis

The numerical value obtained by simulating the experimental results of tensile creep behaviour analysis of polyester nanocomposite(PNC) conducted at constant stress 1 MPa is given in table 6-7 and 6-8 respectively for creep compliance and creep strain. Table 6-9 and 6-10 indicate the same data that for glass fiber reinforced polyester nanocomposite (GFRPNC) at stress 1 MPa. Table 6-11 and 6-12 corresponds to the data for GFRPNC at constant stress 2MPa. Figure 6-19 and 6-20 respectively display the variation of creep strain and creep compliance of polyester nanocomposite at stress 1 MPa, which are the master curves [105] obtained at stress 1 MPa with reference temperature 30°C. Tensile creep properties of polyester nanocomposite(PNC) with 1% and 2% cloisite15A as nano filler as well as pure polyester (0% filler) is indicated by the curves. The creep strain as well as creep compliance is almost

constant up to 100000 seconds of loading. After that the creep compliance and creep strain increase with time. The rate of increase of creep compliance as well as creep strain for pure polyester (0% filler) is high. Also the creep compliance and strain is low for 1% nanoclay filled specimen. Thus the creep resistance of nanocomposite is high as compared to pure polyester. Also the nanocomposite with 1% nanoclay has showed high creep resistance compared to 2% nanoclay. The improved intercalation of nanoclay in to polyester at 1% filler content reported by the SEM analysis (Chapter 4) may be the reason for high creep resistance.

Similar to polyester nanocomposite, the master curves obtained for creep strain and creep compliance of the glass fiber reinforced polyester nanocomposite (GFRPNC) at stress 1 MPa is indicated by figure 6-21 and 6-22. Similar plots at stress 2 MPa is indicated by figure 6-23 and 6-24. These curves can also be obtained by extrapolating the experimental results for a short period to long period by WLF equation. The plots clearly demonstrating the increase of creep resistance of reinforced polyester with the addition of nanoclay. A similar variation as that of polyester nanocomposite is obtained for the reinforced nanocomposite. Thus the addition of nanoclay (Cloisite15A) enhances the creep resistance and addition of more nanoclay doesnot guarantee any enhancement. The creep strain as well as creep compliance is almost constant up to 100000 seconds of loading. After that the creep compliance and creep strain increase with time. The rate of increase of creep compliance as well as creep strain for reinforced polyester (0% filler) is high as compared to reinforced nanocomposite (1% and 2% nanoclay as filler). Reinforced nanocomposite with 1% nanoclay has creep compliance and strain constant over a long time, which indicates the improvement in the performance of the material by the addition of nano filler and

the sustainable performance of the material at 1% nano clay inclusion. This may be attributed to the restricted motion of the polymer chain by the addition of nano filler which occupies the interface. The nano platelets also help to establish a good bonding between the fiber and polymer matrix, which also restricts the motion of the polymer matrix. For the 2% filled nano composite the possibility for the agglomeration of the clay particles is high which may result in improper mixing [63]. With the creep deformation of nano composites with 1 wt% Cloisite15A shows the minimum value and which also shows improved creep resistance from nano filler. The creep resistance does not show any notable change with the applied stress from the experimental data of 1MPa and 2 MPa applied stress.

### **6.3.3 Statistical Analysis**

Table 6-13 shows the report of the statistical analysis conducted on the data obtained for creep compliance of polyester nanocomposite (PNC). From the table of ANOVA, the significant value for time is 0.486, which is more than the cut off value 0.05. Hence the analysis says that there is no significant relation between time and creep compliance. Thus the creep compliance not much affected by the time ,within the limit the analysis is done. Again the significant value for percentage weight of filler is 0.4.26E-6 which is less than the cut off value 0.05. So there is significant effect for the variation of percentage weight of filler in terms of creep compliance.

The average value of creep compliance is 8.98E-9 at 0% filler, 5.87E-9 at 1% filler and 8.97E-09 for 2% filler incorporated samples, which means the creep compliance is low or creep resistance maximum for 1% nanoclay filled samples. Thus 1% nanoclay is the optimum quantity of filler regards to creep resistance.

**Table 6-13** Statistical analysis, creep compliance of PNCs at stress 1MPa

| <i>SUMMARY</i>             | <i>Count</i> | <i>Sum</i> | <i>Average</i> | <i>Variance</i> |                |               |
|----------------------------|--------------|------------|----------------|-----------------|----------------|---------------|
| Time(s)                    | 62           | 5.48E+08   | 8.8E+5         | 4.88E+12        |                |               |
| 0% filler                  | 62           | 5.56E-07   | 8.98E-09       | 1.23E-16        |                |               |
| 1% filler                  | 62           | 3.648E-07  | 5.87E-09       | 3.15E-17        |                |               |
| 2% filler                  | 62           | 5.56E-07   | 8.97E-09       | 6.67E-17        |                |               |
| ANOVA                      |              |            |                |                 |                |               |
| <i>Source of Variation</i> | <i>SS</i>    | <i>df</i>  | <i>MS</i>      | <i>F</i>        | <i>P-value</i> | <i>F crit</i> |
| Time(s)                    | 7.45E+13     | 61         | 1.22E+12       | 1               | 0.486          | 1.389         |
| % weight of filler         | 3.63E+13     | 3          | 1.21E+13       | 9.92            | 4.26E-06       | 2.653         |
| Error                      | 2.23E+14     | 183        | 1.22E+12       |                 |                |               |
| Total                      | 3.34E+14     | 247        |                |                 |                |               |

The report of statistical analysis conducted on the data obtained for creep compliance at constant stress 1 MPa for GFRPNC is shown in table 6-14. The average value of creep compliance obtained has the lowest value, 2.33E-10, when the filler content is 1%. The significant value for time is 0.485, which is greater than the cut off value 0.05. Hence the null hypothesis (no significant difference between time in terms of creep compliance) accepted. Thus time has no significant effect in terms of creep compliance.

The significant value for % weight of filler is 0.001, which is less than the cut off value 0.05. Hence the % weight of filler has significant effect in terms of creep compliance.

The report of statistical analysis conducted on the data obtained for creep compliance at constant stress 2 MPa for GFRPNC is shown in table 6-15. The average value of creep compliance is 4.21E-10 at 0% filler, 1.19E-10 at 1% filler and 3.13E-10 for 2% filler incorporated samples, which means the creep compliance is low for 1% nanoclay filled samples.

**Table 6-14** Statistical analysis, creep compliance of GFRPNCs at stress 1MPa

| <i>SUMMARY</i>             | <i>Count</i> | <i>Sum</i> | <i>Average</i> | <i>Variance</i> |                |               |
|----------------------------|--------------|------------|----------------|-----------------|----------------|---------------|
| Time(s)                    | 54           | 4.78E+10   | 8.84E+08       | 7.74E+18        |                |               |
| 0% filler                  | 54           | 4.8E-08    | 8.89E-10       | 3.64E-19        |                |               |
| 1% filler                  | 54           | 1.26E-08   | 2.33E-10       | 8.53E-21        |                |               |
| 2% filler                  | 54           | 3.05E-08   | 5.65E-10       | 9.71E-20        |                |               |
| ANOVA                      |              |            |                |                 |                |               |
| <i>Source of Variation</i> | <i>SS</i>    | <i>df</i>  | <i>MS</i>      | <i>F</i>        | <i>P-value</i> | <i>F crit</i> |
| Time(s)                    | 1.03E+20     | 53         | 1.93E+18       | 1               | <b>0.485</b>   | 1.421         |
| % weight of filler         | 3.17E+19     | 3          | 1.06E+19       | 5.456           | <b>0.001</b>   | 2.661         |
| Error                      | 3.08E+20     | 159        | 1.93E+18       |                 |                |               |
| Total                      | 4.42E+20     | 215        |                |                 |                |               |

**Table 6-15** Statistical analysis, creep compliance of GFRPNC at stress 2 MPa

| <i>SUMMARY</i>             | <i>Count</i> | <i>Sum</i> | <i>Average</i> | <i>Variance</i> |                |               |
|----------------------------|--------------|------------|----------------|-----------------|----------------|---------------|
| Time(s)                    | 52           | 17664522   | 339702.4       | 9.81E+11        |                |               |
| 0% filler                  | 52           | 2.19E-08   | 4.21E-10       | 4.23E-20        |                |               |
| 1% filler                  | 52           | 6.16E-09   | 1.19E-10       | 1.21E-21        |                |               |
| 2% filler                  | 52           | 1.63E-08   | 3.13E-10       | 3.37E-20        |                |               |
| ANOVA                      |              |            |                |                 |                |               |
| <i>Source of Variation</i> | <i>SS</i>    | <i>df</i>  | <i>MS</i>      | <i>F</i>        | <i>P-value</i> | <i>F crit</i> |
| Time(s)                    | 1.25E+13     | 51         | 2.45E+11       | 1               | <b>0.485</b>   | 1.431         |
| % weight of filler         | 4.5E+12      | 3          | 1.5E+12        | 6.119           | <b>0.001</b>   | 2.664         |
| Error                      | 3.75E+13     | 153        | 2.45E+11       |                 |                |               |
| Total                      | 5.45E+13     | 207        |                |                 |                |               |

The significant value for time is 0.485, which is more than the cut off value 0.05. Hence time has no significant effect in terms of creep compliance within the time limit for which the analysis is concerned. The significant value for % weight of filler is 0.001, which is less than the cut off value 0.05, so the % weight of filler has significant effect in terms of creep compliance. A similar conclusion as that of the previous case can be reached.

## 6.4 CONCLUSIONS

Dynamic mechanical behaviors at frequency sweep mode and creep resistance were determined for PNCs and GFRPNCs. The following conclusions can be drawn from the studies:

1. The storage modulus of PNC and GFRPNC increased with increase of frequency. However, it decreased with increase of nanoclay content for PNC and GFRPNC.
2. Peaks of loss modulus and  $\tan\delta$  curves shifted to higher values with increase of frequency.
3. 1% nanoclay recorded maximum storage modulus for nanocomposites.
4. Creep compliance of the nanocomposite (PNC) was lowest at 1% nanoclay content and remained almost steady for a long period of time. Similar trend for creep compliance was observed for GFRPNCs also. The creep resistance was maximum at filler content 1% for both PNC and GFRPNC

## **CHAPTER 7**

### **CONCLUSIONS AND SCOPE FOR FURTHER STUDY**

The present work focusing on the effect of nanoclay on the property enhancement of unsaturated polyester and fiber reinforced polyester showed that a small quantity of nanoclay can provide significant property enhancement. Modified nanoclay and unmodified nanoclays were used for the preparation of nanocomposite with isophthalic polyester resin as matrix. The first part of the investigation was conducted with low cost nanokaoline clay. However, the property enhancement was very low. Hence the study was extended to conventional nanoclay, modified Montmorillonite (Cloisite15A). A notable improvement was observed in this case. The tensile modulus improved 15 to 25 % by the addition of 0.5 % Cloisite15A. The impact strength improved from 30 to 50 % by the addition of 0.5 to 1.5 % Cloisite15A. 10 to 40 % increase in tensile modulus was observed in the case of GFRP nanocomposite with the addition of nanoclay of 0.5 to 1 % by weight. However, the improvement in impact strength was only 16 %. Addition of more nanoclay resulted in the reduction of both impact strength and tensile modulus.

Investigation on the performance of PNCs and GFRPNCs for prolonged application was done by the method of time - temperature superposition using WLF equation and master curve was generated for different nanocomposites. The modified nanocomposites were much superior in creep resistance compared to neat polyester as well as reinforced polyester. Incorporation of 1% nanoclay resulted in an appreciable improvement in creep resistance for both PNCs and GFRPNCs.

Mathematical equations were developed to represent variation of mechanical properties such as tensile modulus, impact strength, flexural modulus and dynamic mechanical properties such as storage modulus, loss modulus and damping factor with filler content. The results were also shown to be statistically reliable by the method of ANOVA.

Uniform distribution of the nanofiller was found to be the critical factor deciding the level of reinforcement both in the case of polyester nanocomposites and reinforced nanocomposites.

The study can be further extended to areas such as

1. Water absorption characterization of the composite and the variation in the property of nanocomposite with water absorption.
2. Use of hybrid fillers such as mixture of modified montmorillonite and modified kaolinite for optimizing properties, cost of the nanocomposite and nanofilled glass fiber reinforced composite.
3. Use of coupling agents to improve the adhesion of nanofiller in the nanocomposite and glass fiber filled composite.

## REFERENCES

- [1] **Bhagwan, D. Agarwal, Lawrence J. Broutman, and Chandrashekhara, K.** Analysis and performance of fiber composites, 3<sup>rd</sup> Ed., John Wiley & Sons, 2006.
- [2] Report of BCC Research Gate, report code-NANO21F, May 2014
- [3] **M.A. Motawie, N.M. Ahmed, S.M. ElMesallamy, E.M. Sadek and N.G. Kandile** (2014), Unsaturated Polyesters / Layered Silicate Nanocomposites: Synthesis and Characterization, *IOSR Journal of Applied Chemistry (IOSR-JAC)*, 7(10), 34-43
- [4] **Sabu Thomas, Kuruvilla Joseph, Sant Kumar Malhotra, Koichi Goda, and Meyyarappallil Sadasivan Sreekala**, Polymer Composites, Volume 1, Wiley-VCH Verlag GmbH & Co. KGaA 2012.
- [5] **Farzana Hussain, Mehdi Hojjati, Masami Okamoto, Russell E. Gorga** (2006), Review article: Polymer matrix Nanocomposites, Processing, Manufacturing, and Application: An Overview, *Journal of Composite Materials*, 40, 1511-75
- [6] **Charles Chikwendu Okpala** (2013), Nanocomposites, An Overview, *Int. Journal of Engineering Research and Development*, 8(11), 17-23
- [7] **Kumar, A.P., Depan, D., Tomer, N.S., Singh, R.P.** (2009), Nanoscale particles for polymer degradation and stabilization-Trends and future perspectives, *Progress in Polymer Science*, 479-515.
- [8] **Vineeta Nigam and Gobardhan Lal** (2008), Review on Recent Trends in Polymer Layered Clay Nanocomposites, *Defence Materials and Stores Research and Development Establishment, Proc Indian Natn Acad*, 74(2), 87-96.
- [9] **Paolo Cosoli, Giulio Scocchi, Sabrina Priol and Maurizio Fermeglia** (2008), Many-scale molecular simulation for ABS–MMT nanocomposites: Upgrading of industrial scraps, *Microporous and Mesoporous Materials*, 107, 169–179
- [10] **Quang T. Nguyen and Donald G. Baird** (2007), Preparation of polymer–clay nanocomposites and their properties, *Advances in Polymer Technology, Wiley periodicals, Inc.*, 25(4), 270–285.
- [11] A web page of the Southern Clay Products, [www.southernclayproducts.com](http://www.southernclayproducts.com)
- [12] **Mahmoud M. Shokrieh, Ali Saeedi and Majid Chitsazzadeh** (2013), Mechanical properties of multi-walled carbon nanotube/polyester nanocomposites, *Journal of Nanostructure in Chemistry, Springer*, 3, 1-5

- [13] **Joseph HK**, Polymer nanocomposites- processing, characterization, and applications. *McGraw-Hill Nanoscience and Technology Series.*, 2006
- [14] **Okada, A., Kawasumi, M., Usuki, A., Kojima, Y., Kurauchi, T. and Kamigaito, O.** (1990) In: Schaefer DW, Mark JE, editors. Polymer based molecular composites, vol. 171. Pittsburgh: MRS Symposium Proceedings
- [15] **Michael Alexandre, Philippe Dubois** (2000), Polymer-layered silicate nanocomposites: preparation, properties and uses of a new class of materials, *Materials Science and Engineering*, 28, 1-63
- [16] **Gorga, R.E. and Cohen, R.E.** (2004), Toughness Enhancements in Poly(methyl methacrylate) by Addition of Oriented Multiwall Carbon Nanotube, *Journal of Polym. Sci., Part B: Polym. Phys.*, 42(14), 2690–2702.
- [17] **Arunkumar Lagashetty and A. Venkataraman** (2005), Polymer Nanocomposites, *Resonance*, 10(7), 49-57.
- [18] **Shah V.**, Handbook of Plastic Testing Technology, 2nd Edition, *Wiley-Interscience Publication*, 1998
- [19] **Kevin P. Menard**, Dynamical Mechanical Analysis A Practical Introduction, *CRC Press*, 2008.
- [20] **Duncan M. Price, Douglas J. Hourston and Fabrice Dumont** (2000), Thermogravimetry of Polymers, *Encyclopedia of Analytical Chemistry, John Wiley & Sons Ltd*, Chichester, 8094–8105
- [21] **Li Chang and Klaus Friedrich** (2010) Enhancement effect of nanoparticles on the sliding wear of short fiber-reinforced polymer composites: A critical discussion of wear mechanisms, *Tribology International*, 43, 2355–64
- [22] **Mashaal Alshabanat, Amal Al-Arrash, and Waffa Mekhamer** (2013), Polystyrene/Montmorillonite Nanocomposites: Study of the Morphology and Effects of Sonication Time on Thermal Stability, *Hindawi Publishing Corporation, Journal of Nanomaterials*, 1-12
- [23] **K.V.P.Chakradhar, K.Venkata Subbaiah, M. Ashok Kumar and G.Ramachandra Reddy** (2011), Epoxy/Polyester Blend Nanocomposites: Effect of Nanoclay on Mechanical, Thermal and Morphological Properties, *Malaysian Polymer Journal*, 6(2), 109-118.
- [24] **P. Jawaharlal and M. Balasubramanian** (2006), Preparation and Properties of Polyester-Based Nanocomposite Gel Coat System, *Hindawi Publishing Corporation Journal of Nanomaterials*, 1–7
- [25] **K. Rajkumar, Prem Ranjan, P. Thavamani, P.Jeyanthi and P. Pazhanisamy** (2013), Dispersion Studies of Nanosilica in NBR Based Polymer Nanocomposite, *Rasayan Journal of Chemistry*, 6(2), 122-133

- [26] **J. Rotrekl, L. Matejka, L. Kapralkova, A. Zhigunov, J. Hromadkova and I. Kelnar**(2012),Epoxy/PCL nanocomposites: Effect of layered silicate on structure and behavior, *Express Polymer Letters*,6(12),975–986
- [27] **Byung Chul Kim, Sang Wook Park and Dai Gil Lee** (2008), Fracture toughness of the nano-particle reinforced epoxy composite, *Composite Structures*, 86, 69–77
- [28] **Shahryar Pashaei, Siddaramaiah and Akheel Ahmed Syed** (2010), Investigation on Thermal, Mechanical and Morphological behaviours of Organo Nanoclay incorporated Epoxy Nanocomposites, *ARPJ journal of engineering and applied sciences*, 5(12), 1-11
- [29] **In Yee Pang, K.P. Promoda, Tianxi Liu and Chaobin He** (2004), Crystallization and melting behavior of polyester/clay nano composites, *polymer Int.* 53, 1282-89
- [30] **Charef Harrats and Gabriel Groeninckx** (2008), Features, Questions and future challenges in Layered silicates clay nanocomposites with semi crystalline polymer Matrices, *Macromolecular rapid communication*, 29, 14-26.
- [31] **D.R. Paul, L.M. Robeson** (2008), Polymer nanotechnology: Nanocomposites, *Polymer* 49, 3187–3204
- [32] **Michael Alexandre and Philippe Dubois** (2000), Polymer-layered silicate nanocomposites: preparation, properties and uses of a new class of materials, *Materials Science and Engineering*, 28, 1-63
- [33] **Lagache, M., Agbossou, A., Pastor, J. and Muller, D.**(1994), Role of interphase on the elastic behavior of composite materials: theoretical and experimental analysis. *Journal of Compos Materials*, 28 (12), 1140–57.
- [34] **Kornmann, X., Rees, M., Thomann, Y., Necola, A., Barbezat, M. and Thomann, R.**(2005), Epoxy-layered silicate nanocomposite as matrix in glass fibre-reinforced composites. *Journal of Compos Sci. Technol*, 65, 2259–68.
- [35] **Yuan Xu and Suong Van Hoa** (2008), Mechanical properties of carbon fiber reinforced epoxy/clay nanocomposites, *Composites Science and Technology*,68, 854–861
- [36] **B. Sharma, S. Mahajana, R. Chhibbera, R. Mehtab** (2012), Glass Fiber Reinforced Polymer-Clay Nanocomposites: Processing, Structure and Hygrothermal Effects on Mechanical Properties, *Procedia Chemistry*, 4, 39 – 46
- [37] **Weiping Liu, Suong V. Hoa and Martin Pugh** (2005), Fracture toughness and water uptake of high-performance epoxy/nanoclay nanocomposites, *Compos Sci. Technology*, 65, 2364–73.

- [38] **Mallick, P.K.**, Fiber Reinforced Composites: Materials, Manufacturing and Design, *Marcel Dekker Inc.: New York*, 1997
- [39] **Yosoyima, R., Morimoto, K., Susuki, T., Nakajima, A. and Ikada, Y.**, Adhesion and Bonding in Composites, *Marcel Dekker Inc.: New York*, 1990
- [40] **Pukánszky, B., Maurer-Frans, H.J. and Boode, J.W.** (1995), Impact testing of polypropylene blends and composites, *Polym. Eng. Sci.*, 35, 1962–71.
- [41] **M.A. Rodríguez-Pérez, S. Rodríguez-Llorente and JA. De Saja** (1997), Dynamic mechanical properties of polyolefin foams studied by DMA techniques, *Polymer Engineering & Science*, 37(6), 959-965
- [42] **Amash, A. and Zugenmaier, P.** (1997), Thermal and dynamic mechanical investigations on fiber- reinforced polypropylene composites, *Journal of Applied Polymer Science* , 63(9),1143–54
- [43] **Mehdi Tajvidi, Robert H. Falk and John C. Hermanson** (2006), Effect of Natural Fibers on Thermal and Mechanical Properties of Natural Fiber Polypropylene Composites Studied by Dynamic Mechanical Analysis, *Journal of Applied Polymer Science*, 101, 4341–49.
- [44] **Cho, M.H. and Bahadur, S.** (2005), Study of the tribological synergistic effects in CuO-filled and fiber-reinforced polyphenylene sulfide composites, *Wear*, 258, 835–845.
- [45] **Javad Moftakharian Esfahani, Masoud Esfandeh and Ali Reza Sabet** (2012), High-Velocity Impact Behavior of Glass Fiber-Reinforced Polyester Filled with Nanoclay, *Journal of Applied Polymer Science*, 125, E583–E591
- [46] **Sudirmana, M. Anggaravidyac, E. Budianto and I. Gunawan** (2012), Synthesis and Characterization of Polyester-Based Nanocomposite, *Procedia Chemistry*, 4, 107 – 113
- [47] **Mariana Etcheverry and Silvia E. Barbosa** (2012), Glass Fiber Reinforced Polypropylene Mechanical Properties Enhancement by Adhesion Improvement, *Materials*, 5, 1084-1113
- [48] **Sujesh, G. and C. Ganesan** (2012), Tensile Behavior of Nano Filled GFRP at Different Strain rates, *Proceedings International Conference on Mechanical, Materials and Automotive Engineering*, 13-15
- [49] **S.R. Challa and R.C. Progelhof** (1995), A study of creep and creep rupture of polycarbonate, *Polymer Engineering and Science*, 6, 546-554.
- [50] **R.K. Krishnaswamy** (2005), Analysis of ductile and brittle failures from creep rupture testing of high-density polyethylene (HDPE) pipes, *Polymer*, 28, 11664 -72.

- [51] **A.Greco, Claudio Musardo and Alfonso Maffezzoli** (2007), Flexural creep behaviour of PP matrix woven composite, *Composites Science and Technology*, 67, 1148-58.
- [52] **B.A. Acha, M.M. Reboredo and N.E. Marcovich** (2007), Creep and dynamic mechanical behavior of PP–jute composites: Effect of the interfacial adhesion, *Composites Part A: Applied Science and Manufacturing*, 33, 1507-1516.
- [53] **W.N. Findley and G. Khosla** (1955), Application of the superposition principle and theories of mechanical equation of state, strain, and time hardening to creep of plastics under changing loads, *Journal of Applied Physics*, 26, 821–832.
- [54] **M.Hadid, S.Rechak and A.Tati** (2004), Long-term bending creep behavior prediction of injection molded composite using stress-time correspondence principle, *Materials Science and Engineering*, 385, 54-58.
- [55] **G.E. Novak** (1995), Creep fracture of long fiber reinforced nylon 66, *Polymer Composites*, 16,38-51.
- [56] **K.Banik, J.Karger-Kocsis and T. Abraham** (2008), Flexural creep of all-polypropylene composites: Model analysis, *Polymer Engineering and Science*,48, 941-948.
- [57] **H.Liu, M.A.Polak and A.Penlidis** (2008), A practical approach to modeling time-dependent nonlinear creep behavior of polyethylene for structural applications, *Polymer Engineering Science*, 48, 159-167.
- [58] **C.Subramanian, Abdulrahman Khalfan Hassan Al Mamari , S.Senthilvelan** (2014), Effect of Fiber Length on the Short-Term Flexural Creep Behavior of Polypropylene, *International Journal of Students' Research in Technology & Management*, 2(5),157-162
- [59] **Nunez, A.J., Marcovich, N.E. and Aranguren, M.I.** (2004) Analysis of the creep behavior of polypropylene-woodflour composites, *Polymer Engineering and Science*, 44(8), 1594-1603.
- [60] **Yanjun, X.**(2009) ,Creep behavior of natural fiber reinforced polymer composites. PhD Thesis, Louisiana State University.
- [61] **Feiyi Pang, Chun Hui Wang** (2000), A predictive creep model for unstitched and stitched woven composites, *composites Science and Technology*, 255-261
- [62] **Feiyi Pang, C.H.Wa ng, R.G. Bathgate** (1997), Creep response of woven-fibre composites and the effect of stitching, *Composites Science and Technology*, 57(1), 91–98

- [63] **C.Z. Chen, Y.Li and J. Xu**, Creep and Dynamic Mechanical Behavior of Natural Fiber/Functionalized Carbon Nanotubes Modified Epoxy Composites, *proc. of 18<sup>th</sup> ICCM, School of Aerospace Engineering and Applied Mechanics, Tongji University, Shanghai, China, 1-6*
- [64] **M. Tehrani, M. Safdari and M.S. Al-Haik** (2011), Nanocharacterization of creep behavior of multiwall carbon nanotubes/epoxy nanocomposite, *Int. Journal of Plasticity*, 27,887–901
- [65] **Lubna Ghalib** (2013), Creep Behavior in Fiber-Reinforced Epoxy (DGEBA) Composites, *Eng. & Tech. Journal.*, 31, No.1
- [66] **Vlasveld, D.P.N., Bersee, H.E.N. and Picken, S.J.**(2005), Creep and physical ageing behavior of PA6, *Polymer*, 46, 12539-45.
- [67] **T. Glaskova and A. Aniskevich** (2015), Creep behavior of Epoxy/Clay Nanocomposite, *Institute of Polymer Mechanics, University of Latvia 23, Aizkraules Str., Riga, LV-1006.*
- [68] **Catherine, A. Tweedie and Krystyn J. Van Vlieta** (2006), Contact creep compliance of viscoelastic materials via nanoindentation, *Journal of Mater. Res.*, 21(6), 1576-89.
- [69] **Jayita Bandyopadhyay, Suprakas Sinha Ray and Mosto Bousmina** (2007), Thermal and Thermo-mechanical Properties of Poly(ethylene terephthalate) Nanocomposites, *Journal of Ind. Eng. Chem.*, 13(4), 614-623
- [70] **Liu, H. and Brinson, LC.**(2008), Reinforcing efficiency of nanoparticles: A simple comparison for polymer nanocomposites. *Composite Science and Technology*, 68, 1502-12.
- [71] **Anjana, R. and K.E. George** (2012), Reinforcing effect of nano kaolin clay on PP/HDPE blends, *IJERA*, 2(4), 868-872
- [72] **M.R. Basiri and A.Bigdeli** (2010), The Role of Nanoclay Type and Content in Promoting Microstructure and Properties of Nylon6 Fibre, *Textile Science and Technology Journal*, 4(2), 36-46
- [73] **Newly Joseph, Sinto Jacob, Tresa Sunitha George, Asha Krishnan and George K.E.** (2009), Reinforcing Effect of Organo Modified Kaolin Clay on Polypropylene-Short Glass Fibre Composites, *Academic review*, 16, 152-163
- [74] **Preetha Nair K., Dr. Rani Joseph** (2012), Nanokaolin Clay as Reinforcing Filler in Nitrile Rubber, *Int. Journal of Scientific & Engineering Research* ,3 (3),1-10
- [75] **Tresa Sunitha George, Asha Krishnan K., Anjana R. and K.E. George** (2013), Studies on Nano Kaolin Clay Reinforced PS-HDPE Nanocomposites, *Indian Journal of Advances in Chemical Science* 1(4), 201-206

- [76] **Somaiah Chowdary and Niranjan Kumar** (2014), Effect of Nanoclay on the tensile properties of Polyester and S-glass Fiber (Al), *Int. Journal of Engineering Research & Technology*, 3(5), 1977-80
- [77] **Sambarkar, P.P., Patwekar, Sl. and Dudhgaonkar, Bm.** (2012), Polymer Nanocomposites: An Overview, *Int. Journal of Pharmacy and Pharmaceutical Sciences*, 4(2), 60-65
- [78] **A. Mirmohseni and S. Zavareh** (2010), Preparation and characterization of an epoxy nanocomposite toughened by a combination of thermoplastic, layered and particulate nano fillers, *Materials and Design*, 31, 2699-2706.
- [79] **Krishnan K., Chawla**, Composite Materials Science and Engineering, *Springer*, 2010.
- [80] **Schwartz, M.M.**, Composite materials handbook, *McGraw-Hill*, 1992.
- [81] **Mohan, T.P., Kumar, M.R. and Velmurugan, R.** (2005), Rheology and curing characteristics of epoxy-clay nanocomposites, *Polym Int*, 54, 1653–59.
- [82] **Vikas Dhawan, Sehijpal Singh and Inderdeep Singh** (2013), Effect of Natural Fillers on Mechanical Properties of GFRP Composites, *Journal of Composites*, Volume 2013, Article ID 792620, 1-8
- [83] **Kornmann, X., Thomann, R., Mulhaupt, R., Finter, J. and Berglund, L.** (2002), Synthesis of amine-cured, epoxy-layered silicate nanocomposites: the influence of the silicate surface modification on the properties. *Journal of Appl Polym Sci*, 86 , 2643–52.
- [84] **Kinloch, A.J. and Taylor, A.C.** (2006), Mechanical and fracture properties of epoxy/inorganic micro- and nano-composites. *Journal Mater Sci*, 41, 3271-97.
- [85] **Miyagawa, H. and Drzal, L.T.** (2003), Fracture behaviour of epoxy/clay and epoxy/silica nanocomposites. *ICCM-14, San Diego, California, USA*.
- [86] **Zilg, C., Mulhaupt, R. and Finter, J.** (1999), Morphology and toughness/stiffness balance of nanocomposites based upon anhydride-cured epoxy resins and layered silicates. *Macromol Chem Phys*, 200, 661–70.
- [87] **B.Qi, Q.X. Zhang, M.Bannister, Y-W Mai** (2006), Investigation of Mechanical Properties of DGEBA-based epoxy resin with nano clay additives, *Composite Structures*, 75, 514-519
- [88] **Mushtaq T. Albdiry, Belal F Yousif and Harry Ku** (2013), Fracture toughness and toughening mechanisms of unsaturated polyester-based clay nanocomposites, *proc. 13th Int. Conference on Fracture, Beijing, China*

- [89] **Jeffrey Jordan, Karl I. Jacob , Rina Tannenbaum Mohammed A. Sharaf and Iwona Jasiuk**, (2005), Experimental trends in polymer nanocomposites—a review, *Materials Science and Engineering* ,A 393,1–11
- [90] **Manoj Kumar Shukla and Deepak Srivastava** (2016), DGEBA Epoxy Nano Composite: A Study on Mechanical Properties Characterization, *Int. J. of Sci, and Research*, 5(10), 1692-97
- [91] **Normasmira A. Rahman, Aziz Hassan, R. Yahya and R.A. Lafia-Araga** (2013), Glass Fiber and Nanoclay Reinforced Polypropylene Composites: Morphological, Thermal and Mechanical Properties, *Sains Malaysiana*, 42, 537–546
- [92] **Yaping Zheng, Ying Zheng and Rongchang Ning** (2003), Effects of nanoparticles SiO<sub>2</sub> on the performance of nanocomposites. *J. Mater Letters*, 57, 2940–44.
- [93] **Ma. J., Mo. MS, Du. X-Sh, Rosso, P., Friedrich, K. and Kuan, H-Ch** (2008), Effect of inorganic nanoparticles on mechanical property, fracture toughness and toughening mechanism of two epoxy systems, *Polymer*, 49, 3510–23.
- [94] **Nair, K.C., Diwan, S.M. and Thomas, S.**(1996), Tensile properties of short sisal fiber reinforced polystyrene composites, *Journal Appl. Polym., Sci.*, 60, 1483-97
- [95] **Jitendra Gummadi, G.Vijay Kumar and Gunti Rajesh** (2012), Evaluation of Flexural Properties of Fly Ash Filled Polypropylene Composites, *Int. Journal of Modern Engineering Research (IJMER)*, 2(4), 2584-90
- [96] **Liu WP, Hoa SV and Pugh, M.** (2005), Fracture toughness and water uptake of high- performance epoxy/nanoclay nanocomposites. *Compos Sci. Technology*, 65, 2364–73.
- [97] **A.R. Jeefferie, M.Y. Yuhazri, O. Nooririnah, M.M. Haidir, Haeryip Sihombing, M.A., Mohd Salleh and N.A. Ibrahim** (2010), Thermomechanical and Morphological Interrelationship of Polypropylene-Mutiwalled Carbon Nanotubes (PP/MWCNTs) Nanocomposites, *Int. Journal of Basic & Applied Sciences IJBAS-IJENS* ,10(4), 22-28
- [98] **Yang, S., Tijerina, J.T., Diaz, V.S., Hernandez, K., and Lozano, K.** (2007), Dynamic Mechanical and Thermal Analysis of Aligned Vapor Grown Carbon Nanofibre Reinforced Polyethylene, *Composites Part B*, 38, 228-235.
- [99] **K.T.B.Padal, S.Srikanan and P. Surya Nagendra** (2014), Dynamic mechanical and thermal properties of Jute nano fibre reinforced polymer composite, *5th Int. Manufacturing Technology Design and Research Conference, IIT Guvahati (AIMTDR 2014)*

- [100] **Mansour Rokbia, Hocine Osmani, Abdellatif Imad and Noureddine Benseddiq**,(2011) Effect of Chemical treatment on Flexure Properties of Natural Fiber-reinforced Polyester Composite, *Procedia Engineering* 10, 2092–97
- [101] **Cho MH and Bahadur S** (2005), Study of the tribological synergistic effects in CuO-filled and fiber-reinforced polyphenylene sulfide composites, *Wear*, 258, 835–45.
- [102] **Yang, S., Tijerina, J.T., Diaz, V.S., Hernandez, K. and Lozano, K.**(2007), Dynamic Mechanical and Thermal Analysis of Aligned Vapor Grown Carbon Nanofibre Reinforced Polyethylene, *Composites Part B*, 38, 228-235.
- [103] **Zhang, H. and Zhang, Z.**(2007), Impact Behaviour of Polypropylene Filled with Multi-Walled Carbon Nanotubes. *Macromolecular Nanotechnology, European Polymer Journal*, 43, 3197-3207.
- [104] **J. M. Cervantes-Uc, J. V. Cauich-Rodríguez, H. Vázquez-Torres, L. F. Garfias-Mesías and D. R. Paul** (2007), Thermal degradation of commercially available organoclays studied by TGA-FTIR, *Thermochimica Acta*, 457, 92–102.
- [105] **Yu Jia, Ke Peng, Xing-long Gong and Zhong Zhang** (2011), Creep and recovery of polypropylene/carbon nanotube composites, *International Journal of Plasticity*, 27(8), 1239-51.
- [106] **Wu, C.L., Zhang, M.Q., Rong, M.Z. and Friedrich, K.**(2002), Tensile Performance Improvement of Low Nanoparticles Filled- Polypropylene Composites, *Composites Science and Technology*, 62 ,1327-40.
- [107] **S.Y. Lee, H. S. Yang, H.J. Kim, C.S. Jeong, B.S. Lim and J.N. Lee** (2004), Creep behavior and manufacturing parameters of wood flour filled polypropylene composites, *Composite Structures*, 65, 459-469
- [108] **Banik K., Abraham T. N. and Karger-Kocsis J.**(2007), Flexural creep behavior of unidirectional and cross-ply all poly (propylene) (PURE) composites, *Macromolecular Materials and Engineering*, 292, 1280–88.
- [109] **Venkata S. Chevali, Derrick R. Dean and Gregg M Janowski** (2009), Flexural creep behavior of discontinuous thermoplastic composites: Non-linear viscoelastic modeling and time temperature- stress superposition. *Composites Part A: Applied Science and Manufacturing*, 40, 870–877.
- [110] **Kim KJ., Yu WR. and Harrison P.** (2008), Optimum consolidation of self-reinforced polypropylene composite and its time-dependent deformation behavior. *Composites Part A: Applied Science and Manufacturing*, 39, 1597–1605.
- [111] **Carola Esposito Corcione and Mariaenrica Frigione** (2012), Characterization of Nanocomposites by Thermal Analysis, *Materials*, 5, 2960-2980.
- [112] **Sanaz Abdolmohammadi, Samira Siyamak, Nor Azowa Ibrahim, Wan Md Zin Wan Yunus Mohamad Zaki Ab Rahman, Susan Azizi and Asma Fatehi** (2012), Enhancement of Mechanical and Thermal Properties of

Polycaprolactone/Chitosan Blend by Calcium Carbonate Nanoparticles, *Int. Journal of Molecular Sciences*, 13, 4508-22

- [113] **G. Ragosta, M. Abbate, P. Musto, G. Scarinzi and L. Mascia** (2005), Epoxy-silica particulate nanocomposites: Chemical interactions, reinforcement and fracture toughness, *Polymer* 46, 10506–10516.
- [114] **Nuria Garcia, Mario Hoyos, Julio Guzman and Pilar Tiemblo** (2009), Comparing the effect of nanofillers as thermal stabilizers in low density polyethylene, *Polymer Degradation and Stability*, 94, 39–48
- [115] **Junfeng Xiao, Shaofeng Wang, Ping Lu, and Yuan Hu** (2013), Effect of organically modified montmorillonite on thermal degradation mechanism of polycarbonate nanocomposites, *Procedia Engineering* ,62, 791 – 796
- [116] **Karl W. Putz, Marc J. Palmeri, Rachel B. Cohn, Rodney Andrews and L. Catherine Brinson** (2008), Effect of Cross-Link Density on Interphase Creation in Polymer Nanocomposites, *Macromolecules*, 41, 6752-6756
- [117] **Yu-Hsuan Liao, Olivier Marietta-Tondin, Zhiyong Liang, Chuck Zhang and Ben Wang** (2004), Investigation of the dispersion process of SWNTs/SC-15 epoxy resin nanocomposites, *Materials Science and Engineering*, 385, 175–181

## LIST OF PUBLICATIONS

### I NATIONAL CONFERENCE

1. **Binu P P, K.E. George and M.N. Vinodkumar**, High Temperature behavior of polyester/ Cloisite15A Nano composite, *Proc. of 3<sup>rd</sup> National conference on Modern Trends in Mechanical Engg., Sree Narayana Gurukulam College of Engineering*, 2014, Pg. 42-45.

### II INTERNATIONAL CONFERENCE

1. **Binu P P, K.E. George and M.N. Vinodkumar**,(2016) Effect of nanoclay, Cloisite15A on the Mechanical Properties and Thermal behavior of Glass Fiber Reinforced Polyester, *Procedia Technology* ,25 , 846 – 853
2. **Binu P P, K.E. George and M.N. Vinodkumar**, Preparation, Mechanical and Thermal Characterization of Isophthalic Polyester- Cloisite15A Nanocomposite,*Proc. ICETEM-15, Sree Narayana Gurukulam College of Engineering* (Int. J. Design and Mfg. Tech. Vol.5(3), Dec(2014), pp.148-154 )
3. **Binu P P, K.E. George and M.N. Vinodkumar**, Effect of Nanoclay on Dynamic Mechanical and Tensile creep behavior of Glass Fiber Reinforced Polyester, *Proc. ICETEM-16, Sree Narayana Gurukulam College of Engineering* (Int. J. of Mechanical and Civil Engineering , Jan(2016),PP 25-34)

# CURRICULUM VITAE

1. **NAME** : Binu P P

2. **DATE Of BIRTH** : 24 March 1975

## 3. **EDUCATIONAL QUALIFICATION**

### **1997 Bachelor of Technology (B.Tech)**

Institution : M A College of Engineering,  
Kothamangalam

Specialization : Mechanical Engineering

### **2009 Master of Technology (M.Tech)**

Institution : School of Engineering, CUSAT

Specialization : Mechanical (Production)

### **Doctor of Philosophy**

Institution : School of Engineering, CUSAT

Registration Date : 03 August 2009